STRATIGRAPHY OF THE JURASSIC TECOCOYUNCA GROUP, MEXICO

BIOSTRATIGRAPHY AND LITHOSTRATIGRAPHY

OF

THE MIDDLE JURASSIC TECOCOYUNCA GROUP,

MEXICO

By

MICHAEL CAMERON MARSHALL, B.Sc.

A Thesis

Submitted to the School of Graduate Studies

in Partial Fulfilment of the Requirements

for the Degree

Master of Science

McMaster University

June 1986

MASTER OF SCIENCE (1986) McMASTER UNIVERSITY
(Geology) Hamilton, Ontario

TITLE: Biostratigraphy and Lithostratigraphy of the Middle Jurassic Tecocoyunca Group, Mexico

AUTHOR: Michael Cameron Marshall, B.Sc.
(McMaster University)

SUPERVISOR: Professor G.E.G. Westermann

NUMBER OF PAGES: xiii, 281

Abstract

The Middle Jurassic Tecocoyunca Group of northeastern Guerrero, Mexico is situated on the allochthonous Mixteca tectostratigraphic terrane. This group represents an overall transgressive trend with a few minor fluctuations of base level. Foreshore, shoreface, barrier island, washover, and lagoonal facies are identified within five coarsening-upward sequences. Abundant hummocky cross stratification, low-angle inclined stratification, and swash cross stratification indicate dominance of wave processes. These nearshore sequences are overlain by offshore marine shales, which are thought to represent a major global eustatic sea-level rise in the latest Bathonian, continuing into the Early Callovian. During the transgression, deep portions of the basin developed anoxic bottom conditions, resulting in the deposition of bituminous black shales. The combined effects of basinal subsidence and eustatic sea-level rise resulted in a rapid rate of transgression which exceeded that of sedimentation; ca. 110 cm/Ka.

Five ammonite associations date the Tecocoyunca Group as Upper Bathonian (Retrocostatum Zone) to Lower Callovian (Calloviense Zone). Biogeographic affinity of the ammonite fauna is mostly Andean with significant

west-Tethyan/Mediterranean elements and a few endemic species. The ammonite faunas show: 1) a rapid faunal replacement, 2) shell morphology trends, and 3) varying degrees of endemism/cosmopolitanism, all in relation to sea level variation.

Biostratigraphy and lithostratigraphy of the Tecocoyunca Group suggest that: 1)the Mixteca terrane had a paleoposition, during the Middle Jurassic, near the Pacific opening of the Hispanic Corridor (proto-Atlantic), 2) the Hispanic corridor provided marine connections between the eastern Pacific Ocean and the western Tethys Sea, and 3) preponderance of nearshore sediments suggests close proximity to the Andes of South America.

Acknowledgements

I would like to express my sincere gratitude to Dr. G.E.G. Westermann who provided me with a chance to study under his supervision. This research project was fascinating from the outset but its connotations became much more profound than either of us ever expected.

I would like to thank Dr. Jose Sandoval for his ammonite expertise and companionship in the field. The people at the Instituto de Geologia, Universidad Nacional Autonoma Mexico were also very helpful.

I am also extremely indebted to my "spouse" Shelley. She spent many frustrating hours proof reading my rough drafts and providing comments which were always constructive. I would also like to thank her for helping me with the typing, drafting, and layout. I don't know how I can ever thank you Shelley.

Jack Whorwood's advice and expertise were invaluable in helping me with the photography. Jack worked wonders in the dark room and I know he would rather develop and print almost anything but "wretched little ammonites".

I would also like to express my thanks to Len Zwicker for making excellent thin sections of my samples. Dr. M.J. Risk was very generous in allowing me access to his personal computer. I would like to sincerely thank Dr. R.G. Walker for providing a forum for discussion of my

research during an informal seminar at his home. Lastly, I would like to thank Dr. Guy Plint and Dr. Roger Walker for constructive criticism in the sedimentological aspects of my thesis.

Table of Contents

List of Figures

List of Plates

List of Tables

CHAPTER 1: INTRODUCTION

1.1 OVERVIEW

The Middle Jurassic Tecocoyunca Group crops out near Cualac in the northeastern part of the state of Guerrero, Mexico (Fig. 1.1). Areal extent of the outcrop does not exceed 100 km^2, but the structural and topographic characteristics of the area create excellent stratigraphic exposures. Continuously exposed clastic marine sequences between 750 and 900 metres thick are common. Some units of the Tecocoyunca Group are highly fossiliferous and are considered classic ammonite localities. Ammonite biostratigraphy dates the Tecocoyunca Group as Late Bajocian to Callovian.

The only other known outcrop of the Tecocoyunca Group is located approximately 100 km east of Cualac in neighbouring Oaxaca state. This outcrop contains older sediments of the Taberna, Otatera and Simon Formations (Lower to Middle Bajocian and Lower Bathonian) which are not the concern of this study (See Fig. 1.6).

1.2 STATEMENT OF PROBLEM

The Tecocoyunca Group near Cualac was made known by Burckhardt (1927) and Erben (1956) who concentrated their efforts on the ammonite fauna. The stratigraphic boundaries of the Tecocoyunca Group are unconformable and may be

Figure 1.1: Location of the Middle Jurassic Tecocoyunca Group (labelled 1) near Cualac, state of Guerrero (dotted border), Mexico.

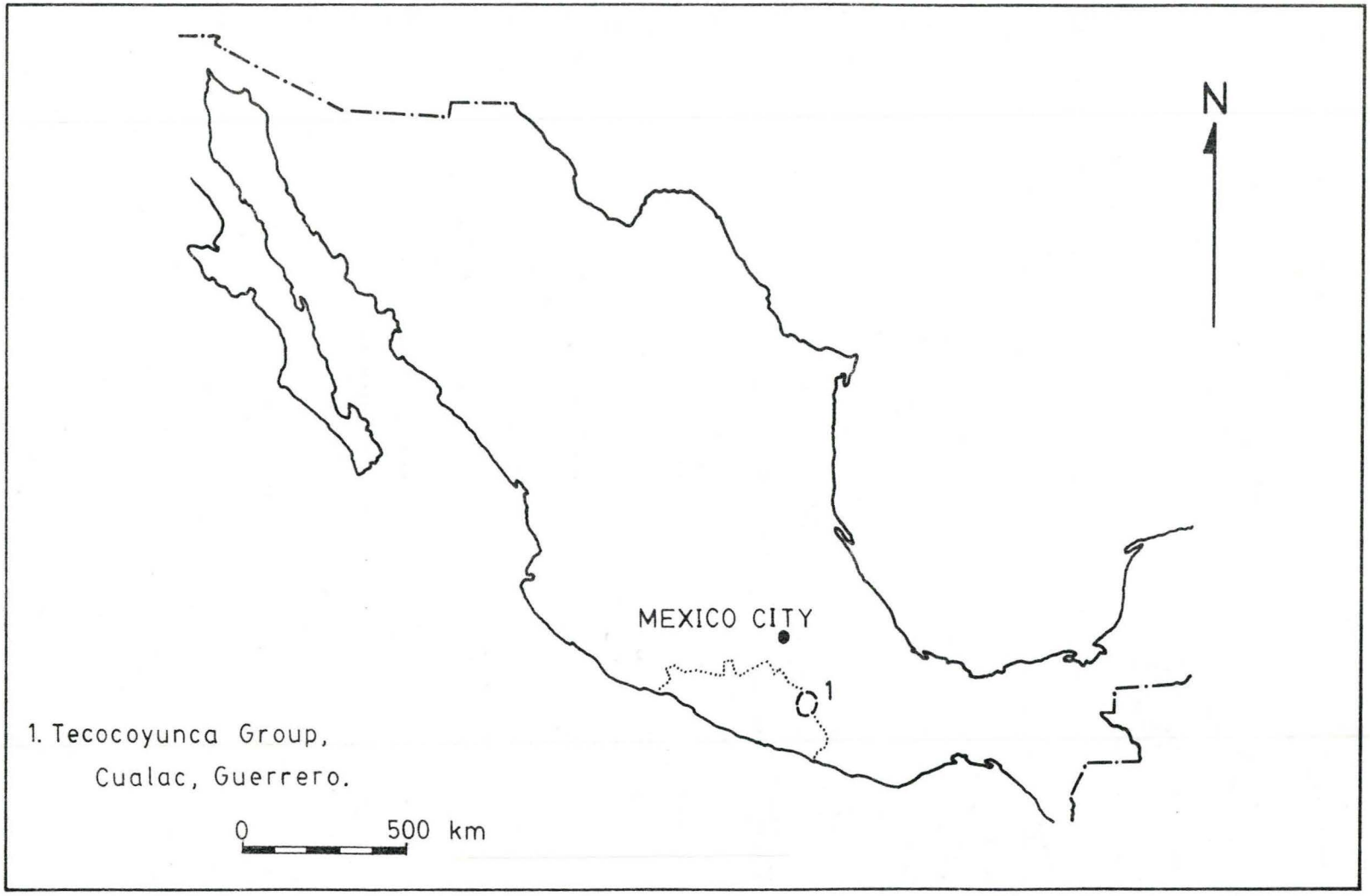
N
MEXICO CITY
1
1. Tecocoyunca Group,
Cualac, Guerrero.
0
500 km

faulted. Coney et al. (1980) and Campa and Coney (1983) have referred to the Tecocoyunca Group outcrop and other, similar areas in the North American Cordillera as 'suspect terranes' of which many are thought to be allochthonous to the North American craton. The accretion of numerous microplates onto the Pacific coast of North America occurred during the Mesozoic.

Other workers (Erben, 1957b; Imlay, 1980) believed that the Mesozoic marine sediments of the Tecocoyunca Group and similar sequences were deposited in marine embayments of the craton. Alencaster (1984) placed the origin of the Tecocoyunca Group in the Oaxaca-Guerrero Embayment (Fig. 1.2). More recently, many workers (e.g. Westermann, 1984c;Westermann et al., 1984; Taylor et al., 1984; Bartok et al., 1985) have considered the possibility of an epicontinental seaway south of the Mexican portion of the continent with marine connections to the Tethys Sea via the Proto-Atlantic seaway (Hispanic Corridor) (Fig. 1.5). Paleontological studies may provide information regarding the origin of the Tecocoyunca Group. Studies indicated high ammonite affinities with the Tethyan and Andean regions (Westermann, 1984b; Westermann et al., 1984). These affinities suggest some sort of marine connection with the Tethys Sea such as the epicontinental seaway located south of Mexico and including the northern Andes of South America.

Prior to the study of Westermann et al. (1984),

Figure 1.2: Proposed pre-Oxfordian location of the Huayococotla Embayment, Oaxaca Basin and hypothesized marine connections. (After Alencaster, 1984)

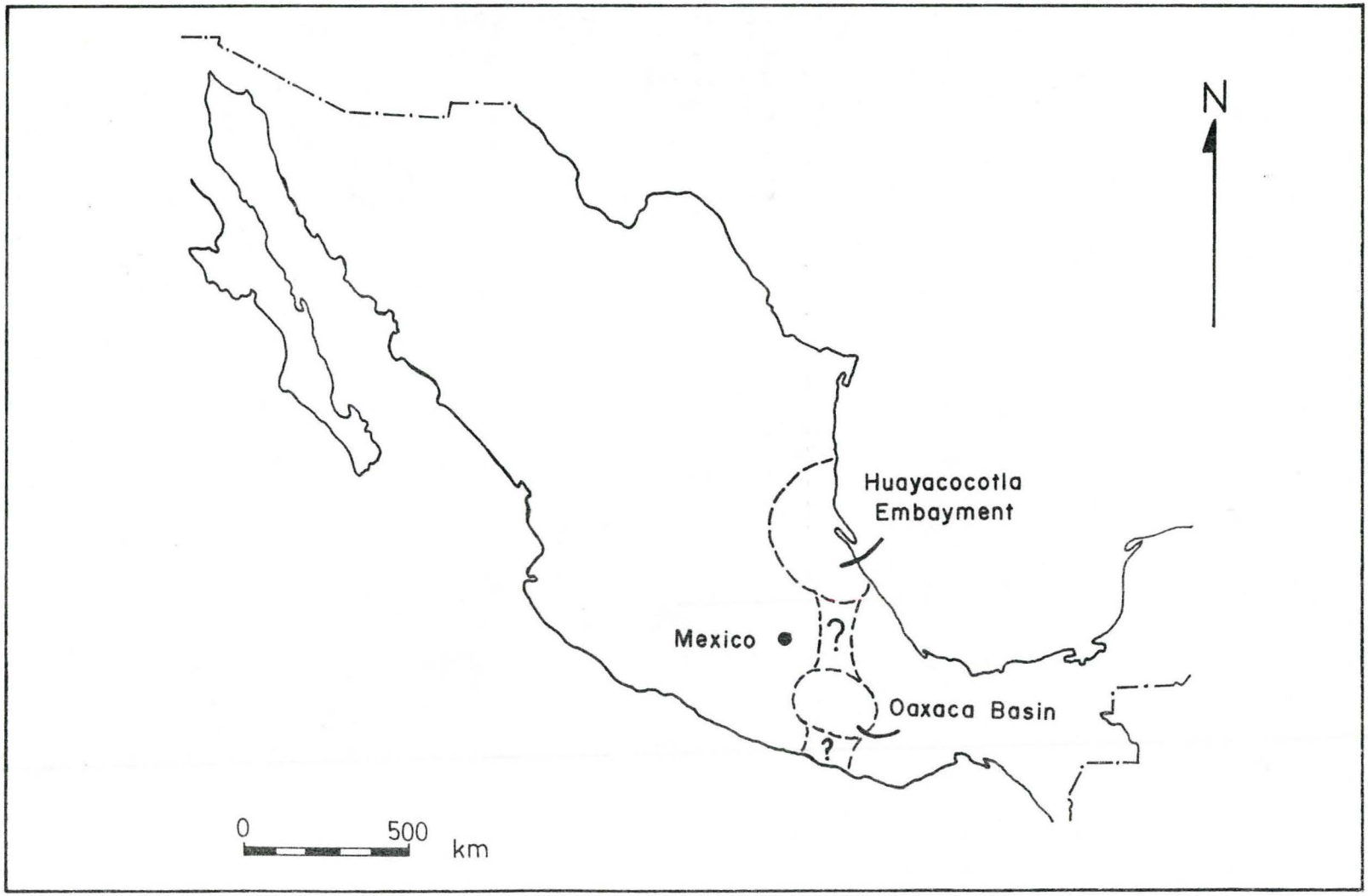
N
Huayacocotla
Embayment
Mexico
?
Oaxaca Basin
?
0
500
km

investigations of the Tecocoyunca Group near Cualac were few and incomplete. Recent field work by the author has revealed much additional paleontologic and geologic information. Whereas previous studies dealt principally with paleontology and biostratigraphy, this study incorporates both paleontologic and lithologic investigations of the clastic marine sequences.

1.3 PURPOSES OF THE PRESENT STUDY

Study of the Tecocoyunca Group outcrop near Cualac has very important global tectonostratigraphic and paleogeographic implications in addition to local paleontological, sedimentological, and paleoenvironmental applications. Previous investigations have focused on the ammonite fauna. The present study will extend the previous ones and present a comprehensive study of the Tecocoyunca Group by examining:

1. Ammonite fauna. Field work in 1984-1985 has yielded many additional ammonite genera and species than those previously known. The vertical distributions of the genera and species are more extensive than previously believed and therefore a fuller stratigraphic and taxonomic revision is imperative. Such a revision will also facilitate a more precise chronostratigraphic correlation with the European ammonite zonation.

2. Affinities, biogeography and evolution of the ammonite

fauna and its global associations and implications.

3. Other paleontological aspects of the study area including paleoecology of bivalves, brachiopods, gastropods and trace fossils.

4. Sedimentological aspects. A detailed facies analysis will provide the sedimentological information necessary for the environmental and depositional interpretations. The science of sedimentology has developed greatly since the early studies of the Tecocoyunca Group by Burckhardt (1927) and Erben (1956). The exposures near Cualac are well suited for such investigation.

5. Petrography of the various facies. Petrographic studies will compliment the facies analysis and provide added information for rock classification which will help interpret the depositional environments.

1.4 PREVIOUS WORK

The earliest study by Jenny (1933) mentioned the Tecocoyunca Group as part of a geological reconnaissance survey of northeastern Guerrero. Other studies of the general geology of the area of Cualac followed with those of Salas (1949), Guzman (1950) and Benavides (1978).

The first study of the ammonite fauna was by Burckhardt (1927) and it became the foundation for later investigations. Erben (1956) revised the Jurassic of Guerrero and Oaxaca states and gave the most recent account

of the Jurassic lithostratigraphy and biostratigraphy of the region, based on Guzman's field work. Ochoterena (1966) further examined some of the Middle Jurassic ammonites of the area. A general stratigraphic study of Corona (1981) concentrated primarily on the Paleozoic strata of the region but included brief discussions of the Mesozoic strata. Westermann et al. (1984) improved on Erben (1956) emphasizing vertical distribution of the ammonite fauna plus taxonomic additions and revisions. Westermann (1984) examined the Duashnoceras Assemblage found in the Bajocian Taberna Formation of the Tecocoyunca Group in neighbouring Oaxaca state.

Alencaster (1963) described the pelecypods of Oaxaca and Guerrero, particularly those from the Tecocoyunca Group near Cualac.

1.5 SUSPECT TERRANES - THE STATE OF KNOWLEDGE

Coney et al. (1980) noted that over 70 % of the North American Cordillera is composed of 'suspect terranes' creating a mosaic or collage. This increases to 80 % in the southern part of the North American Cordillera within Mexico (Campa and Coney, 1983). These terranes are considered to be allochthonous for two reasons: a) their paleogeographical setting with respect to the North American craton through Phanerozoic time cannot be determined unequivocally, and b) they cannot be proven to be underlain by autochthonous North

American basement. Most appear to have collided and accreted onto the North American cratonic margin during the Mesozoic and Cenozoic. The accreted terranes became detached from Pacific Ocean plates (eg. Farallon and Kula plates) due to the formation of subduction zones in the Mesozoic (Campa and Coney, 1983).

A 'terrane' possesses certain characteristics which include internal homogeneity, continuity of stratigraphy, and similar tectonic style and history. Some terranes are 'composite'and consist of a number of smaller plates. The boundaries between terranes appear as stratigraphic discontinuities which are difficult to explain by conventional facies changes or unconformities (Coney et al., 1980). Most boundaries separate terranes whose rock sequences are temporally or physically distinct and often contain different faunas. Most terranes are bounded by known or suspected faults. Many are definitely sutures which frequently were reactivated in the Cenozoic by concurrent and post-collisional right-lateral strike-slip movements (Coney et al., 1980). Coney and others point out that the identification of a terrane is based on tectonostratigraphic criteria and does not imply any genetic or plate-tectonic origins. Most terranes have sedimentary and volcanic rock sequences which are of oceanic rather than continental origin thus implying an allochthonous origin. The mechanical process of accretion involved thrust

faulting. The process of intra-plate thrusting and strike-slip translation created concurrent and post-accretionary telescoping and consolidation of terranes (Coney et al., 1980).

The Mojave-Sonora Megashear (Silver and Anderson, 1974), extending from N.W. to S.E. Mexico (Fig. 1.3, unshaded dashed line), was active during the Late Triassic-Middle Jurassic opening of the Gulf of Mexico (Taylor et al., 1984). The Terreon-Monterrey Megashear cut the eastern terranes of the Mexican Cordillera during the Jurassic. The portion of Mexico southwest of the Mojave-Sonora Megashear could have moved 1000 km southeastward and such a translation combined with accretion and counter-clockwise rotation of terrane blocks prevents the overlap of Mexico with South America in the reconstruction of Pangea (Taylor et al., 1984).

Paleomagnetic studies (Beck, 1976; Irving, 1979) have indicated that extensive northward translation and clockwise rotation of the terranes occurred suggesting oblique convergence from a generally northward Pacific 'mega-drift' (Coney et al., 1980). Most of the terranes are thought to have originated much farther south of their present locations. North America's northwestward and westward motion against the generally northward moving accretionary terranes may have been important (Coney, 1972). It is noted by Coney et al. (1980) that Cordilleran telescoping on the

Figure 1.3: Tectonostratigraphic terranes of Mexico. Basement terrane boundaries are shaded black lines. The Mojave-Sonora Megashear is the unshaded dashed line extending from northwestern to southeastern Mexico. (After Campa and Coney, 1983)

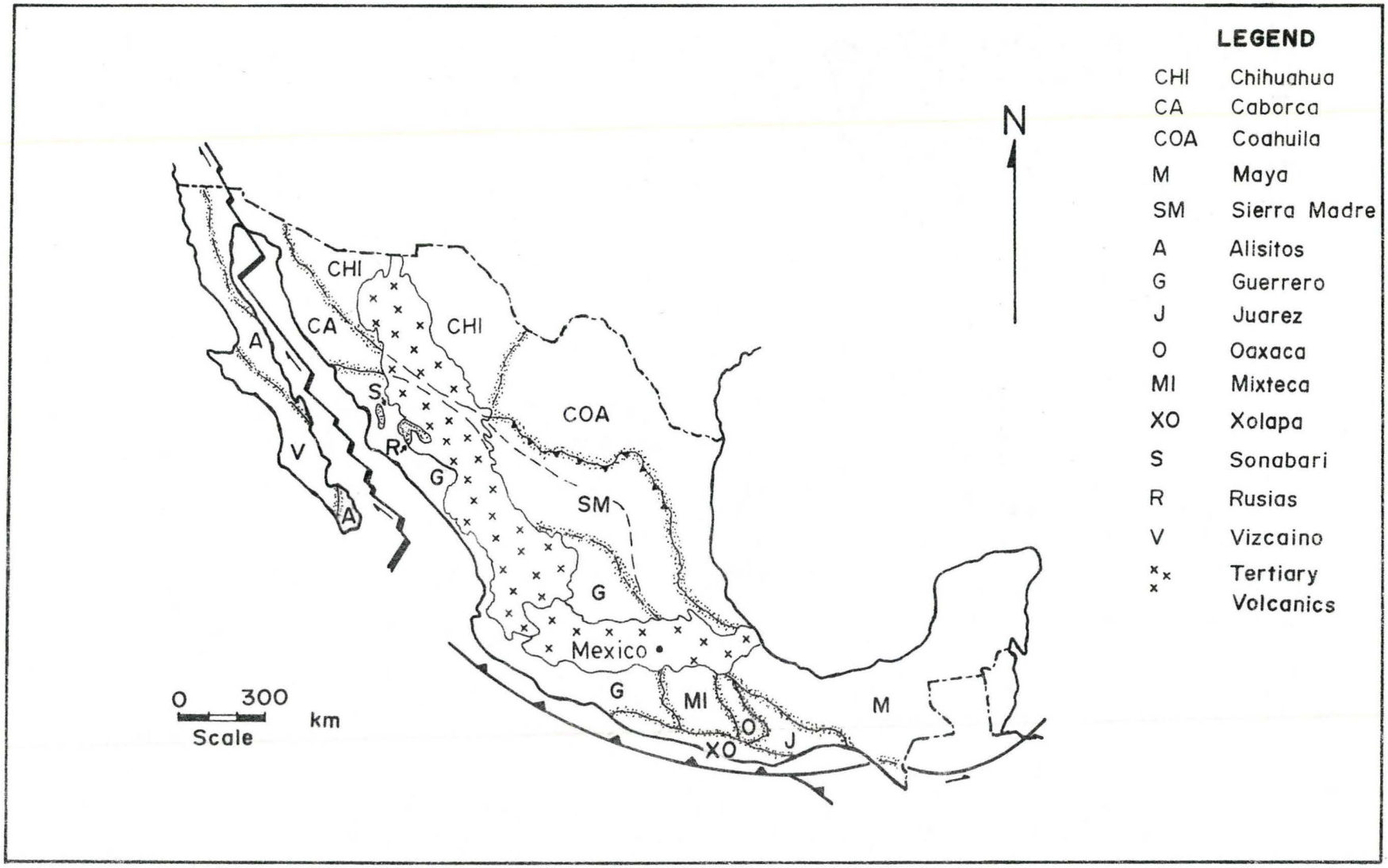
LEGEND
CHI Chihuahua
CA Caborca
COA Coahuila
M Maya
SM Sierra Madre
A Alisitos
G Guerrero
J Juarez
O Oaxaca
MI Mixteca
XO Xolapa
S Sonabari
R Rusias
V Vizcaino
Tertiary Volcanics
N
CHI
CA
CHI
A
S
R
V
A
G
COA
SM
G
Mexico
G
MI
O
J
XO
M
0 300
Scale
km

foreland began only after the Middle Jurassic initiation of the Opening of the central Atlantic Ocean, which moved the North American plate northwestward and then westward over the Pacific Ocean. As a final stage to consolidation of the Cordilleran mosaic, the Laramide Orogeny (Late Cretaceous to Early Tertiary) and the possibly elevated convergence rates between the North American plate and the Farallon and Kula plates, may have created deep-seated tectonism and shifting of the terranes (Coney et al., 1980).

A tectonostratigraphic terrane map of Mexico of Campa and Coney (1983) (Fig. 1.3) shows the distribution of major terranes each with an internally homogeneous basement assemblage within the boundaries of the terrane. Campa and Coney (1983) group the terranes into three major tectonostratigraphic subdivisions; 1) northwestern zone, 2) eastern zone, and 3) western zone, which will be discussed in more detail. The western zone covers almost half of Mexico and consists of the Alisitos, Guerrero, Juarez, Mixteca, Oaxaca, Xolapa and Sonabari terranes of which many are composite. Campa and Coney (1983) suggest that the terranes of western Mexico were accreted onto North America during the Laramide Orogeny (Late Cretaceous to Early Tertiary). Folding, faulting and volcanism were widespread during this time and the extensive superjacent Tertiary volcanics were emplaced during the latter portion of Laramide tectonism.

The Mixteca terrane is the most interesting because it contains the Tecocoyunca Group near Cualac and is the only terrane with a well documented Late Bajocian-Early Callovian ammonite faunas. The terrane consists of a "tectonically juxtaposed two-part metamorphic basement with an intervening ultramafic body" according to Campa and Coney (1983). Radiochronology from metamorphic rocks of the lower part of the basement indicates Early Paleozoic (Cambrian to Ordovician) ages (Ortega, 1978). The Jurassic and Paleozoic rocks are overlain by Neocomian shales and limestones followed by Aptian-Cenomanian limestones and a flysch-like Upper Cretaceous sequence as shown in Figure 1.4 (Campa and Coney, 1983).

Faunal investigations have provided the best evidence for the longitudinal paleopositions of terranes. The Late Bajocian Parastrenoceras and Duashnoceras ammonite associations suggest that the Mixteca terrane was positioned in proximity to the opening of the Hispanic Corridor (Westermann, 1984). The Late Bathonian Neuqueniceras association of ammonites suggests a position near the central and southern Andes (Taylor et al., 1984). Faunal evidence clearly indicates that during the Jurassic the Mixteca terrane was associated with the eastern Pacific Ocean. Westermann et al. (1984) used ammonite faunas to suggest that the Mixteca terrane had a paleoposition near the Pacific opening of the Hispanic Corridor which connected

Figure 1.4: Tectonostratigraphic column of the Mixteca terrane. Vertical arrow beside column shows the extent of the basement terrane. Rocks above are superjacent (overlap) terrane (After Campa and Coney, 1983).

MIXTECA

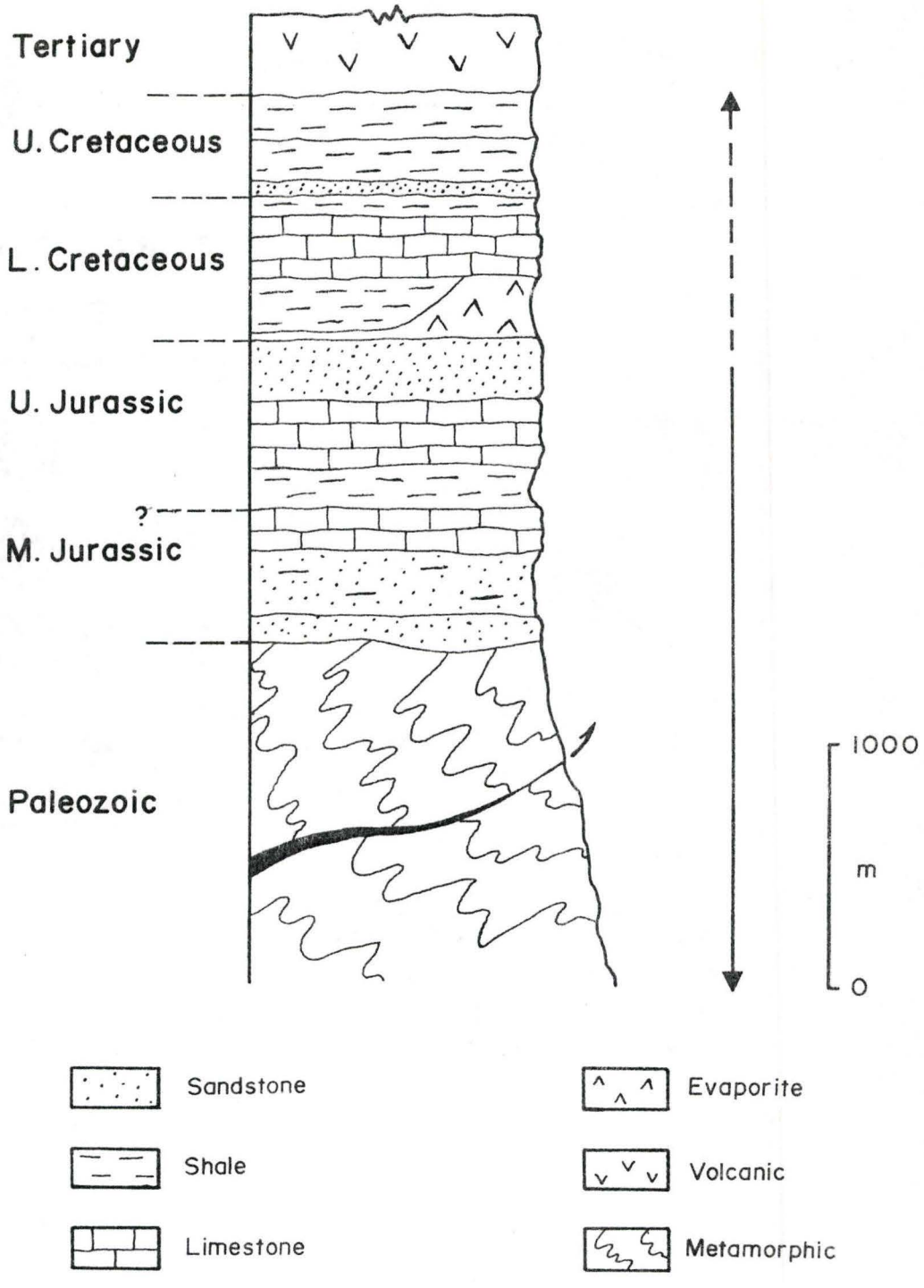
Tertiary
U. Cretaceous
L. Cretaceous
U. Jurassic
?
M. Jurassic
Paleozoic
1000
m
0
Sandstone
Shale
Limestone
Evaporite
Volcanic
Metamorphic

with the western Tethys Sea, but not too distant from the Andes of Peru, Chile and Argentina.

Tectonostratigraphic investigations of the Mexican Cordillera are still in the early stages and even as recently as 1980 the concept of collage tectonics was not integrated into paleogeographic studies of the North American Cordillera. Imlay (1980) failed to mention plate tectonics and remained supportive of the idea proposed by Erben (1957b) that the marine sequences in the Mexican Cordillera are remnants of marine embayments. Paleontological evidence of Westermann et al. (1984) suggests that the marine sequences and their associated faunas within the Mexican Cordillera may be the result of a combination of; a) accreted terrane blocks, and b) an epicontinental marine seaway south of Mexico connected with the Tethys Sea via the Hispanic Corridor (Proto-Atlantic) as shown in Figure 1.5.

1.6 GEOLOGIC SETTING

The Tecocoyunca Group crops out in the northeastern part of the state of Guerrero and northwestern Oaxaca state as part of the Mixteca tectonostratigraphic terrane within the Sierra Madre del Sur. The oldest rocks are schists of the Acatlan Formation which have been dated as Early Paleozoic by Ortega (1978) (See Map 1). The Permian Los Arcos Formation lies superjacent and unconformably on the

Figure 1.5: Proposed paleogeographic reconstruction of Middle Jurassic North America and neighbouring continents. The approximate paleopositions of the major terrane blocks, including the Mixteca terrane (labelled M), are indicated before and after accretion (After Westermann, 1984). Note the relationship between the East Pacific Ocean, epicontinental marine connection, Hispanic Corridor and the Tethys Sea with respect to the paleoposition of the Mixteca terrane. Many of the North American terranes are not shown.

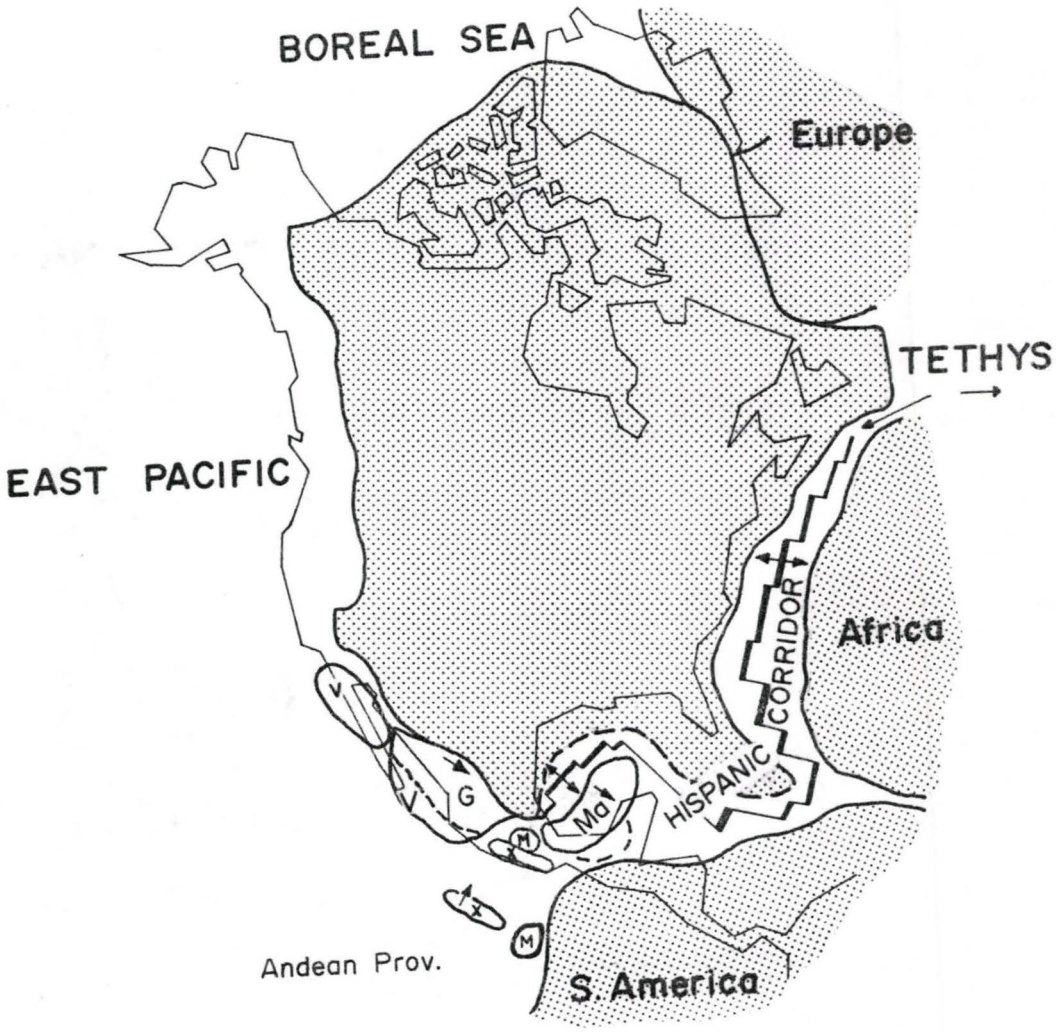
BOREAL SEA
Europe
TETHYS
EAST PACIFIC
CORRIDOR
Africa
HISPANIC
G
Ma
M
Andean Prov.
S. America

Map 1: Geology of the region near Coauilote, Guerrero, Mexico. The measured stratigraphic sections are labelled C1-C4. (Modified from Corona, 1981)

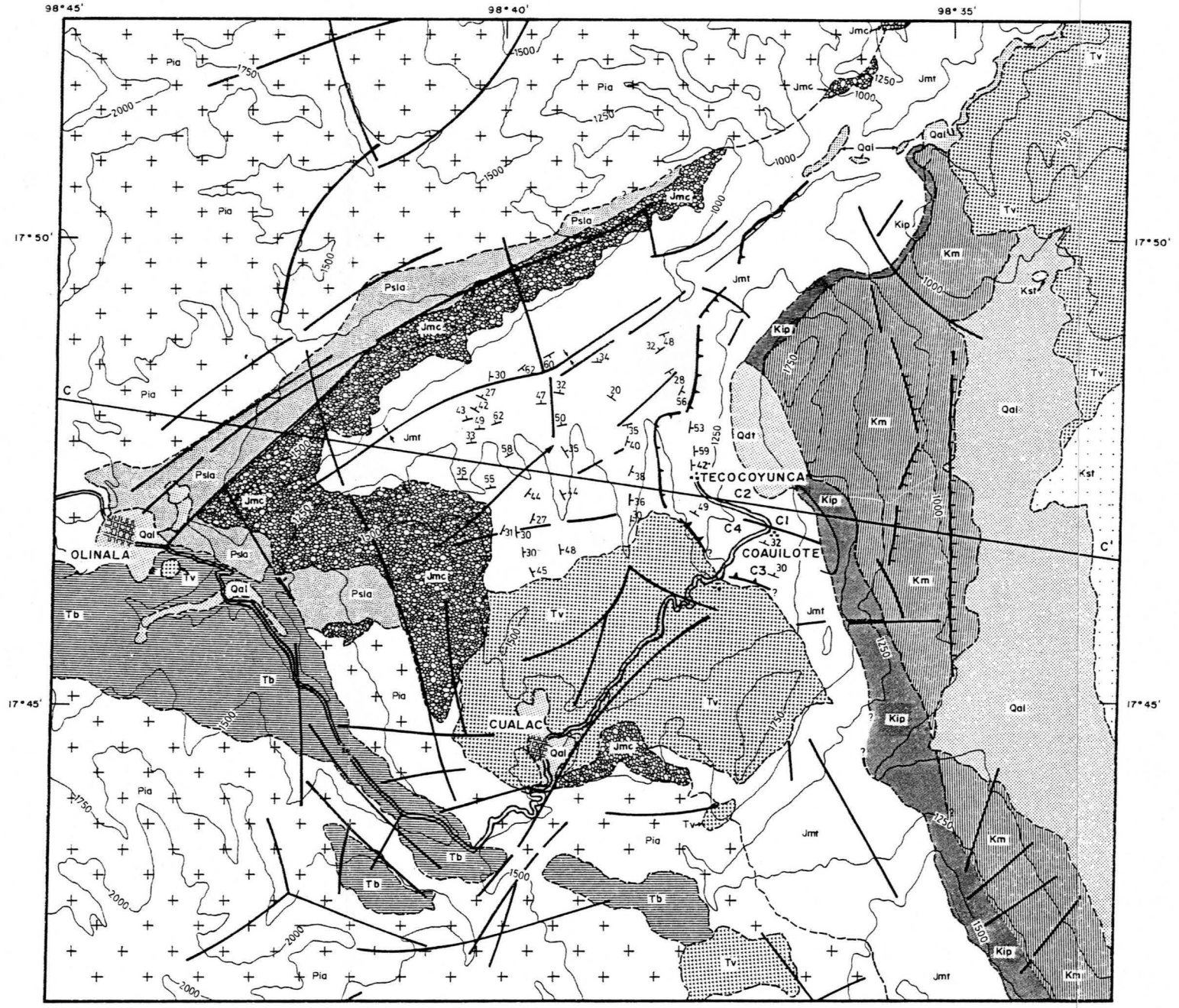

LEGEND

ERA	PERIOD	EPOCH	AGE	SYMBOL	DESCRIPTION
CENOZOIC	QUAT.		RECENT	Qal	Alluvium and Soil
			PLEIST.	Qdt	Talus Deposits
	TERTIARY		PLIOCENE MIOCENE	Tv	Andesite Tuffs and Flows
			OLIGOCENE EOCENE	Tb	Balsas Fm. Conglomerates and Red Continental Breccia, Limestone with Volcanic Material
			PALEOCENE		
MESOZOIC	CRETACEOUS	UPPER		Kst	Tialtepexi Chalk, Chalk, Anhydrite and Thin Lenses of Limestone
			ALBIAN APTIAN	Km	Morelos Fm. Massive Limestone, Dolomitized
		LOWER	NEOCOMIAN	Kip	Puebla Group. Sandstone Horizons and Conglomerate Lenses
	JURASSIC	UPPER			
		MIDDLE	CALLOVIAN BATHONIAN	Jmt	Tecocoyunca Group. Sandstones, Limestones, Shales with Coal Layers and Conglomerate Horizons
			BAJOCIAN	Jmc	Cualac Conglomerate. Quartzitic
	TRIASSIC				
PALEOZOIC	PERMIAN			Psla	Los Arcos Fm. Sandstones with Ferruginous Concretions, Black Shales, Marls and Limestones
	ORDOVICIAN CAMBRIAN			Pia	Acatlan Fm. Micaceous Schists and Phyllites with Abundant Quartz Veins
PRECAMBRIAN					

GEOLOGIC SYMBOLS

- GEOLOGIC CONTACT
- STRIKE AND DIP (Number) — 30
- FRACTURE (No apparent movement)
- FAULT
- THRUST FAULT
- ANTICLINE
- SYNCLINE
- SECTION LINE — C C'
- MEASURED SECTION — C2

TOPOGRAPHIC SYMBOLS

- TOWN
- VILLAGE
- ELEVATION CONTOURS (m) — 1000
- DIRT ROAD

CONTOUR INTERVAL 250 m

SCALE 1:50 000

N

0 1 2.5 5
Kilometres

SECTION C-C'

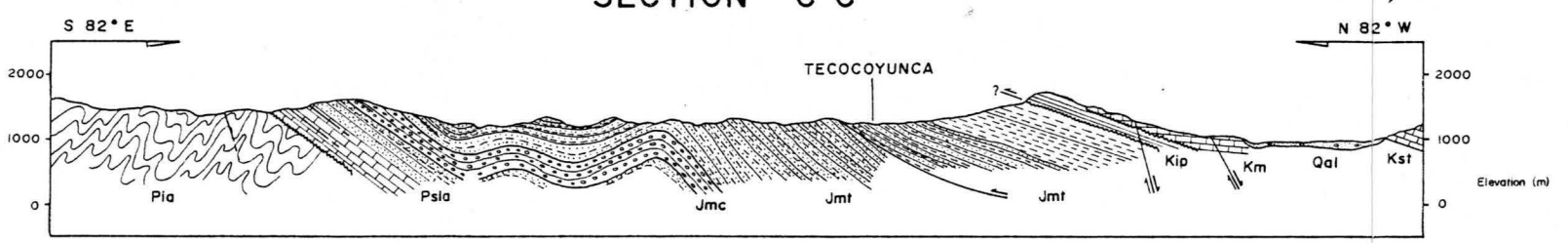

GEOLOGY OF THE CUALAC REGION, STATE OF GUERRERO, MEXICO.

Adapted from Corona, 1982.

Paleozoic Acatlan Formation and is composed of sandstones, black shales, marls and limestones. Corona (1981) reported Permian ammonoids in the Los Arcos Formation which was formerly considered Early Mesozoic. The Lower Jurassic Cualac Conglomerate lies unconformably (?) on the Permian sediments. This is followed by the Tecocoyunca Group of sandstones, limestones and shales with coal-bearing horizons. Lower Cretaceous (Neocomian) sandstones of the Puebla Group lie unconformably (?) (faulted) on the Tecocoyunca Group. The Puebla Group forms the basal portion of an escarpment in the local topography which is the result of thrust faulting. The massive dolomitized limestones of the Aptian-Albian Morelos Formation follow superjacent (unconformably ?) on the Puebla Group. The upper Cretaceous Tlaltepexi Chalk lies above the Morelos Formation. The Tertiary (Oligocene-Eocene) Balsas Formation of conglomerates and limestones is situated on the Paleozoic Acatlan Formation indicating local uplift and erosion. Tertiary (Miocene-Pliocene volcanics are superjacent to all of the sedimentary rocks in the region, except for the Quaternary talus and alluvial deposits which fill the intermittent stream and river valleys.

This study is concerned with the Tecocoyunca Group, an 850 metre thick clastic sequence of marine and continental origin. Erben (1956) divided the Tecocoyunca Group into five formations separated by transitional 'boundaries'(See

Fig. 1.6). They are listed here from top to bottom (from Westermann et al., 1984):

Yucunuti Formation. Ca. 600 m of calcareous shales often with calcareous iron-rich concretions and some interbedded siltstones. There is an abundant invertebrate fauna at several levels. Late Bathonian-Early Callovian.

Otatera Formation. 50 to 70 m of sandstones with well developed sedimentary structures and some shales with ferruginous concretions. Oyster horizons are also present. Late Bathonian.

Simon Formation. 80 to 100 m of sandstones with conglomerate, coaly horizons and abundant plant debris.

Taberna Formation. 50 to 60 m of siltstones and shales with ferruginous concretions. Rich invertebrate fauna of the Late Bajocian.

Zorillo Formation. 20 to 80 m of ferruginous sandstone and shales with plant debris and coal horizons.

Only the Yucunuti, Otatera and Simon Formations crop out near Cualac and are the focus of this study.

The region near Cualac underwent considerable tectonism during the Laramide Orogeny (Late Cretaceous to Early Tertiary). The Jurassic sequence near Coauilote, east of Cualac, forms part of the western limb of a large synclinorium (Westermann et al., 1984). Within the Tecocoyunca Group outcrop there is a syncline and an anticline both of which have been eroded. They trend

Figure 1.6: Summary of the stratigraphic position, age and important ammonite genera of the diachronous formations within the Tecocoyunca Group from N.W. Oaxaca and N.E. Guerrero (Modified from Westermann, 1984b). Formation thicknesses are not to scale.

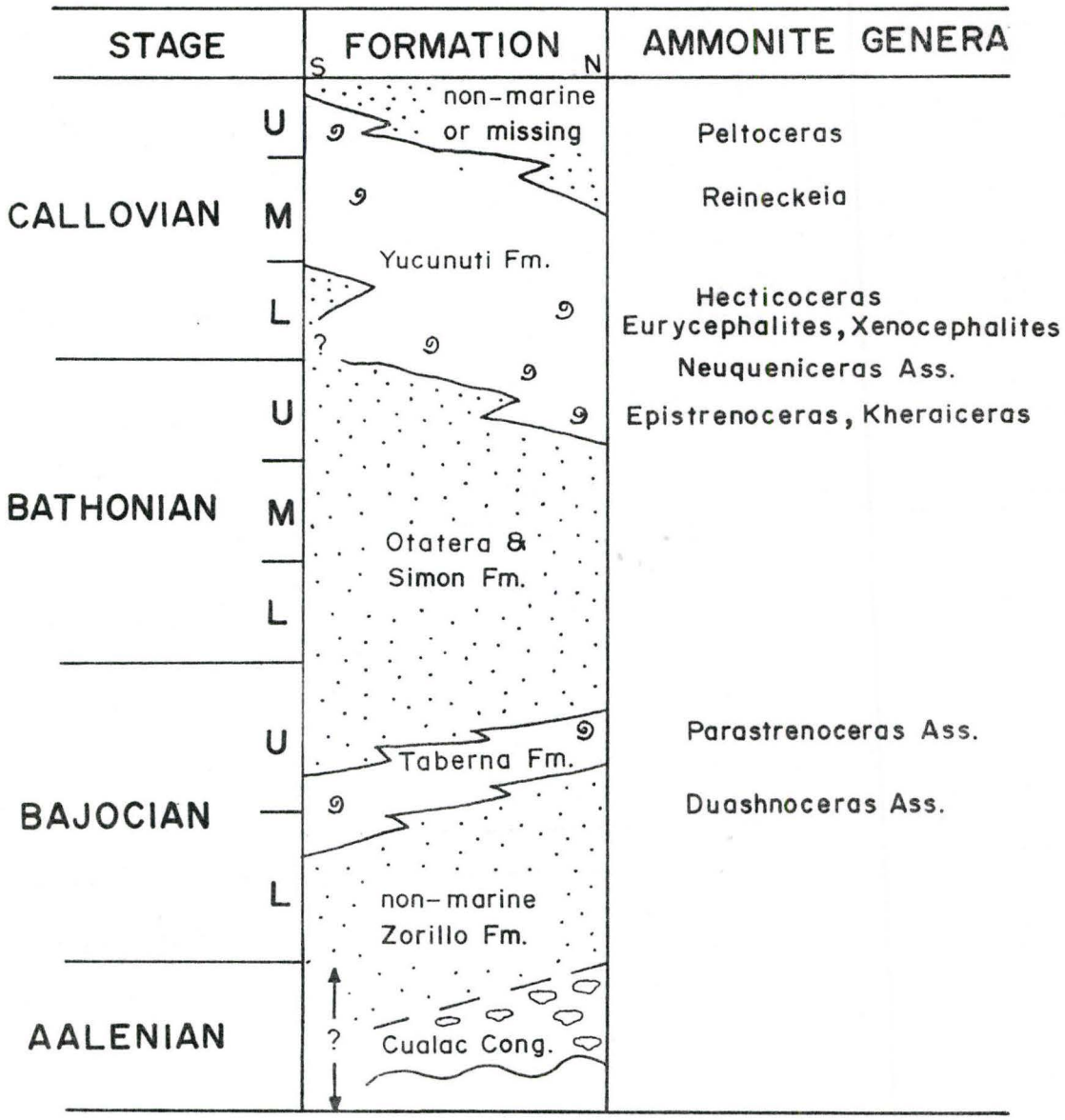
STAGE
FORMATION
S
N
AMMONITE GENERA
non-marine
or missing
Peltoceras
U
CALLOVIAN
M
Reineckeia
Yucunuti Fm.
L
Hecticoceras
Eurycephalites, Xenocephalites
?
Neuqueniceras Ass.
U
Epistrenoceras, Kheraiceras
BATHONIAN
M
Otatera &
Simon Fm.
L
U
Parastrenoceras Ass.
Taberna Fm.
BAJOCIAN
Duashnoceras Ass.
L
non-marine
Zorillo Fm.
AALENIAN
?
Cualac Cong.

northeast-southwest and the anticline plunges to the northeast. The bedding of the area generally dips in a northeasterly to easterly direction. Field work by Corona (Westermann et al., 1984) and recent work by the author indicate the presence of many faults of varying magnitude. Map 1 shows the locations of thrust and dip-slip faults, as well as many other possible stike-slip faults. In many cases, displacement along faults is not apparent and these are called fractures. Small Tertiary andesite sills intruded the sedimentary sequence in several small areas and have imparted noticeable contact metamorphism especially on the shales.

Westermann et al. (1984) suggest that the rate of sedimentation for the Yucunuti Formation was high; on the order of 20 cm/ka as calculated from ca. 550 m of shale deposited during 3 to 4 ammonite chronozones. This refers to the shale thickness measured in outcrop. The actual rate of mud sedimentation could have been on the order of 1.1 m/ka based on the commonly quoted mud to shale compaction ratio of 6:1 (Dr. M.J. Risk, pers. comm.).

1.7 STUDY AREAS AND STRATIGRAPHY

The principal area of study is just north of the village of Coauilote extending to the village of Tecocoyunca (Map 1). The outcrop area can be reached from Cualac by travelling northeast over 7.5 km of dirt roads.

The most important measured section is along the creek bed of Arroyo El Rincon (labelled C1 on Map 1). The topography of the lower part of this outcrop is reasonably flat, but the upper portion above the road from Coauilote to Tecocoyunca, becomes steeper as the creek head cuts back into a ridge. The reference level for studies of Westermann et al. (1984) and Erben (1956) is the andesite sill at the level of the road from Coauilote to Tecocoyunca. The 180 m of shales with interbedded siltstones and calcareous, iron-rich concretions above the reference andesite sill contain abundant ammonite faunas at several levels. The 160 m of shales with interbedded siltstones and concretions below the reference level also contain very abundant ammonite faunas at several levels. The lower boundary of the Arroyo El Rincon section (C1) is located at the junction of Arroyo El Rincon and Arroyo Tecocoyunca.

The Arroyo Tecocoyunca section (labelled C4 on Map 1) is stratigraphically below and continuous with the Arroyo El Rincon section. This section consists of 100 m of sandstones with well developed sedimentary structures. Thin coal horizons are found within the lower portion of the exposed sandstones. The sandstones are overlain by 50 m of interbedded sandstones and shales. A rich pelecypod fauna is present in the shales.

Approximately 0.6 km north of Coauilote is another well exposed section within Arroyo El Campamento (labelled C2 on

Map 1). The section is 210 m in thickness and passes from shales with interbedded siltstones and concretions in the basal 170 m, upward into limey shales, limestone and shales with abundant sandstone interbeds. The fauna permits correlation of the lower 145 m with the upper portion of the Arroyo El Rincon section (C1). The upper 65 m of the El Campamento section are stratigraphically above the uppermost portion of the El Rincon section and they are the youngest Jurassic rocks of the area near Coauilote.

Southeast of Coauilote, near the head of Agua Amarga Creek and Alto de Teeolutla, is a sequence of interbedded buff-coloured sandstone and shale beds with a rich, shallow infaunal pelecypod fauna. The 50 m exposure (locality C3 on Map 1) yields an ammonite fauna which is typically Late Bathonian in age including the Tethyan guide ammonite Epistrenoceras hystricoides Rollier.

The overall stratigraphic situation of the Tecocoyunca Group for Guerrero and Oaxaca is shown in Figure 1.6 as modified from Westermann (1984b).

1.8 GENERAL PROCEDURES

The field work involved the measurement of a number of outcrop sections. These sections were subdivided into units based on lithology and numbered sequentially. Detailed lithologic descriptions were compiled for each unit and grain sizes were estimated using a half-phi interval grain

size comparator. Hand samples of each unit were collected. Paleontological investigations of each unit included a description of the fauna, notes on the type and state of preservation, relative abundance, and any other features. Macrofossil specimens were collected and numbered according to which section and unit they originated.

CHAPTER 2: FACIES DESCRIPTIONS

2.1 OVERVIEW

Data collected from 900 metres of continuous stratigraphic section near Coauilote, Guerrero have resulted in a total of 78 units identified on the basis of lithology, sedimentary structures, macrofossils and ichnofossils. These units have been further grouped into 22 facies.

Figures 2.2 to 2.6 are stratigraphic columns detailing the position of facies. Figure 2.1 is a legend describing all symbols used.

2.2 FACIES A: INTERBEDDED SANDSTONES, SILTSTONES, AND SHALES

Facies A is an association of interbedded sandstones, siltstones, and shales. Total thickness of Facies A is approximately 155 metres thick in sections C3-Alto de Teeolutla and C4-Arroyo Tecocoyunca (Plate 2.1).

The shales are poorly fissile and often extensively bioturbated. Sandstone and siltstone beds typically have sharp erosional bases which occasionally show undulatory scouring into the underlying shales. Upper surfaces are planar and sharp, with some beds exhibiting symmetrical wave ripples. The wave ripples are sharp-crested and have amplitudes of 1-2 cm and wavelengths of 10-30 cm. Parallel lamination is evident in many of the sandstone and siltstone

Figure 2.1:

Legend of all symbols used in the stratigraphic columns measured near Coauilote, Guerrero.

LEGEND

LITHOLOGY

- Shale
- Metamorphosed Shale
- Limestone
- Silty Limestone
- Limey Siltstone
- Modern Soil
- Coal
- Pebbles
- Oyster Coquina
- Concretion
- Andesite

FOSSILS

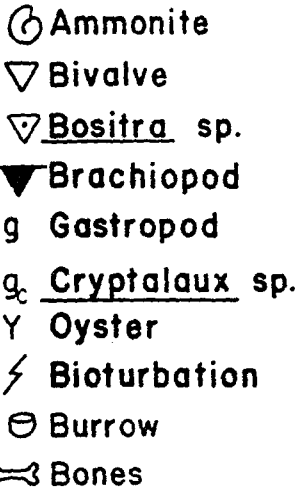

- Ammonite
- Bivalve
- Bositra sp.
- Brachiopod
- g Gastropod
- g_c Cryptalaux sp.
- Y Oyster
- Bioturbation
- Burrow
- Bones

SEDIMENTARY STRUCTURES

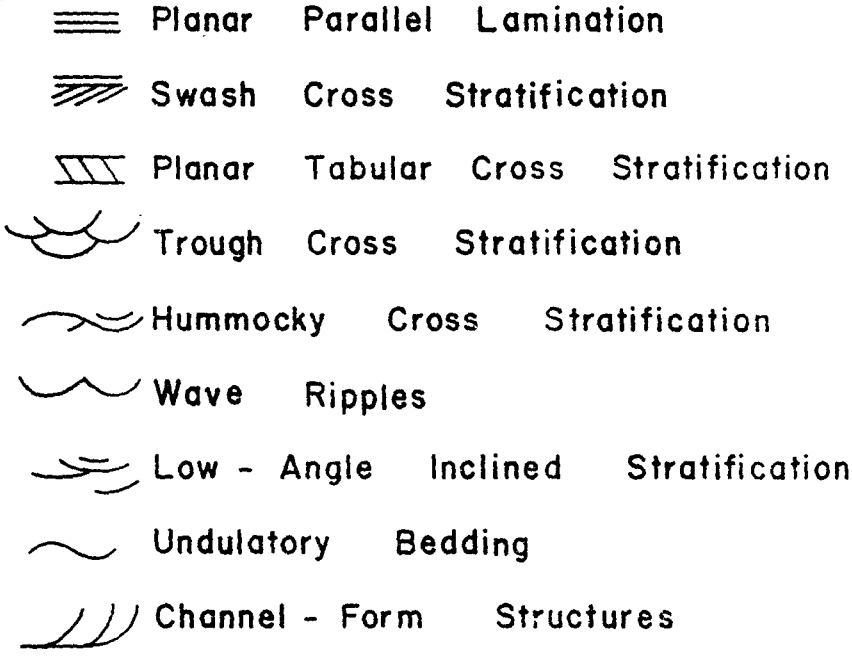

- Planar Parallel Lamination
- Swash Cross Stratification
- Planar Tabular Cross Stratification
- Trough Cross Stratification
- Hummocky Cross Stratification
- Wave Ripples
- Low - Angle Inclined Stratification
- Undulatory Bedding
- Channel - Form Structures

OTHERS

- Unconformity

Figure 2.2: Lithofacies and fauna of Section C3-Alto de Teeolutla.
Note: The arrows on the sections represent coarsening-upward (curve to right) and fining-upward (curve to left) trends.

C3 - Alto de Teeolutla

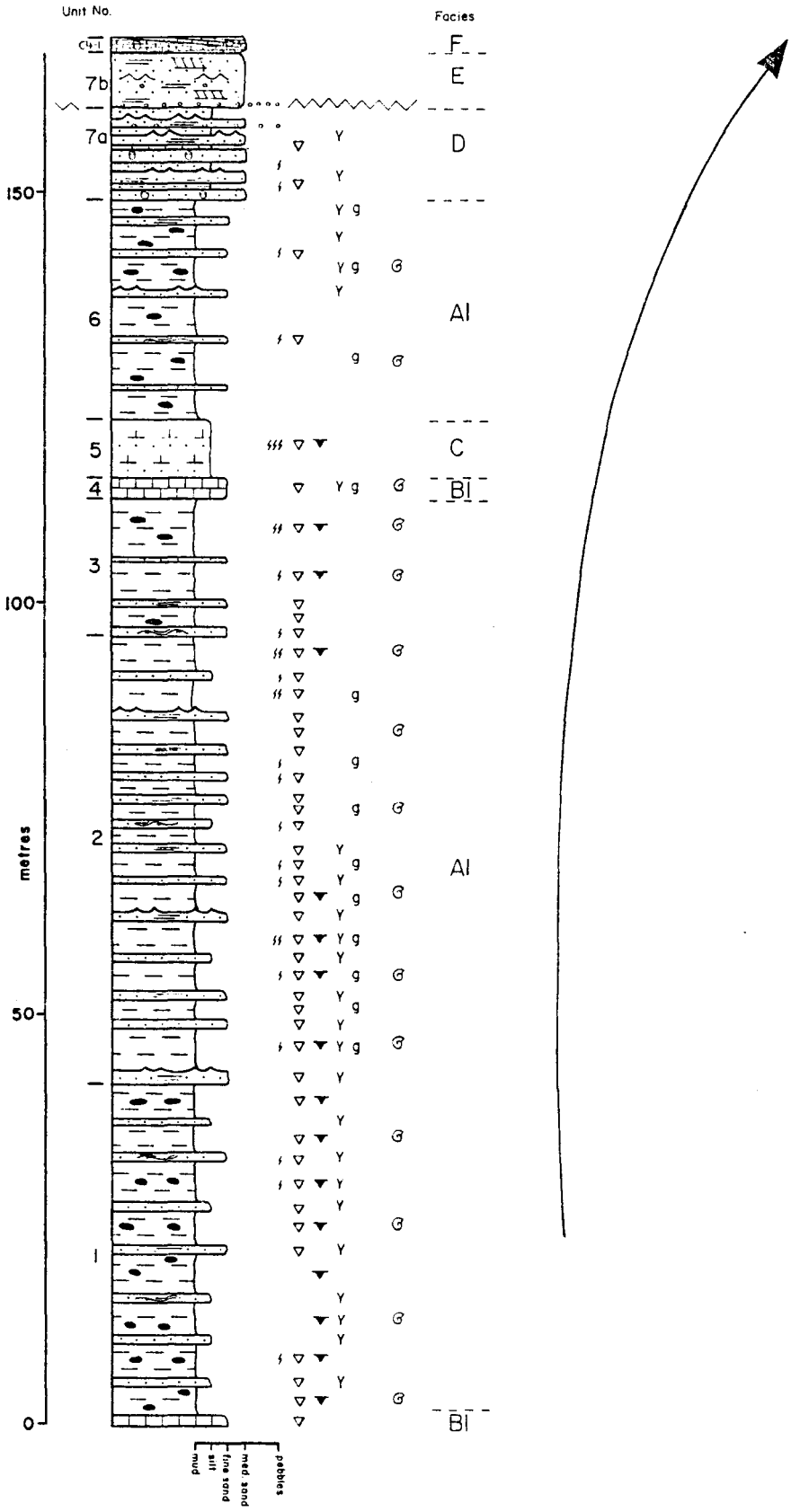

Figure 2.3:

Lithofacies and fauna of Section C5-Alto El Variado. This section correlates with a portion of Unit 2, Section C3.

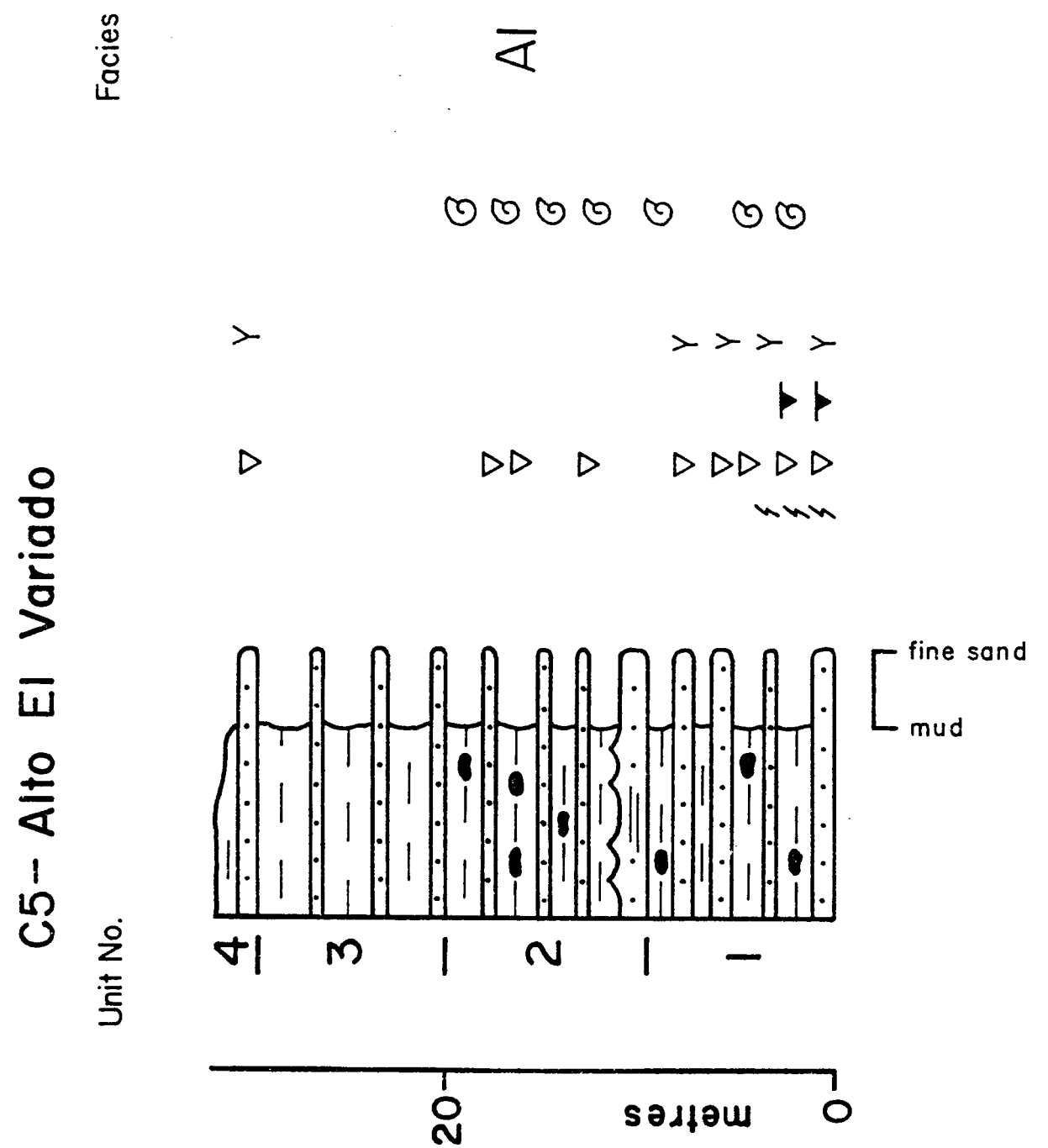
C5- Alto El Variado
Unit No.
Facies
AI
4
3
2
1
20
0
metres
fine sand
mud

Figure 2.4: Lithofacies and fauna of Section C4-Arroyo Tecocoyunca.

C4 - Arroyo Tecocoyunca

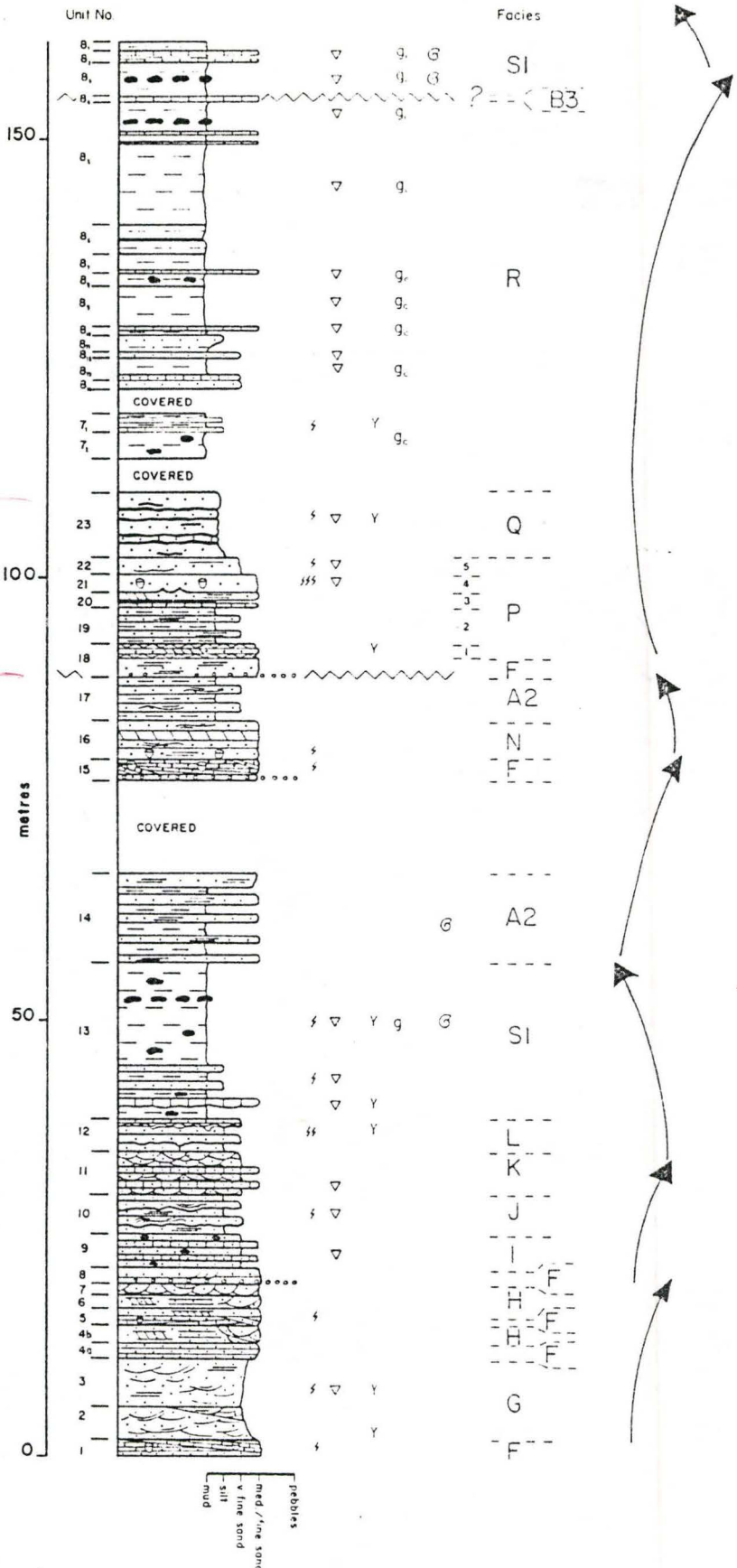

Figure 2.5: Lithofacies and fauna of Section C1-Arroyo El Rincon.

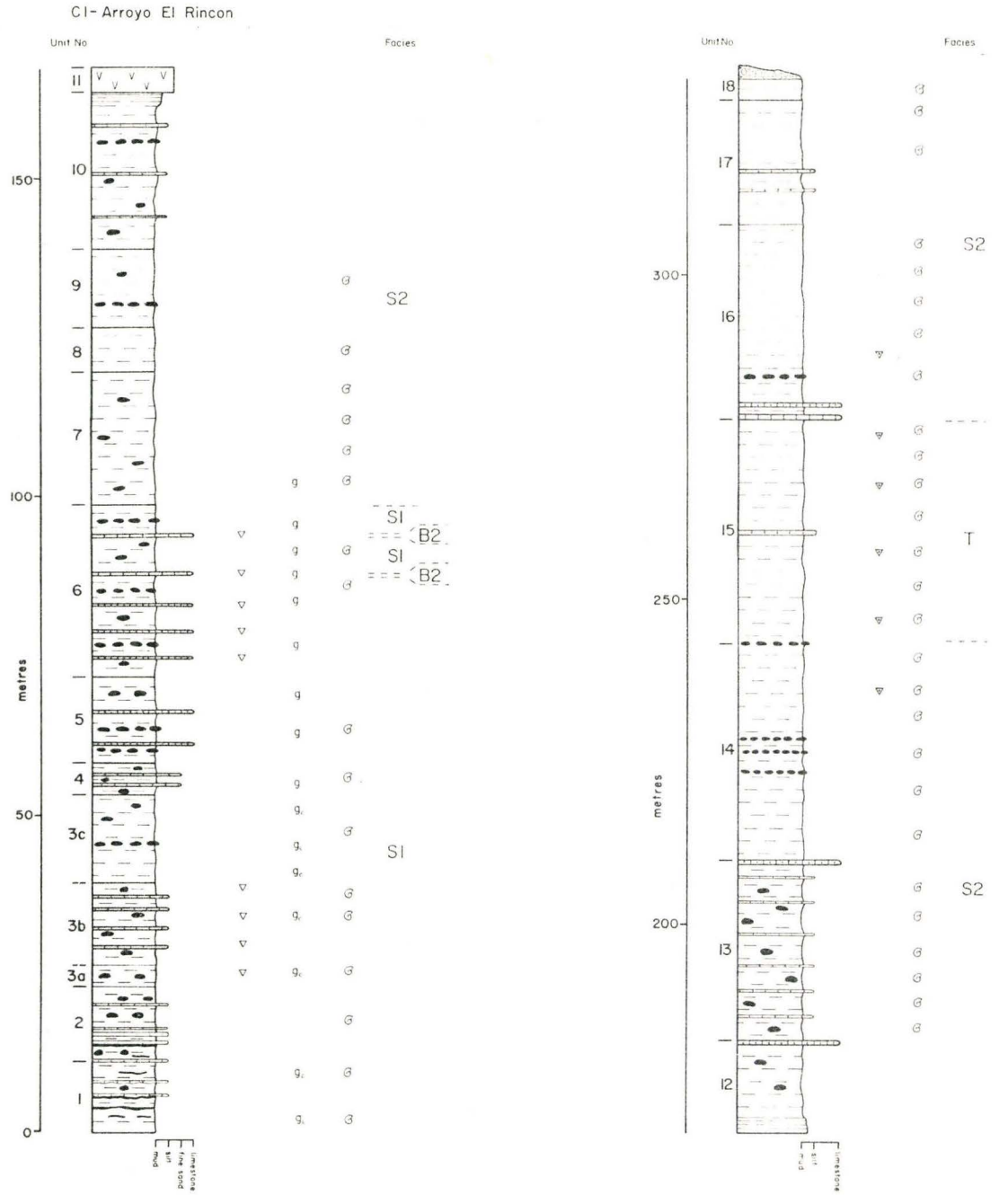
C1- Arroyo El Rincon
Unit No
Facies
metres
0
50
100
150
200
250
300
11
10
9
8
7
6
5
4
3c
3b
3a
2
1
12
13
14
15
16
17
18
S2
S1
B2
T
mud
silt
fine sand
limestone

Figure 2.6: Lithofacies and fauna of Section C2-Arroyo El Campamento.

C2- Arroyo El Campamento

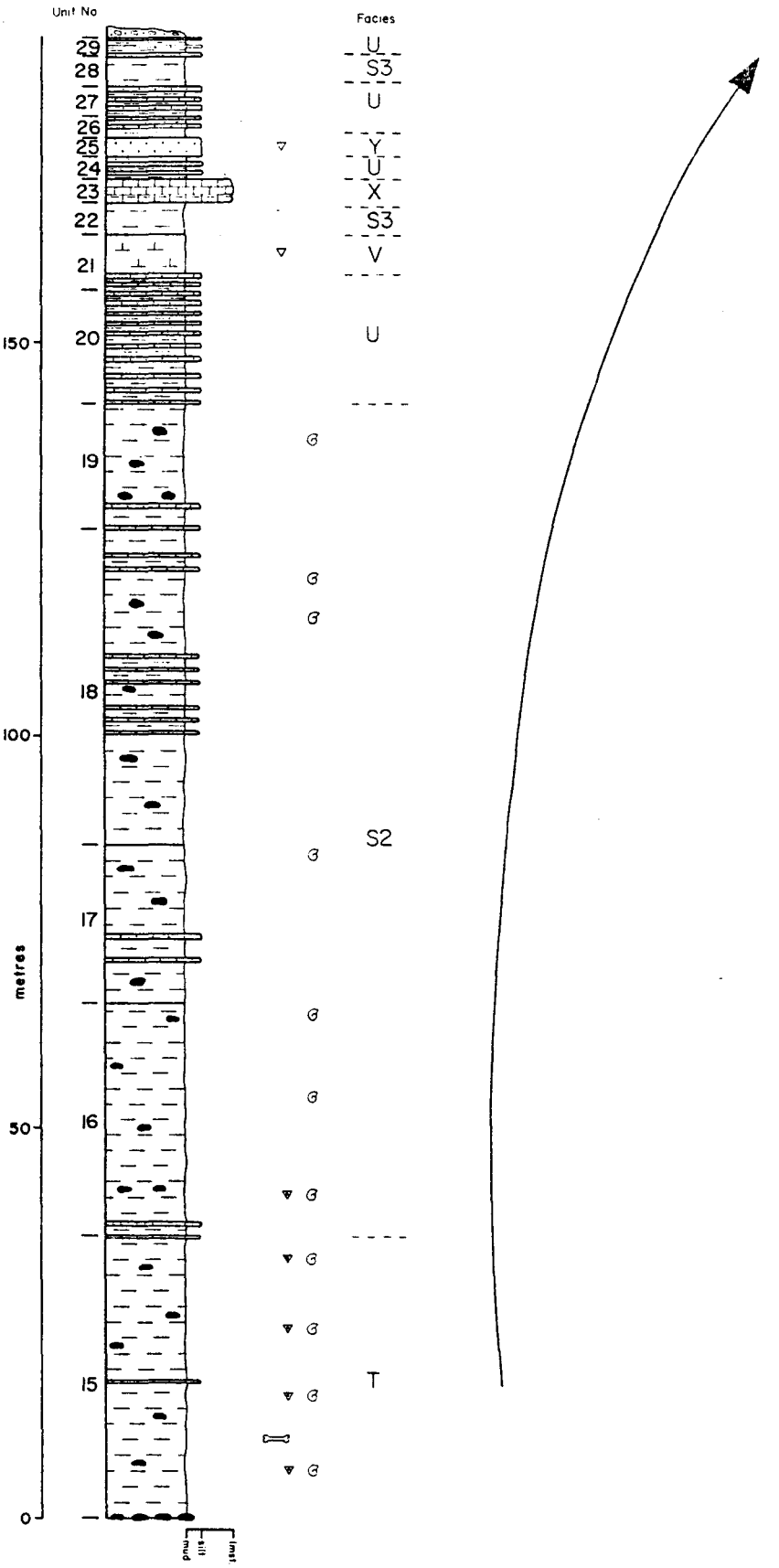

Plate 2.1: Subfacies A1. Unit 2, Section C3. A sandstone interbed is in the lower left foreground.

beds. Normal grading is observed in some sandstone beds. Many of the sandstone and siltstone beds are characterised by broad swales and hummocks, with low-angle intersections of laminae. The hummocks range in amplitude from 10-20 cm with wavelengths on the order of 1.2-2.0 metres. Upper surfaces of the sandstone and siltstone interbeds often contain Chondrites and Planolites feeding traces. Sedimentary structures, in more massive sandstone and siltstone beds, are often obliterated by extensive bioturbation. Two subfacies have been distinguished primarily on the basis of fossil content.

SUBFACIES A1: FOSSILIFEROUS SANDSTONES, SILTSTONES, AND SHALES

Subfacies A consists of buff-coloured interbedded sandstones, siltstones and shales. The sandstone to siltstone to shale ratio is approximately 2.5:1:15. Siltstones decrease in abundance upwards and are completely replaced by sandstones at the top of the subfacies. Subfacies A is well exposed at Alto de Teeolutla (Section C3, Units 1-3, 6) and comprises approximately 135 metres of outcrop.

The sandstone and siltstone beds range in thickness from 0.5 to 1.0 m. Shale beds range in thickness from 0.6 to 5.0 metres. Limey-ferruginous concretions, 2.0-10.0 cm in diameter, are found within some shale beds. Grain size of the sandstones ranges .25 -.125 mm (2.0-3.0 Ø).

Siltstone grain size ranges .0625-.031 mm (4.0-5.0 ∅).

The distinguishing feature of Subfacies A1 is its rich faunal assemblage consisting of bivalves, brachiopods, oysters, gastropods, and ammonites. Preservation of all fossils is excellent, with most bivalves and brachiopods still articulated. Disarticulated valves, which account for less than 20% of the total valves, occur almost exclusively in the sandstones and siltstones. Bivalves appear in all lithologies, while brachiopods and gastropods appear almost exclusively in the shales. Ammonites are found only in the shales. The fossil taxa are listed in the pelecypod listing of Sections 4.1 and 4.4.

SUBFACIES A2: NON-FOSSILIFEROUS INTERBEDDED GREY SHALES AND SANDSTONES

Subfacies A2 consists of non-fossiliferous medium grey shales with medium- to fine-grained sandstone interbeds (Plate 2.2). Some shale beds are silty. Total thickness of Subfacies A2 is 10 m and 4 m respectively in Units 14 and 17 of Arroyo Tecocoyunca (C4). The shale to sandstone ratio is approximately 1:1 but the sandstone beds thicken and increase in abundance upward within the subfacies.

Basal and upper bounding surfaces of Subfacies A2 are sharp and distinct. Sandstone interbeds are 10-30 cm thick. Grain size of the sandstones is .25-.08 mm (2.0-3.5 ∅).

The distinctive characteristic of Subfacies A2 is the

Plate 2.2: Subfacies A2. Unit 17, Section C4. Interbedded, non-fossiliferous grey shales and sandstones.

absence of macrofossils.

INTERPRETATION

Facies A is an association of shales with interbedded erosive, sharp-based sandstones and siltstones. The sharp-based character implies episodic emplacement which was capable of scouring into pre-existing shales. Parallel lamination within the sandstones and siltstones also suggests high velocity flows. Facies A was most likely deposited in a quiet nearshore marine environment. Mud accumulation in the low energy environment was interrupted episodically by sediment-laden gradient currents generated by storm and/or ebb currents (Aigner, 1985).

Sandstone and siltstone beds containing hummocks and swales may be interpreted as hummocky cross stratification (HCS) formed by reworking of sands below fairweather wave base by storm waves (Dott and Bourgeois, 1982; Walker, 1984). The presence of wave ripples on the upper surfaces of these beds could also be attributed to storm waves touching the bottom.

The fossil assemblage of Subfacies A1 is typical of a nearshore, open marine environment with normal to brackish salinities. The excellent preservation of the fossils and predominance of articulated shells indicates rapid sedimentation with little reworking of sediments. Shell fragments and disarticulated shells within the sandstone and siltstone beds indicates transport by currents.

In summary, Facies A appears to have been deposited in a quiet offshore marine environment below fairweather wave base (10-20 m) but within storm wave base.

2.3 FACIES B: LIMESTONES

Facies B consists of slightly arenaceous medium to coarsely crystalline, fossiliferous, grey limestone. In outcrop, they often display a patchy colour due to iron staining. No sedimentary structures are apparent. The tabular geometry of the beds is accentuated by sharp erosional bases and abrupt planar upper surfaces. Unsorted and randomly oriented fragments of gastropods, bivalves, brachiopods, bryozoans, and ostracods are abundant. The thickness of Facies B ranges from 0.4 to 2.4 metres. Three subfacies can be distinguished based on the carbonate rock classification scheme of Folk (1962). Examples of each subfacies are given but occurrences of Facies B are too numerous to list.

SUBFACIES B1: BIOSPARITES

Subfacies B1, grey biosparite, is the dominant subfacies. It contains abundant shell fragments (1.5-7.0 mm) cemented by coarsely crystalline (.25-.5 mm) sparry calcite. Spar cement accounts for approximately 85 %, fossil fragments 5-20 %, and silts 1-5 %. Microstylolites are present as a result of pressure solution. Exposures of Subfacies B1 are located in Units 1 and 4 of the Alto de

Teeolutla section (C3) with total thickness of 1.2 and 2.4 m respectively.

SUBFACIES B2: BIOMICRITES

The grey biomicrites contain shells and shell fragments ranging in size from .25 to 7.0 mm cemented by micrite and sparry calcite. The shell component accounts for 10-20 % of the total volume. The sparry calcite occurs as void infills and crystal sizes range from .15 to .6 mm. The micrite to spar cement ratio is 3:1. Subfacies B2 is exposed as a .4 m thick bed in Unit 6 of the Arroyo El Rincon section (C1).

SUBFACIES B3: BIOPELMICRITES

The biopelmicrites are composed of 75 % pelmicrite, and 25 % calcite spar which cements shell and shell fragments 0.2-2.0 mm in size. Shells account for less than 10 % of the total rock volume. Subfacies B3 is exposed in Arroyo Tecocoyunca (C4, Unit 8) and its thickness is .6 m.

INTERPRETATION

Facies B is an association of fossiliferous limestones differentiated by the cement type. The sharp erosive bed contacts, combined with the fragmented and unsorted nature of the shells, is suggestive of episodic emplacement. Facies B is interbedded with shales, suggesting deposition in a basinal environment below fairweather wave base. Storm waves most likely eroded shallow nearshore deposits rich in fauna, transferring them as shell layers into deeper basinal regions (Aigner, 1985).

2.4 FACIES C: BIOTURBATED LIMEY SILTSTONE

Facies C is a green limey siltstone, approximately 5.0 m in total thickness. It is exposed at Alto de Teeolutla (Section C3, Unit 5). The siltstone is massive and structureless due to intense bioturbation, but has sharp upper and lower bounding surfaces. Primary sedimentary structures have not been preserved. Grain size ranges from .0625 to .031 mm (4.0-5.0 ∅). Bivalves and brachiopods are prevalent, bivalves being the most abundant.

INTERPRETATION

The silt sediments within Facies C were favourable for colonization and bioturbation by bivalves and brachiopods. Confinement of Facies C above and below by Facies A suggests deposition below fairweather wave base.

2.5 FACIES D: INTERBEDDED SILTSTONES AND SANDSTONES

Facies D is well exposed at Alto de Teeolutla (Section C3, Unit 7a) and is approximately 11 m thick. This facies consists of buff-coloured interbedded medium sandstone and siltstone. Sandstone to siltstone ratio is approximately 1.5:1. The sandstones increase slightly in abundance and thicken upward within Facies D.

Sandstone beds are 1.2-1.6 m thick. The beds are sharp-based and occasionally show undulatory scouring into underlying siltstones. Upper bounding surfaces are planar, often bioturbated and sometimes scoured into by overlying

beds. Symmetrical wave ripples with amplitudes of 1-2 cm and wavelengths 5-10 cm are seen on some upper bedding surfaces. Parallel lamination is common in the basal portion of sandstone beds. Some of the more massive sandstone beds appear to have been extensively bioturbated. The uppermost sandstone bed within Facies D contains a sparse basal lag of rounded pebbles 1-1.5 cm in diameter. Grain size of the sandstones ranges from .35 to .25 mm (1.5-2.0 ∅).

Siltstone beds range from 0.6 to 1.4 m thick and often have erosional bases and tops. The siltstones are structureless and pervasively bioturbated. The lowermost siltstone bed has shale horizons and partings. Grain size of the siltstones is .06-.04 mm (4-4.5 ∅).

Facies D contains a meager bivalve fauna consisting mostly of oysters. A few vertical dwelling burrows Skolithos and Monocraterion are found in the lower half of Facies D but they disappear almost entirely toward the top.

INTERPRETATION

Facies D is an association of interbedded, erosionally bedded siltstones and sandstones which are parallel laminated but often bioturbated. This is typical of lower shoreface environments (McCubbin, 1982; Reinson, 1984). The erosional nature of bedding surfaces in Facies D is similar to that described by Howard (1972) for lower shoreface sediments. Such erosion was most likely the result of

high-energy conditions such as storms (Aigner, 1985).

The trace fossils belong to the Skolithos ichnofacies typically associated with shifting substrates in a moderate to high-energy lower littoral/infralittoral environment (Frey and Pemberton, 1984). Upwardly decreasing abundance of traces within this facies is typical of the lower shoreface (Howard, 1972).

Facies D is interpreted to have been deposited in a lower shoreface environment under the influence of high-energy conditions such as storms.

2.6 FACIES E: BLOCKY SANDSTONE

Facies E is a clean, well sorted, light buff-coloured sandstone. It is 6.8 m thick at Alto de Teeolutla (Section C3, Unit 7b).

The base of this facies is sharp, erosional and slightly undulatory. A basal lag of 1.0-1.5 cm pebbles is also present. Individual beds average 10-30 cm in thickness and are distinguished from other beds by erosional bounding surfaces. Sediment grain size ranges from .4 to .25 mm (1.25-2.0 Ø) and coarsens upward within the facies.

Facies E contains several physical sedimentary structures which include planar parallel lamination, planar tabular cross- bedding and symmetrical wave ripples. Planar parallel lamination is prevalent and occurs in low-angle wedge-shaped sets. Individual laminae are 2-5 cm thick.

The wedge-shaped sets are the result of planar erosion surfaces which truncate the lamination. Tabular cross-bedding (foreset angle = 20 degrees) occurs as 8-10 cm sets with slightly asymptotic foreset toes. The sets are interbedded with horizons of planar parallel lamination and comprise 30 to 50 percent of Facies E. Foreset orientation indicates deposition by currents trending along the strike of the planar parallel sets. Symmetrical wave ripples with amplitudes of 1-2 cm and wavelengths 5-10 cm are sometimes seen on the upper surfaces of planar parallel and cross-bedded sets.

Macrofossils are absent except for a few disarticulated bivalves associated with the basal pebble lag. Sparse Skolithos burrows are occasionally observed in the upper portion of planar parallel laminated sets. The burrows are often truncated by planar erosion surfaces of overlying beds.

INTERPRETATION

The blocky sandstone of Facies E is characterised by low- angle wedge-shaped sets of planar lamination, some planar tabular cross-beds and symmetrical wave ripples. The planar laminated sets and wave ripples are the result of fairweather waves reworking the sands (Clifton et al., 1971; Harms et al., 1975). Wave ripples can also be attributed to wave reworking. Orientation of the tabular cross-bedded sets suggests deposition by longshore currents. The paucity

of biogenic structures and macrofossils is typical of the upper shoreface (Howard, 1972).

The types and predominance of sedimentary structures suggest that this facies E was deposited within an upper shoreface environment (Howard, 1972; McCubbin, 1982; Reinson, 1984).

2.7 FACIES F: PLANAR LAMINATED SANDSTONES

The planar laminated sandstones composing Facies F are clean and well sorted. This facies is well exposed at the base of the Arroyo Tecocoyunca (Section C4, Units 1, 4a, 5, 8, 15, and 18) (Plate 2.3). Total thicknesses are 1.9, 1.6, 1.0, 1.6, 2.1, and 2.0 m in Units 1, 4a, 5, 8, 15, and 18 respectively.

The base of Facies F is sharp and erosional, and often contains a pebble lag. The upper bounding surface is abrupt and is sometimes characterised by many Monocraterion burrows (Plate 2.3). Gently dipping planar subparallel laminae averaging 0.3-1.0 cm in thickness compose the entire facies (Plates 2.4, 2.5). The laminae occur as wedge-shaped sets occasionally bounded by high-angle planar truncation sets. Other set boundaries are non-erosional but display a gradual change in the bedding angle. Set thicknesses average 5-40 cm. Grain size range is .35-.5 mm (1.5-1.0 ø), while pebbles from the lags average 1.0-1.5 cm.

A scour-like feature measuring .75 m in depth and 2.0 m

Plate 2.3:

Bedding plane exposure of Facies F. Unit 1, Section C4. The indentations on the upper bedding surface are Monocraterion.

Plate 2.4:

Planar parallel lamination (swash cross stratification) within Facies F. Unit 1, Section C4.

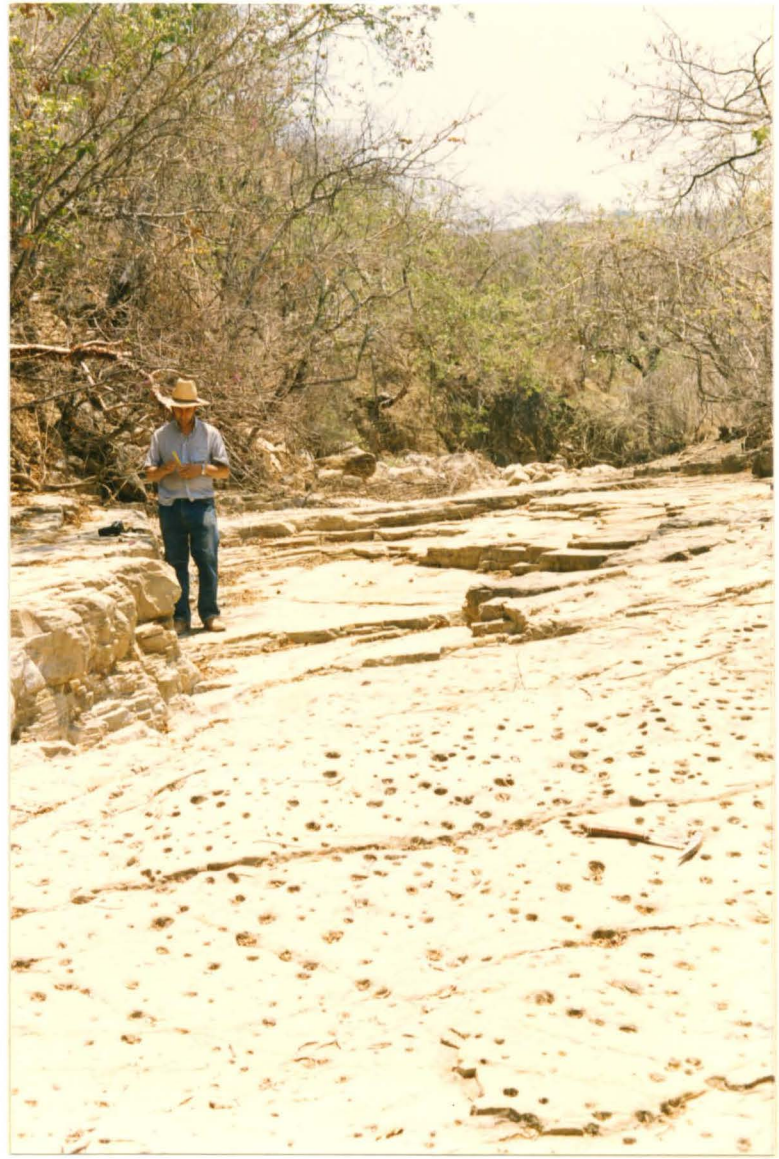

Plate 2.5: Gently dipping swash cross stratification of Facies F, Unit 4a, Section C4.

Plate 2.6: A channel-form scour incised into the top of Facies F (near hammer handle), Unit 8, Section C4.

in width is located in the upper portion of this facies in Unit 8. It displays a channel form in cross section. Infilling laminae within the scour are thickest (2-5 cm) in the bottom of the scour but thin toward the margins where they drape the sides (Plate 2.6). Scours are found almost exclusively in the uppermost portion of Facies F, and are oriented perpendicular to the gently dipping subparallel lamination. Similar smaller structures are also seen in the upper portion of Unit 1.

Only trace fossils are present in Facies F. Monocraterion occur in the uppermost 15 cm of the facies, where they are present in high densities (as many as 125/m^2 in Units 1 and 15). Some coalified pieces of driftwood, 5-30 cm in size, are frequently found on bedding surfaces of Facies F.

INTERPRETATION

The low-angle wedge-shaped sets of planar parallel lamination may be interpreted as swash cross stratification formed within the wave swash zone of the foreshore (Harms et al., 1975). The wedge-shaped characteristic of the lamination is thought to be the result of changing slope of the beachface with varying wave conditions (McCubbin, 1982). Planar erosional surfaces which truncate the lamination may be attributed to storms which eroded the beach episodically.

A lack of macrofossils and biogenic structures is

typical of the foreshore (Howard, 1972). Monocraterion burrows most likely formed slightly seaward of the foreshore. Their high density is generally associated with a few metres of water depth rather than the swash zone (Dr. M. J. Risk, pers. comm.).

The scour features within Units 1 and 8 may be interpreted as rip-current channels, based on their position and orientation within the swash zone sands (Reineck, 1973).

Facies F is interpreted to represent a foreshore beach deposit which was periodically eroded by storm waves.

2.8 FACIES G: LOW-ANGLE INCLINED STRATIFICATION

Facies G is a buff-coloured, very fine-grained sandstone which is dominated by low-angle stratification. It occurs in Arroyo Tecocoyunca (Section C4, Units 2, 3) where its total thickness is 11 m. This facies contains approximately 65 % swales, 20 % subparallel lamination, 10 % bioturbated horizons, and 5 % upward curving hummocks. The basal and upper bounding surfaces of Facies G are well defined, but not sharp. Grain sizes range from .088 to .125 mm (3.5-3.0 ø).

The swales within Facies G can be described as a mutually intersecting stacked sequence (Plate 2.7). Bed thickness ranges from 5 to 15 cm. The dominant sedimentary structure within these beds is low-angle inclined stratification. The swales have wavelengths of

Plate 2.7: Low-angle inclined stratification in Facies G. Note the bioturbated and planar laminated horizons.

approximately 1.0-1.5 m and amplitudes of 7-12 cm. The sedimentary structure contained within these swales is referred to as low-angle ($<10^{\circ}$) inclined stratification. The laminae composing the stratification are 2-5 m in thickness and conform to the concave-upward lower bounding surfaces of the swales. The laminae are often found gradually flattening upwards, creating gently undulating subparallel stratification between the erosional surfaces. The swales within Facies G may be characterised by the following features: (1) swales become shallower and beds thin upwards, (2) shale beds are absent throughout, and (3) the stratification appears identical in all vertical orientations. Bioturbated beds commonly occur as laterally continuous horizons 10-15 cm thick at the top of the swaley units.

The hummocks within Facies G are found randomly distributed between swales. They have amplitudes of 5-10 cm and wavelengths of 1.5-2.0 m. Several large planar erosional surfaces which truncate all of the previously mentioned structures occur in the lowest part of Facies G.

Macrofossils are rare in Facies G, but some fragmented bivalve shells, namely oysters are present.

INTERPRETATION

Stratification of Facies G closely resembles swaley cross stratification (SCS), a storm-dominated structure formed in shallow water above fairweather wave base (Leckie

and Walker, 1982). The stratification of Facies G differs slightly from SCS described by Leckie and Walker (1982) in that it lacks the significant amounts of subparallel stratification.

Planar truncation surfaces may be attributed to storm erosion of the nearshore profile (McCubbin, 1982). Organisms were able to pervasively bioturbate the sediment during slack periods of storm activity.

Facies G is interpreted to have been deposited in a storm-dominated nearshore environment above fairweather wave base i.e. upper shoreface. Storm activity was so prevalent as to exclude the sedimentary record of fairweather processes and a major portion of the bioturbation usually associated with such an environment (Walker, 1982; Howard, 1972).

2.9 FACIES H: PARALLEL LAMINATED, TABULAR, AND TROUGH CROSS-STRATIFIED SANDSTONES

Facies H consists of clean, well sorted, buff-coloured sandstones dominated by sets of parallel lamination, tabular cross stratification and trough cross stratification. Exposures are found in Units 4b, 5, 6 and 7 of Arroyo Tecocoyunca (Section C4). Thicknesses are 2.0, .8, 1.4 and 1.2 m respectively.

Basal and upper bounding surfaces of Facies H are distinct. Individual beds range from 10 to 40 cm in

thickness. Grain size is .25-.35 mm (2.0-1.5 ø). All sedimentary structures are stacked and amalgamated but laterally continuous (Plates 2.8, 2.9). Equal proportions of all three sedimentary structures are present.

Parallel laminated beds, 10-20 cm thick, consist of laminae averaging .5-1.2 cm in thickness. Planar tabular cross- stratified beds average 10-20 cm thick (Plate 2.8). The beds have planar bounding surfaces and the planar foreset laminae intersect the bottomset at an angle of 22-25 degrees. Paleocurrent measurements made on the foresets indicate deposition parallel and perpendicular to the strike of the planar parallel laminated sets.

Three-dimensional exposure allows both longitudinal and transverse views of the trough cross-bedding (Plate 2.9). Longitudinal views appear as wedge-shaped sets each with a concave-upward lower bounding surface. Individual laminae, 1-3 cm thick, intersect at a low angle and asymptotically with the lower bounding surface of each set. Transverse views display a series of troughs which scour into one another. Laminae conform to the lower bounding surfaces of the troughs. Individual troughs average 1-2 m long and .4-.8 m wide. Trough cross-stratified beds are often not laterally extensive for more than 10-15 metres, but occur as packages which scour downward and laterally into planar parallel stratified sandstones. Paleocurrent measurements illustrate that the long axes of the troughs trend

Plate 2.8: Parallel laminated, planar tabular and trough cross-stratified sandstone of Facies H. Unit 5, Section C4.

Plate 2.9: Trough cross stratification within Facies H. Unit 7, Section C4.

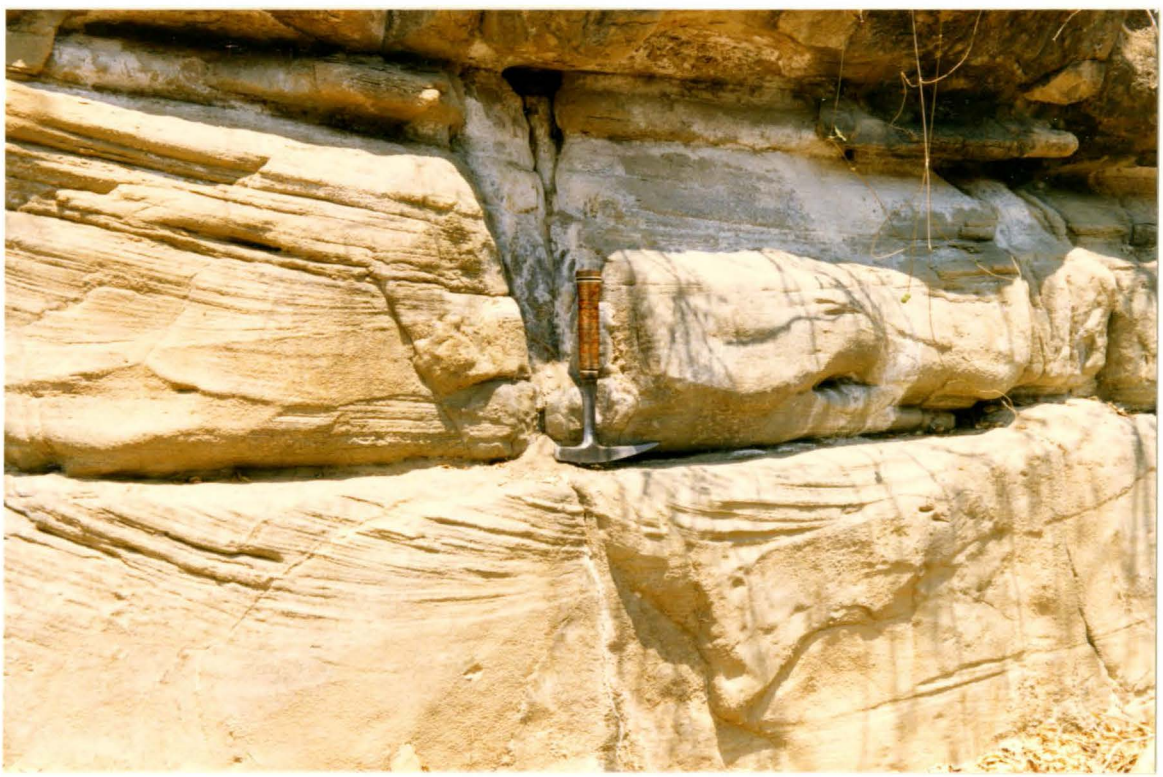

approximately perpendicular to the strike of the planar parallel lamination, but some horizons have randomly oriented troughs.

Macrofossils and bioturbation are absent in this facies.

INTERPRETATION

The sandstones of Facies H were most likely deposited in a relatively shallow nearshore environment dominated by fairweather processes. Planar parallel lamination can be attributed to fairweather wave action (Clifton et al., 1971). Planar tabular cross-bedding was formed by low amplitude (10-20 cm) straight-crested sand waves migrating parallel and perpendicular to shore by longshore currents and rip-currents respectively (Davidson-Arnott and Greenwood, 1976; Hunter et al., 1979). Trough cross-stratified sands resulted from the migration of sinuous crested dunes (Harms et al., 1975). Trough cross stratification is often multi-directional in the upper shoreface (Clifton et al., 1971). Longshore currents develop in the surf zone by wave action and may produce trough cross stratification by the migration of lingoid megaripples (Reineck, 1973).

Other characteristics suggestive of an upper shoreface environment are: (1) domination of fairweather processes, (2) absence of body fossils and ichnofossils due to high energy conditions and shifting substrates, (3) clean, well

sorted coarse sediments, and (4) close proximity to Facies F beach sediments (Howard, 1972; Davis and Hayes, 1984).

2.10 FACIES I: GREENISH-GREY SANDSTONE WITH LIMESTONE INTERBEDS

Greenish-grey coloured very fine sandstones with silty limestone interbeds are exposed in Arroyo Tecocoyunca (Section C4, Unit 9) and have a total thickness of 3.8 m. The sandstone to silty limestone ratio is approximately 2:1.

The lower bounding surface of Facies I is sharp, whereas the upper bounding surface is gradational. The siltstones are poorly and thinly bedded with individual beds ranging from 2 to 5 cm in thickness. Some horizons are pervasively bioturbated and others contain limey-ferruginous concretions 2-5 cm in diameter.

Limestone interbeds are 15-30 cm thick and characterised by sharp erosive bases. The interbeds are silty and highly fossiliferous with a large component of disarticulated shells and shell fragments. These limestones are similar to Facies B, Subfacies B1.

The bivalve Anisocardia is found in the siltstones and was probably responsible for much of the bioturbation. Unidentifiable shell fragments are abundant in the limestone interbeds.

INTERPRETATION

Facies I is interpreted as being deposited in a shallow

nearshore environment of intermediate water depth. Bioturbating activities of the fauna partially obliterated the record of fairweather processes. Limestone interbeds are probably the result of storm-winnowed shell layers (Aigner, 1985).

The lithology and biological characteristics of this facies are typical of a lower shoreface environment (Howard, 1972; Reineck and Singh, 1980).

2.11 FACIES J: HUMMOCKY CROSS-STRATIFIED SANDSTONE

Facies J consists of 4.6 m of greenish-grey amalgamated hummocky cross-stratified sandstones (Plate 2.10). The sandstone grain size is fine sand verging on coarse silt (.08-.05 mm) (3.5-4.25 $\emptyset$). These sandstones are exposed in Unit 10, Arroyo Tecocoyunca (Section C4).

Facies J sandstones occur as stacked fining-upward sets which range in thickness from 20 to 50 cm. The bases of these sets show erosive scouring into underlying sandstones. The tops typically contain a 5-15 cm thick horizon of bioturbation, while some show no bioturbation due to deeper scouring of overlying sandstones.

Primary sedimentary structures include approximately 30 percent planar parallel lamination and 50 percent low-angle inclined hummocky beds. Broad upward curving hummocks with amplitudes of 10-20 cm and wavelengths of 1.0-1.5 m occur in sets 10-50 cm thick. Laminae within the hummocks average

Plate 2.10: Amalgamated hummocky cross-stratified sandstone in Facies J. Unit 10, Section C4.

Plate 2.11: Facies L interbedded siltstones and sandstones. Unit 12, Section C4.

2-5 cm in thickness and form low-angle (10°) intersections with adjacent stratification. Within this facies, the hummocky beds are characterised by a lack of shale partings and the amalgamation of hummocks. Often a bioturbated horizon containing Chondrites and Planolites distinguishes the separation between sets of hummocks. Planar parallel lamination occurs in beds 10-25 cm thick and overlies the hummocky beds.

A sparse fauna of the bivalve Anisocardia occurs within the hummocky beds and bioturbated horizons. Carbonaceous plant fragments 1-5 mm in size are abundant and disseminated throughout the sandstones of Facies J.

INTERPRETATION

Similar sedimentary structures to those of Facies J were interpreted by Walker (1982) as amalgamated hummocky cross stratification (HCS). Occurrences of amalgamated HCS sandstones have previously been interpreted as rapidly emplaced storm deposits (Dott and Bourgeois, 1982; Walker et al., 1983). These authors also suggest that amalgamated HCS beds may indicate intense and/or frequent storm events. This implies close proximity to shore in shallow water depths below fairweather wave base (10-20 m) but above storm wave base (Dott and Bourgeois, 1982).

2.12 FACIES K: TROUGH CROSS-BEDDED SANDSTONES WITH SILTY LIMESTONE INTERBEDS

Greenish-grey, fine-grained sandstones with silty limestone interbeds have a total thickness of 5 m in Unit 11 of Arroyo Tecocoyunca (Section C4). The sandstones are five times more abundant than the limestones.

The sandstones contain a series of small-scale troughs with concave-upward lower bounding surfaces which scour into one another. Laminae conform to the lower bounding surface and average 1-2 mm thick. Individual troughs range 2-10 cm deep and 10-20 cm wide. Grain size of the sandstone is .08-.125 mm (2.5-3.0 ø).

Some Anisocardia bivalves are present in the basal 80 cm of Facies K. Disseminated plant fragments are found scattered throughout the sandstones.

The silty limestone interbeds range from 10 to 30 cm thick and have sharp erosional bases. They are packed with fossil fragments and are similar to those described in Subfacies B1.

INTERPRETATION

The small-scale trough cross-bedded sandstones of Facies K are the result of migrating megaripples (Harms et al., 1975). Dimensions of the troughs and their orientation perpendicular to shore are similar to the trough cross-bedding of the Lunate Megaripple (outer rough) facies described by Clifton et al. (1971) and Davidson-Arnott and Greenwood (1976). This facies occurs in the wave build-up zone (2-5 m water depth) of the lower to middle shoreface

(Clifton et al., 1971).

The silty limestone interbeds in this facies were most likely deposited episodically as storm-winnowed shell layers (Howard and Reineck, 1972).

2.13 FACIES L: GREENISH-GREY SILTSTONES AND SANDSTONES

Greenish-grey siltstones with interbeds of sandstone total 3.8 m in thickness in Unit 12 of the Arroyo Tecocoyunca section (C4). The siltstone to sandstone ratio is about 1.5:1 (Plate 2.11).

The base of Facies L is sharp but undulatory. Siltstone beds are 30-130 cm thick, poorly bedded and often pervasively bioturbated. Grain size is .06-.05 mm (4-4.25 ø).

Sandstone interbeds range in thickness from 15 to 35 cm. They typically have erosional bases which are undulatory and often scour into underlying siltstones. The upper surfaces of the interbeds are often bioturbated. Planolites and Chondrites are common. The sandstone interbeds are parallel laminated with individual laminae averaging 1-3 mm thick. Grain size range is .08-.12 mm (3.5-3.0 ø).

Facies L is unfossiliferous except for a 15 cm thick oyster coquina bed which has an erosional base scouring into underlying siltstones. Disseminated carbonized plant fragments, 1-5 mm in size, are abundant.

INTERPRETATION

The interbedded siltstones and sandstones of Facies L seem to have been deposited in the nearshore environment of the lower shoreface. The lithology, grain size, and prevalence of bioturbation support this interpretation (Howard, 1972; Howard and Reineck, 1972). Storm and ebb currents were capable of sweeping sand and silt from nearshore areas and transporting it seaward (Reineck et al., 1967). The oyster coquina bed was deposited episodically as a storm-winnowed shell layer (Howard and Reineck, 1972; Aigner, 1985).

2.14 FACIES N: PARALLEL LAMINATED, TABULAR CROSS-BEDDED, AND HUMMOCKY CROSS-STRATIFIED SANDSTONES

The blocky, buff-coloured, fine-grained sandstone is characterised by sequential beds of subparallel lamination, planar tabular cross-bedding, and hummocky cross stratification (Plates 2.12, 2.13). All beds are laterally continuous for several tens of metres but are vertically separated by silty clay drapes. Total thickness of this facies is 4.3 m as exposed within Unit 16 of Arroyo Tecocoyunca (C4). Facies N sandstones are clean with well sorted and rounded grains.

The base of this facies N is sharp but undulatory and appears to be erosional. The upper bounding surface is planar and abrupt. The basal 1.5 m of Facies N is massive

Plate 2.12: Facies N is characterised by beds of subparallel lamination and hummocky cross stratification separated by silty drapes. Unit 16, Section C4.

Plate 2.13: A closer view of stratification in Facies N.


16

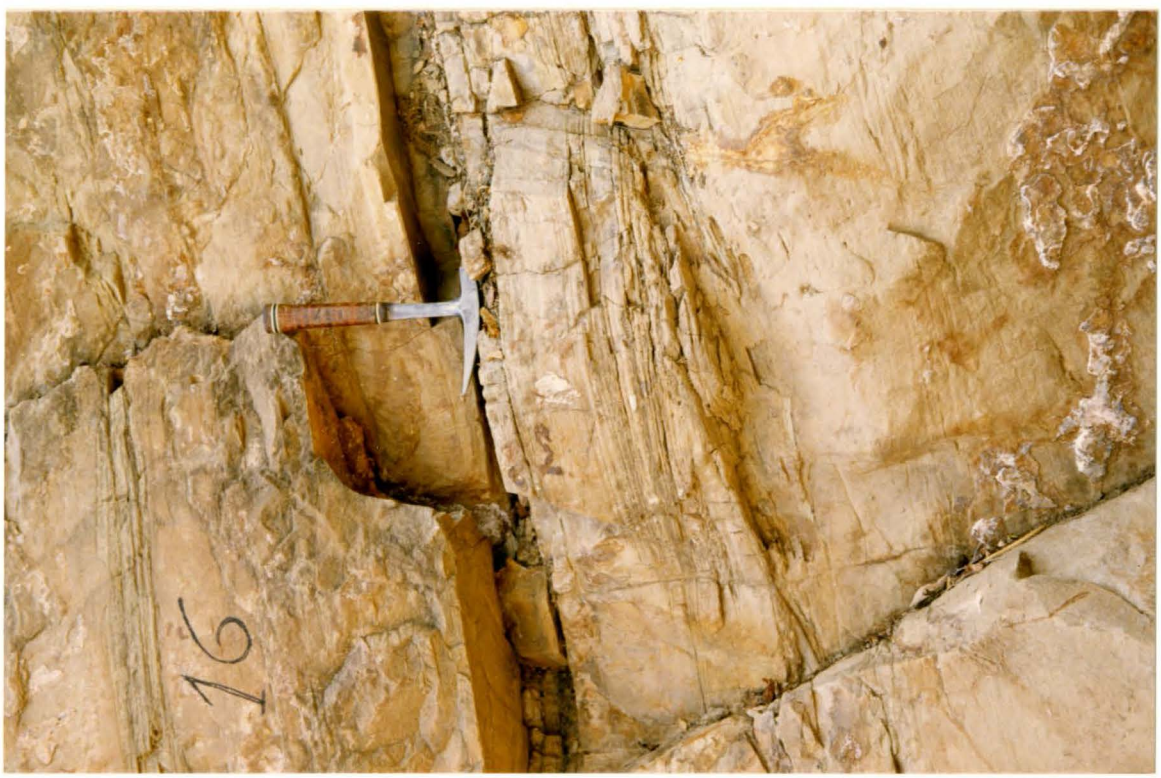
16

and contains parallel to subparallel lamination. Individual laminae are .5-1 cm thick. All sedimentary structures form distinct sets stacked upon one another but often separated by the thin silty clay drapes. Grain size of Facies N ranges from .125 to.18 mm (3.0-2.5 ∅).

Several sandstone beds contain broad hummocks and swales with amplitudes of 20-30 cm and wavelengths of 2.0-2.5 m. Laminae within the hummocks form low-angle intersections (10°) with adjacent stratification (Plate 2.12, 2.13). Silty clay often drapes the hummocks and swales to thicknesses of 2-8 cm. Drapes often show subparallel lamination. Some of the upper surfaces of hummocks and silty clay drapes are bioturbated. Planolites and Chondrites are common.

Planar tabular cross-bedding occurs in 10-20 cm thick sets with planar foresets intersecting the bottomset at an angle of 22-25 degrees. Such sets are observed in the upper 2.5 m of Facies N, interbedded with parallel lamination and hummocky beds. Paleocurrent orientation of the planar tabular cross-bedding is perpendicular to the dip of Facies F beach sediments. Parallel laminated beds averaging 15-30 cm thick are seen interbedded with other sedimentary structures in the upper 2.5 m of Facies N.

Body fossils are absent whereas trace fossils are common in some horizons. Skolithos and Monocraterion occur within the massive and parallel laminated sandstones of the

lowermost 1.5 m of Facies N. Chondrites and Planolites are often observed on the upper surfaces of hummocks and within the silty clay drapes.

INTERPRETATION

The sedimentary structures within Facies N suggest deposition in a shallow nearshore marine environment. The massive parallel laminated sandstones at the base of facies N were most likely deposited in the lower shoreface under the influence of fairweather waves (Clifton et al., 1971). Constantly shifting substrates deterred fauna except for marine worms and sea anenomes which constructed dwelling burrows of the Skolithos ichnofacies.

The overlying hummocky beds suggest slightly deeper water and may be interpreted as hummocky cross stratification (HCS) formed below fairweather wave base (10-20 m) by storm waves (Walker, 1984). Silty clay draped the hummocks and swales during lulls in storm activity. Marine worms colonized and bioturbated the upper portions of the HCS sands and silty clay drapes also during the quiescent periods.

Planar tabular cross stratification was formed by the migration of low amplitude (10-25 cm) straight crested sand waves within shore-parallel currents (Clifton et al., 1971; Parker, 1975; Reinson, 1984).

In summary, Facies N was deposited in a nearshore environment in water depths near fairweather wave base

(10-20 m).

2.15 FACIES P: INTERBEDDED SANDSTONE, SILTSTONE, SILTY SHALE AND COAL

Facies P consists of interbeds of grey sandstone, siltstone, silty shale, and coal (Plate 2.14). Total thickness is 11.4 m and this facies extends throughout Units 18 (upper 1.6 m) to 22 in the Arroyo Tecocoyunca section. Facies P is subdivided into five subfacies based on sedimentary structures and degree of bioturbation. Each subfacies has sharp upper and lower bounding surfaces due to erosion.

SUBFACIES P1: PLANAR TABULAR CROSS-BEDDED SANDSTONE WITH OYSTER COQUINID BEDS

Subfacies P1 is characterised by a 30 cm thick bed of planar tabular cross-bedding bounded erosionally above and below by 30 cm thick oyster coquinid beds (Liostrea). Foreset dip of the planar tabular cross-bedding is 25 degrees. Sandstone grain size is .25-.35 mm (2.0-1.5 Ø). Subfacies P1 occurs in the uppermost .9 m of Unit 18.

SUBFACIES P2: SILTY SHALES WITH SANDSTONE INTERBEDS

Grey silty shales with sharp, erosionally based interbeds of very fine sandstone compose Subfacies P2. The sandstone interbeds range from 10 to 40 cm in thickness and are dominated by planar parallel lamination. Macrofossils are absent. Total thickness is 4 m as exposed in Unit 19.

Plate 2.14: Interbedded sandstone, siltstone, shale, and coal of Facies P. Unit 20, Section C4.

Plate 2.15: Facies Q bioturbated carbonaceous siltstone. Unit 23, Section C4.

SUBFACIES P3: SANDSTONES AND COAL

Subfacies P3 has an upper sandstone bed .4 m thick and a lower planar laminated bed .3 m thick. These two sandstone beds are separated by a thin, 20 cm thick, coal bed. Total thickness of Subfacies P3 is 1.8 metres within Unit 20. Grain size of the sandstones is .25-.5 mm (2.0-1.0 ∅). The medium-grained grey sandstone is characterised by 25 cm thick sets of angle-of-repose planar tabular cross-bedding, 10-25 cm thick sets of planar parallel lamination and symmetrical wave ripples. Foreset dip is 22-25 degrees within the planar tabular cross-beds. The parallel lamination contains individual laminae which are 2-3 mm thick. Symmetrical wave ripples average 1-2 cm in amplitude and wavelengths of 5-10 cm.

Some surface traces of Planolites and Chondrites are seen on the upper bedding surface of Subfacies P3 but macrofossils are absent.

SUBFACIES P4: PERVASIVELY BIOTURBATED SANDSTONE

Subfacies P4 is a .2 m thick, pervasively bioturbated medium-grained sandstone exposed in Unit 21. Grain size is .25-.35 mm (2.0-1.5 ∅). The bivalve Anisocardia is very abundant and was probably responsible for the extensive bioturbation.

SUBFACIES P5: MASSIVE SANDSTONE

Subfacies P5 is a 2 m thick massive, fine-grained (.06-.125 mm; 4.0-3.0 ∅); grey sandstone in Unit 22. The

base is sharp and erosional. Bedding averages .5-2 cm in thickness. Some planar parallel lamination is seen but most was destroyed by bioturbation especially toward the top of the subfacies. Some Anisocardia bivalves are found within Subfacies P5 and their abundance increases upwardly within the sandstone.

INTERPRETATION

The association of thin beds of several interbedded lithologies is typical of lagoonal sequences with a number of overlapping subenvironments (McCubbin, 1982; Phleger, 1969; Schwartz, 1975; Leatherman, 1981). The abundance of plant debris supports this interpretation and indicates a proximal marsh environment (McCubbin, 1982).

The erosionally based siltstone and sandstone beds are interpreted as storm washover deposits emplaced episodically into a lagoon. Planar lamination and planar tabular cross-bedding observed within these beds are typical of washover deposits (Reinson, 1984; McCubbin, 1982; Schwartz, 1975). The horizontal planar lamination is formed during deposition by shallow flows above normal high tide (McCubbin, 1982). Medium-scale foreset stratification is formed as the washover fan builds into the shallow, standing water of the lagoon (Schwartz, 1975). Sand avalanches down the front of the washover fan in a 'Gilbertian' manner.

In summary, Facies F is an association of fine-grained

lagoonal sediments and coarser-grained interbeds deposited by storm washovers. Oyster coquinid beds are most likely winnowed storm washover deposits. Plant matter was supplied to the lagoonal environment from proximal marshes.

2.16 FACIES Q: CARBONACEOUS SILTSTONE

Facies Q is a bioturbated medium grey siltstone which contains abundant carbonaceous plant matter. Total thickness is 7.5 m and this facies is found within Unit 23 of the Arroyo Tecocoyunca section (C4) (Plate 2.15).

The base of Facies Q is gradational and the upper surface is covered by modern soil. The siltstone is poorly bedded due to extensive bioturbation. Grain size is .05-.06 mm (4.25-4.0 Ø).

Carbonaceous plant fragments are copious and often form carbonaceous horizons and coal seams averaging 5-6 cm in thickness. Some plant fragments attain sizes up to 10 cm.

Facies Q also contains a large population of the bivalve Anisocardia which were presumably responsible for much of the bioturbation. Oyster shell fragments are common and randomly distributed throughout the siltstone.

INTERPRETATION

Facies Q may be interpreted as a mixed intertidal flat for several reasons: (1) high abundance of bivalves, (2) pervasive bioturbation, (3) apparent lack of tidal channel deposits, and (4) profusion of plant debris indicating

proximal marsh environments. Such characteristics have been extensively discussed by Weimer et al.(1982), Reineck (1972) and Ginsburg (1975).

2.17 FACIES R: BIOTURBATED DARK GREY SHALES

Thinly bedded bioturbated dark grey shales with interbedded siltstones, sandstones, and silty limestones are exposed in Arroyo Tecocoyunca (Section C4, Units 7_1, 7_2, 8_{14}-8_4). Total thickness is 38 metres. The ratio of shale to other lithologies is approximately 8:1.

Shale beds are thin (1-5 mm) but are often obliterated by extensive bioturbation. Some shale horizons contain sparse limey-ferruginous concretions which average 3-6 cm in diameter. All shales contain abundant carbonaceous plant debris, but some levels are extremely rich in plant debris often resulting in thin coal seams (e.g. Unit 8_6).

Sandstone and siltstone beds range from 2 to 90 cm in thickness and display sharp erosional bases. Little or no stratification is preserved within these beds due to varying degrees of bioturbation. Most interbeds are calcareous and contain abundant shell fragments which average 5-10 mm in size and are poorly sorted, but angular. Grain size is .1-.06 mm (3.25-4.0 ϕ) for the sandstones and .06-.04 mm (4-4.5 ϕ) for the siltstones.

Limestone interbeds, similar to those described in Facies B, are found randomly distributed throughout Facies

R.

The fauna of Facies R is abundant but low in diversity, consisting of the bivalve Anisocardia and the small gastropod Cryptalaux.

INTERPRETATION

Facies R appears to have been deposited by slow accumulation of mud in a low-energy, restricted, nearshore environment, probably a lagoon. Reinson (1984) noted that lagoonal sequences generally consist of interbedded shale, sandstone, siltstone, and coal facies due to overlapping of a number of subenvironments. Disseminated carbonaceous plant material and thin coal beds are common in the shales. This suggests interfingering of proximal marsh and subaqueous lagoonal environments (Reinson,1984). Coarser-grained sediments were most likely carried into the lagoon by storm wave activity and deposited as sharp, erosionally based beds in a manner similar to washover deposits (Leatherman, 1981).

The fauna is characterized by high abundance and low diversity, which is suggestive of a high stress environment. The gastropod Cryptalaux is indicative of lowered salinity (brackish) environments (J. Szabo, pers. comm.).

2.18 FACIES S: GREY SHALES

Facies S consists of thinly bedded, light to medium

grey shales with thin interbeds of siltstone, sandstone and limestone(Plate 2.16). The surfaces of the shales often weather to a coffee- brown colour. Facies S accounts for approximately 400 m of section in Arroyo Tecocoyunca (Section C4, Units 8_3-8_1), Arroyo El Rincon (Section C1, Units 1-14, 16-18) and Arroyo Campamento (Section C2, Units 16-19). The ratio of shale to other lithologies is approximately 10:1 (Plate 2.16, 2.17).

The shales are thinly bedded (1-2 cm) and fissile except when slightly bioturbated (Plate 2.18). Many horizons contain limey-ferruginous concretions ranging in size from 3-20 cm. Concretions are spherical to oblate in shape (Plate 2.19). Fossils sometimes form the core of these concretions.

Siltstone and sandstone beds range from 5 cm to 60 cm in thickness and have planar to irregular, sharp bases which are erosional (Plate 2.20). Parallel lamination is often present but many beds are massive and structureless. The interbeds are often limey and contain many bivalve shell fragments averaging 5 to 10 mm in size. Fragments are poorly sorted and angular. The siltstone and sandstone interbeds often exhibit a crude normal grading of sediments. Grain size of the siltstones ranges from .06 to .03 mm (4.0-5.0 ø). Sandstone grain size is .08-.06 mm (3.5-4.0 ø). Limestone interbeds are silty and contain abundant shell fragments. They are similar to those

Plate 2.16: Facies S (Subfacies S2) shales with thin siltstone interbeds. Unit 14, Section C1.

Plate 2.17: Facies S (Subfacies S2) shales within Section C1-Arroyo El Rincon, Units 16, 17, 18 are exposed.

Plate 2.18: Facies S (Subfacies S1) shales. Unit 7, Section C1.

Plate 2.19: A concretionary horizon containing large limey-ferruginous concretions. Subfacies S2. Unit 19, Section C2.

Plate 2.20: A sharp based sandstone interbed. Subfacies S2, Unit 13, Section C1.

described in Facies B (Subfacies B1).

Fossil content and degree of bioturbation may be used to distinguish three subfacies.

SUBFACIES S1: SLIGHTLY BIOTURBATED GREY SHALES

Subfacies S1 contains horizons of slight bioturbation which partially destroys the fissile nature of the shales. Total thickness is approximately 100 metres in Arroyo Tecocoyunca (Section C4, Units 13, 8_3-8_1) and Arroyo El Rincon (Section C1, Units 1-6) (Plate 2.18).

The invertebrate benthic fauna consists of the bivalve Anisocardia and the gastropod Cryptalaux but in much lower abundance than in Facies R. Ammonites are an important pelagic/nektobenthic faunal component. Disseminated carbonaceous plant debris is abundant and a few thin (2-3 cm) coaly horizons are found in Units 1 and 2 of Arroyo El Rincon (C1).

SUBFACIES S2: FISSILE GREY SHALES

Finely laminated fissile grey shales compose Subfacies S2. Total thickness is approximately 300 metres in Arroyo El Rincon (Section C1, Units 7-14, 16-18) and Arroyo El Campamento (Section C2, Units 16-19) (Plates 2.16, 2.17, 2.19, 2.20). Subfacies S2 contains an entirely nektobenthic/pelagic fauna of ammonites.

SUBFACIES S3: NON-FOSSILIFEROUS GREY SHALES

These shales are finely laminated, fissile and grey and occur in Arroyo El Campamento (Section C2) with a total

thickness of 4.0 m and 3.8 m in Units 22 and 28 respectively. Subfacies S3 lacks the fossils, coarser-grained interbeds, and limey- ferruginous concretions which are characteristic of Subfacies S1 and S2.

INTERPRETATION

Facies S is an association of offshore shales deposited in a quiet, shallow to moderately deep water environment below fairweather wave base. The sandstone, siltstone and limestone interbeds were deposited episodically as indicated by their abrupt, erosional bases and shell fragments. Storm-generated density currents were probably the causative agent for deposition of these interbeds (Aigner, 1985).

Subfacies S1 may have been deposited closer to shore and in shallower water than Subfacies S2 as indicated by: (1) an abundant benthic invertebrate fauna, (2) influx of freshwater creating slightly brackish conditions suggested by the presence of Cryptalaux, and (3) the abundance of plant fragments. Subfacies S3 was apparently deposited in an area of the basin which was not susceptible to influxes of coarser-grained sediments. Substrate conditions of Subfacies S2 and S3 may not have been conducive to benthic invertebrates, although the shales do not possess anoxic characteristics.

2.19 FACIES T: BLACK SHALES

Monotonous black fissile shales compose Facies T, which is found in Unit 15 of the Arroyo El Rincon (C1) and Arroyo El Campamento sections. Total thickness is approximately 36 metres (Plate 2.21).

The base and top of Facies T are slightly gradational as they pass into grey shales, but the boundaries are marked by a distinct colour change. The shales are moderately fissile and composed of thin planar beds, 1-3 cm in thickness. All the shales are carbonaceous and have a bituminous odour when freshly broken.

A massive, structureless siltstone bed 0.8 m in thickness is located in the middle of Facies T. The grain size range is .05-.06 mm (4.25-4.0 Ø).

The well preserved pelagic fauna consists of ammonites as the major faunal component, but the planktonic bivalve Bositra is also abundant. Vertebrae of the Tethyan crocodile genus Steneosaurus are also present.

INTERPRETATION

Facies T is a moderately fissile black shale deposited in relatively deep water. Anoxic bottom conditions are suggested by: (1) the black colour and bituminous nature of the shales, (2) lack of a benthic community of organisms, (3) absence of bioturbation, and (4) the presence of a well preserved pelagic fauna.

2.20 FACIES U: INTERBEDDED DARK GREY SHALES AND SILTSTONES

Plate 2.21: Facies T black shales. Unit 15, Section C1.

Facies U encompasses a number of dark grey fissile shales with interbedded siltstones exposed in the upper portion of Arroyo El Campamento (Section C2, Units 20, 24, 26, 27 and 29). Total thickness of the facies is 28 metres. Shale to siltstone ratio is approximately 3:1.

Shale beds average .4-1.6 m thick and have well developed fissility. Bases of the shale beds are slightly gradational but distinct.

The siltstone beds have sharp, erosional bases and contain planar parallel lamination. Upper bounding surfaces of the beds are distinct but are gradational into the overlying shales. Individual bed thicknesses range from .1 to .6 metres. Average grain size is .04 mm (4.5 Ø), but some siltstone beds fine upward to .015 mm (6.0 Ø).

Fossils are absent in Facies U.

INTERPRETATION

The interbedded dark grey shales and siltstones of Facies U seem to have been deposited in an offshore environment of moderate water depth. Siltstone beds were probably the result of sediment-laden density flows generated by storms and/or ebb currents (Aigner, 1985). Supporting evidence is the sharp erosional bases which imply episodic emplacement by currents. Bottom conditions may have been unfavourable for inhabitation by benthic invertebrate organisms.

2.21 FACIES V: LIMEY GREY SHALE

These poorly bedded, limey grey shales are exposed in Unit 21 of Arroyo El Campamento (Section C2). Total thickness is 4.8 metres.

Individual bed thickness averages 5 cm. Bedding planes are abrupt but undulatory and irregular. The basal and upper bounding surfaces of Facies V are distinct and moderately sharp. Fossils are very sparse. Rare Anisocardia occur near the base of this facies.

INTERPRETATION

The limey grey shales of Facies V appear to be the result of mud accumulation in a moderately quiet offshore environment. Conditions of this environment were marginal for the survival of a very sparse bivalve population.

2.22 FACIES X: NON-FOSSILIFEROUS GREY LIMESTONE

The light grey, thickly bedded limestone of Facies X is 2.9 m thick in Arroyo El Campamento (Section C2, Unit 23). Upper and lower bounding sufaces of the facies are abrupt. Individual beds average 20-30 cm and are often separated by thin partings of grey shale. Bed contacts are abrupt and distinct. Average parting thickness is 1-3 cm. Shale partings are most abundant in the basal 1.0 metre but thin and disappear entirely in the uppermost metre of Facies X.

Body fossils and bioturbation are absent.

INTERPRETATION

Facies X limestone may be termed a micrite using the carbonate rock classification scheme of Folk (1962). The limestone was most likely the result of carbonate mud settling out of suspension in a quiet basinal environment. Rapid rates of sedimentation and the extremely fine mud probably deterred all suspension-feeding organisms from colonizing the sediments (McKerrow, 1978).

2.23 FACIES Y: MASSIVE CALCAREOUS SILTSTONE

The massive, light grey calcareous siltstone of Facies Y is exposed in Unit 25 of the Arroyo El Campamento section (C2). Total thickness is 2.4 m.

The base of Facies Y is sharp and erosional. Numerous rip-up clasts of the underlying mud are seen at the base of the facies and average 1-4 cm in size. The upper bounding surface is distinct but slightly gradational as it passes into the overlying shales. The only sedimentary structure seen in this facies is parallel lamination. Individual laminations are .5-1.5 cm thick. Grain size ranges from .04 to .06 mm (4.5-4.0 Ø) and fines upward especially in the uppermost 5-10 cm.

Macrofossils are very rare. A few internal moulds of articulated and disarticulated valves of Anisocardia are apparent and may have been eroded from pre-existing sediments. They are found randomly scattered at the base of the facies, along with the mud rip-up clasts.

INTERPRETATION

The sharp base and mud rip-up clasts imply rapid emplacement by currents which were capable of eroding pre-existing shales. Parallel lamination and transported bivalves also suggest current emplacement. Facies Y seems to have been deposited by a storm and/or ebb current-related, sediment-laden, density current in a quiet basinal environment (Aigner, 1985).

CHAPTER 3: PETROLOGY

3.1 INTRODUCTION

Thin sections were prepared from samples collected in the stratigraphic sections C1-Arroyo El Rincon, C2-Arroyo El Campamento, C3-Alto de Teeolutla, C4-Arroyo Tecocoyunca, and C5-Alto El Variado. An attempt to define the sandstones and siltstones was made by counting 300 points per thin section. Ternary diagrams of quartz (Q), feldspar (F), and rock fragments (R) were plotted for both sandstones and siltstones (McBride, 1963). Limestones were classified according to Folk's (1962) carbonate rock and texture classification scheme.

3.2 METHODS

All thin sections were stained using the method developed by Lindholm and Finkelman (1971) to identify ferroan/non-ferroan calcite and dolomite. Preparation details are given in Appendix 1. A ferroan calcite comparison chart was then used to estimate the ferrous iron content of calcite. Porosity was enhanced in some thin sections by impregnation with blue epoxy. This also provided consistency with poorly consolidated samples. Textural and mineral relationships seen in thin section were photographed using a standard petrographic microscope. Sample numbers correspond to the unit numbers of the

stratigraphic sections.

3.3 SANDSTONES AND SILTSTONES

The major detrital components of the sandstones and siltstones in decreasing abundance are: quartz, feldspar, mica, rock fragments, chert, and authigenic pyrite and hematite. Trace amounts of chlorite, glauconite, zircon, and epidote are present. Alteration products and cements include clays, sericite, calcite, and dolomite (Plates 3.1-3.10). Tables 3.1 and 3.3 list modal percentages of all mineral components.

The sandstones and siltstones plot in the subarkose and arkose fields of McBride's (1963) ternary diagram (Figs. 3.1, 3.3). This classification scheme was designed for sandstones, but it seems reasonable to extend its use to very fine sandstones and siltstones. Modal percentages of rock fragments may be artificially low due to identification problems at silt and fine sand sizes.

Rock porosity is minimal (1-2%), which may be attributed to compaction, pressure solution, and the development of carbonate cements and authigenic clays.

3.3.1 Quartz

Quartz grains appear moderately well sorted to well sorted (Pettijohn et al., 1972). Grains are commonly subangular to angular (Powers, 1953). Grain sizes of the

sandstones range from very fine to fine sand (4.0 ∅–2.0 ∅; 0.0625–0.25 mm.), with some occurrences of medium sand (2.0 ∅–1.75 ∅; 0.25–0.30 mm). Quartz grains in the siltstones are coarse silt size (4.5 ∅–4.0 ∅; 0.044–0.0625 mm).

Quartz cements and syntaxial overgrowths, though uncommon, are sometimes observed in "clean" sandstones (i.e. high percentage of cement and other detrital minerals) which have microcrystalline quartz cement. A "welded" texture is very common with sutured and interpenetrating contacts of quartz grains. This degree of development is enhanced in "clean" sandstones. Fracturing of quartz grains is seen in the highly "welded" sandstones (Plate 3.1).

Quartz grains have been classified and plotted under four subdivisions (Basu et al., 1975). These types are: 1) monocrystalline, non-undulatory grains, 2) polycrystalline grains with two or three crystals per grain, 3) polycrystalline grains with greater than three crystals per grain, 4) monocrystalline grains exhibiting undulatory extinction requiring more than a 5°rotation of the stage under crossed nicols. Thin section point counts were made for each type of quartz and are listed in Tables 3.2 and 3.4. Most quartz grains are monocrystalline and undulatory. The majority of the polycrystalline grains have greater than three crystals per grain.

Basu et al. (1975), proposed that quartz crystallinity is indicative of provenance. They suggested that

Plate 3.1: A 'clean' sandstone with a tight 'welded' texture. Quartz grains are fractured. There are minimal amounts of carbonate cement. Note the bent mica flake in the lower right. Unit 1, Section C4. XN, 63X.

Note: Dimensions of the field of view in all 63X photos are 1.5 X 1.0 mm.

Plate 3.2: Poikilotopic texture of the calcite cement in a sandstone. Note the shell fragment in the lower right and calcite replacement of a feldspar grain in the upper left. Unit 7b, Section C4. XN, 63X.

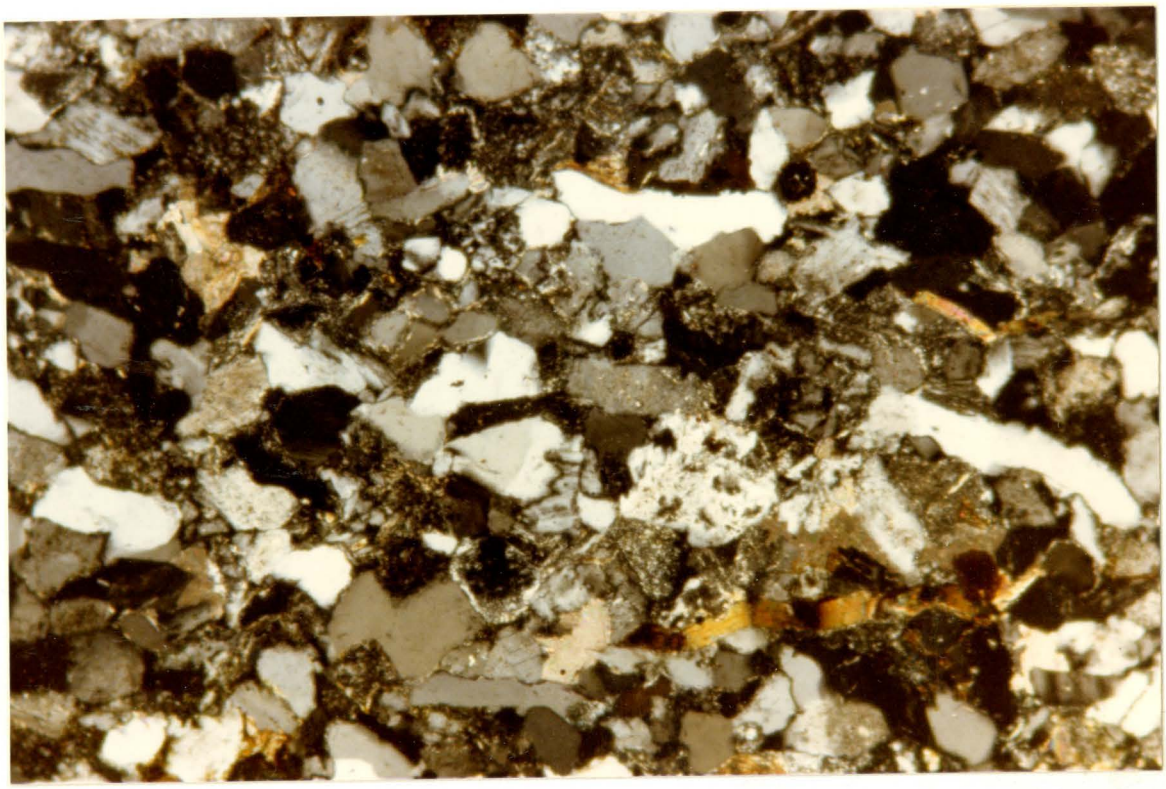

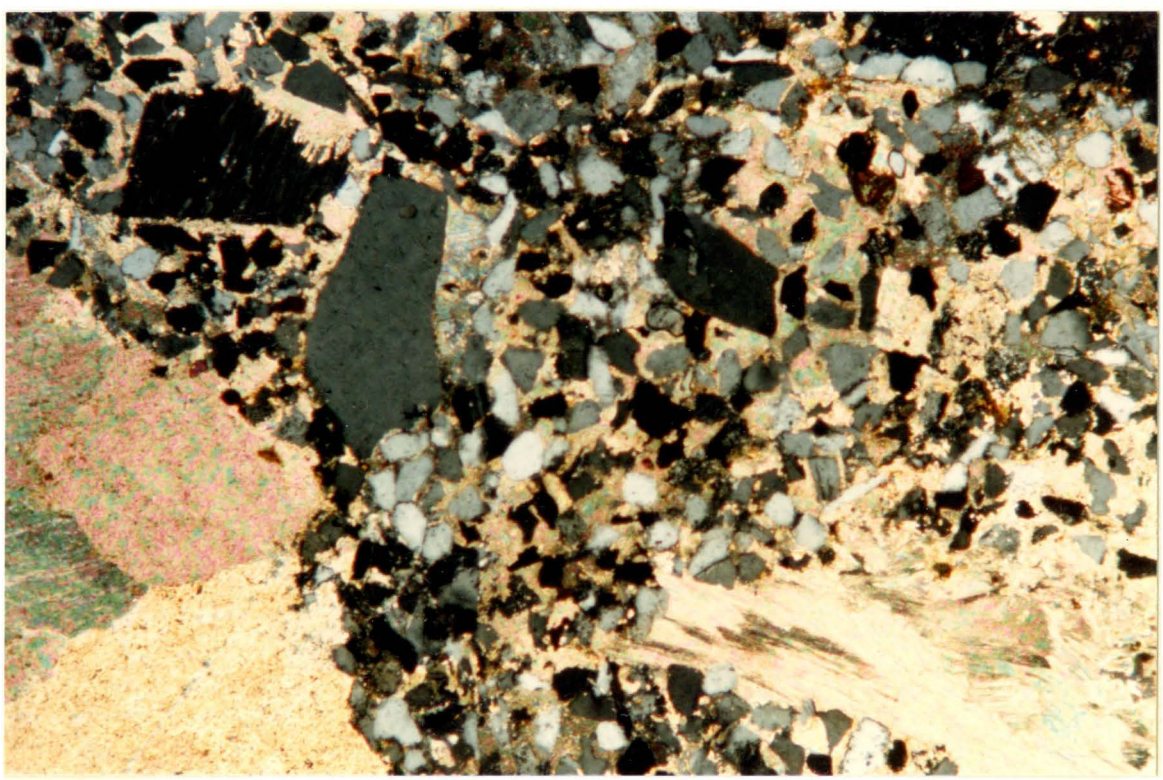

Table 3.1: Modal percentages of sandstone constituents.

Section #	Quartz	Chert	Feldspars	Rock Fragments	Calcite Cement	Quartz Cement	Chlorite	Biotite	Muscovite	Glauconite	Pyrite	Hematite	Clays	Zircon	Epidote	Sericite	Fossils
C3-7	30.6	—	6.8	.32	58.1	—	.32	.64	.64	.32	.32	.64	1.3	—	—	—	—
C4-5a	58.7	14.9	19.7	.63	1.9	—	.63	1.59	.63	—	.37	.63	—	.32	—	—	—
C4-7b	12.2	—	24.9	.31	57.7	—	.62	.62	.31	.31	.31	—	—	.31	—	2.49	Yes
C4-1	50.5	16.0	23.5	.3	4.2	2.06	.64	1.3	.3	—	.6	.3	—	.3	—	—	—
C4-4a	14.3	14.9	34.0	.62	32.6	—	.93	1.2	.31	.31	.31	.31	—	—	—	—	—
C4-8	29.8	4.9	40.4	.29	1.7	19.2	—	.29	.29	.29	.29	2.0	—	.29	.29	—	—
C4-18	35.3	2.8	33.1	.64	—	—	—	1.26	1.58	.32	1.58	.32	—	.32	.32	3.15	—

Table 3.2: Modal percentages of quartz types in the sandstones.

Section Number	Monocrystalline, Non-Undulatory, Extinction (%)	Polycrystalline, 2-3 Crystals Per Grain (%)	Polycrystalline, 3 Crystals Per Grain (%)	Monocrystalline, Undulatory, Extinction (%)	Total Quartz (#)
C3-7	14.7	6.3	29.5	49.5	95
C4-5a	2.8	1.1	2.8	93.3	179
C4-7b	2.5	2.5	2.5	92.5	40
C4-1	1.3	—	9.9	88.8	152
C4-4a	2.2	—	17.8	80.0	45
C4-8	—	2.1	6.2	91.7	97
C4-18	—	5.6	14.0	80.4	107

Table 3.3: Modal percentages of siltstone constituents.

Section #	Quartz	Chert	Feldspar	Rock Fragments	Calcite Cement	Chlorite	Biotite	Muscovite	Glauconite	Pyrite	Hematite	Clays	Zircon	Epidote	Sericitic Matrix	Staurolite	Fossils
C2-21	35.2	—	5.57	—	17.6	4.46	.3	.6	.3	.3	.88	20.0	—	—	14.5	.3	—
C2-25	31.35	—	3.3	—	54.5	2.21	.35	.35	.35	1.65	.7	—	—	—	5.28	—	—
C2-27	18.0	—	5.1	—	—	2.87	.66	.99	.99	.66	5.1	—	.33	—	65.0	—	—
C3-5	23.4	—	27	—	28.9	.28	.55	.55	—	.28	1.93	—	.55	—	16.56	—	Yes
C4-7a	39.6	—	18.5	—	18.2	2.95	.33	.66	.33	.33	2.97	—	.33	—	15.8	—	Yes
C1-13 int	3.1	—	21.4	—	71.6	—	.3	.3	.3	1.55	.93	—	.3	.3	—	—	Yes
C1-18 int	3.3	—	9.6	—	83.3	.3	.3	.3	.3	2.0	.3	—	.3	—	—	—	Yes

Table 3.4: Modal percentages of quartz types in the siltstones.

Section Number	Monocrystalline, Non-Undulatory, Extinction (%)	Polycrystalline, 2-3 Crystals Per Grain (%)	Polycrystalline, 3 Crystals Per Grain (%)	Monocrystalline, Undulatory, Extinction (%)	Total Quartz (#)
C2-21	32.0	--	4.1	63.9	122
C2-25	27.6	2.0	10.2	60.2	98
C2-27	9.4	--	3.8	86.8	53
C3-5	10.7	--	2.4	86.9	84
C4-7a	1.8	2.6	3.5	92.1	114
C1-13int	33.3	11.2	22.2	33.3	9
C1-18int	--	--	--	100.0	10

Figure 3.1: Ternary diagram illustrating the classification of the sandstones.

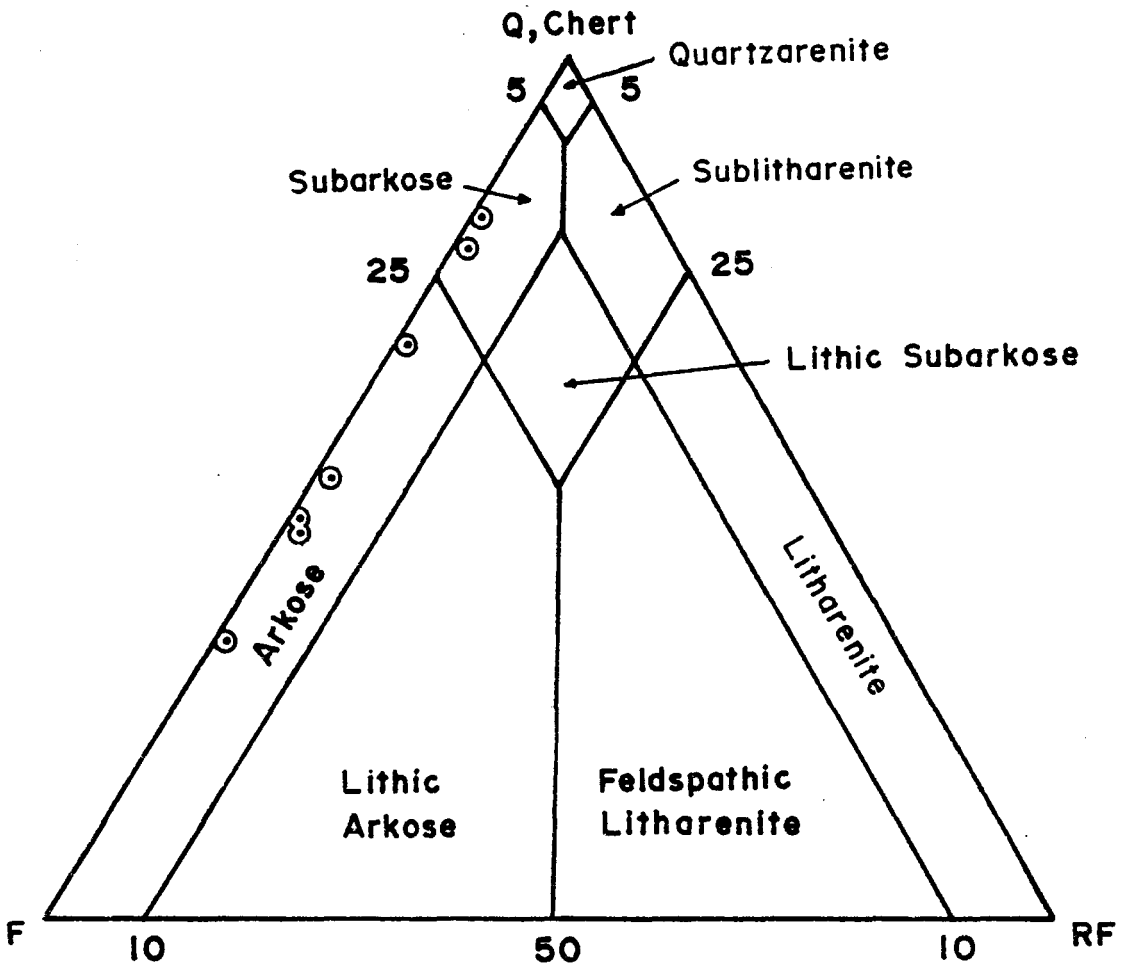

McBride, 1963

Figure 3.2: Diamond plot illustrating quartz variety and provenance for the sandstones.

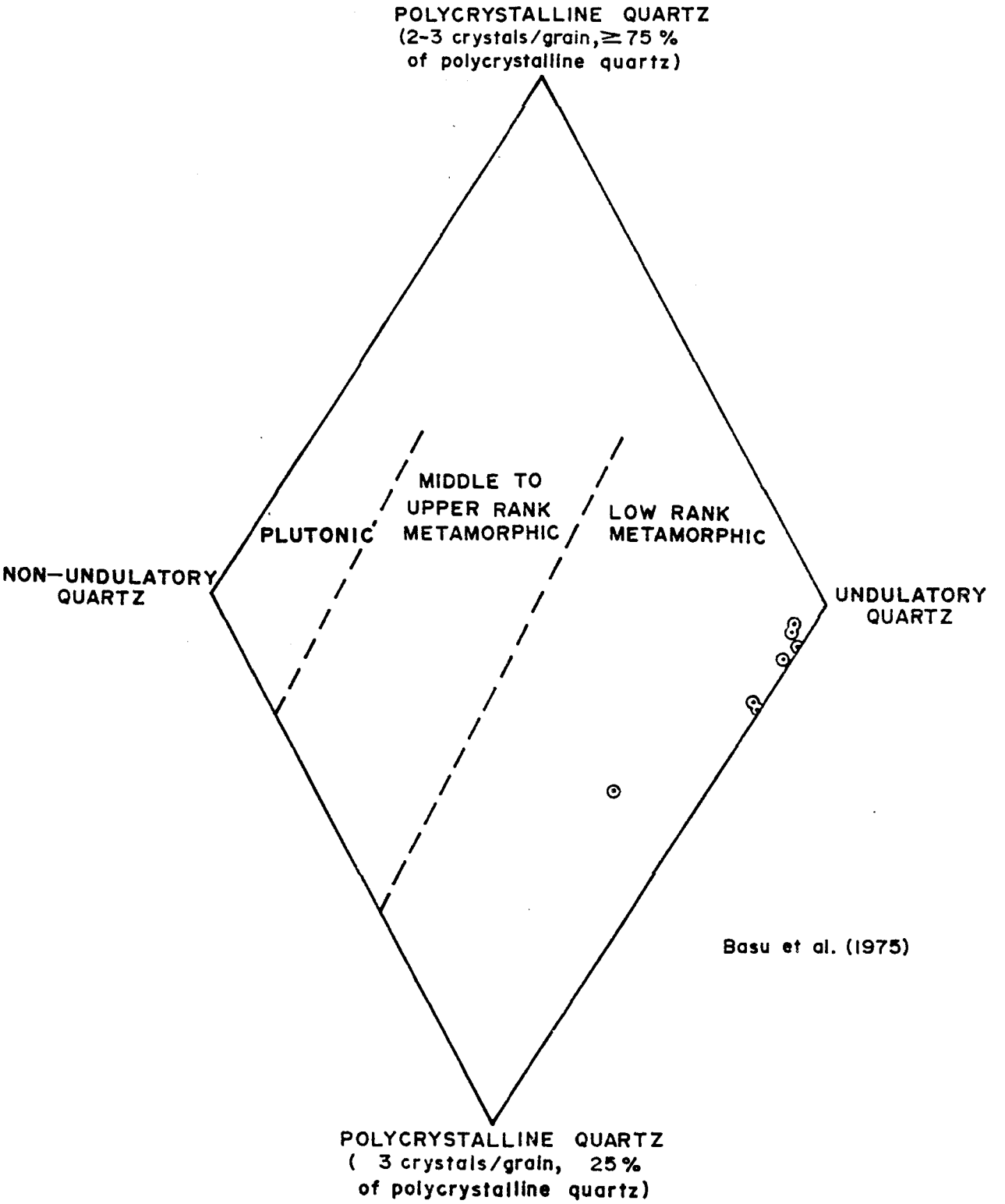

Basu et al. (1975)

Figure 3.3: Ternary diagram illustrating the classification of the siltstones.

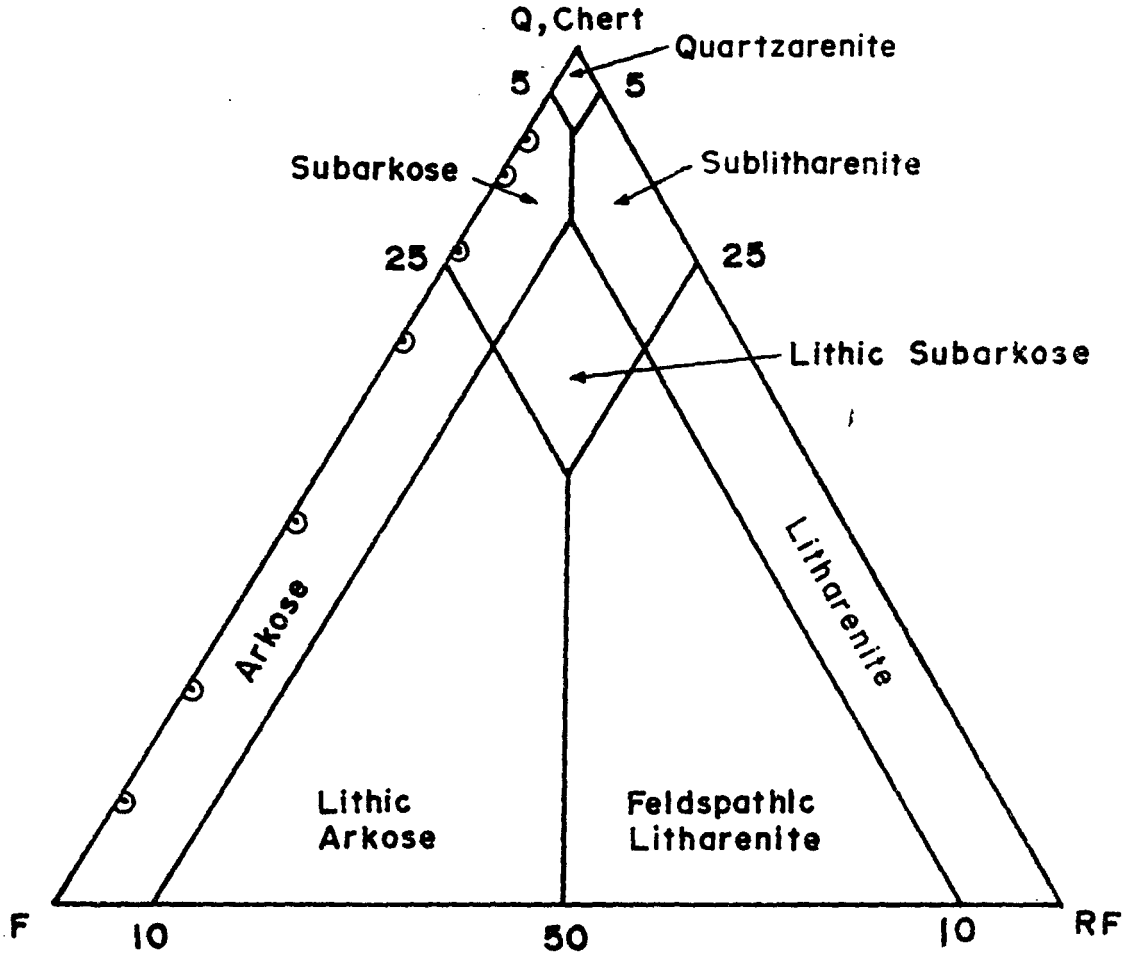

McBride, 1963

Figure 3.4: Diamond plot illustrating quartz variety and provenance for the siltstones.

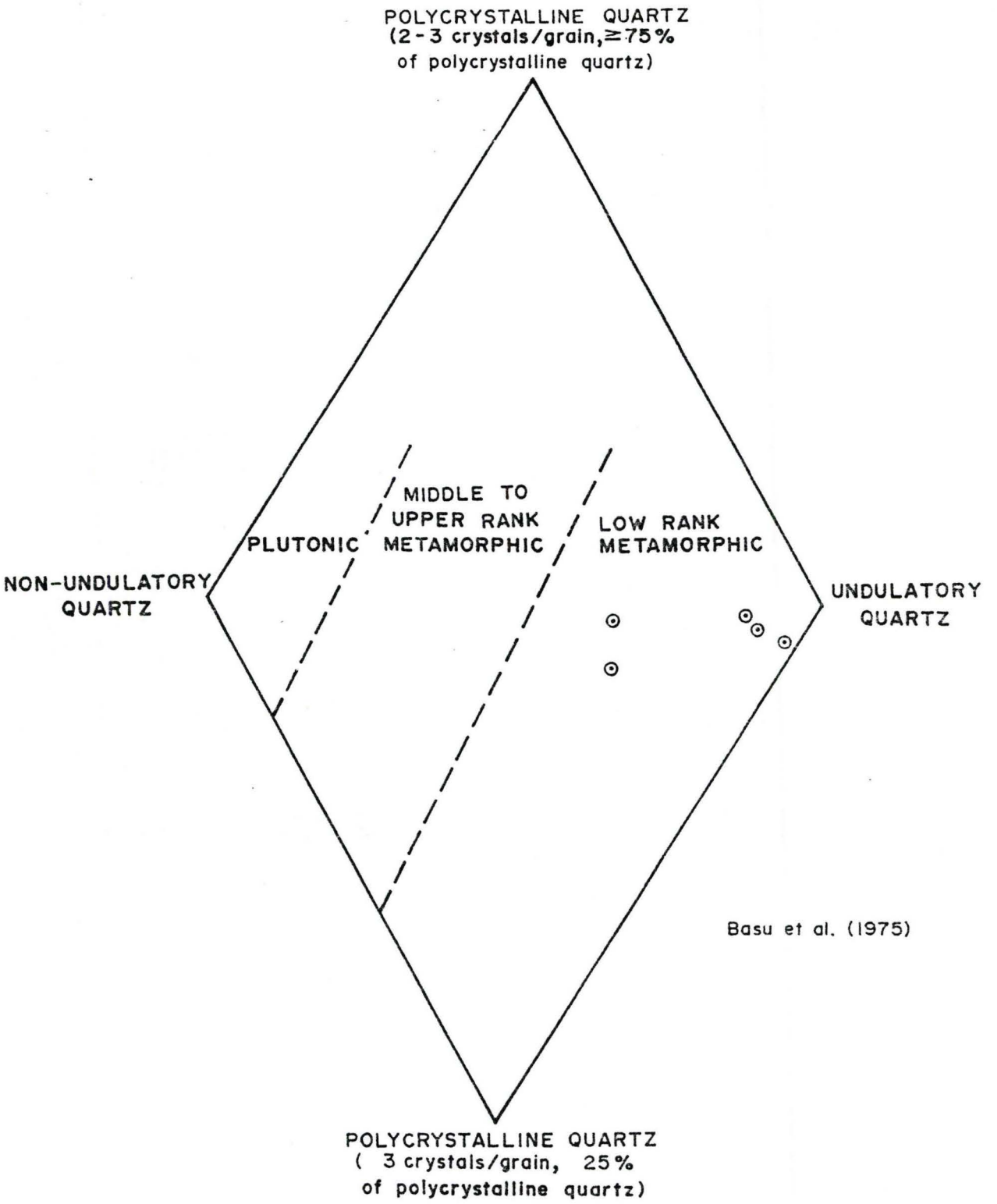

Basu et al. (1975)

polycrystalline quartz grains of Type 2 are derived from plutonic source regions, and those of Type 3 are derived from metamorphic rock sources. Figure 3.2 and 3.4 are diamond plots of quartz variety and illustrate that the provenance is from low rank metamorphic rocks.

3.3.2 Chert

Chert is abundant in all sandstones (See Table 3.1). It is aphanitic in texture and light brown in colour under plane light. Grain sizes range from very fine to fine sand (3.5 Ø-2.75 Ø; .08-.14 mm). Chert grains display a distinct roundness not apparent in other mineral grains.

3.3.3 Feldspar

The high feldspar content evident in the studied thin sections has resulted in the classification of the sandstones and siltstones as arkose to subarkose according to McBride (1963) (see Figs. 3.1, 3.3, and Tables 3.1, 3.3). Grain size of the feldspars in the sandstones and siltstones ranges from coarse silt to fine sand (5.0 Ø-2.25 Ø;.03-.2 mm). Grain shapes vary between angular to subrounded (Powers, 1953).

The alkali feldspar, microcline, and the plagioclase feldspars, labradorite, andesine, and oligoclase are present in all samples. Microcline is readily identified by its "crosshatch" transformation twinning. Plagioclase feldspars

were identified using the Michel-Levy extinction angle method. Labradorite and andesine are most abundant, while oligoclase is present in lesser amounts. All the plagioclase feldspars are characterised by albite, Carlsbad, and pericline twinning.

Potassium feldspars show some alteration to clays, and sericite. Sericitization appears to initiate and propagate along twinning planes, resulting in "honeycomb" texture. Sericite alteration of the feldspars appears to be a major contributor to the microcrystalline sericite matrix which cements and partially supports the detrital components of the siltstones.

Orthoclase feldspars are frequently observed to be altering to calcite. Calcite alteration often initiates at the grain boundaries creating scalloped and irregular edges. Unstained calcite rims are observed on some feldpar grains, and appear to be an alteration "proto-calcite", midway between calcite and feldspar.

3.3.4 Rock Fragments

Sedimentary, igneous, and metamorphic rock fragments have been identified in the sandstones but have not been differentiated (see Table 3.1). Sedimentary rock fragments are composed of microcrystalline chert grains. These have been included with quartz in McBride's ternary classification diagram (1963). Igneous and metamorphic rock

fragments contain polycrystalline quartz, biotite, and feldspars. All of these rock fragments are exceptionally fine grained, which may result in artificially low percentages (Table 3.1 and Fig. 3.1). For this reason, the siltstones plot along the Quartz-Feldspar axis (Fig 3.3).

3.3.5 Accessory Minerals

Accessory minerals found within the sandstones and siltstones include: biotite, muscovite, glauconite, chlorite, pyrite, hematite, zircon, epidote, and clays.

Biotite and muscovite occur as small, lath-shaped grains, ranging in size from 3.25 Ø-1.75 Ø; .1-.3 mm. Some grains show alignment of their long axes parallel to bedding, while others show bending and deformation around quartz and feldspar grains. Deformation of the micas is not apparent in the siltstones containing a high percentage of calcite and sericite cements. Glauconite occurs as subrounded to rounded detrital grains, and is easily identified by its characteristic speckled green birefringence. Grain sizes range from 2.25-6.0 Ø;0.2-0.02 mm. Compactional deformation of the glauconite grains causes them to appear similar to an interstitial authigenic mineral or cement. Chlorite most commonly occurs as lath-shaped, detrital grains which range in size from 2.25-6.0 Ø;0.2-0.02 mm. Chlorite also occurs as authigenic interstitial masses with a fibrous texture. Authigenic

chlorite is three times more abundant than detrital chlorite. Compactional deformation has resulted in "squeezing" of the chlorite between quartz grains.

Pyrite occurs as subhedral crystals, and framboidal grains of authigenic origin. Crystal sizes range from 6.0 Ø-4.25 Ø; .01-.05 mm, but framboidal grains often coalesce into aggregates up to 1.75 Ø;.3 mm. Pyrite may also be detrital, showing concentrations along bedding planes, and associated with organic matter such as fossils and plant debris.

Hematite is often associated with pyrite, as aggregates of tiny (4.25 Ø;.05 mm) subhedral, authigenic crystals. Patchy iron staining is often associated with hematite and pyrite.

Zircon and epidote occur as subrounded to rounded grains averaging 5.5 Ø-4.25 Ø;.02-.05 mm in size. They appear randomly scattered, but occasionally show concentrations along bedding planes in the sandstone beds. Epidote is associated with low grade metamorphic rocks (Greenschist, Epidote-Amphibolite Facies, Winkler, 1979) consistent with the low rank metamorphic source for quartz as shown in figures 3.2 and 3.4.

Clays and sericite are present in the sandstones in small quantities within interstitial regions. Both appear to have an authigenic origin.

3.3.6 Cements

Sparry calcite is the most abundant cement, filling pore spaces and significantly reducing porosity (Plates 3.3-3.6). Iron content of the calcite in the sandstones is 1.0-1.5% FeO (ferroan calcite I) and greater than 3.5% FeO (ferroan calcite III) using the scheme of Lindholm and Finkelman (1971). The siltstones contain ferroan calcite types I, II, and III. Zonation of increasing FeO content away from the centers of the pore spaces is observed within the sparry calcite cement. This most likely reflects ferrous iron enrichment of meteoric waters with increasing burial depth. Corroded calcite crystals are also apparent and show a patchy, intermingled distribution of ferroan calcite types I, II, and III. This textural relationship suggests cycles of partial dissolution followed by precipitation of more highly iron-enriched calcites. The extent of this process appears dependant on the permeability of the rock. Interconnected pores have ferroan calcite I and II completely replaced by ferroan calcite III. Low permeability regions contained only ferroan calcite I. Calcite exhibits poikilotopic texture in some sandstones (eg. C4-7b) (Plate 3.2) and siltstones (Plates 3.4-3.6). Crystal sizes range between 1.0-4.0 mm. This texture is suggestive of only partial consolidation of the sands when they were cemented.

Shell fragments are important in the cementation

Plate 3.3: Calcite cement resulted in a reduction of porosity in this poorly sorted siltstone. Unit 7a, Section C4. XN, 63X.

Plate 3.4: Poikilotopic texture in a poorly sorted siltstone. Unit 25, Section C2. XN, 63X.

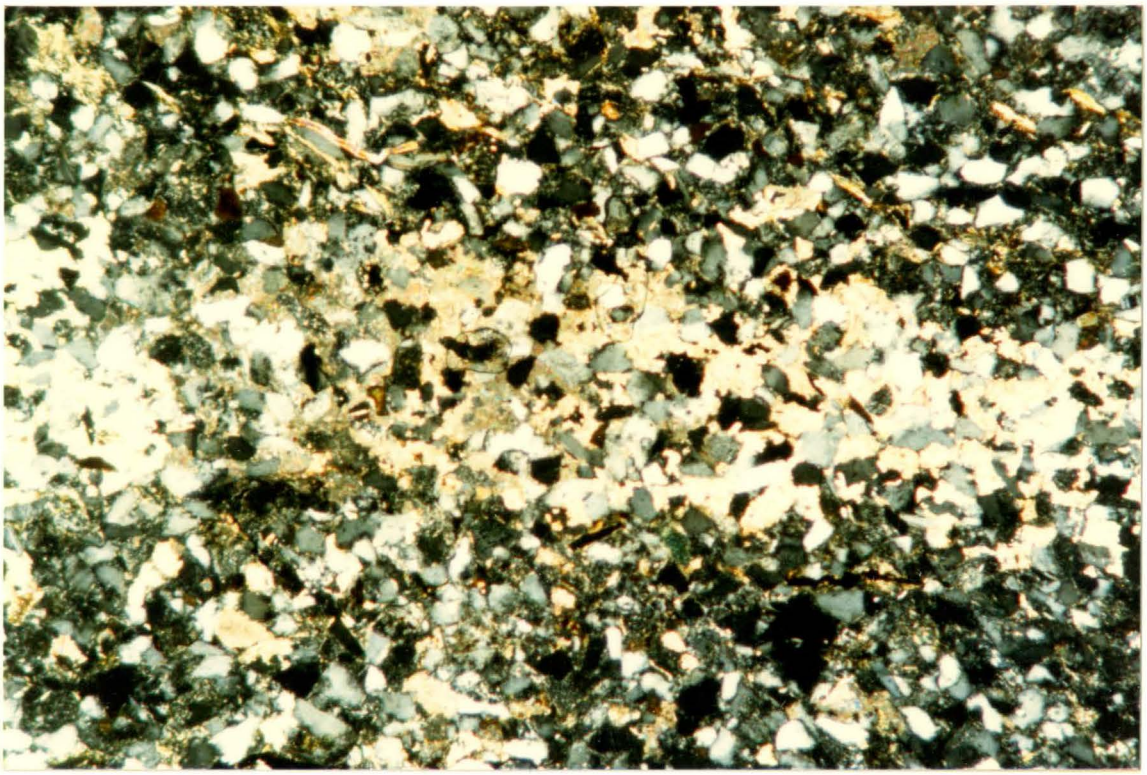

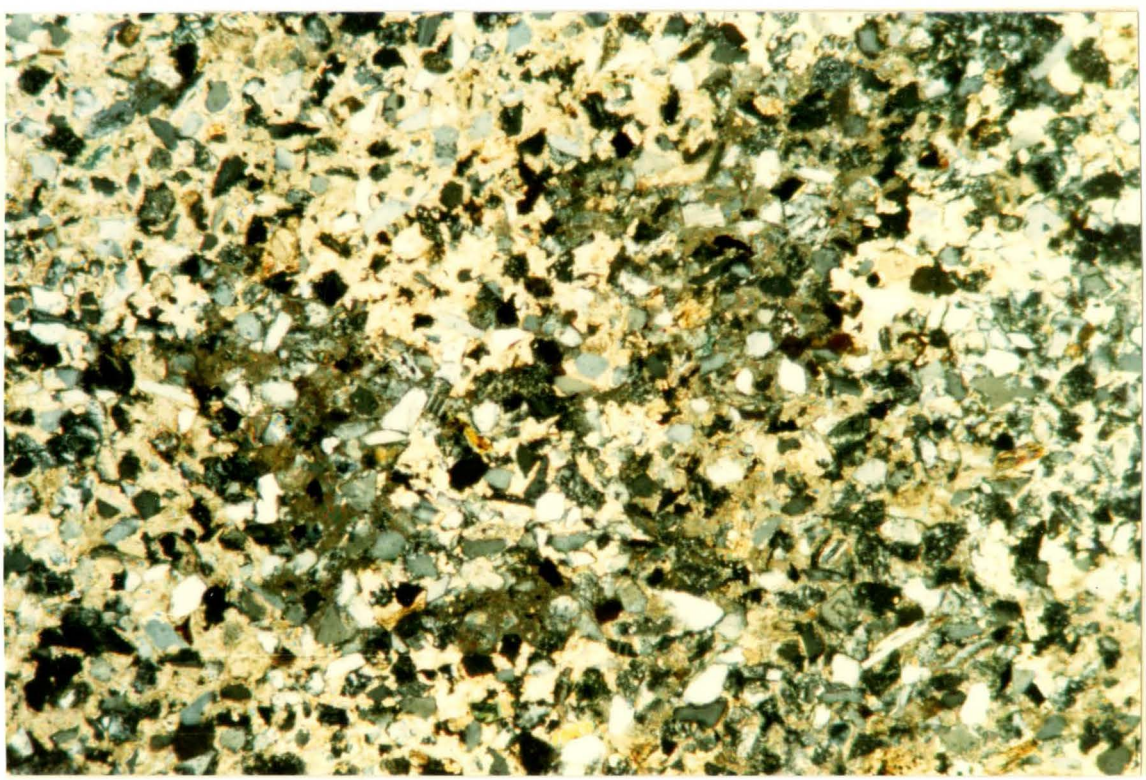

Plate 3.5: Uneven distribution of calcite cement in certain bedding plane horizons which appears to be related to the amount of shell material which subsequently recrystallized. Unit 13int, Section C1. XN, 63X.

Plate 3.6: A similar uneven distribution of well developed poikilotopic texture in a siltstone. Unit 18int, Section C1. XN, 63X.

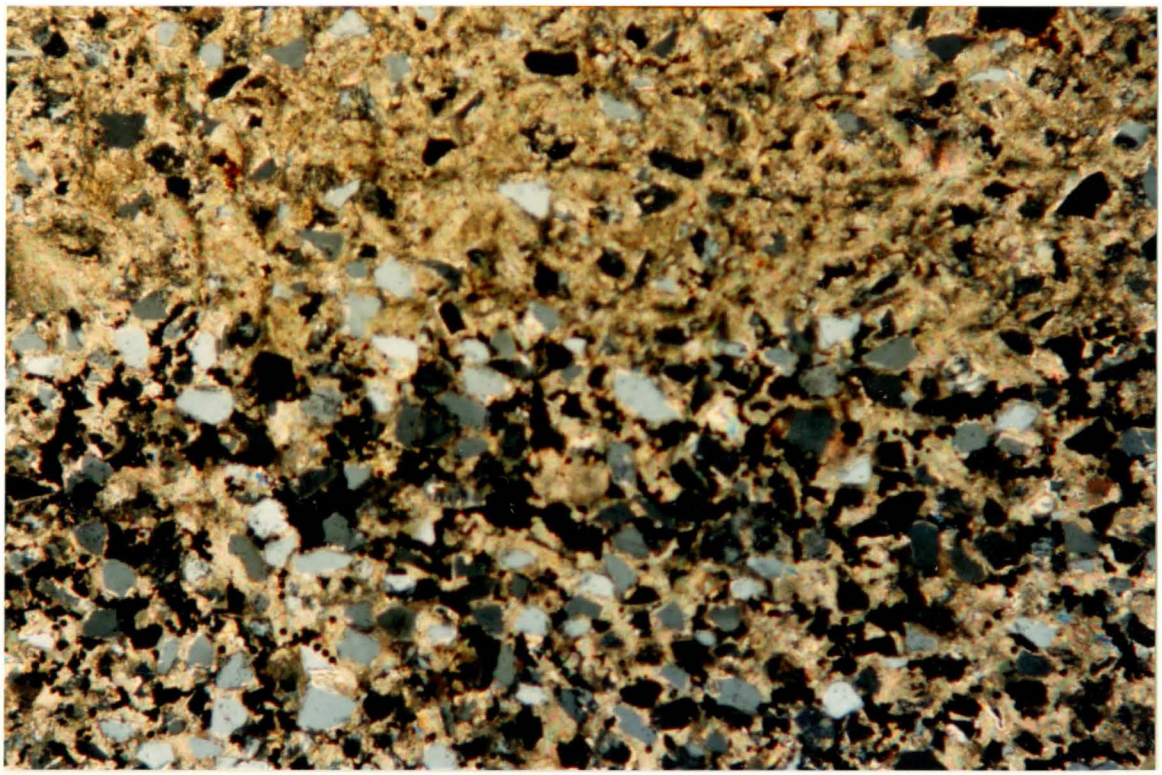

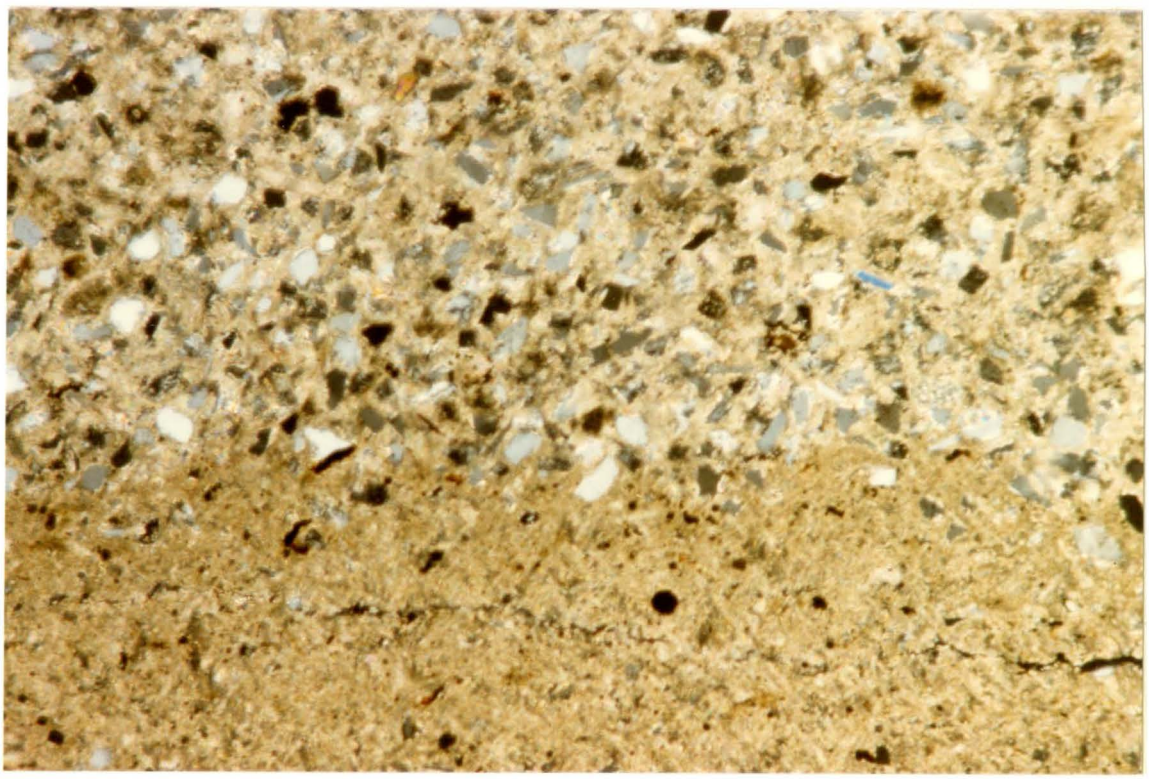

history of the sandstones and siltstones. They are uncommon in the sandstones, but account for approximately 10% in the siltstones. Disarticulated bivalves and brachiopods are the most important shell components, but some articulated ostracods are found in C4-7a. Bivalve and brachiopod shells average 0.1-0.2 mm in size. Most valves are oriented in the stable convex-up position. Details of the shell microstructure are discussed in Section 3.4.1. Sample C4-7a, a fossiliferous sandstone, is representative of the cementation history. After deposition, the bivalve shells were dissolved which resulted in biomoldic void spaces. The void spaces were infilled with radiaxial fibrous, ferroan calcite cement. Following this was neomorphism of micrite to ferroan calcite, forming a poikilotopic texture (Plate 3.7). The neomorphic calcite nucleated syntaxially on the radiaxial fibrous calcite within the biomoldic voids. Evidence supporting this interpretation is: 1) increasing crystal size away from the biomoldic voids, 2) detrital grains sometimes "pushed" away from biomoldic void boundaries due to the propagation of neomorphic calcite crystals. The result is that portions of the infilled biomoldic voids have boundaries which remain only as remnant "ghosts" between the radiaxial fibrous calcite of the infilled void and the smaller crystals of the neomorphic calcite.

Dolomite cement is present in thin section sample C3-7,

Plate 3.7: Fossiliferous siltstone with shell fragments showing a preserved outer prismatic layer (non-ferroan red) and a recrystallized ferroan calcite inner layer. The other shell fragment has been completely dissolved and the resultant biomoldic void infilled with ferroan calcite. Note how the ferroan cement propagated from the biomoldic void and spread out laterally. Unit 7b, Section C4. PL, 25X. Stained.

Note: Dimensions for the field of view in all 25X photos is 4.0 X 2.5 mm.

Plate 3.8: Siltstone cemented by dolomite (unstained). The bulk of the dolomite is xenotopic and hypidiotopic crystals. 'Baroque' or saddle dolomite occurs as unstained euhedral crystals protruding into the fracture-filling non-ferroan calcite in the lower right. Unit 7, Section C3. PL, 25X. Stained.

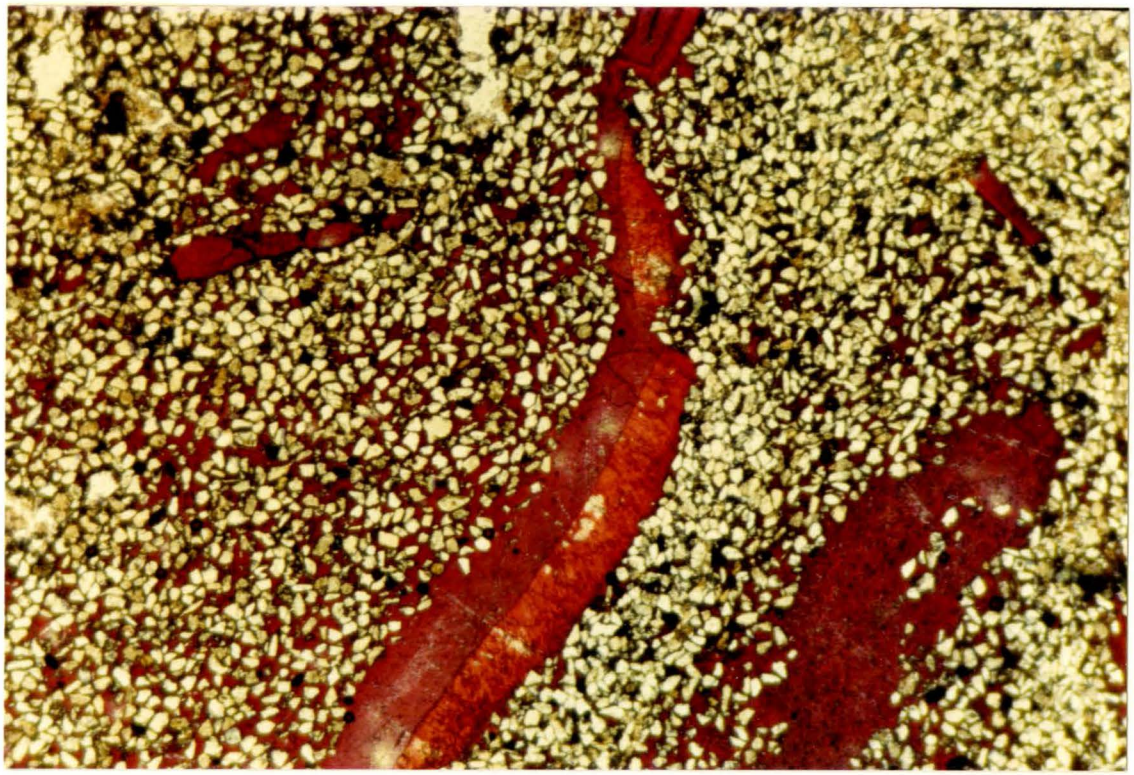

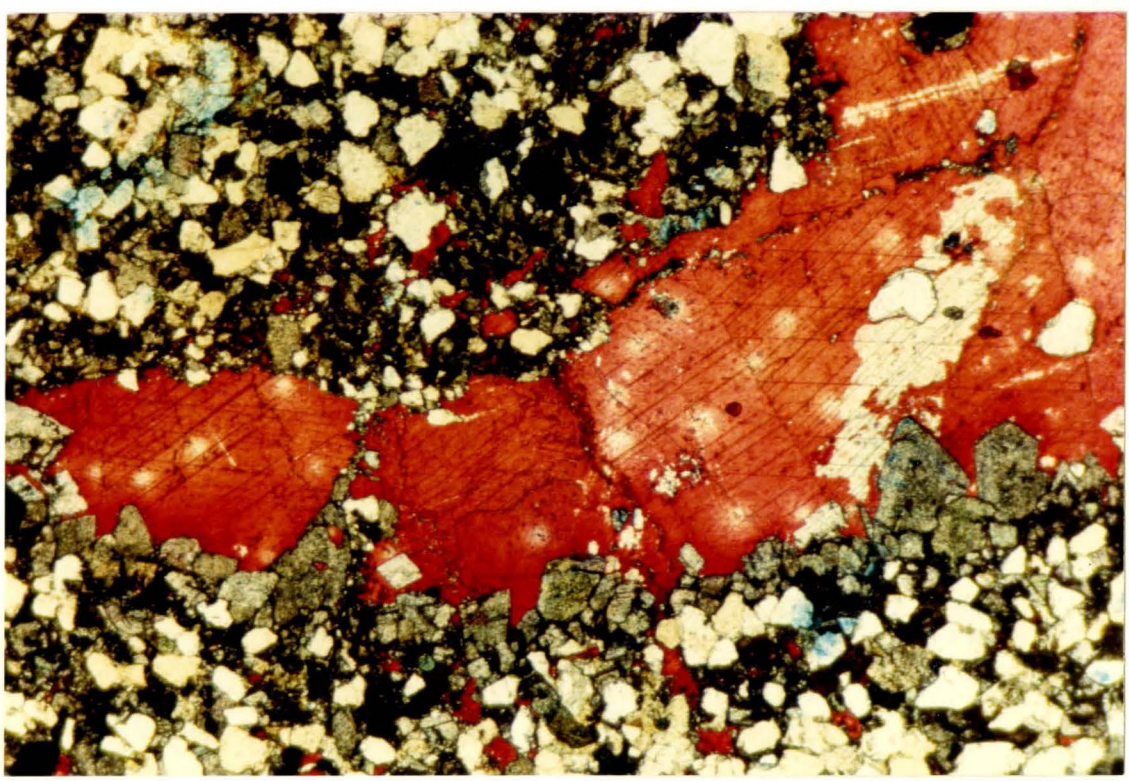

as detected by staining methods. The bulk of the cement is composed of xenotopic, and hypidiotopic crystals which average .02 mm in size (Plate 3.8). Saddle or "baroque" dolomite accounts for approximately 20% of the total dolomite, and is located in cross-cutting fractures. These dolomites have an idiotopic crystal form, ranging in size from .3-.4 mm, with well developed crystal zonation. Saddle dolomites are commonly characterised by slightly curved crystal edges and undulose extinction,interpreted as late diagenetic burial dolomite (Mattes and Mountjoy, 1980).

De-dolomitization is responsible for corrosion of some of the dolomite crystals. Calcite is sometimes observed within dolomite crystals along twinning planes.

3.3.7 Diagenetic Features

Diagenetic features are visible within many of the siltstones. Microstylolites are well developed, indicating pressure solution effects. Compactional deformation is indicated by the bent mica flakes and crushed shell fragments (Plate 3.1). Sample C1-18int contains pressure shadows. They appear as fibrous calcite aggregates growing on opposed sides of the host detrital grains, and have been interpreted to be the direct result of deformational stresses during diagenesis (Hobbs et al., 1976).

3.3.8 Interesting Petrographic Features

Plant fragments are common in the siltstones but comprise only 1-2% of the rock volume. They are aligned parallel to bedding, and often show excellent preservation accentuated by pyrite and hematite crystals. In the process of decay, the plant material created a microenvironment characterised by the presence of sulfur and reduced pH, both of which are conducive to the precipitation of pyrite and hematite.

Sample C4-7a contains a burrow approximately 1.5 mm in diameter which has been compacted to an oval shape (see Plates 3.9, 3.10). The burrow contains finer grained material in the center and is surrounded by detrital grains on the margins. Non-selective use of several types of mineral grains appears to have been employed by the organism as it constructed its tube-lining wall. Grains are oriented with their long axes tangential to the burrow outline. This type of dwelling is typical of polychaete worms or similar tube-constructing organisms.

3.4 LIMESTONES

The limestones may be classified as biosparite (C3-4 and C3-1L), biomicrite (C1-6), and biopelmicrite (C4-8_4) based on Folk's (1962) classification of carbonate rock and textures. The limestones may also be regarded as medium calcirudite using the average size for the transported shell fragments of 4 mm (Folk, 1962). The most common fossil

Plate 3.9: Cross-sectional view of a burrow which has been compacted to an oval shape. Note the fine-grained sediment infill and orientation of grains in the tube-lining wall (long axes of grains tangential to the burrow outline). Also note the ostracod shell fragment in the bottom center. Unit 7a, Section C4. PL, 63X.

Plate 3.10: View of the same burrow in polarized light. Note the ostracod shell fragment in the bottom center. XN, 63X.

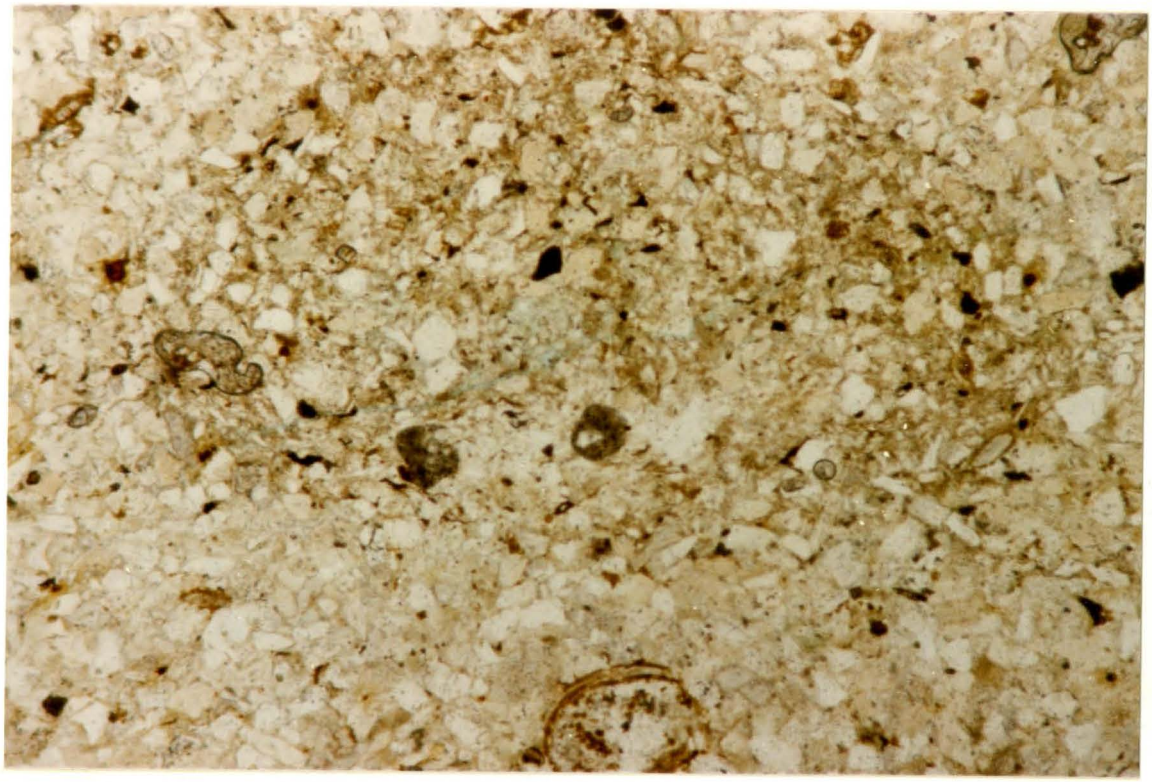

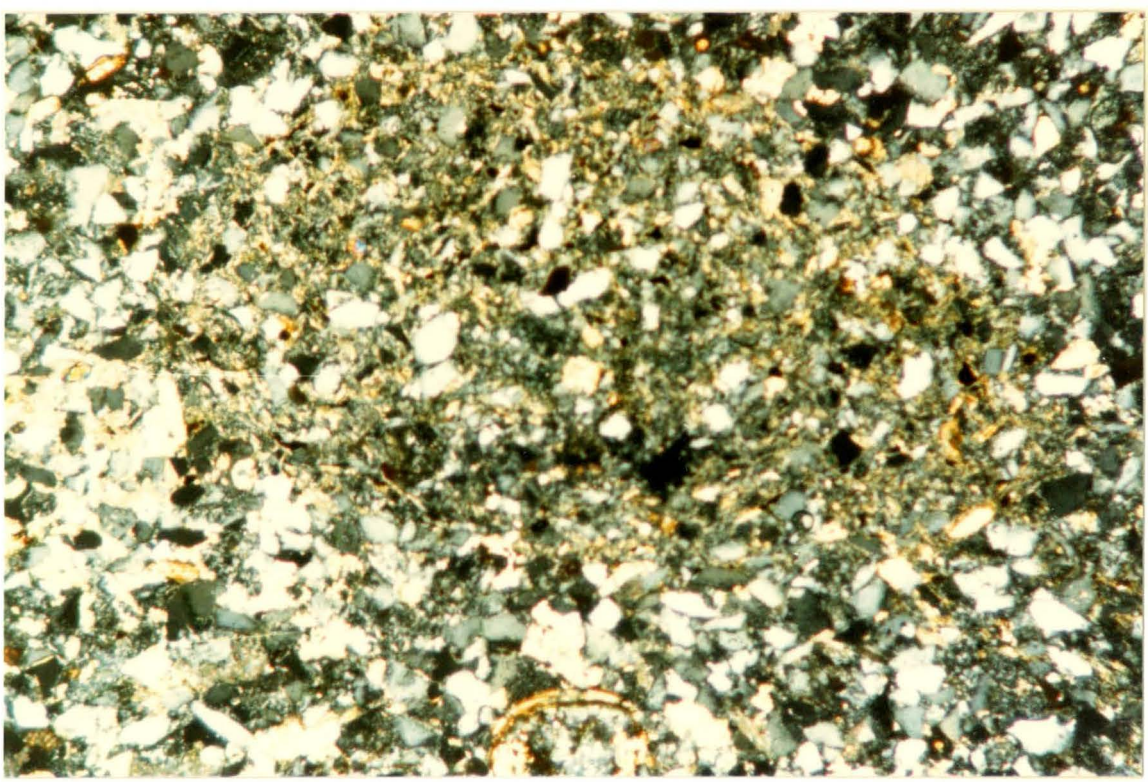

constituents are bivalves, brachiopods, gastropods, ostracods, and bryzoans. Non-carbonate detrital grains are quartz, feldspar, phosphate, and celestite. Authigenic pyrite and hematite are ubiquitous. Stylolitization is present on a minor scale.

3.4.1 Fossil Fragments

Bivalves, brachiopods, gastropods, and ostracods account for the vast majority of the fossil material, in that order of descending importance. Some fragments display well preserved shell microstructure while others have had their structure obliterated by replacement (Plates 3.11-3.13). Characteristics of the shell fragments are identical in all three lithologies and therefore are discussed here under one subsection.

Fossil fragments may be distinguished taxonomically using shell microstructure as the criterion. Bivalve fragments contain two or three distinct shell microstructure layers. The outermost simple— prismatic layer is characterised by perpendicularly oriented short prismatic crystals. Thickness of this layer ranges from 25 to 65 u. The middle layer (in a triple layer shell) is the 'homogeneous' structure. It has no visible organization but individual crystals can be observed. Overall thicknesses range from 50 to 125 u. Crossed-lamellar structure forms the innermost layer. Laminae which construct this layer

Plate 3.11: Biosparite with large calcite crystals and a bryozoan fragment (center). Note the microstylolite with concentrations of insoluble material (brown), quartz, and feldspar grains along the seam. Unit 4, Section C3. XN, 63X.

Plate 3.12: Biopelmicrite containing recrystallized pelecypod fragments and a non-recrystallized brachiopod fragment showing the subparallel fibrous foliated microstructure. The pelecypod fragments show increasing crystal size of the calcite toward the centre, which is typical of a void-filling cement. Acicular cement (tiny hair-like crystals) can be seen in the large fragment (lower left). Pyrite crystals have been 'pushed' to the center of one fragment (top center) by calcite crystal growth. Note the pelmicrite cement which has a brown colour and peloidal texture. It is being neomorphosed to sparry calcite in places (upper left). Unit 8_4, Section C4. XN, 63X.

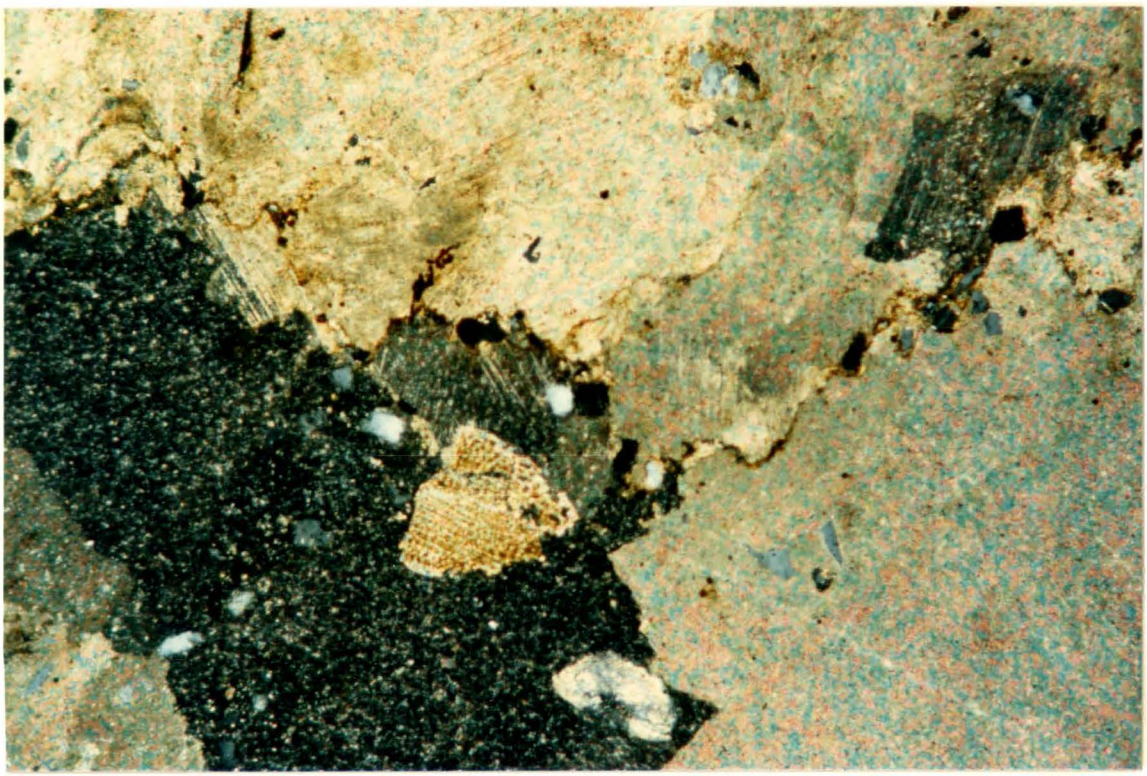

Plate 3.13: Biosparite containing intraclasts of reworked carbonate sediment (left side). The intraclast contains detrital quartz and feldspar. Unit 1L, Section C3. XN. 63X.

Plate 3.14: A biomicrite showing non-ferroan (red) shell fragments with preserved microstructure and recrystallized ferroan (purple) shell fragments. A gastropod is in the center. Some opaque pyrite crystals are visible. Note the micrite cement. Unit 6, Section C1. PL, 25X. Stained.

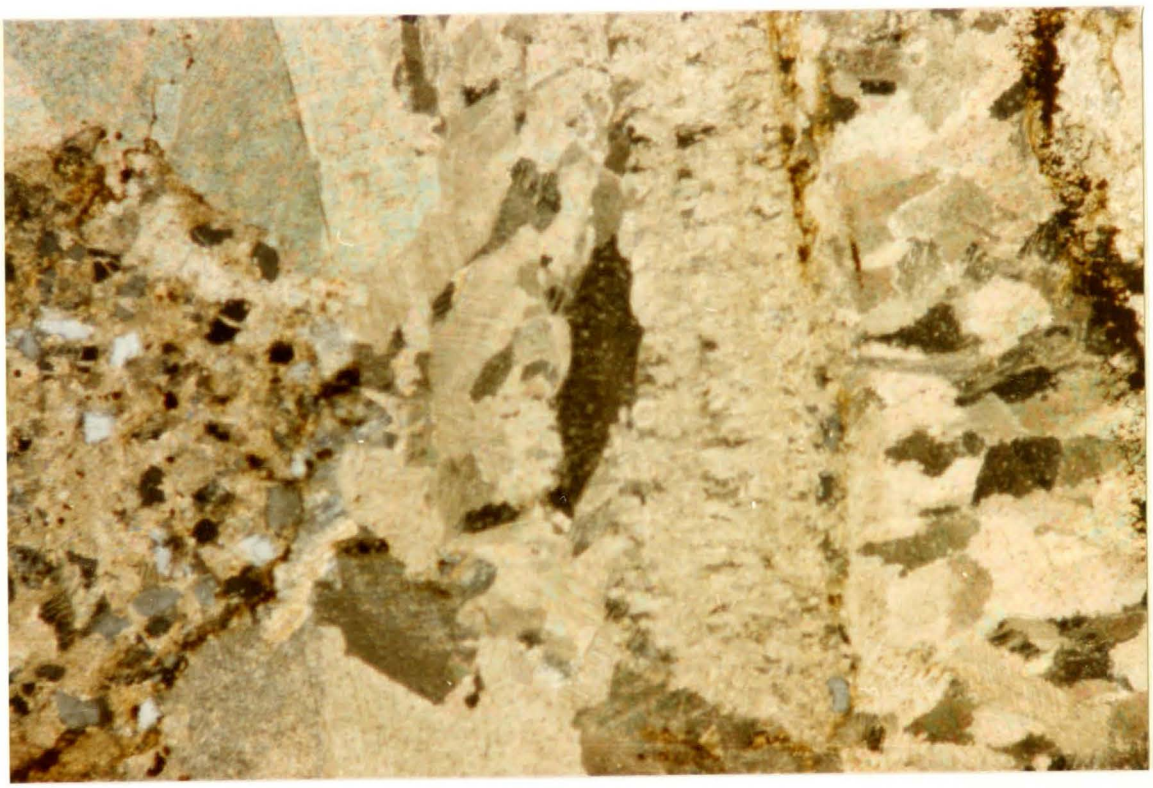

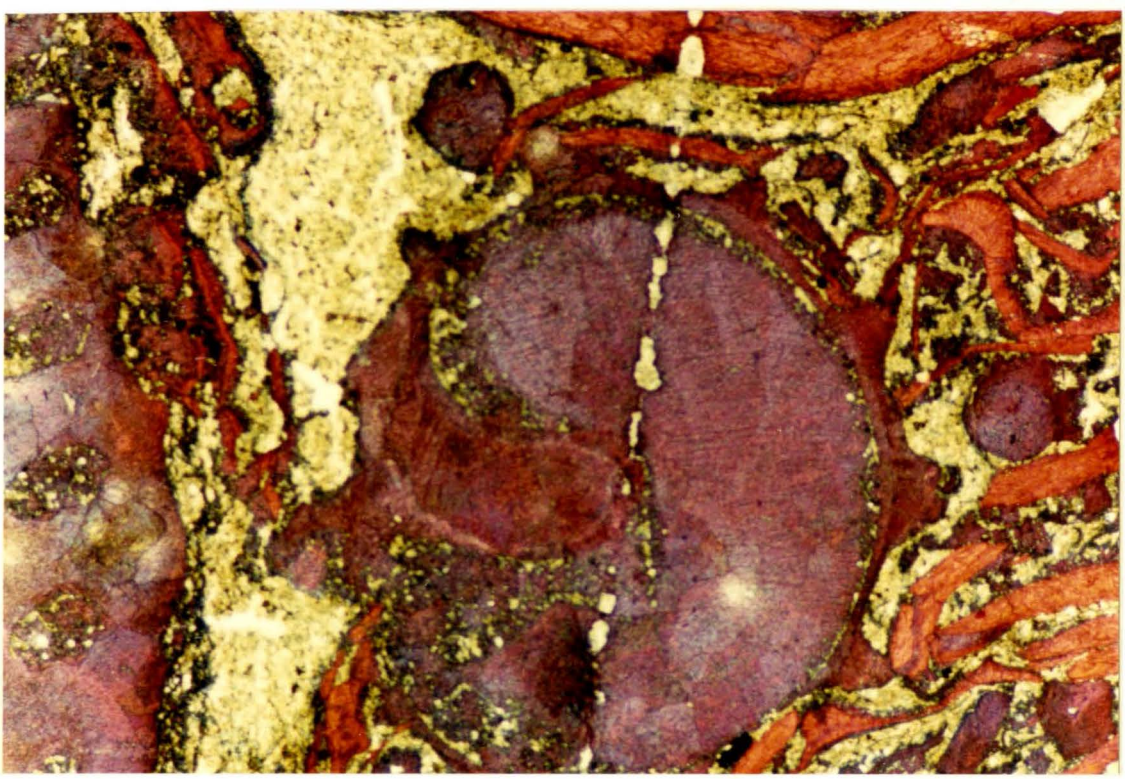

are oriented in alternating directions to provide strength to the shell (Tasch, 1980). Thicknesses of this layer span from 75 to 200 u.

Brachiopods are easily identified by their subparallel fibrous foliated microstructure which is inclined 15-20 degrees to the shell margin (Plate 3.12). It always composes a major thickness of the shell (100-200 u). Occasionally a thin (20 u) simple-prismatic layer is present on the external shell margin as a second layer. Calcite crystals are oriented perpendicular to the shell margin in this layer. Punctae are evident in some brachiopod fragments.

Gastropods observed within the samples usually have two layers preserved. The outer layer is simple-prismatic, whereas the inner layer is crossed-lamellar structure. The inner layer often consists of two or three sub-layers which are discernible because of alternating laminae directions.

Ostracods have a distinctive microstructure, consisting of a non-ferroan, finely fibrous calcite layers (20 u thick). The c-axes of the crystals are perpendicular to the surface of the shells (Dickson, 1966). The calcite layer is enveloped on its inner and outer surfaces by chitinous/proteinaceous layers approximately 10 u in thickness. These layers appear brown in colour when viewed in thin section.

Carbonate staining reveals that shells and shell

fragments with preserved microstructure are composed of non-ferroan calcite (Plate 3.14). Richter and Fuchtbauer (1978) suggest that skeletons remain almost free of iron due to the lack of recrystallization because the original shell composition was stable under diagenetic conditions. Low-magnesian calcite is more stable than high-magnesian calcite and aragonite. Recrystallization of aragonite to calcite destroys the shell microstructure. Formerly high-magnesian calcite shells are difficult to distinguish from primary low-magnesian calcite shells. The reason for this is that the transition from high- to low-magnesian calcite does not destroy the shell microstructure (Richter and Fuchtbauer, 1978). An example of this is shown in brachiopods which are always preserved as non-ferroan calcite with excellent microstructure because they used low-magnesian calcite for their shells (Tasch, 1980).

Some shell fragments display a well preserved non-ferroan, simple-prismatic outer layer. Ferroan, radiaxial fibrous or sparry calcite cement fills the remainder of the void. Using the criteria of Richter and Fuchtbauer (1978), these shells must have had an outer prismatic layer composed of low-magnesian calcite. The inner shell layers were composed of high-magnesian calcite which dissolved, leading to the infilling of remaining void space with ferroan calcite.

Bryzoan zoaria fragments comprise only a minor portion

of the fossil fragment content in the limestones, and are all composed of non-ferroan calcite. Fragment sizes range from 0.5 to 0.75 mm (Plate 3.11).

3.4.2 Detrital Mineral Grains

Most of the limestones contain detrital grains of feldspar, quartz, phosphate, celestite, and intraclasts. All are present in minor quantities accounting for only 1-3% of the rock volume. Feldspar is ubiquitous and appears as small (.01-1.0 mm) subangular to subrounded grains scattered throughout the samples (Plate 3.11). The feldspars are often concentrated along microstylolite seams and swarms, due to pressure solution of the surrounding carbonate material (Plate 3.11). Some of the larger grains exhibit albite twinning and have been identified as andesine and labradorite using the Michel-Levy extinction angle method. In sample C3-4, the feldspar grains have altered to calcite and display very irregular grain boundaries. Quartz is present as small (.03-.05 mm) subangular grains scattered throughout samples C3-4 and C3-1L. There are some concentrations of quartz grains along microstylolite seams. Phosphate fragments ranging in size from 0.2 to 1.25 mm are seen in sample C3-1L and $C4\text{-}8_4$. The fragments are amber coloured when viewed under plane light and isotropic under crossed nicols. Structural organization and the shape of the fragments suggest a

biogenic derivation. Sample C1-6 contains a trace of celestite grains averaging .3-.5 mm in size. The grains exhibit well defined cleavage with the planes oriented at right angles. Alteration of the celestite to calcite is apparent on all celestite grains. Intraclasts of reworked carbonate sediment are present in sample C3-1L (Plate 3.13). They are composed of micritic matrix encompassing subangular to subrounded feldspar grains, which average .05-.10 mm in size. Opaque mineral grains of a similar size are also present within these intraclasts. Reworked carbonate sediments do not survive long distance transport, which suggests a near-source depositional site for these sediments (Scholle, 1978).

3.4.3 Cementation and Diagenesis

Sparry calcite appears to have cemented the limestones shortly after deposition. This cement typically has a low ferrous iron content (ferroan calcite I type, .5-1.5 % FeO), and is found as interparticle void-filling sparry mosaic and radiaxial cement. Crystal size range is .05-.75 mm, increasing towards the center of the void. Several samples contain considerable amounts of very fine grained non-carbonate material (silt, mud, clay) which infills some of the interparticle void spaces.

Pelmicrite cement is present in sample C4-8_4 which has been classified as a biopelmicrite, and contains

approximately two-thirds pelmicrite. It is described as fine, brown calcite matrix with peloidal texture (Plate 3.12).

Sample C4-8_4 contains acicular calcite cement (type A according to Richter and Fuchtbauer, 1978) which occupies less than 5% of the interparticle and biomoldic void space. The crystals are fibrous and acicular in habit.

Carbonate staining revealed that the acicular cement is ferroan calcite I type (Lindholm and Finkelman,1971). Acicular cement forms during early diagenesis (Richter and Fuchtbauer, 1978). Later cementation resulted in infilling of the void spaces with slightly more ferroan sparry calcite mosaic. Isometric calcite cement within the biomoldic voids suggests a considerable time gap between dissolution of the shells and cementation of the voids (Richter and Fuchtbauer, 1978) The sparry mosaic calcite is easily distinguished from the acicular cement because it is not in optical continuity.

Pyrite precipitation is also thought to occur early in the diagenetic history of these limestones. Tiny (.005-.01 mm) subhedral and euhedral crystals precipitated as crustal linings, and in the basal portions of the biomoldic voids, resulting in geopetal structures. Occasionally there is a concentration of pyrite in the center of the voids, surrounded by calcite cement. The calcite cement is thought to have nucleated on the walls of the void spaces and

propagated towards the center, pushing the pyrite crystals towards the center (Plate 3.12).

A final calcite event cemented the remaining pore spaces and infilled the biomoldic voids. This is an isometric sparry calcite mosaic cement and radiaxial fibrous cement of ferroan calcite II type (1.5-2.0% FeO). Crystal sizes range from .05 to .5 mm in pore spaces and from .5 to 1.0 mm within the biomoldic voids. Occasional pore spaces show remnants of ferroan calcite type 1 cement (first cementation event) which appears to have been partially or completely dissoved and replaced by ferroan calcite II.

Micrite is observed to be recrystallized to sparry calcite mosaic in a neomorphic process (Plate 3.12). This process took place within gastropod shells and interparticle pore spaces which were originally infilled with lime mud. Early developmental stages of micrite replacement initiated at fossil fragment or biomoldic void margins, where calcite was already present.

The initial stage of pressure solution is represented by sutured crystal contacts. This is followed by the development of microstylolite swarms or "horsetails", which are in the process of amalgamation to one distinct "microstylolite" seam (Plate 3.11). All the stages of development can be observed in the thin sections. The concentrated material which composes the microstylolite consists of insoluble organic matter, feldspars, and

opaques.

3.5 SHALES

3.5.1 Concretions

Shale units throughout the stratigraphic sections contain limey ferruginous concretions. Most concretions are randomly scattered, but some are concentrated along distinct horizons or beds. Concretion shapes are oblate spherical, and spherical. Many contain gastropods, bivalves, brachiopods, and ammonites. Most concretions also contain well preserved plant debris, and small amounts of quartz, feldspar, pyrite, and hematite. Modal percentages from point counts are given in Table 3.5.

Berner (1971) suggested that the causative factor of calcite concretion formation is heterogeneous nucleation by shell fragments. Decaying organisms, rich in proteins may be responsible for calcite precipitation during early diagenesis (Weeks, 1957). Ammonia generated by tissue decay, creates a high-pH microenvironment causing calcium carbonate to precipitate from the pore fluids to form a concretion. Berner (1971) also suggested that calcium carbonate may not be the first product precipitated during alkaline putrefaction. Both field and experimental evidence indicate that natural calcium soaps, called adipocere, are precipitated first (Berner, 1968a). Eventual breakdown of

Table 3.5: Modal percentages of concretion constituents.

Section Number	Microspar Matrix	Sparry Calcite	Feldspar	Quartz	Pyrite	Hematite	Plant Fragments	Fossils
C1-15c	73.0	4.2	1.8	—	2.4	.3	19.2	Yes
C1-17c	87.95	3.26	1.95	.33	4.23	.65	1.63	Yes
C3-1c	85.0	3.3	—	—	2.5	3.0	6.2	Yes
C4-8c	82.0	10.0	—	—	5.0	—	3.0	Yes

the soap results in the calcium carbonate concretion. The time of the concretion formation was probably during early diagenesis (Berner, 1971). Supporting evidence comes from the presence of uncrushed fossil fragments, plant debris, and mineral grains (e.g. feldspar) all of which are well preserved in the concretions, but absent in the surrounding shales.

3.5.2 Calcium Carbonate

Concretions are composed of 77-93% calcium carbonate, most of which is microcrystalline sparry calcite matrix (Plates 3.15-3.18). The average calcite crystal size is 5-15 u. Ferrous iron content in the calcite averages 1.0-1.5% (ferroan calcite I type; Lindholm and Finkelman, 1971). The remaining calcite occurs as fracture-filling and void filling cement, classified as either non-ferroan or ferroan I and II type. Crystal sizes range from .1 to .75 mm for these cements.

3.5.3 Fossils

Complete shells and fragments of bivalves, brachiopods, gastropods, and ammonites are present in some concretions. The average size of shells ranges from 0.01 to 1.0 cm, and account for approximately 10% of the volume. All shell fragments, except brachiopods have been dissolved out, and the remaining biomoldic voids have been infilled with sparry

Plate 3.15: A concretion with microcrystalline calcite matrix. Void-filling sparry calcite is seen within part of a gastropod shell (right side). Unit 8, Section C4. XN, 63X.

Plate 3.16: Concretion showing hematite staining around pyrite crystals and as 'oxidation fronts'(left side). Displacement of the front can be seen along a small microfracture (infilled with sparry calcite). A shell fragment can be seen in the lower right. Unit 1, Section C3. XN, 63X.

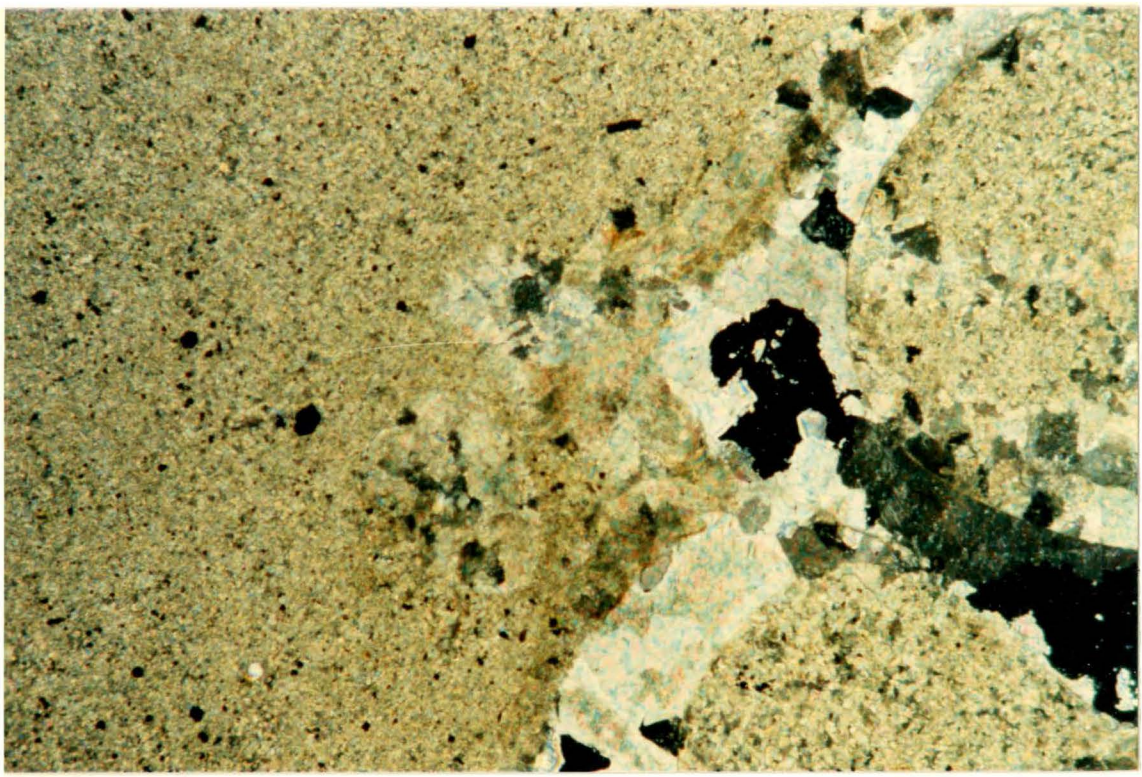

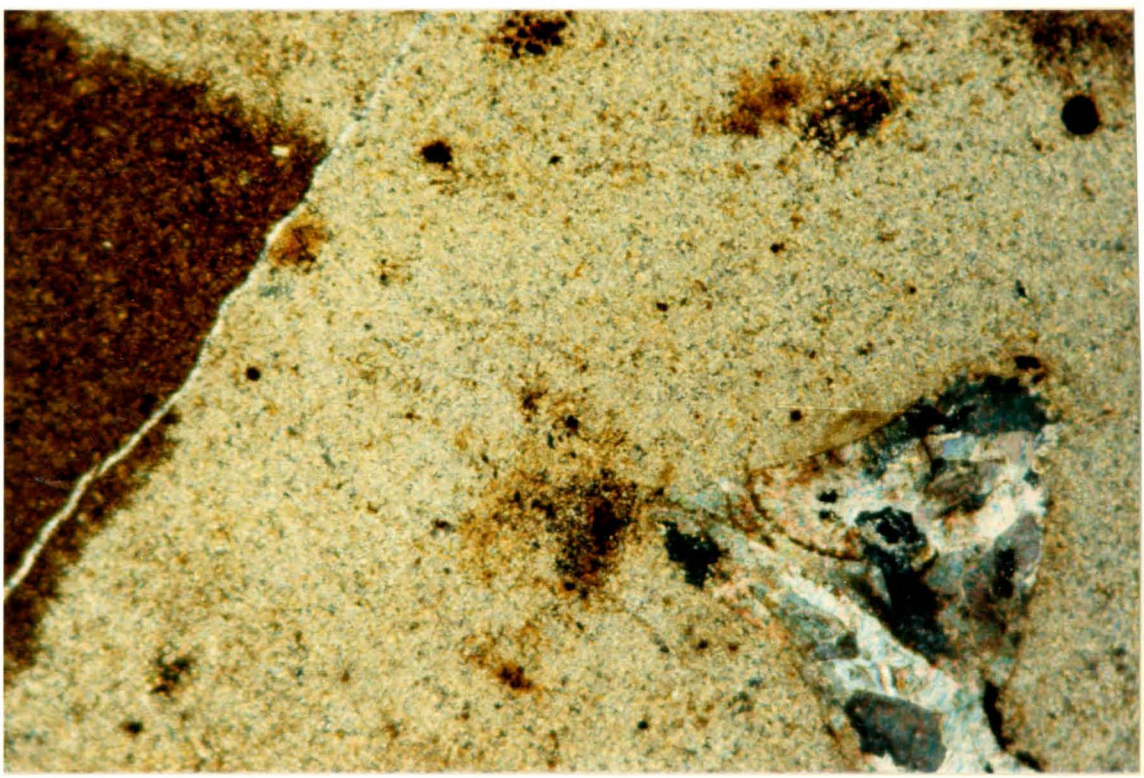

Plate 3.17: Microcrystalline calcite matrix of a concretion containing detrital quartz and feldspar. A large plant fragment can be seen in the upper right. Unit 15, Section C1. XN, 63X.

Plate 3.18: Three plant fragments within a concretion. Note the hematite, pyrite and calcite associated with the fragments. Unit 15, Section C1. XN, 63X.

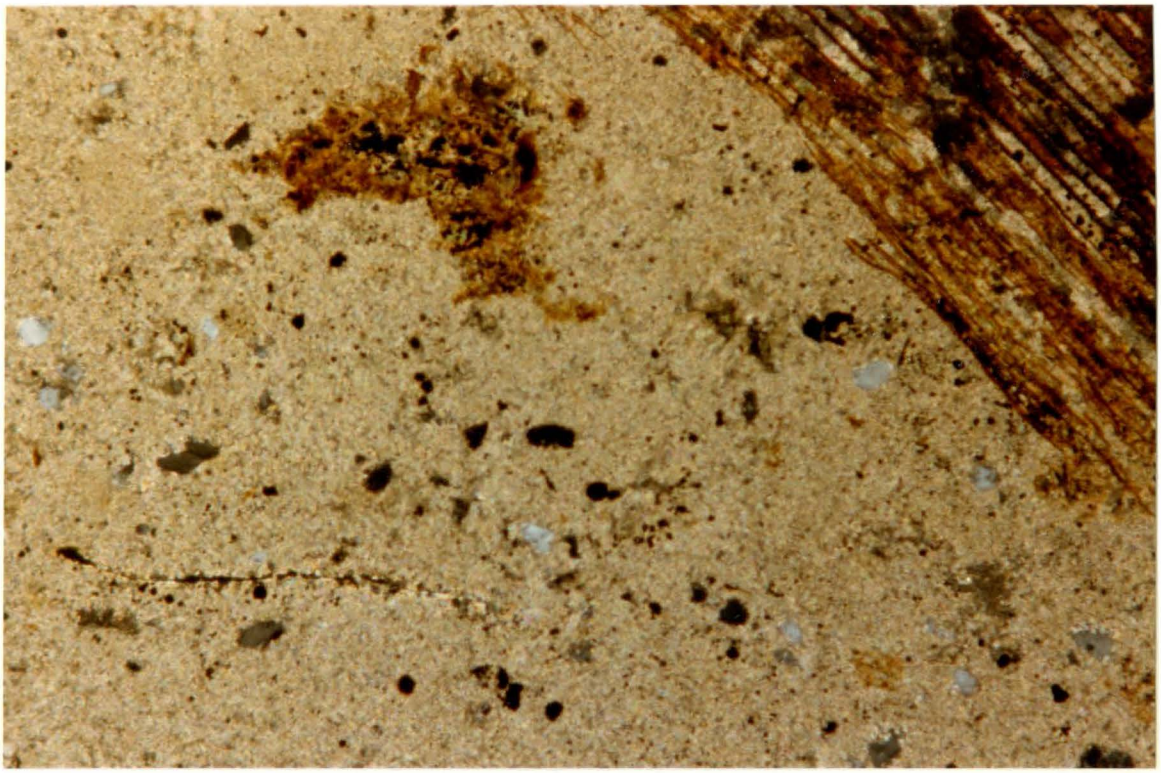

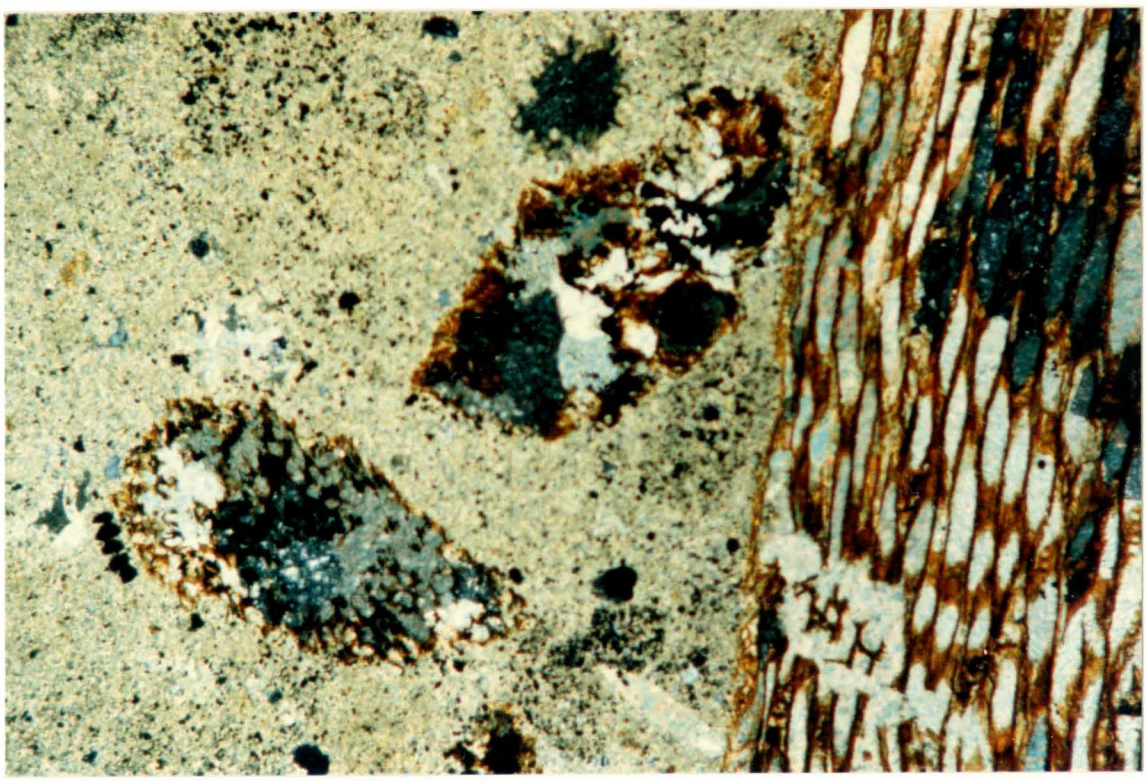

calcite cement (Plate 3.15). Crystal sizes for the sparry calcite cement range from .01-.5 mm, and increase in size towards the void centers. This cement is consistently the most ferroan calcium carbonate in the concretions (ferroan calcite types I and II; Lindholm and Finkelman, 1971). Brachiopod shell fragments are composed of non-ferroan calcite and have retained their microstructure. Identifiable fossils include the bivalve Bositra sp. in samples C1-15c and C1-17c, and the gastropod Cryptalaux sp. in C3-4 and C4-8_4.

3.5.4 Plant Fragments

Plant fragments are very abundant in the concretions. Well preserved woody, cellular structure is evident and often accentuated by pyrite and hematite. Organic cell walls are brown in colour and the hollow cells are infilled with sparry calcite cement (Plates 3.17, 3.18).

3.5.5 Mineral Components

Concretion samples of C1-15 contain trace amounts of subangular monocrystalline quartz grains. The quartz grains average .06 mm in size and show undulatory extinction (Plate 3.17). Concretions at levels C1-15 and C1-17 contain 5-10% subangular feldspar grains, which range in size from .02-.08 mm (Plate 3.17).

Traces of authigenic pyrite are ubiquitous except in

void-filling calcite. Crystals show random distribution throughout the concretion, but sometimes show concentrations along the margins of fossil and plant fragments (Plates 3.17, 3.18). Pyrite crystallized as crustal linings, and geopetal structures within biomoldic voids prior to infilling by ferroan calcite cement.

Authigenic hematite is found throughout the concretions, except in the void-filling calcite. Hematite is associated with plant debris and pyrite, but also occurs as iron staining. Textures exhibited by the hematite include dendritic patterns associated with microfractures, and oxidation halos around pyrite crystals. Concretions often exhibit banding due to differential hematite staining, and bands reminiscent of "oxidation" fronts created by pore fluid movement (Plate 3.16). These bands or zones are often cross-cut by microfractures infilled with clean sparry calcite. Displacement along such microfractures is shown in Plate 3.16.

CHAPTER 4: PALEONTOLOGY

4.1 AMMONITE SYSTEMATICS

Ammonite shell dimensions used throughout the systematic descriptions are summarized diagrammatically in Figure 4.1.1.

Class Cephalopoda

Order Ammonoidea

Family Tulitidae Buckman, 1921

Genus *Bullatimorphites* Buckman, 1921

Subgenus *Kheraiceras* Spath, 1924

Bullatimorphites (*Kheraiceras*) *bullatus* (d'Orbigny) ♀

Pl. 1, figs. 1a-b, 4a-c.

Material: Six complete specimens and six phragmocone fragments from Units 3, 6 of C3-Alto de Teeolutla and Unit 2 of C4-Alto El Variado.

Description: Inner whorls of these macroconch specimens have very tight sphaeroconic coiling but the mature body chamber portion of the outer whorl becomes elliptical and egresses strongly. The spindle-shaped whorls are very depressed in the phragmocone but the ultimate half-whorl, consisting of the body chamber, is strongly contracted such that it is markedly narrower than the phragmocone.

Figure 4.1.1: Ammonite shell dimensions used throughout the systematic descriptions.

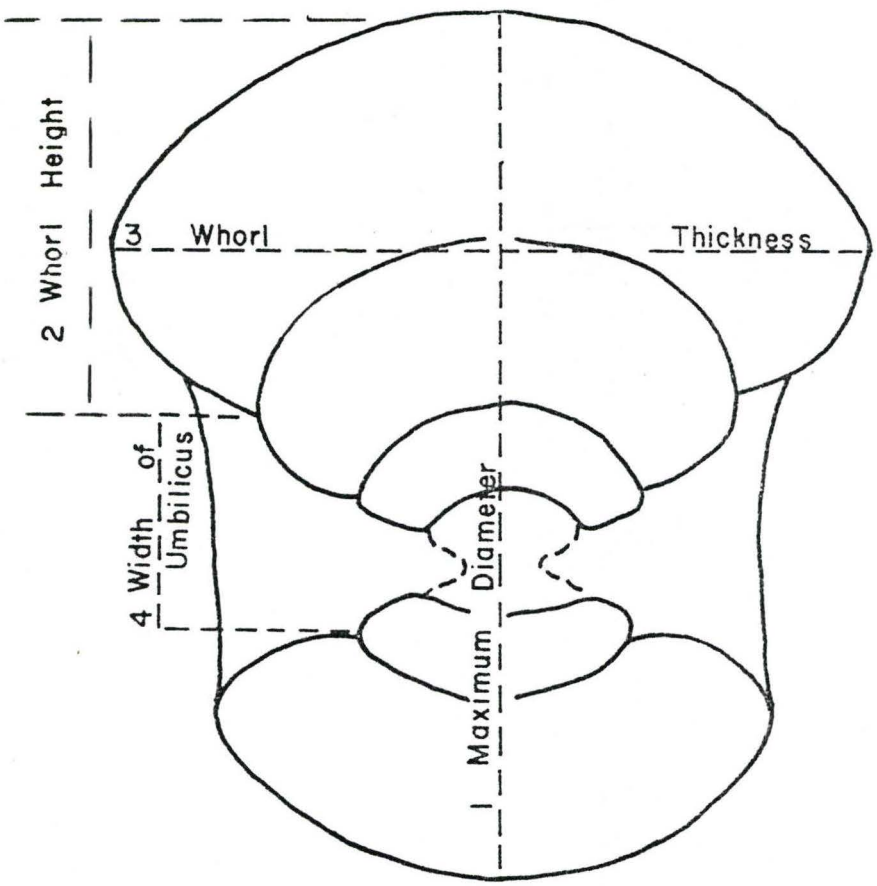
2 Whorl Height
3 Whorl Thickness
4 Width of Umbilicus
1 Maximum Diameter

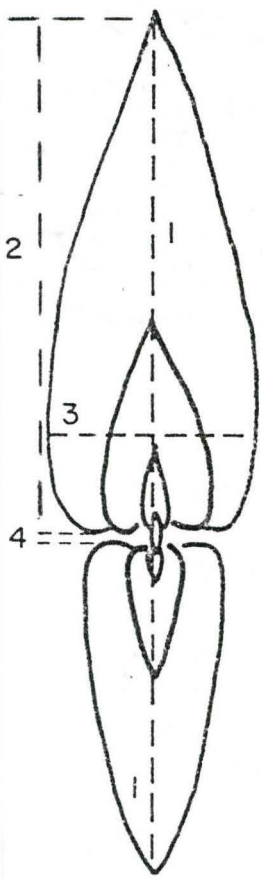
2
1
3
4
1

Phragmocone whorls are almost as wide as the shell diameter. Whorl shape combined with the sphaeroconic coiling develops a very inflated, globular phragmocone (Fig. 4.1.2). Specimen diameter ranges from 60 to 80 mm.

The narrow umbilicus is funnel-shaped. With the beginning of the body chamber, the whorl is contracted and deviates from the spiral of the phragmocone causing the umbilical seam to extend radially and then bend adorally through an angle of 90 to 100 degrees. There is a well developed, almost vertical, umbilical wall with rounded umbilical edge.

The blunt ribs are straight and pass evenly over the venter. The single indistinct primary ribs at the umbilical edge, divide into two or three secondary ribs at approximately one-third whorl height, and increase slightly in prominence as they pass over the venter. Primary ribs are very blunt on the body chamber and disappear completely near the peristome. Secondary ribs are continuous to the peristome but become less prominent and more widely spaced on the body chamber. The body chamber occupies one-half whorl and the aperture is simple and contracted.

The septal suture is only partially visible on a slightly abraded specimen at a diameter of 67 mm (Fig. 4.1.3). The median saddle is slender with two incisions. The external lobe (E) is slender and shorter than the lateral lobe (L). The lateral saddle is broad and

Figure 4.1.2: Cross-section of Bullatimorphites (Kheraiceras) bullatus at a diameter of 67 mm. 1X.

Figure 4.1.3: Incomplete external septal suture of B. (Kheraiceras) bullatus. 1X.

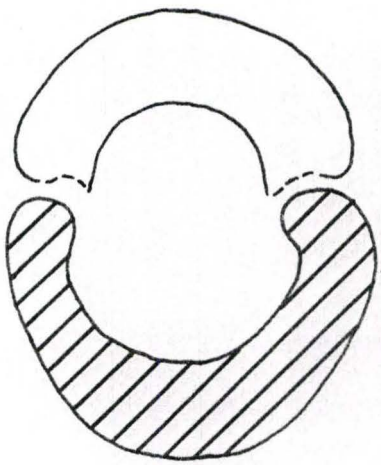

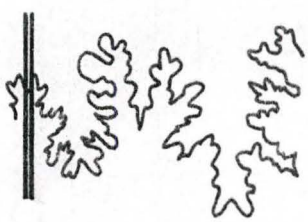

bifid with a well developed incision. L is trifid, broad and almost symmetrical. This suture is very similar to the one figured by Quenstedt (1847).

Remarks: The Coauilote specimens are identical to B. (Kheraiceras) bullatus figured by Westermann et al. (1984) who noted that both the subgenus and species are widespread. The only other Kheraiceras specimen figured previously from Mexico is the holotype of B. (K.) v-costatus (Burckhardt). It differs in the curved secondary ribs of the intermediate whorls forming blunt ventral chevrons but unfortunately the holotype is lost making specific comparison difficult (Westermann et al., 1984). The type species of the subgenus Kheraiceras, K. cosmopolita, was designated by Parona and Bonarelli (1895) based on the holotype figured by Waagen (1875).

At Coauilote, B. (Kheraiceras) bullatus is associated with Epistrenoceras hystricoides Rollier which is known to be from the Retrocostatum Zone of the Upper Bathonian of Europe (Elmi, 1967; Westermann and Callomon, unpublished).

Bullatimorphites (Kheraiceras) bullatus (d'Orbigny) ♂

Pl. 1, figs. 2a-b, 3a-c.

Material: One complete and one phragmocone specimen from Unit 2 of C4-Alto El Variado. The phragmocone is severely abraded.

Description: This microconch specimen attains sizes of 25-35 mm. The phragmocone has elliptical coiling but the mature body chamber becomes strongly elliptical and egresses. The spindle-shaped whorls of the phragmocone are strongly depressed but the ultimate three-quarters whorl is contracted becoming narrower and less depressed than the phragmocone. The phragmocone is globular with a wide and broadly rounded venter. The contracted body chamber has a depressed subovate whorl section with flattened whorl sides. The body chamber occupies three-quarters of a whorl and the aperture is incomplete. The funnel-shaped umbilicus has an almost vertical umbilical wall. The umbilical edge is sharp in the phragmocone but becomes increasingly rounded in the body chamber.

The ribs are blunt, straight and pass evenly across the venter. Primary ribs are indistinct at the umbilical edge and divide into three secondary ribs at approximately one-third whorl height. The costulation increases in prominence as it passes over the venter. Secondary ribs are most prominent on the phragmocone and gradually become more blunt and widely spaced on the body chamber. The septal suture is not visible.

Remarks: Inner whorls and costulation of the Coauilote specimens are very similar to the macroconch B. (Kheraiceras) bullatus. In view of the morphological similarity and the coexistence of the two forms in the same

horizons and localities, it is very likely that these smaller forms are the corresponding microconchs.

These specimens are most similar to Treptoceras laurenti figured by Enay (1959) but this genus is no longer considered valid. Arkell (1952) proposed the genus Bomburites for these small globular 'bullati'. Several of the figured Bomburites sp. (e.g. Grossouvre, 1891; Parona and Bonarelli, 1897) have a flared collar and lappets at the peristome immediately following the terminal constriction. The flared collar is often preceeded by a contracted, smooth band. These features distinguish the small forms from the macroconchs of Kheraiceras and Bullatimorphites which have simple peristomes. The specimens of Bullatimorphites "(Bomburites)" microstoma microstoma figured by Westermann (1958) lack the flared collar and contracted bands but the apertures are probably incomplete.

Family Parkinsoniidae Buckman, 1920

Genus Epistrenoceras Bentz, 1928

Epistrenoceras hystricoides Rollier

Pl. 1, figs. 6a-b, 7, 8a-b.

Material: Nine complete or almost complete specimens and 124 body chamber and phragmocone fragments from Units 1-3, 6 of Section C3-Alto de Teeolutla and Units 1-2 of C4-Alto El Variado.

Description: Septate specimens, 25 to 40 mm in diameter, have serpenticone coiling and the whorl section varies from subcircular to ovate with the maximal whorl width at two-fifths whorl height (Fig. 4.1.4).

The moderately strong prosiradiate ribbing has an adoral inflexion at approximately three-fifths whorl height. Specimens average 18 primary ribs per half-whorl. The dense secondary ribs end in blunt nodes along the sulcate venter; prominence depends on the development of blunt nodes. Some specimens have pronounced nodes while they are very blunt on others. On one small phragmocone fragment (20 mm diameter), the ventrolateral nodes are sharper, more prominent and develop into ventrolateral spines on the ultimate quarter-whorl. Bisected complete specimens show the development of ventrolateral spines at a diameter of 8 to 10 mm. The spines increase in length to approximately 20 mm diameter, with some spines attaining lengths of 1.8 mm. Beyond 20 mm diameter, the spines become abruptly reduced to ventrolateral nodes which persist on the remaining whorls. Two of the the bisected complete specimens (29.5 and 33.5 mm diameter) appear to be mature because the last 4 to 6 septae are approximated.

The adult body chamber occupies approximately three-eighths of a whorl and is subcircular to ovate. The aperture is simple. A portion of the septal suture is visible on one small phragmocone (20.25 D) and is shown in

Figure 4.1.4: Cross-section of Epistrenoceras hystricoides. 1X.

Figure 4.1.5: Incomplete external suture of Epistrenoceras hystricoides at a diameter of 20.25 mm. 1X.

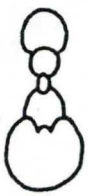

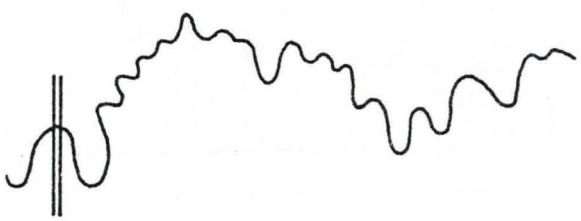

Figure 4.1.5. The suture of E. hystricoides has not previously been figured thus rendering comparison impossible.

Remarks: The Coauilote specimens are more involute than E. contrarium (d'Orbigny, 1846, Pl. 145, figs. 1,2 only) and have variocostate secondary ribbing. These differences along with the presence of ventrolateral spines during the adolescent growth stage ally the Coauilote specimens with E. hystricoides Rollier. Dietl (1978) considered E. hystricoides Rollier as a descendant of Strenoceras/Parastrenoceras rather than Spiroceras sp. This places E. hystricoides in the Parkinsoniidae rather than the Spiroceratidae. Dietl (1978) also suggested that E. hystricoides was the forerunner of the Parapatoceratids. The suture line of E. hystricoides (Fig. 4.1.5) is very reduced and similar to that of Parapatoceras sp.. Ventrolateral spines in juvenile stages and the character of the ventral interruption throughout ontogeny of E. hystricoides are similar to those observed in Parapatoceras distans. E. hystricoides displays some shell aberration (Dietl, 1978).

Subfamily Parapatoceratinae Buckman, 1926

Genus Parapatoceras Spath, 1924

Parapatoceras distans (Baugier & Sauze)

Pl. 5, figs. 5-9.

Material: Numerous phragmocone and body chamber fragments found almost exclusively within limey concretions of Units 15 and 16 of Sections C1-Arroyo El Rincon and C2-Arroyo El Campamento.

Description: The whorls form is a loose, planar but irregular spiral of which the ultimate mature quarter whorl may be straight. The first three-quarters whorl is involute but deviates into the loose spiral. The spiral form of the subsequent whorls is variable because W (expansion rate) varies throughout the ontogeny of some specimens (Fig. 4.1.6).

The whorl section changes shape slightly throughout ontogeny; being transversely oval in the juvenile whorls, circular in the middle whorls and dorso-ventrally oval in the last whorls. Whorl height and width exceeds 1 cm only in very large specimens.

Ribs are straight and unsubdivided with some variability. The protoconch and first whorl lack costulation; weak ribs appear early in the second whorl. The first few ribs are rectiradiate, gradually becoming slightly prosiradiate. In the middle whorls, the ribs regain a rectiradiate orientation and they become very prominent in the middle and outer whorls. There are approximately 22 ribs per half-whorl, normally evenly spaced, but occasionally some irregularity appears. The

Figure 4.1.6: Reconstruction of shell spirals for *Parapatoceras distans*. 1X.

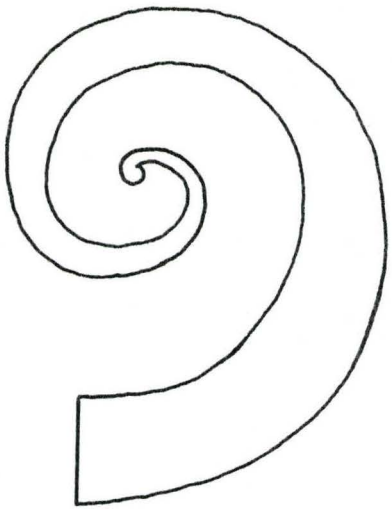

a

b

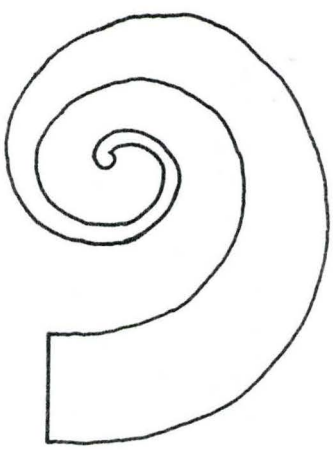

c

ribs are slightly weaker but pass evenly and straight across the venter. In the siphonal region, the ribs are strongly interrupted by a smooth band, and each rib has a sharp and prominent terminal tubercle. Each rib also has a much less prominent dorso-lateral tubercle. The body chamber occupies approximately one-half whorl and the ultimate quarter whorl is straight in some specimens and extends radially from the spiral. Ribs and tubercles lessen in prominence toward the apertural end of the body chamber. The aperture is simple and the septal suture is not visible on the specimens from Coauilote.

Remarks: The specimens collected near Coauilote are identical to Parapatoceras distans as figured by Dietl (1978). P. tenue (Baugier & Sauze) occurs in northern Chile together with P. distans (Westermann et al., 1984). P. distans has more prominent tubercles and rectiradiate ribbing than P. tenue which has more closely spaced prosiradiate ribbing and weak tubercles. At Coauilote, P. distans is associated with typically Lower Callovian ammonite species. Dietl (1978) notes that P. tenue is found only in the Upper Bathonian of Europe, whereas P. distans extends into the Lower Callovian.

Dietl (1978), based on investigation of Dogger heteromorphs of Europe, concluded that shell coiling aberration must be related to a specific mode of life, i.e. stillwater basinal areas according to abundance and

maximum variation of the specimens. He suggested that the high degree of variability within one species, especially the loss of bilateral symmetry, indicates that the heteromorphs were not selected for active swimming. He suggested a crawling locomotion, mainly on plants, for the Dogger heteromorphs based on their frequent association with "Posidonae" bivalves (eg. Bositra sp.) and plant debris.

This heteromorph-Bositra association occurs at Coauilote and many other Middle Jurassic outcrops of Europe (Arkell, 1956) in black shales. The conclusions of Dietl (1978) are based on the premise that "Posidonae" bivalves are benthic. This seems erroneous based on; (1) the lithologic facies association and lack of benthos which suggest oxygen-deficient conditions, and (2) the work of Jefferies and Minton (1965) which concludes that it is feasible and probable that "Posidonae" bivalves had a planktonic mode of life. Further paleoecological discussion may be found in Section 5.5; Black Mud Community.

Dietl's (1978) reasoning of non-selection for streamlining of the heteromorphs neglected the possibilty that they may have been neutrally buoyant which allowed them to float in the water column. Ward (1976) modelled heteromorph ammonite replicas from sculpting wax. He concluded that the heteromorphs were nearly neutrally bouyant for the complete living animal and shell and that they hung vertically in the water column (see

Fig. 4.1.6 for probable orientation of P. distans). Based on buoyancy and living position studies, Ward (1976) concluded that many heteromorphs were adapted to a planktonic rather than benthic mode of life. Thus it seems more likely that the Dogger heteromorphs did not need streamlined shell morphologies because they were planktonic floaters and not active swimmers. This conclusion also agrees with the lithologic facies association.

Dietl (1978) suggested that Parapatoceras is the evolutionary intermediate between the Upper Bathonian Epistrenoceras hystricoides and the Callovian Paracuariceras sp..

Genus Paracuariceras Schindewolf, 1963

Paracuariceras cf. incisum Schindewolf

Pl. 4, fig. 4.

Material: One body chamber fragment from Unit 15 of Section C1-Arroyo El Rincon.

Desription: The body chamber fragment is 4.61 mm in length and has a diameter of 6.8 mm at the apertural end tapering to 4.7 mm at the apical end of the fragment. The whorl section is circular and the shell has an orthoconic form except for a slight dorsally upward curvature of the apical portion and the tight coiling of the protoconch (Fig. 4.1.7) (Dietl, 1978).

Ornamentation consists of rursiradiate labial ridges

Figure 4.1.7: Reconstruction of the shell spiral for Paracuariceras incisum. (After Dietl, 1978). 2.25X.

and furrows which are strongest on the flanks and less prominent on the dorsal and ventral surfaces. Normally a ridge is preceeded adapically by a furrow but the converse also occurs infrequently. The general appearance is one of alternating ridges and furrows.

Remarks: Dietl's (1978) plate illustrating Paracuariceras incisum Schindewolf allowed identification at least to the generic level. Paracuariceras sp. is strictly Callovian in age. It appeared in the middle Macrocephalus Zone and became extinct in the Jason Zone (Dietl, 1978). He also discussed an evolutionary sequence of; Upper Bathonian Epistrenoceras hystricoides Rollier, followed by Upper Bathonian-Lower Callovian Parapatoceras sp., followed by Paracuariceras sp. which is Callovian in age. An identical evolutionary sequence is observed in the Tecocoyunca Group.

Family Phylloceratidae Zittel, 1884

Subfamily Phylloceratinae Zittel, 1884

Genus Phylloceras Suess, 1865

Phylloceras cf. plicatum Neumayr

Pl. 2, figs. 2a-b, 3, 5.

Material: Numerous complete specimens were found in Units 6, 7 of Section C1-Arroyo El Rincon.

Remarks: This species is characterised by an involute,

compressed shell, deep umbilicus with rounded shoulder, dense fine radial lirae on the test and some less pronounced radial folds appearing periodically on the whorl sides. Shell diameter generally does not exceed 50 mm.

Subfamily Calliphylloceratinae Spath, 1927

Genus Ptychophylloceras Spath, 1927

Ptychophylloceras plasticum (Burckhardt)

Pl. 2, figs. 1a-b, 4a-b, 6a-b, 7.

Material: Complete phragmocone specimens from Units 1-4, 5-7, 14-18 of Section C1-Arroyo El Rincon, Units 13-15 of Section C2-Arroyo El Campamento, Units 2-6 of Section C3-Alto de Teeolutla, and Units 1, 2, 8 of C4- Alto El Variado.

Description: Specimens are compressed and very involute with rapidly expanding inner whorls. The venter is broadly rounded and the flanks flattened. The transverse whorl section is much higher than wide with the maximal whorl width at about 1/2 whorl height (Fig. 4.1.8).

Ornamentation consists of very fine flexuous biconvex lirae which are most visible on the whorl flanks near the umbilical edge and lessen in prominence as they pass evenly over the venter. The lirae have an adoral inflexion at approximately 1/3 whorl height, extend radially, and then have a less pronounced adapical curvature at about 2/3 whorl

Figure 4.1.8: Whorl section of Ptychophylloceras plasticum. 1X.

Figure 4.1.9: Septal suture of Ptychophylloceras plasticum.
a) Specimen J2119 at 50 mm diameter. 1X.
b) Specimen C2-13 at 27 mm diameter. 1X.

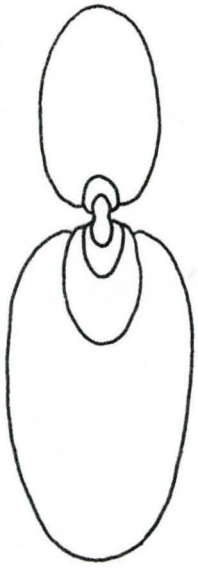

a

b

height. More prominent ornamentation observed on the specimens is furrows and labial ridges. The furrows appear at the umbilical edge and are moderately deep to approximately 1/3 whorl height beyond which they are shallow. At approximately 2/3 whorl height, the furrows are accompanied by a labial ridge immediately adoral of the furrow. The ridge is most prominent as it passes over the venter. Paired furrow and ridge ornamentation averages seven per half-whorl and it is visible even on internal molds. Furrows and ridges follow the same flexuous pattern as the fine lirae. Figure 4.1.9 illustrates the septal suture for two different specimens. The suture is characterised by broad lobes and diphyllic principal saddles.

Remarks: Ptychophylloceras plasticum has a large vertical range at Coauilote and is associated with typically Bathonian and Callovian Ammonitina. The genus Ptychophylloceras is Tethyan (Westermann, 1984) but its long range renders it useless for biostratigraphy. However, the Phylloceratina have long been considered an oceanic suborder associated with deep, oceanic areas. Callomon (1984) described the phylloceratids as pelagic ocean-dwellers rather than shelf-dwellers as were most ammonites. It now seems that the significance of their distribution is as indicators of proximity to former oceans. Their occurrence in the Jurassic of Oaxaca, Guerrero and parts of the North

American Cordillera reflect the proximity of the Pacific Ocean (Callomon, 1984).

Genus Holcophylloceras Spath, 1927

Holcophylloceras sp.

Pl. 2, figs. 8, 9a-b.

Material: Several specimens from Unit 15 of C1-Arroyo El Rincon and C2-Arroyo El Campamento.

Remarks: Small (1 cm) smooth, compressed involute forms with a rounded venter and periodic sigmoid constrictions on the internal mold. Holcophylloceras is a cosmopolitan genus ranging from the Middle Jurassic to Lower Cretaceous.

Family Sphaeroceratidae Buckman, 1920

Subfamily Eurycephalitinae Thierry, 1976

Genus Lilloettia Crickmay, 1930

Lilloettia steinmanni Spath ♀

Pl. 3, fig. 3a-c; Pl. 4, fig. 1a-b.

Material: Several specimens collected from Units 3 and 6 of Section C1-Arroyo El Rincon.

Remarks: L. steinmanni has a slightly compressed, globose involute form with simple costulation on the inner and middle whorls. The ribbing disappears on the body chamber. The whorl section is ovate to subtriangular. Specimens

average 70-80 mm in diameter.

Callomon (1984) indicated that the age of Lilloettia in northwestern North America was early Lower Callovian. However, the most recent review of the Eurycephalitinae of S. America by Riccardi (1985) suggested that L. steinmanni and the genus Lilloettia in Argentina are Upper Bathonian in age in South America.

Lilloettia boesei (Burckhardt) ♀

Pl. 3, fig. 1a-b.

Material: Numerous specimens from Units 3 and 6 of C1-Arroyo El Rincon.

Remarks: This species averages 55-60 mm in diameter and the ribbing is coarser than in L. steinmanni Spath. The primaries of L. boesei are more reduced than those of L. steinmanni resulting in smoother inner flanks. L. boesei is also more inflated than L. steinmanni. The identical stratigraphic range of the two species suggests that they may be variants of a single species. Callomon (1984) suggested that L. boesei may also be conspecific with the North-Cordilleran L. buckmani Crickmay. However, L. buckmani is more coarsely ribbed on the flanks than the Mexican species (Westermann et al., 1984).

Genus Eurycephalites Spath, 1928

Eurycephalites cf. vergarensis (Burckhardt) ♀

Pl. 4, fig. 4a-c.

Material: Two specimens from Unit 8 of C1-Arroyo El Rincon.
Remarks: This species has an inflated and globose shell shape. Primary ribs are prominent on the venter but disappear on the whorl flanks. Secondary ribbing appears to be absent. E. vergarensis was reported from the basal Callovian of the Andes (Riccardi, 1985). The appearance of E. cf. vergarensis in Unit 8 of Section C1-Arroyo El Rincon is very important for placing the Bathonian-Callovian boundary. It occurs slightly above the Bathonian Lilloettia-Neuqueniceras Association.

Eurycephalites cf. rotundus (Tornquist) ♀

Pl. 4, fig. 2a-b.

Material: Several complete specimens and body chamber fragments were found in Units 14, 15 and 16 of Sections C1-Arroyo El Rincon and C2-Arroyo El Campamento.
Remarks: This species is characterised by its inflated globose involute shell. The flanks of the inner whorls are smooth, but the body chamber has faint primaries. Secondary ribs are faint but present toward the venter. Some shallow radial grooves appear periodically near the umbilical shoulder fading rapidly as they approach mid-flank.

Riccardi (1985) suggested that there are transitional morphological characters and an advance in evolutionary grade from the Upper Bathonian Lilloettia steinmanni Spath to Eurycephalites vergarensis (Burckhardt) and E. rotundus (Tornquist) both of which are Callovian. The trends are; (1) an inflation of the globose shape culminating with E. vergarensis and maintained by E. rotundus, (2) decrease in prominence of secondary ribbing which disappeared completely in E. vergarensis but reappeared in E. rotundus and, (3) progressive disappearance of the lateral primary ribs which culminated with E. rotundus which has smooth whorl flanks on the inner whorls.

The association of E. cf. rotundus with other species of the Frickites bodenbenderi and Clydoniceras inflatum Associations suggests that the age of E. rotundus is Lower Callovian.

Genus Xenocephalites Spath, 1928

Xenocephalites gr. "nikitini-vicarius" (Burckhardt)/Imlay ♂

Pl. 3, fig. 2a-b; Pl. 4, fig. 3a-b; Pl. 5, fig. 1a-c.

Material: Several specimens were collected from Units 3-6, 13-15 of Section C1-Arroyo El Rincon.

Remarks: This species has very small (10-15 mm diameter), strongly ribbed shells. The primary ribs increase in prominence as they pass from the shoulder of the deep

umbilicus and over the venter. X. nikitini is considered to be the microconch of Lilloettia boesei (Burckhardt) and they occur within the same horizons (Units 3-6, Section C1). Callomon (1984) considered X. nikitini (Burckhardt) to be conspecific with X. vicarius Imlay. This author agrees with this synonymy and placed the Coauilote specimens within the designation Xenocephalites gr. "nikitini-vicarius".

The Callovian specimens from Units 13-16 of Arroyo El Rincon appear identical to the Bathonian specimens suggested to be the microconchs of E. boesei. However, the specimens of Units 13-16 are associated with E. rotundus and may be the coresponding microconch.

Xenocephalites neuquensis Stehn ♂

Material: This species has a limited range within Unit 15 of Section C1-Arroyo El Rincon.

Remarks: This microconch is very similar to X. gr. "nikitini-vicarius". The ornamentation is similar but weaker than that of X. gr. "nikitini-vicarius". X. neuquensis is found within the Callovian Clydoniceras inflatum Association at Coauilote. This species is found in the Upper Bathonian of the Andes but disappears in the early Lower Callovian according to Riccardi (1985).

Family Oppeliidae Bonarelli, 1894

Subfamily Oppeliinae Bonarelli, 1894

Genus Oxycerites Rollier, 1909

Oxycerites (Alcidellus) cf. tenuistriatus Grossouvre

Pl. 6, figs. 1a-b, 2a-b, 11a-b.

Material: This species is found in Units 2, 3, 6 of C3-Alto de Teeolutla, Units 3, 6, 7, 14-16 of C1-Arroyo El Rincon, and Units 17, 18 of C2-Arroyo El Campamento.

Remarks: The large macroconch attains sizes up to 150 mm diameter, but most specimens are 50-70 mm. The inner whorls are very involute and discoidal with a tricarinate venter. The body chamber is slightly more rounded. Ribbing is well developed on the outer half of the whorl sides. Secondaries are rursuridate and sickle-shaped while fine tertiaries are seen near the ventrolateral edge. Similar forms are known from the Upper Bathonian of Western Europe and the Argentine-Chilean Andes (Westermann et al., 1984).

Oxycerites (Paroecotraustes) davaicensis Lissajous ♂

Pl. 6, figs. 7, 8.

Material: Mature specimens were found in Units 14 and 15 of C1-Arroyo El Rincon.

Remarks: This microconch species is similar to O. cf. tennistrictus but much smaller in size, i.e. 20-25 mm. The shell is slightly evolute, the umbilicus relatively

wide and has vertical walls. The venter is rounded but unicarinate. Ornamentation consists of rursuridate, sickle-shaped secondary ribs on the outer half of the whorl sides. These become more prominent toward the venter and possess minor ventrolateral nodes which give the venter a crude tricarinate appearance. A sulcus at mid-flank is prominent on all specimens and the primary ribs are very faint between the sulcus and the umbilical shoulder.

Westermann et al. (1984) suggested that this species may be the microconch of O. tenuistriatus found widely distributed near Coauilote.

Oxycerites cf. prahecquense Petitclerc ♀

Pl. 13, fig. 4a-b.

Material: Specimens were collected from Units 16 and 17 of Section C1-Arroyo El Campamento.

Remarks: This species is very similar to O. cf. tenuistriatus. The shell is very compressed with weaker ribbing but the tricarinate venter is much sharper than that of O. tenuistriatus.

Oxycerites (Paroecotraustes) waageni Stephanov ♂

Pl. 6, figs. 9, 10.

Material: Several specimens from Unit 8 of Section C1-Arroyo

El Rincon.

Remarks: The diameter of the specimens approximates 25-30 mm. Shell shape and ornamentation is similar to O. cf. tenuistriatus but the ribbing is reduced compared to O. cf. tenuistriatus resulting in much smoother whorl sides. A prominent mid-flank furrow is present. The tricarinate venter has very weak shoulders.

Subfamily Hecticoceratinae Spath, 1925

Genus Prohecticoceras Spath, 1928

Prohecticoceras dominjoni Elmi ♀

Pl. 13, fig. 5a-b.

Material: Two specimens were collected from Unit 2 of C3-Alto de Teeolutla.

Material: This species is typified by a slightly evolute shell with strong falcoid ribs and a unicarinate venter. The ribs are strongest on the outer half of the whorl side and terminate with nodes at the ventrolateral shoulder. Diameter of the largest specimen is approximately 55-60 mm. This is a typically Upper Bathonian Tethyan genus.

Genus Jeanneticeras Zeiss, 1956

Jeanneticeras cf. malbosi Elmi ♂

Pl. 6, figs. 3, 4a-b, 5, 6a-b.

Material: This species is known mostly from Unit 15 of Section C1-Arroyo El Rincon but a few were found in Unit 14.
Remarks: This microconch only attains diameters of 20-25 mm. It has an evolute compressed, unicarinate shell shape with strong ornamentation. The ribs curve adorally to approximately one-third whorl height and are abruptly reduced to form a very slight furrow. The ribs are prominent again on the upper half of the whorl side and terminate at the ventrolateral shoulder with high nodes. This is a typically Early Callovian species previously known only from the Lower Callovian of Europe (Elmi, 1967).

Subfamily Phlycticeratinae Spath, 1928

Genus Phlycticeras Hyatt, 1900

Phlycticeras cf. pustulatum (Reinecke) ♀

Pl. 5, figs. 2, 3a-b, 4a-b.

Material: Two septate fragments from Unit 6 of C1-Arroyo El Rincon and two body chamber fragments from Unit 13 of the same section. One complete phragmocone obtained from villagers (Corona and Westermann-1980).
Description: The only complete phragmocone is involute and moderately compressed, approximately one-third higher than wide with pronounced shoulders and flattened whorl sides. The hollow-floored keel is preserved on two specimens while the other three have only the floor. The keel is highly

serrated. The umbilicus is deep, moderately large with a vertical umbilical wall and rounded umbilical shoulder.

The costae are distant and strong. There are three lines of tubercles. Each primary rib commences at a prominent, rounded tubercle on the umbilical shoulder and increases in height as it passes radially to the second set of tubercles at mid-flank. There are eight primaries per half-whorl. The primary ribs bifurcate at the second set of tubercles. Secondary ribs are stronger than the primary ribs. Each secondary rib terminates with a rounded tubercle at the whorl shoulder. Secondary ribs average sixteen per half-whorl. At this third set of tubercles, secondary ribs bifurcate to form tertiary ribs. These are weaker than the secondary ribs but stronger than the primaries. The tertiary ribs are slightly adorally convex and extend to meet the serrated keel. Tertiary ribs average thirty-two per half-whorl.

The tubercles are large, rounded and blunt. The first set of tubercles occurs at the umbilical shoulder followed by the second set at mid-flank and the third at four-fifths whorl height. The second set is the strongest and largest while the first set is the weakest.

Specimens are strongly strigate. Infrequently, a whorl constriction marks a previous position of the aperture. The septal suture is well preserved in one specimen from C1-6 and is illustrated in Figure 4.1.10 at a whorl height of

Figure 4.1.10: Septal suture of Phlycticeras cf. pustulatum at a whorl height of 42 mm and whorl thickness of 32 mm. 2X.

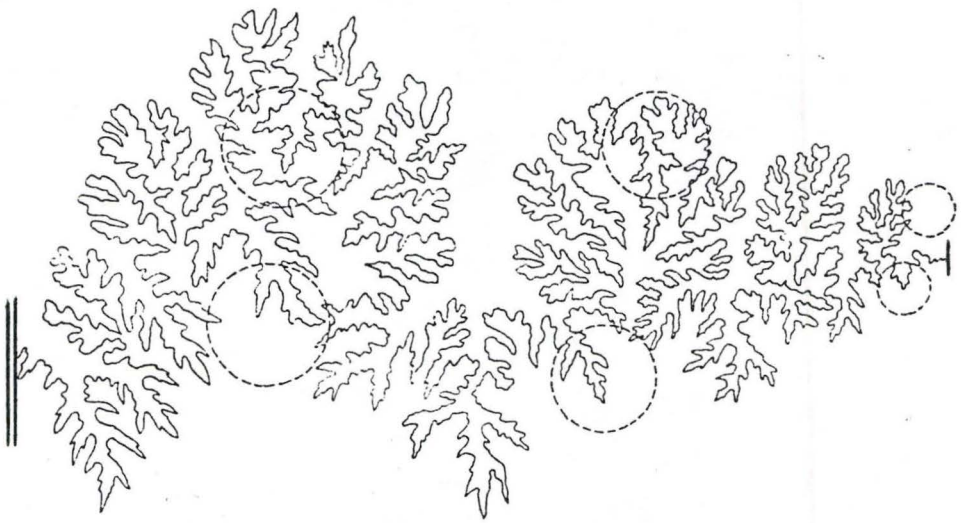

approximately 42 mm and whorl thickness of 32 mm.

Remarks: The figure of Quenstedt (1846) is small and difficult to use for comparison. Ammonites pustulatus figured by d'Orbigny (1846) has weaker ribbing and a less serrated keel than the specimens from Coauilote. Mid-flank tubercles are strongest in Coauilote specimens but the ventrolateral ones are strongest in d'Orbigny's specimens. The whorl section of the Mexican forms is more compressed.

Amaltheus pustulatus Waagen (1873) has a keel which is identical to that of the Mexican specimens but ribbing in the latter is more complicated and bifurcates at tubercles. The whorl section of the Mexican specimens is less quadratic and more compressed than those figured by Waagen. The most important feature of the Mexican specimens is the third set of tubercles at the umbilical shoulder.

This is the first reported find of Phlycticeras cf. pustulatum in North America. Its age is upper Upper Bathonian to Lower Callovian.

Family Clydoniceratidae Buckman, 1924

Genus Clydoniceras Blake, 1905

Clydoniceras inflatum Westermann

Pl. 6, figs. 13a-b, 14, 15, 16.

Material: Numerous specimens from Unit 15 of C1-Arroyo El Rincon and C2-Arroyo El Campamento.

Remarks: The shell is involute and inflated with prominent, flexed ribbing. The venter is bisulcate. Raised ventrolateral shoulders define the two ventral furrows which are separated by a narrow but prominent keel. Maximum diameter is approximately 50 mm but some larger body chamber fragments were also found. Westermann et al. (1984) suggested that the smaller forms may be microconchs of Clydoniceras i.e. Delecticeras. This species is more inflated than any known species of Clydoniceras s.l. which ranges from late Middle to latest Bathonian of Western Europe, north Africa and Madagascar (Westermann et al., 1984).

Family Perisphinctidae Steinmann, 1890

Genus Choffatia Siemiradzki, 1898

[?Choffatia] "Peltoceras" constrictum (Burckhardt)

Pl. 1, fig. 5a-b.

Material: Numerous specimens from Unit 2 of Section C3-Alto de Teeolutla.

Remarks: These small forms (40-50 mm diameter) are evolute and strongly ribbed. The whorl shape is circular. Westermann et al. (1984) noted that they appear to be intermediate between Perisphinctidae and Reineckeiidae. "P." constrictum resembles the inner whorls of Neuqueniceras (Frickites) bodenbenderi (Tornquist) from Coauilote and

"Perisphinctes" boehmi (Steinmann) from Caracoles, Chile (Westermann et al., 1984).

Choffatia aberrans (Burckhardt)

Pl. 11; Pl. 14, fig. 1.

Material: This species is very abundant in Units 2-6 of Section C1-Arroyo El Rincon.

Remarks: This very evolute species is typified by a subrounded whorl section bearing strong radial blade-like primary ribs at approximately one-third whorl height. The whorls are somewhat segmented by strong constrictions. Secondary ribs are fine and pass over the venter with a very slight ventral costal interruption. Many specimens are large; up to 160 mm. Ch. aberrans is associated with other typically Upper Bathonian ammonite species.

Choffatia suborion (Burckhardt)

Pl. 12, fig. 2a-b; Pl. 13, fig. 2.

Material: Many specimens were found in Units 2-6 of Section C1-Arroyo El Rincon.

Remarks: Ch. suborion is generally smaller than Ch. cf. aberrans and averages 100-120 mm diameter. The former also possesses a more subquadratic whorl section, stronger blade-like primary ribs which become most prominent

and protrusive on the outer whorls. These primaries are also located lower on the whorl flanks than those of Ch. cf. aberrans. A ventral costal interruption is present and usually less well developed on the outer whorls.

Choffatia cf. subbackeriae (d'Orbigny)

Pl. 11, figs. 1a-b, 2.

Material: Many specimens were collected in Units 3-5 of Section C1-Arroyo El Rincon.

Remarks: This species is characterised by very evolute whorls and dense, fine ribbing. The whorl section is slightly compressed and much higher than the other species of Choffatia found near Coauilote. The primary ribs occur on the lower third of the whorl flanks and are straight and radial. The primaries subdivide at approximately one-half whorl height. The secondary ribs are almost as strong as the primaries. A very slight ventral interruption of the secondary ribs is present on most specimens.

Choffatia gottschei (Steinmann)

Pl. 8, fig. 5a-b.

Material: Many specimens from Units 1-3 and 5-6 of Section C1-Arroyo El Rincon.

Remarks: This species contains small (70-80 mm diameter),

densely ribbed specimens. The primary ribs are narrow and bifurcate into less prominent secondary ribs at approximately mid-flank. There is a moderately well developed ventral interruption of the secondary ribs as they pass over the venter.

Choffatia cf. jupiter (Steinmann)

Pl. 13, fig. 1a-b, 3.

Material: Many specimens from Units 1-6 of Section C3-Alto de Teeolutla and Units 3-6 of C1-Arroyo El Rincon.

Remarks: This species attains shell diameters up to 160 mm with evolute whorls which are depressed, especially in the body chamber. The primary ribs are strong, narrow and blade-like. They bifurcate into dense secondary ribs at approximately two-thirds whorl height. The secondaries pass uninterrrupted over the venter. The body chamber has weak blade-like primaries but the secondaries are very weak.

Subgenus Homeoplanulites Buckman, 1922

Ch. (Homeoplanulites) cf. ybbsensis (Jussen) ♂

Pl. 8, fig. 3a-b.

Material: A few specimens from Unit 6 of C1-Arroyo El Rincon.

Remarks: This is a very evolute microconch species with

dense ribbing. The primary ribs bifurcate at approximately mid-flank. The point of bifurcation carries a small but sharp blade-like tubercle. The secondary ribs are almost as strong as the primaries and pass over the venter without interruption.

Ch. (Homeoplanulites) sp.

Pl. 12, fig. 4a-b.

Material: Numerous specimens collected from Units 1-6 of Section C1-Arroyo El Rincon.

Remarks: These are small microconchs with shell characteristics similar to those of Choffatia sp.

Family Reineckeiidae Hyatt, 1900

Genus Reineckeia Bayle, 1878

Reineckeia (Rehmannia) gr. "rehmanni-pictava" (Oppel)/(Burckhardt)

Pl. 16, figs. 1a-b, 2, 3a-b.

Material: Numerous specimens from Units 17 and 18 of Sections C1-Arroyo El Rincon and C2-Arroyo El Campamento.

Remarks: This species is represented by large, evolute forms which are strongly ornamented. The whorl section is quadratic. Ribbing consists of radial primary ribs with small, blade-like spines at one-third whorl height in the

inner whorls. The primaries bifurcate into strong secondary ribs which experience a strong ventral interruption as they pass over the venter. The middle whorl primaries carry small punctiform tubercles. These develop into large mammiform tubercles on the body chamber. Secondary ribs are also very strong, bundled and widely spaced on the body chamber. These outer coronate whorls are referred to as 'reineckeiid' stages by Cariou (1980). This species appears to be Lower Callovian in age at Coauilote.

Reineckeia franconica (Quenstedt)

Pl. 11, fig 3a-b.

Material: Several specimens from Unit 18 of C2-Arroyo El Campamento.

Remarks: This species is very similar to R. (Rehmannia) gr. "rehmanni-pictava" except that R. franconica has a slightly depressed oval whorl section and punctiform tubercles are present even on inner whorls. This species is restricted to the Lower Callovian of Europe (Cariou, 1980).

Subfamily Neuqueniceratinae Cariou, 1980

Genus Neuqueniceras Stehn, 1924

Neuqueniceras (Neuqueniceras) cf. plicatum (Burckhardt)

Pl. 7, figs. 1a-b, 4a-b, 5a-b.

Material: Numerous specimens from Units 2-6 of Section C1-Arroyo El Rincon.

Remarks: This species has very evolute coiling and a depressed subquadratic whorl section. Many specimens average 80-100 mm diameter. Ornamentation consists of prominent blade-like primaries which divide at mid-flank. The blade-like character of the primaries increases in outer whorls to the point of developing elongate bullae. Secondary ribbing is strong and dense. A slight ventral interruption of the secondary ribs is apparent in most specimens. The whorls also contain some constrictions. The age of this species appears to be upper Late Bathonian at Coauilote.

Neuqueniceras (Neuqueniceras) steinmanni (Stehn)

Pl. 7, fig. 7a-b; Pl. 8, figs. 1a-b, 2a-b.

Material: Numerous specimens were collected from Units 6 and 7 of Section C1-Arroyo El Rincon.

Remarks: Neuqueniceras (N.) steinmanni is characterised by small to medium-sized macroconchs (70-80 mm diameter) which bear blade-like primary ribs on the phragmocone. The ribbing is dense and forms a typically 'perisphinctid' juvenile stage i.e. no tubercles. Thin but strong primary ribs bifurcate at mid-flank and pass into strong, dense secondary ribs. There is a distinct ventral costal

interruption on the phragmocone. The body chamber has prominent mid-lateral bullae which bear conical spines. The age of this species at Coauilote is late Upper Bathonian.

Neuqueniceras sp. ♂

Pl. 7, figs. 2a-b, 3a-b, 6a-b; Pl. 8, figs. 4a-b, 6a-b.

Material: Numerous specimens from Units 6 and 7 of Section C1-Arroyo El Rincon.

Remarks: These small forms are similar to the inner whorls of N. (N.) cf. plicatum and N. steinmanni and may be the corresponding microconchs.

Subgenus Frickites Jeannet, 1951

Neuqueniceras (Frickites) bodenbenderi (Tornquist)

Pl. 10; Pl. 12, fig. 3a-b.

Material: Many specimens from Units 13-16 of Section C1-Arroyo El Rincon.

Remarks: This species possesses an extremely evolute form, is strongly tuberculate except in the 'perisphinctid' juvenile stages which are characterised by very elongate blade-like primary ribs. The whorl section is depressed. The primary ribs subdivide slightly above mid-flank into secondary ribs which are dense and strong. A slight ventral interruption of the secondary ribs is apparent. Middle

whorls contain moderately short primary ribs with mid-lateral tubercles. The outer two whorls contain very prominent conical mid-lateral spines. This species appears to be restricted to the Lower Callovian of Mexico and South America (Cariou, 1980).

4.2 AGE AND DISTRIBUTION OF THE COAUILOTE AMMONITE FAUNA

The ages and vertical distribution of the ammonite faunas near Coauilote are described within five associations which are illustrated in Figure 4.2.1.

1. The oldest faunal association is named the Epistrenoceras hystricoides Association. It is found in the Simon Formation. Within Europe, the range of Epistrenoceras is restricted to the middle Upper Bathonian, i.e. Retrocostatum Zone. Prohecticoceras dominjoni is also confined to the Middle amd lower Upper Bathonian of Europe (Elmi, 1967). Bullatimorphites (Kheraiceras) bullatus ranges through the Upper Bathonian-Lower Callovian. Therefore, the age of the E. hystricoides Association is middle Upper Bathonian, Retrocostatum Zone.

2. The Lilloettia-Neuqueniceras Association occurs near the base of the Yucunuti Formation, approximately 200 m above the E. hystricoides Association. This association has not previously been documented in the Tecocoyunca Group. The age is probably latest Bathonian, based on the presence of Lilloettia steinmanni and L. boesei. Riccardi (1985)

Figure 4.2.1: Columnar section of the Tecocoyunca Group near Coauilote with the age and vertical distribution of the ammonite fauna.

COAUILOTE COMPOSITE SECTION

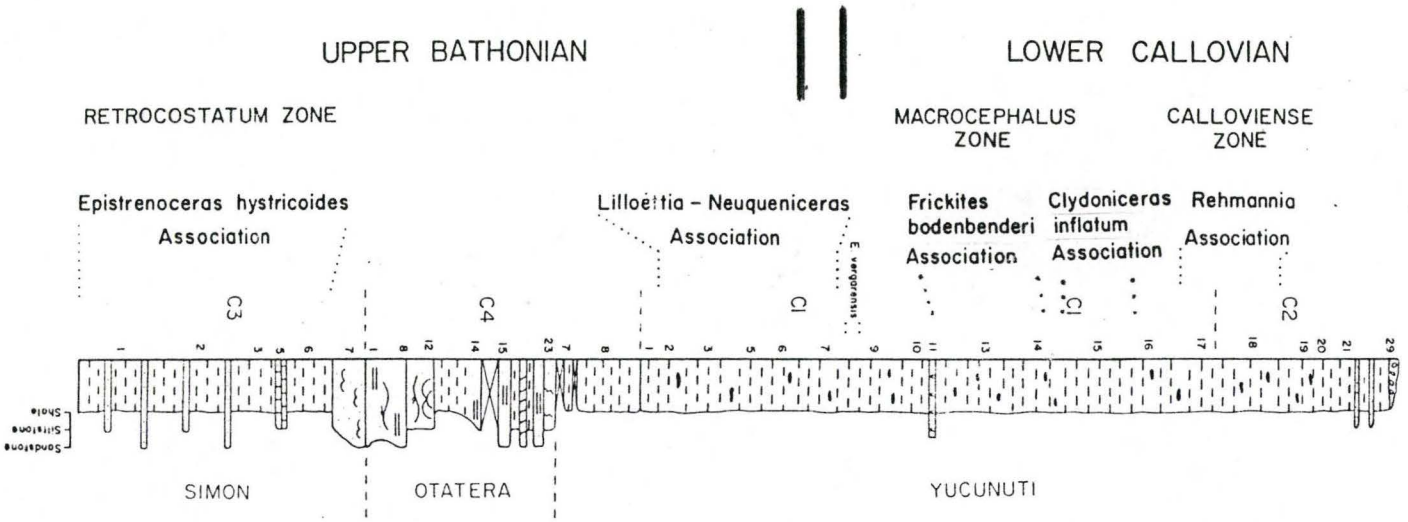

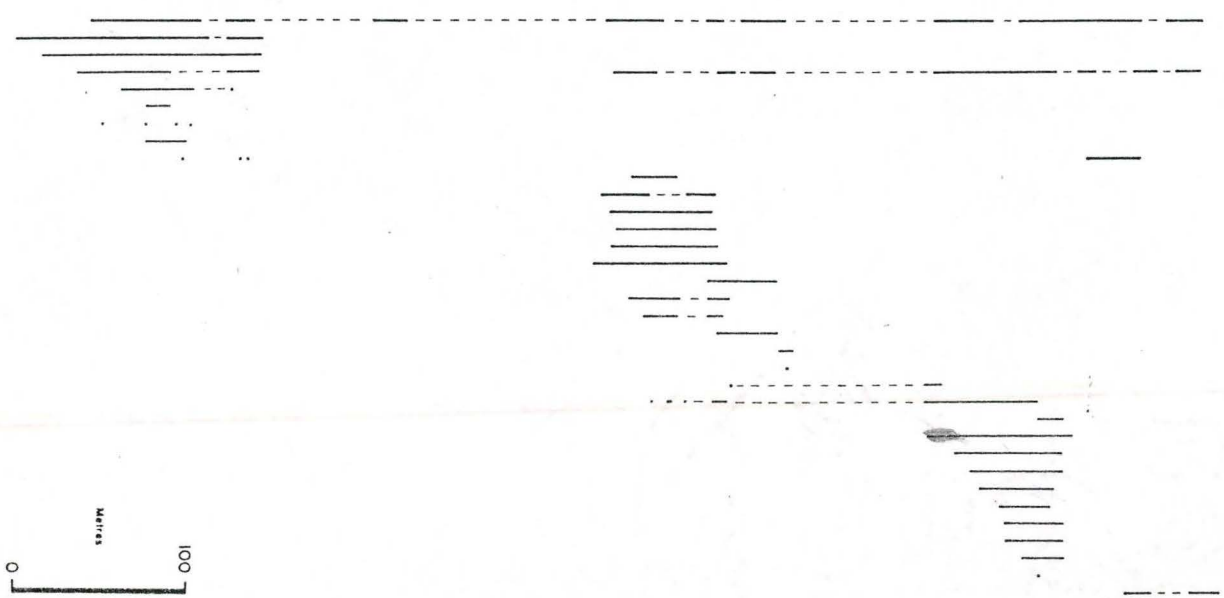

AMMONITE SPECIES

Ptychophylloceras plasticum
Epistrenoceras hystricoides
Choffatia aff. jupiter
Oxycerites (Alcidellus) cf. tannistrictus
Bullatimorphites (Kheraiceras) bullatus ♀
Bullatimorphites (Kheraiceras) bullatus ♂
Prohecticoceras dominjoni
"Peltoceras" constrictum
Oxycerites cf. praehecquense
Choffatia cf. subbackeriae
Choffatia gottschei
Choffatia cf. aberrans
Choffatia cf. jupiter
Choffatia suborion
Neuqueniceras (Neuqueniceras) cf. plicatum
Neuqueniceras (N.) steinmanni
Lilloettia boesei
Lilloettia steinmanni
Phylloceras cf. plicatum
Eurycephalites cf. vergarensis
Oxycerites (Paroecotraustes) waageni
Phlycticeras cf. pustulatum
Xenocephalites gr. "nikitini-vicarius"
Xenocephalites neuquensis
Neuqueniceras (Frickites) bodenbenderi
Oxycerites (Paroecotraustes) daraicensis
Eurycephalites cf. rotundundus
Jeanneticeras cf. malbosi
Parapatoceras distans
Clydoniceras inflatum
Phylloceras sp.
Holcophylloceras sp.
Paracuriceras cf. incisum
Reineckeia (Rehmannia) gr. "rehmanni-pictava"
Reineckeia franconica

recently determined that in the Andes, Lilloettia is confined to the upper Upper Bathonian, followed immediately by Eurycephalites vergarensis placed in the Callovian. It is proposed here that the Bathonian-Callovian boundary lies in the poorly fossiliferous 25 m interval between the last appearances of Lilloettia steinmanni and L. boesei and the first appearance of Eurycephalites cf. vergarensis.

Neuqueniceras (N.) cf. plicatum and five species of Choffatia appear just slightly below Lilloettia. Therefore, the first appearance of the Neuqueniceras Assemblage (Westermann et al., 1984) is latest Bathonian.

3. The Frickites bodenbenderi Association appears approximately 75m above the range of Eurycephalites cf. vergarensis. Phlycticeras cf. pustulatum is documented for the first time in North America. P. pustulatum is known to range from uppermost Bathonian through the Lower Callovian in Europe. A typically Callovian species, Jeanneticeras cf. malbosi Elmi known from the lower Calloviense Zone of Europe also occurs in this association. Eurycephalites rotundus is also an entirely Callovian species (Riccardi, 1985). Therefore, the age of this association is earliest Callovian, (?) Macrocephalus Zone.

4. The Clydoniceras inflatum Association occurs within the upper portion of the Neuqueniceras (Frickites) bodenbenderi range zone and dates the upper range limit of the latter. This association contains the first known

occurrence of the Tethyan genus Paracuariceras outside of Europe. The age of P. incisum in Europe is Macrocephalus to Jason Zone (Dietl, 1978). Parapatoceras distans is also present and ranges in Europe from Retrocostatum Zone to the Calloviense Zone (Dietl, 1978). Therefore, the age of the Clydoniceras Association is upper Macrocephalus Zone.

5. The Rehmannia Association, also in the Yucunuti Formation, can probably be dated as lower Calloviense Zone. This association contains Reineckeia (Rehmannia) gr. "rehmanni-pictava" and Reineckeia cf. franconica. These species are known from the Mediterranean Province and were placed in the upper Macrocephalus Zone, Rehmanni Subzone of the Lower Callovian by Cariou (1980). They were then placed in the lower Calloviense Zone by Callomon (pers. comm.). There is a morphological gradation from Neuqueniceras (Frickites) bodenbenderi into Reineckeia and Rehmannia in Mexico. Westermann (1984) and Cariou (1985) suggested an East Pacific origin of the Reineckeiids.

Figure 4.2.2 summarizes the biostratigraphic correlation of the Coauilote ammonite fauna with respect to the Andean Province and Europe. Zonation of the Andean Province is from Westermann and Riccardi (in press).

4.3 AMMONITE BIOGEOGRAPHY

The biogeographic affinity of the Late Bathonian-Early Callovian ammonite fauna of Coauilote, Guerrero is firstly

Figure 4.2.2: Proposed biostratigraphic correlation of the Coauilote ammonite fauna with respect to the Andean Province and Europe. Zonation of the Andean Province is from Westermann and Riccardi (in press).

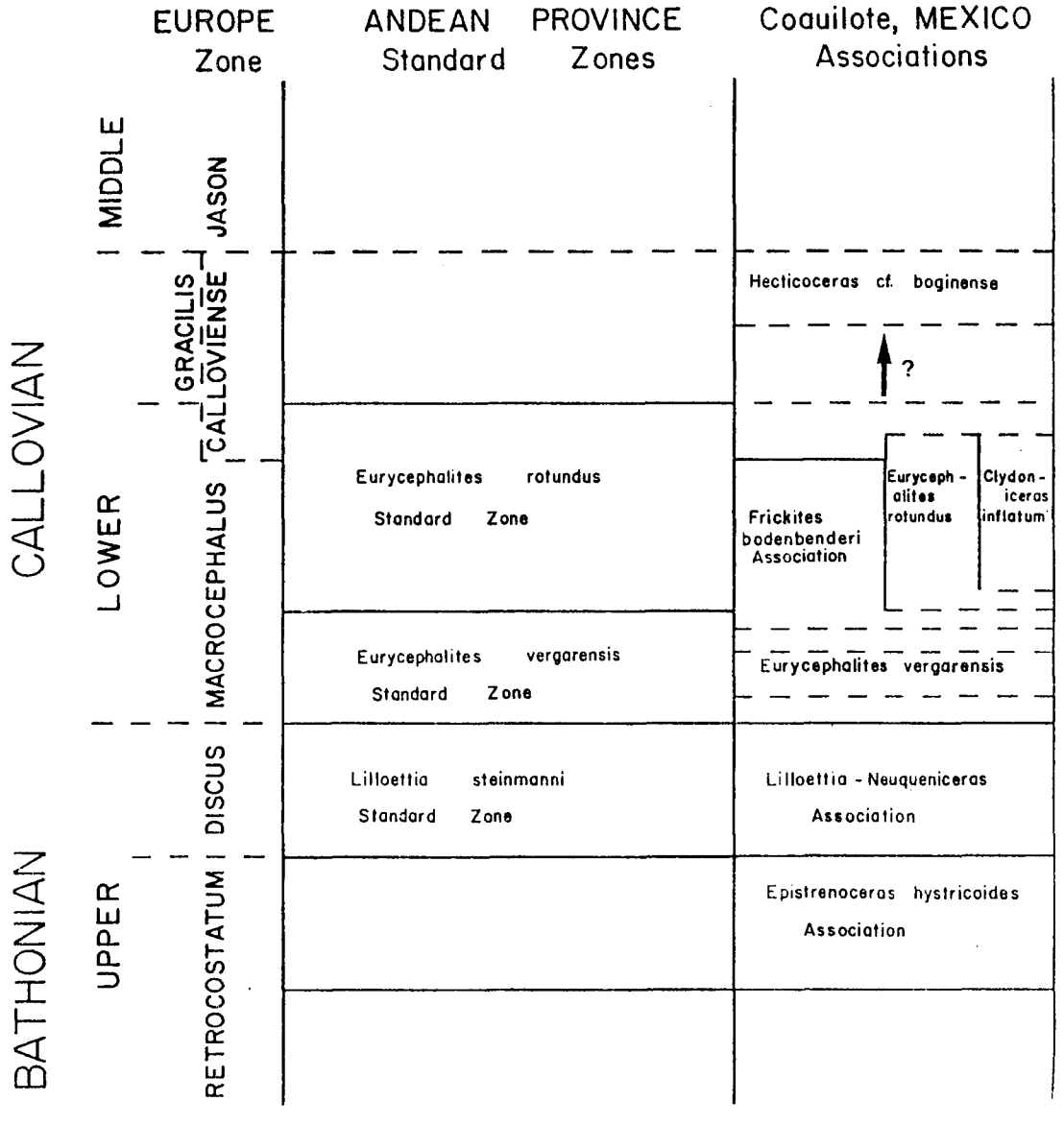
EUROPE
Zone
ANDEAN
Standard
PROVINCE
Zones
Coquilote, MEXICO
Associations
BATHONIAN
CALLOVIAN
UPPER
LOWER
MIDDLE
RETROCOSTATUM
DISCUS
MACROCEPHALUS
GRACILIS
CALLOVIENSE
JASON
Hecticoceras cf. boginense
?
Eurycephalites rotundus
Standard Zone
Frickites bodenbenderi Association
Eurycephalites rotundus
Clydoniceras inflatum
Eurycephalites vergarensis
Standard Zone
Eurycephalites vergarensis
Lilloettia steinmanni
Standard Zone
Lilloettia - Neuqueniceras
Association
Epistrenoceras hystricoides
Association

to the Andean Province and secondly to the west-Tethyan/Mediterranean Province (Table 4.3.1 and Fig. 4.3.1). At the species-level, the Coauilote fauna has 5 (12 %) strictly endemic taxa. There are 19 (46 %) and 15 (37 %) species in common with the Andean and Tethyan/Mediterranean Provinces respectively. Ten species are common to both the Andean and Tethyan/Mediterranean Provinces. Only 2 (5%) species are conspecific with ones from the North Cordilleran Province.

Therefore, biogeographic affinities of the Coauilote, Guerrero fauna are mostly Andean with significant West-Tethyan elements and a few endemic species. The exceptionally close taxonomic affinities with the rich Andean fauna of Chile and Argentina has previously been discussed by Taylor et al. (1984) and Westermann (1984).

This study documents the first known occurrences of three ammonite species in North America. Phlycticeras cf. pustulatum is known from Europe and South America. Jeanneticeras cf. malbosi is common in Europe. The heteromorph Paracuariceras cf. incisum has previously been found only in southern Germany, southern France and the Romanian Carpathians (Dietl, 1978). It is now reported from Mexico and has very important biogeographic implications.

The East Pacific Realm existed from the Late Bajocian to the Early Callovian due to constriction of the Hispanic Corridor (Westermann, 1981). Such constriction limited the

Figure 4.3.1: Affinities of the Coauilote ammonite fauna, Guerrero, at species level. Solid lines indicate taxa shared with another province, solid circle endemic taxa. Numbers indicate the actual number of shared species.

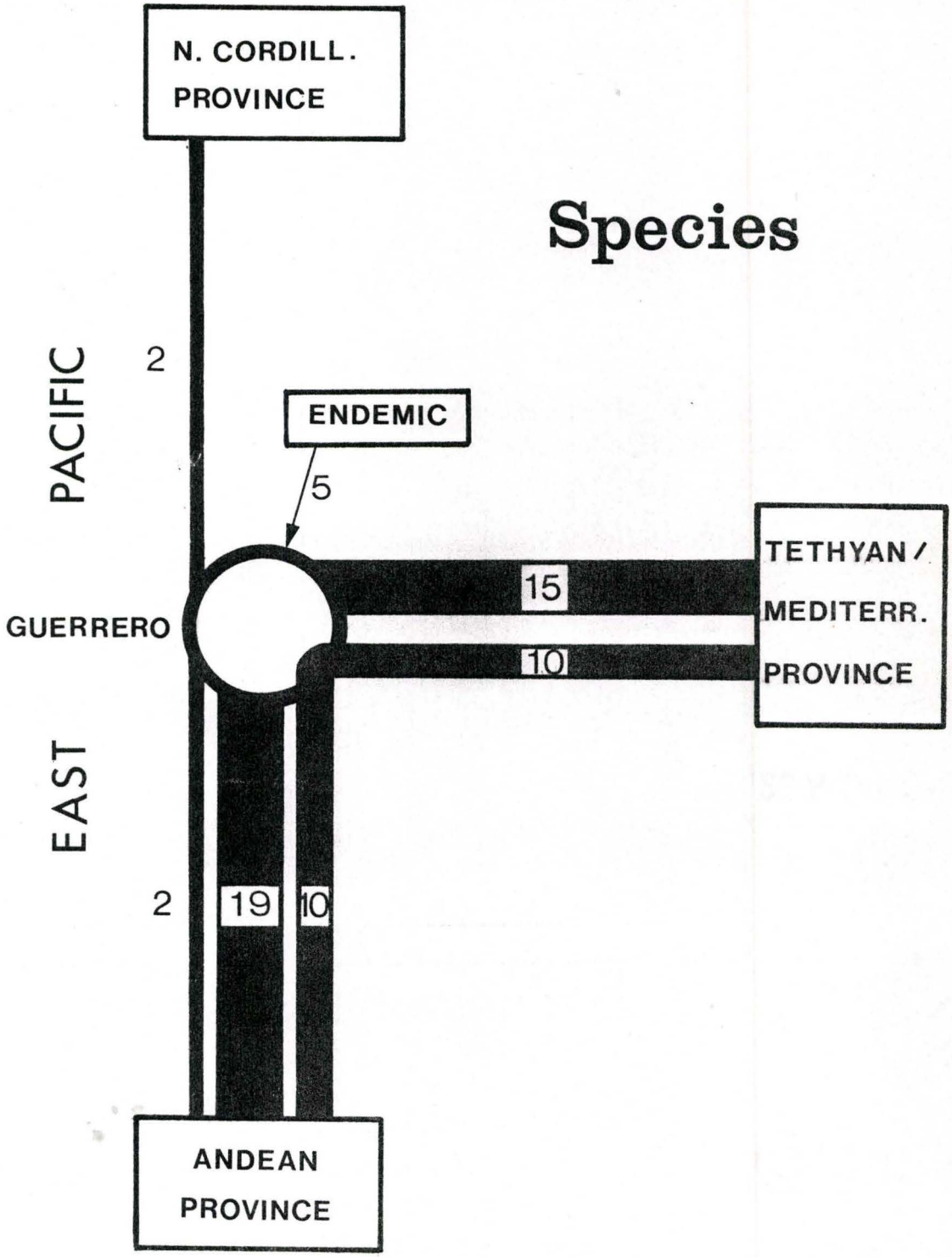
N. CORDILL.
PROVINCE
Species
PACIFIC
2
ENDEMIC
5
TETHYAN /
MEDITERR.
PROVINCE
15
GUERRERO
10
EAST
2
19
10
ANDEAN
PROVINCE

Table 4.3.1: Biogeographic affinities of the Coauilote ammonite fauna.

AMMONITE SPECIES	Endemic	N. Cord.	Andean	Tethyan
Reineckeia (Rehmannia) gr. "rehmanni-pictava				+
Ptychophylloceras plasticum	+			
Epistrenoceras hystricoides			+	+
Bullatimorphites (Kheraiceras) bullatus			+	+
Prohecticoceras dominjoni			+	+
"Peltoceras"constrictum	?+			
Choffatia cf. jupiter			+	
Oxycerites (Alcidellus) cf. tennistrictus				+
Oxycerites cf. prahecquense			+	+
Holcophylloceras sp.				
Phylloceras cf. plicatum				+
Clydoniceras inflatum	+			
Lilloettia steinmanni		+	+	
Lilloettia boesei	+			
Eurycephalites rotundus			+	
Eurycephalites cf. vergarensis			+	
Xenocephalites gr."nikitini-vicarius"		+	+	
Xenocephalites neuquensis			+	
Phlycticeras cf. pustulatum			+	+
Parapatoceras distans				+
Jeanneticeras cf. malbosi				+
Oxycerites (Paroecotraustes) davaicensis			+	+
Oxycerites (Paroecotraustes) waageni				+

cont'd

AMMONITE SPECIES	Endemic	N. Cord	Andean	Tethyan
Paracuariceras cf. *incisum*				+
Neuqueniceras (*Neuqueniceras*) cf. *plicatum*			+	
Neuqueniceras steinmanni			+	
Neuqueniceras (*Frickites*) *bodenbenderi*			+	
Choffatia suborion			+	
Choffatia gottschei			+	
Choffatia aff. *jupiter*			+	
Choffatia cf. *subbackeriae*			+	+
Choffatia cf. *aberrans*	+			

ability of ammonites to migrate between the Pacific Ocean and Tethys Sea thus creating a higher degree of endemism and provincialism. Existence of the East Pacific Realm coincides with globally lowered eustatic sea-levels in the Late Bajocian and throughout the Bathonian (Fig. 4.3.2). Cosmopolitanism increased during the Late Bathonian-Early Callovian global eustatic sea-level rise (See Section 7.4.2).

The Middle Jurassic ammonite fauna of Coauilote occurs on the Mixteca tectonostratigraphic terrane (Campa and Coney, 1983). Biogeographic affinities of the ammonite fauna places this terrane, during the Middle Jurassic, in the vicinity of the Central Andes and the proto-Atlantic seaway (Hispanic Corridor) which connected the west Tethys Sea and East Pacific Ocean (Westermann, 1984). Abundant nearshore and shoreline sediments of the Tecocoyunca Group also suggest close proximity to a major continent i.e. South America.

In summary, ammonite biogeography tends to sustain the hypothesis of an allochthonous Mixteca terrane influenced by the proximity of South America and the Hispanic Corridor (Fig. 1.5), rather than a marine Oaxaca Embayment as suggested by Imlay (1980) and Alencaster (1984) (Fig. 1.2).

4.4 PELECYPOD FAUNA

The pelecypod species listed below may be seen in

Figure 4.3.2: Biogeographic evolution of the eastern Pacific ammonoid realms, regions, and provinces during the Middle Jurassic. Note the overlap of Tethyan/East-Pacific realms in the Mixteca terrane of Southern Mexico (Bathonian-Callovian boundary), which has predominantly Andean faunas at this time. (After Westermann, 1984).

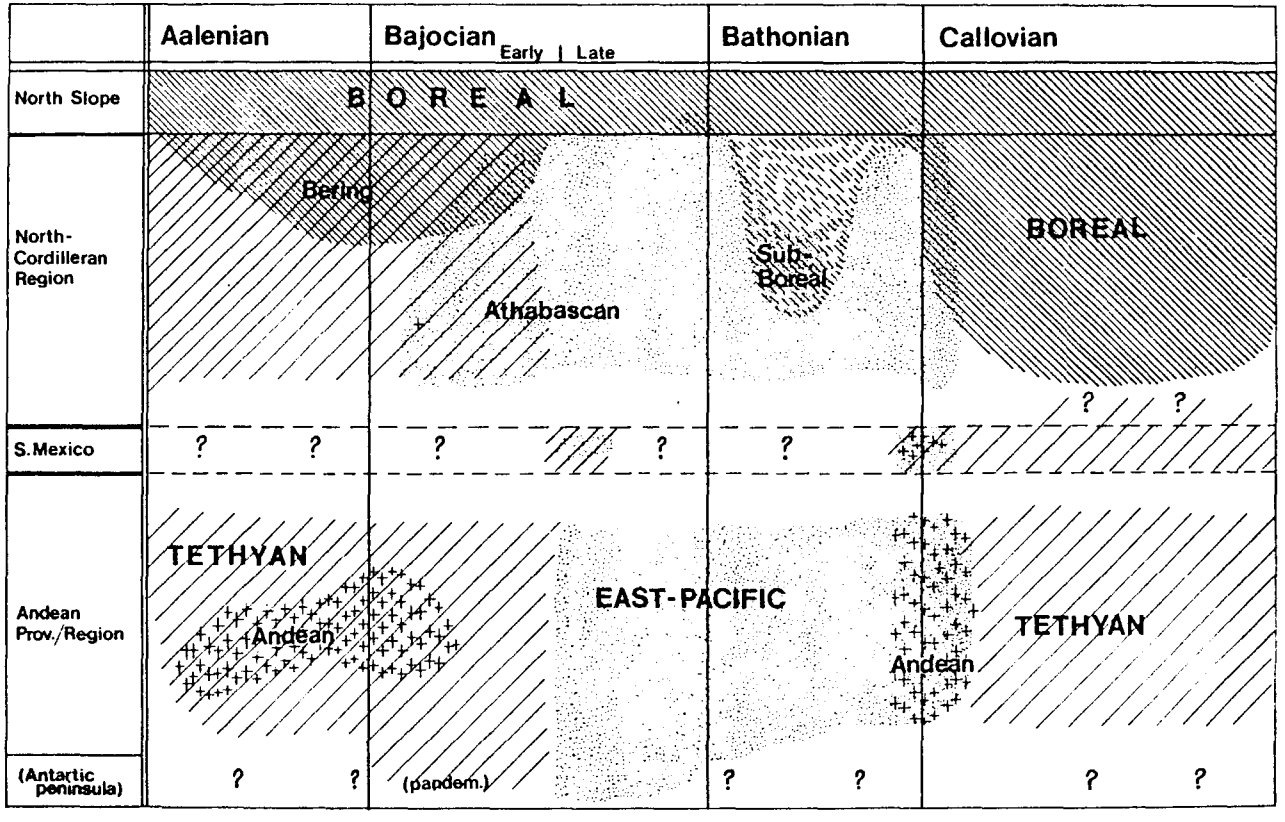
Aalenian
Bajocian
Early | Late
Bathonian
Callovian
North Slope
B O R E A L
North-Cordilleran Region
Bering
Athabascan
Sub-Boreal
BOREAL
S.Mexico
?
Andean Prov./Region
TETHYAN
Andean
EAST-PACIFIC
Andean
TETHYAN
(Antartic peninsula)
(pandem.)

Plates 15 and 16. The letters and numbers within this list indicate the locations of the species i.e. C1-5 means Section C1 and Unit 5.

Class Bivalvia

Subclass Pteriomorpha

Family Mytilidae

Subfamily Mytilinae

Mytilus (Falcimytilus) cf. stricapillatus Hayami

C3-2, 3; C4-1, 2

Family Inoceramidae

Inoceramus cf. fuscus Quenstedt

C2-16, 17

Family Posidoniidae

Bositra sp.

C1-14, 15, 16; C2-15, 16

Subclass Paleoheterodonta

Family Trigoniidae

Vaugonia (Vaugonia) v-costata mexicana Alencaster

C3-2, 6; C4-1, 2

Subclass Heterodonta

Family Lucinidae

Subfamily Lucininae

Lucina magna Alencaster

C3-6

Family Mactromyidae

Unicardium varicosum (Sowerby)

C3-2; C4-1, 2, 8

Family Corbulidae

Subfamily Corbulinae

Corbula oaxaquena Alencaster

C3-2, 3

Family Arcticidae

Anisocardia coxi Alencaster

C3-2; C4-1, 2, 3, 8; C1-6, 8

Family Glossidae

Isocardia mixteca Alencaster

C3-1, 2, 3

Superfamily Ostreacea

Family Gryphaeidae

Subfamily Gryphaeinae

Liostrea sp.

C4-1, 2; C3-2

4.5 OTHER

Order Rhynchonellida

Superfamily Rhynchonellacea

Family Rhynchonellidae

?Capillirhynchia sp.

C3-2, 5, 6; C4-1, 2

Order Caenogastropoda

Superfamily Cerithiacea

Family Procerithiidae

Cryptalaux sp.

C4-8; C1-1-7

Vertebrate

Crocodile

Steneosaurus sp.

C2-15

PLATE 1

Figure 1a-b: Bullatimorphites (Kheraiceras) bullatus ♀ (d'Orbigny), C4-2, 1X.

Figure 2a-b: Bullatimorphites (Kheraiceras) bullatus ♂ C4-2, 1X.

Figure 3a-c: Bullatimorphites (Kheraiceras) bullatus ♂ C4-2, 1X.

Figure 4a-c: Bullatimorphites (Kheraiceras) bullatus ♀ C4-2, 1X.

Figure 5a-b: "Peltoceras" constrictum (Burckhardt), C4-2, 1X.

Figure 6a-b: Epistrenoceras hystricoides (Rollier), C3-3, 2X.

Figure 7: Epistrenoceras hystricoides, C4-3, 1X.

Figure 8a-b: Epistrenoceras hystricoides, C3-6, 1X.

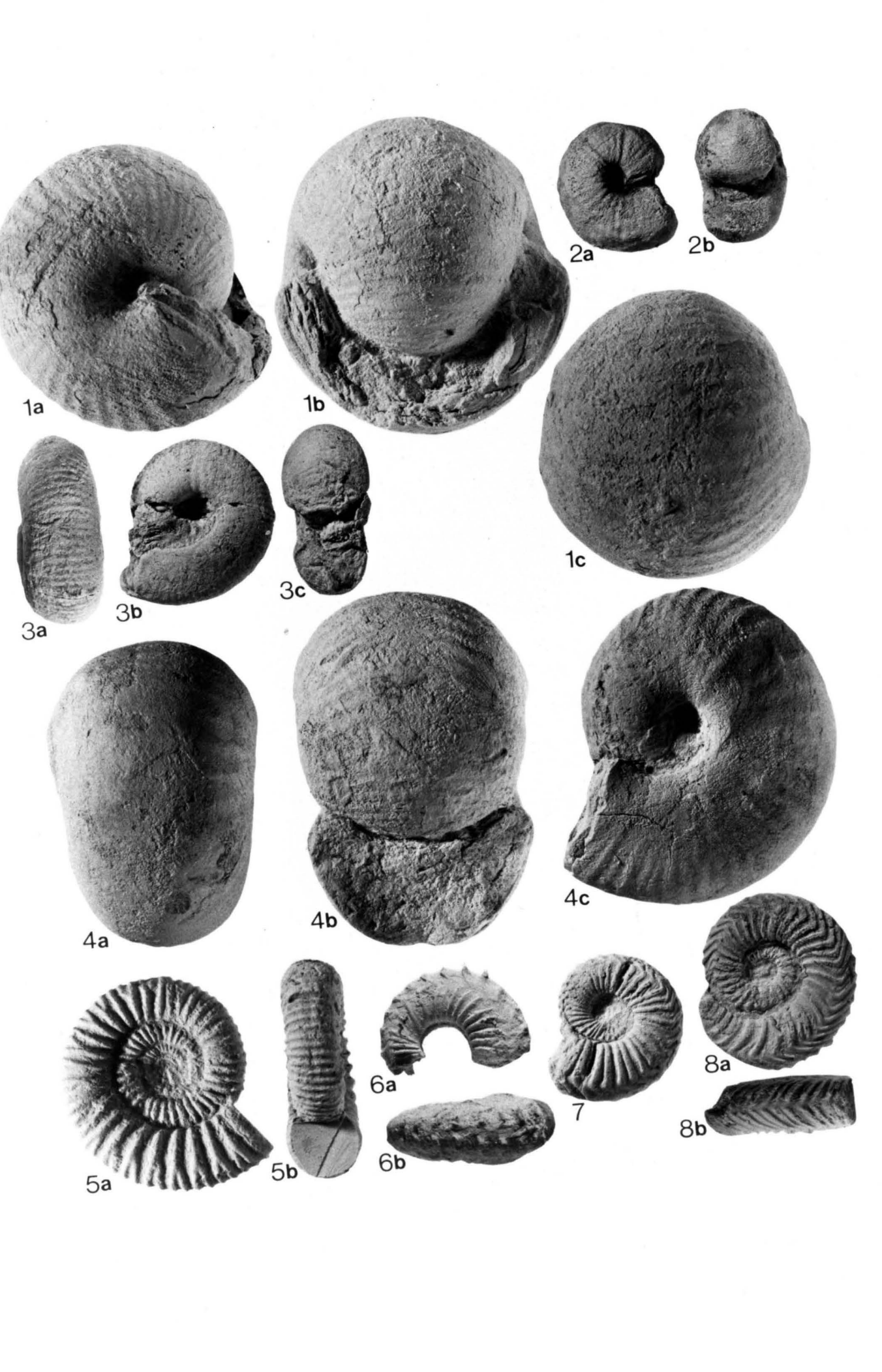
1a
1b
2a
2b
1c
3a
3b
3c
4a
4b
4c
5a
5b
6a
6b
7
8a
8b

PLATE # 1

Figure 1a-b: Ptychophylloceras plasticum (Burckhardt), C1-14, 1X.
Figure 2a-b: Phylloceras cf. plicatum Neumayr, C1-16, 1X.
Figure 3: Phylloceras cf. plicatum, C1-7, 1X.
Figure 4a-b: Ptychophylloceras plasticum, C1-13, 1X.
Figure 5: Phylloceras cf. plicatum, C1-6, 1X.
Figure 6a-b: Ptychophylloceras plasticum, C1-6, 1X.
Figure 7: Ptychophylloceras plasticum, C1-15, 1X.
Figure 8: Holcophylloceras sp., C1-15, 2X.
Figure 9a-b: Holcophylloceras sp., C1-15, 2X.

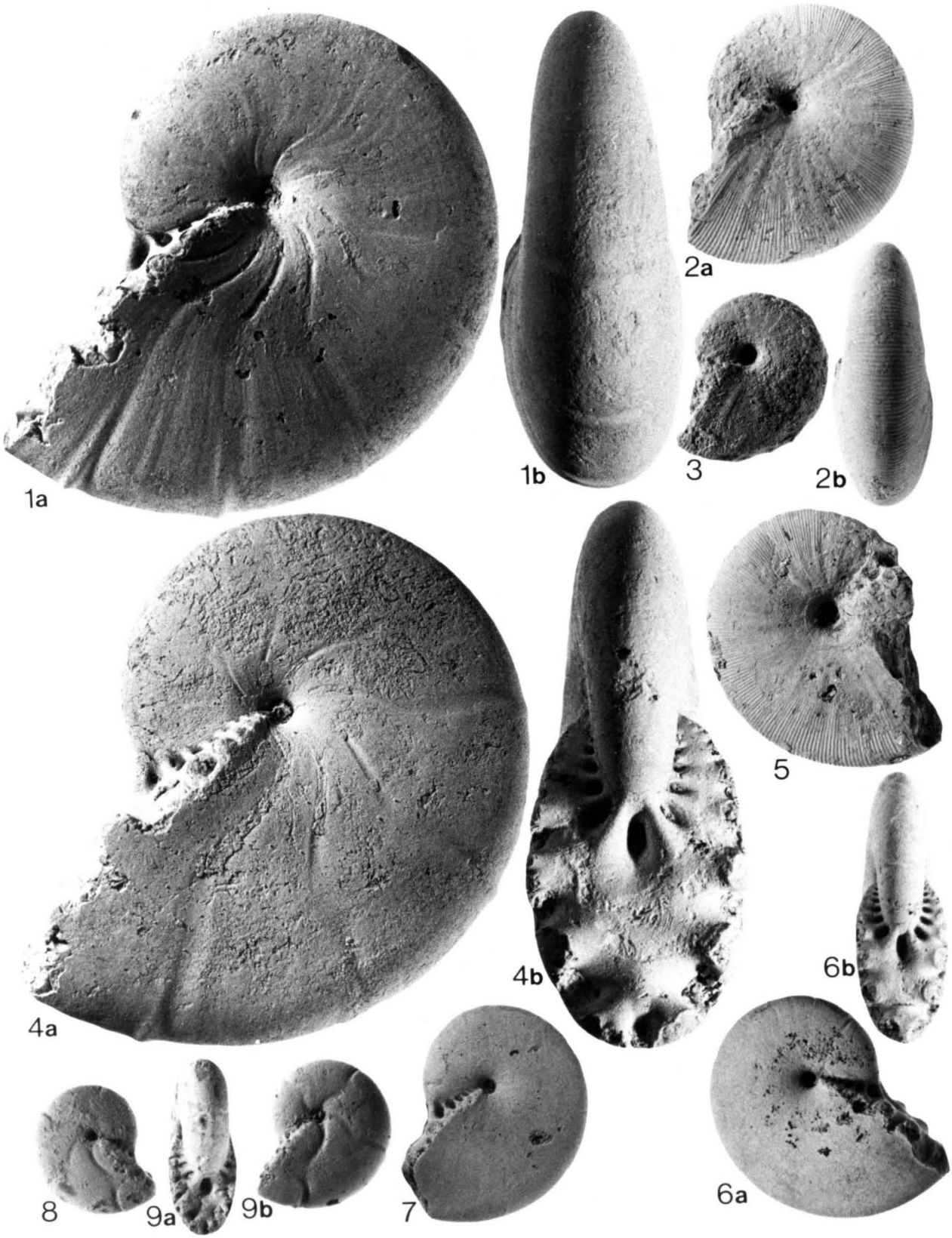
1a
1b
2a
3
2b
4a
4b
5
6b
6a
8
9a
9b
7

PLATE 3

Figure 1a-b: Lilloettia boesei (Burckhardt), C1-3, 1X.
Figure 2a-b: Xenocephalites gr. "nikitini-vicarius" (Burckhardt)/Imlay, C1-15, 2X.
Figure 3a-c: Lilloettia steinmanni Spath, C1-6, 1X.
Figure 4a-c: Eurycephalites cf. vergarensis, (Burckhardt), C1-8, 1X.

1a

1b

3a

3b

3c

2a

2b

4a

4b

4c

PLATE 4

Figure 1a-b: Lilloettia steinmanni Spath, C1-6, 2X
Figure 2a-b: Eurycephalites cf. rotundus (Tornquist), C1-15, 2X.
Figure 3a-b: Xenocephalites gr. "nikitini-vicarius", (Burckhardt)/Imlay, C1-15, 2X.
Figure 4: Paracuariceras cf. incisum Schindewolf, C1-15, 1X.

1a

1b

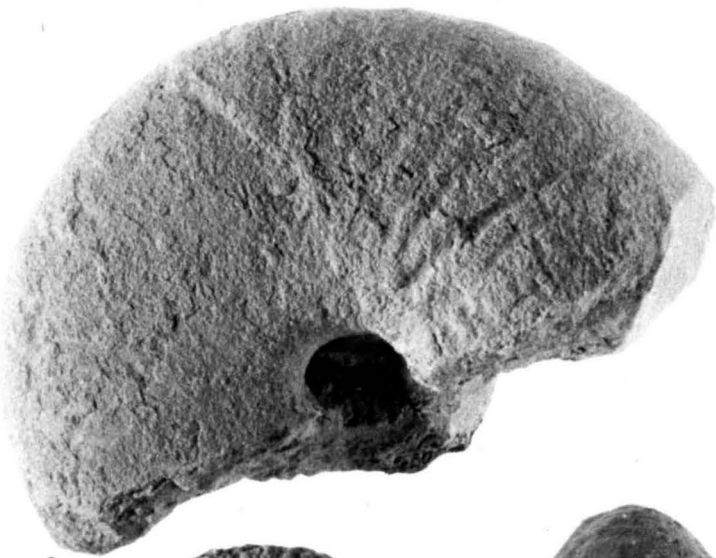

2a

2b

3a

3b

4

PLATE 5

Figure 1a-c: Xenocephalites gr. "nikitini-vicarius" (Burckhardt)/Imlay, C1-6, 2X.
Figure 2: Phlycticeras cf. pustulatum Reinecke, C1-6, 1X.
Figure 3a-b: Phlycticeras cf. pustulatum, C1-13, 1X.
Figure 4a-b: Phlycticeras cf. pustulatum, C1-6, 1X.
Figures 5-9: Parapatoceras distans (Baugier & Sauze), C1-15, 1X.

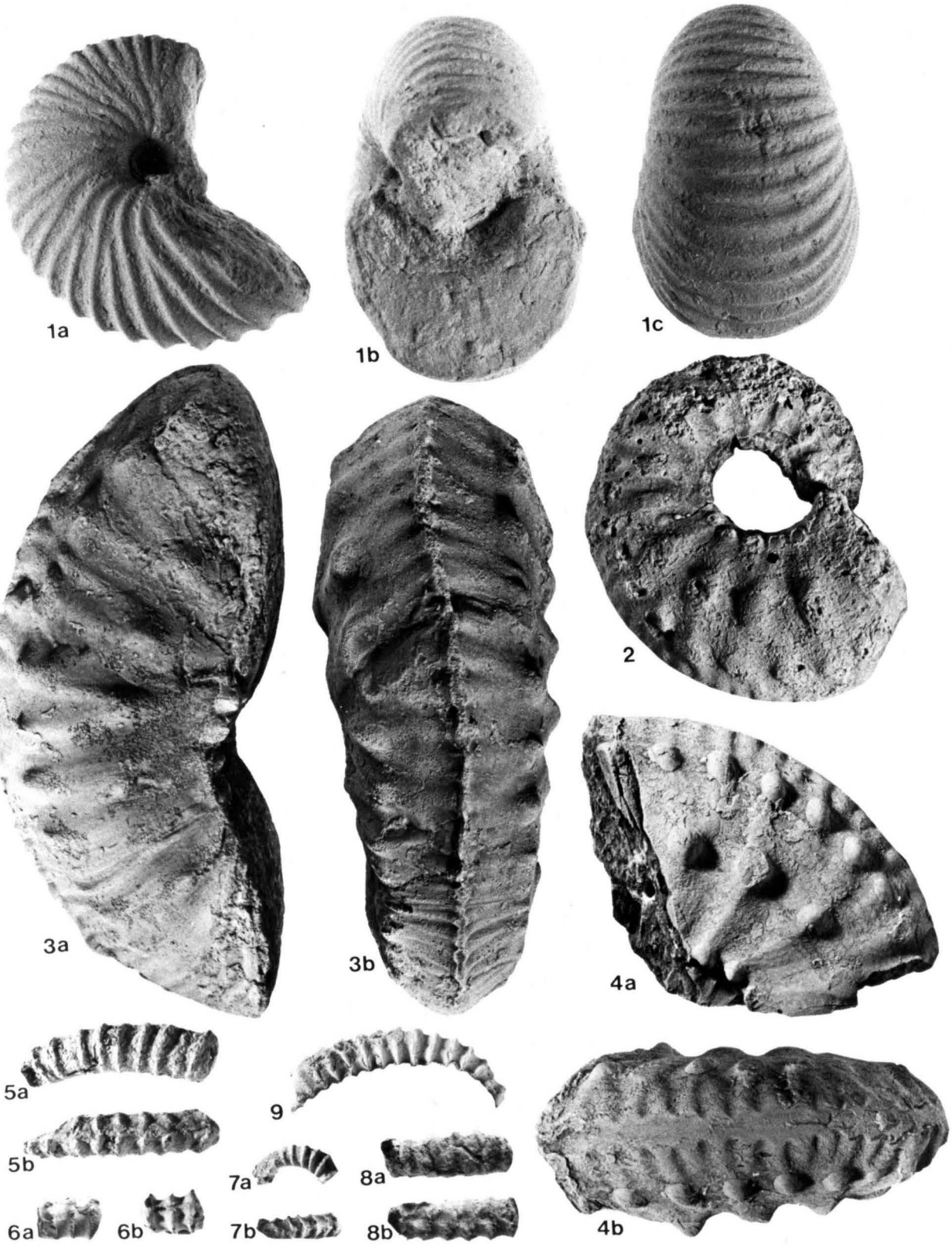
1a
1b
1c
2
3a
3b
4a
4b
5a
5b
6a
6b
7a
7b
8a
8b
9

PLATE 62

Figure 1a-b: Oxycerites (Alcidellus) cf. tenuistriatus (Grossouvre), C1-17, 1X.
Figure 2a-b: Oxycerites (Alcidellus) cf. tenuistriatus, C1-17, 1X.
Figure 3: Jeanneticeras cf. malbosi Elmi, C1-15, 2X.
Figure 4a-b: Jeanneticeras cf. malbosi, C1-15, 2X.
Figure 5: Jeanneticeras cf. malbosi, C1-16, 2X.
Figure 6a-b: Jeanneticeras cf. malbosi, C1-15, 2X.
Figure 7: Oxycerites (Paroecotraustes) davaicensis Lissajous, C2-15, 1X.
Figure 8: Oxycerites (Paroecotraustes) davaicensis, C1-15, 1X.
Figure 9: Oxycerites (Paroecotraustes) waageni Stephanov, ♂, C1-15, 1X.
Figure 10: Oxycerites (Paroecotraustes) waageni ♂, C1-15, 1X.
Figure 11a-b: Oxycerites (Alcidellus) cf. tenuistriatus, C4-8, 1X.
Figure 12a-b: Clydoniceras inflatum Westermann, C2-15, 1X.
Figure 13a-b: Clydoniceras inflatum, C1-15, 1X.
Figure 14: Clydoniceras inflatum, C1-15, 1X.
Figure 15: Clydoniceras inflatum, C2-15, 1X.
Figure 16: Oxycerites (Alcidellus) cf. tenuistriatus, C4-8, 1X.

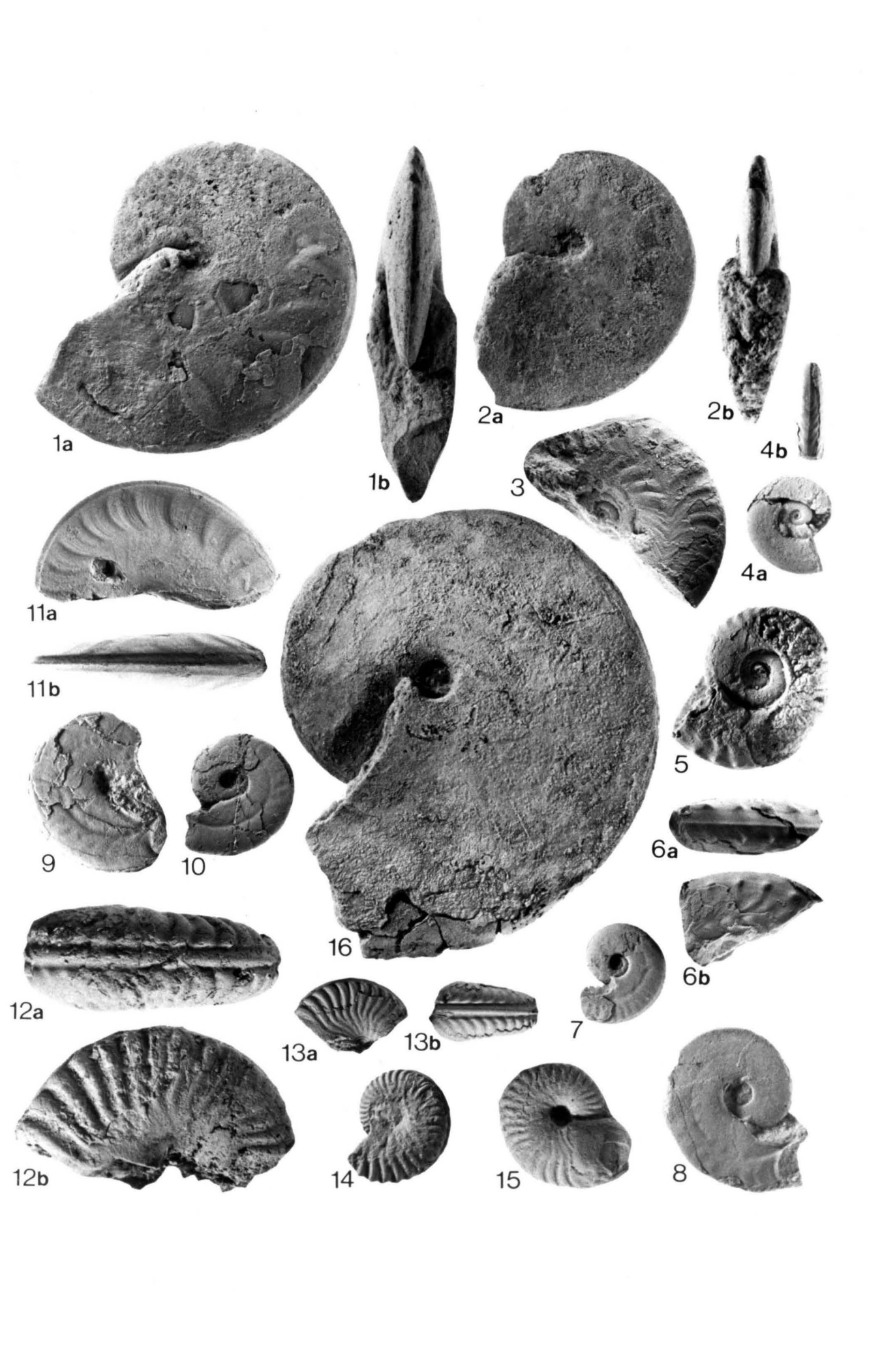
1a
1b
2a
2b
4b
3
4a
11a
11b
5
9
10
16
6a
6b
12a
7
13a
13b
12b
14
15
8

PLATE 7

Figure 1a-b: Neuqueniceras cf. plicatum (Burckhardt), C1-6, 1X.
Figure 2a-b: Neuqueniceras sp. ♂, C1-7, 1X.
Figure 3a-b: Neuqueniceras sp. ♂, C1-7, 1X.
Figure 4a-b: Neuqueniceras cf. plicatum, C1-6, 1X.
Figure 5a-b: Neuqueniceras cf. plicatum, C1-7, 1X.
Figure 6a-b: Neuqueniceras sp. ♂, C1-6, 1X.
Figure 7a-b: Neuqueniceras steinmanni (Stehn), C1-6, 1X.

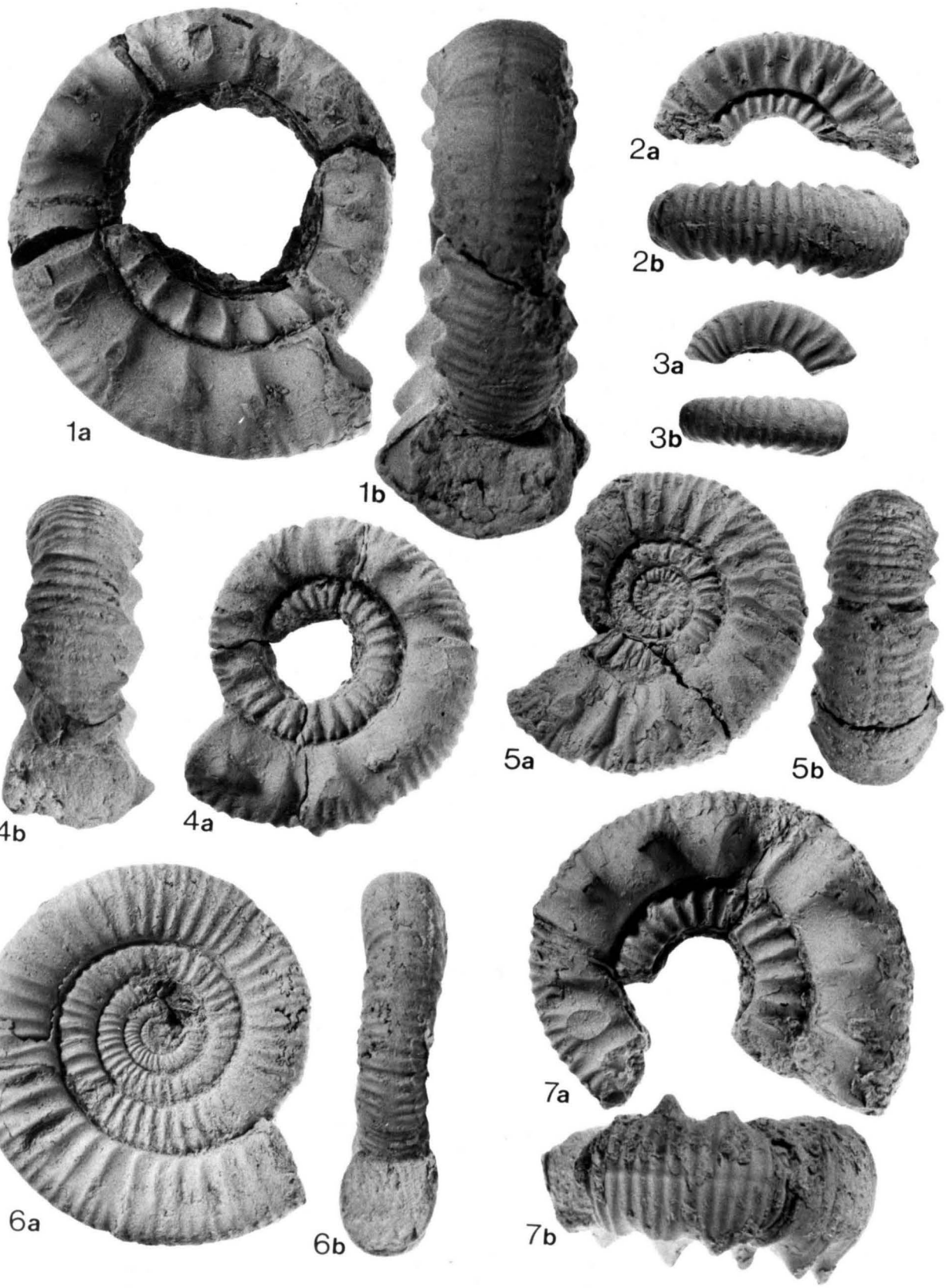
1a
1b
2a
2b
3a
3b
4b
4a
5a
5b
6a
6b
7a
7b

PLATE 8

Figure 1a-b: Neuqueniceras steinmanni (Stehn), C1-6, 1X.
Figure 2: Neuqueniceras steinmanni (Stehn), C1-7, 1X.
Figure 3a-b: Choffatia (Homeoplanulites) cf. ybbsensis (Jussen), C1-6, 1X.
Figure 4a-b: Neuqueniceras sp. ♂, C1-4, 1X.
Figure 5a-b: Choffatia gottschei (Steinmann), C1-4, 1X.
Figure 6a-b: Neuqueniceras sp. ♂, C1-6, 1X.

1a

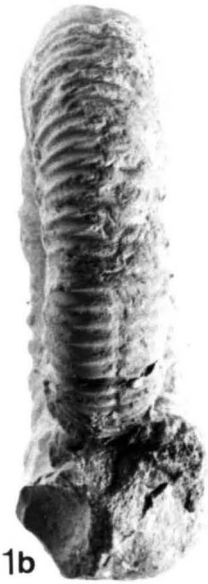

1b

2

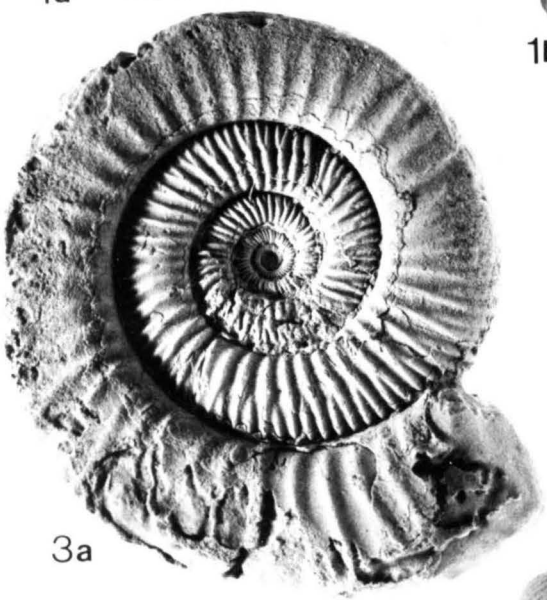

3a

4a

4b

3b

5a

5b

6a

6b

PLATE 9

Figure 1a-b: Choffatia aberrans (Burckhardt), C1-3, 1X.

1a

1b

PLATE 10

Figure 1a-b: Neuqueniceras (Frickites) bodenbenderi (Tornquist), C2-14, 1X.

1a

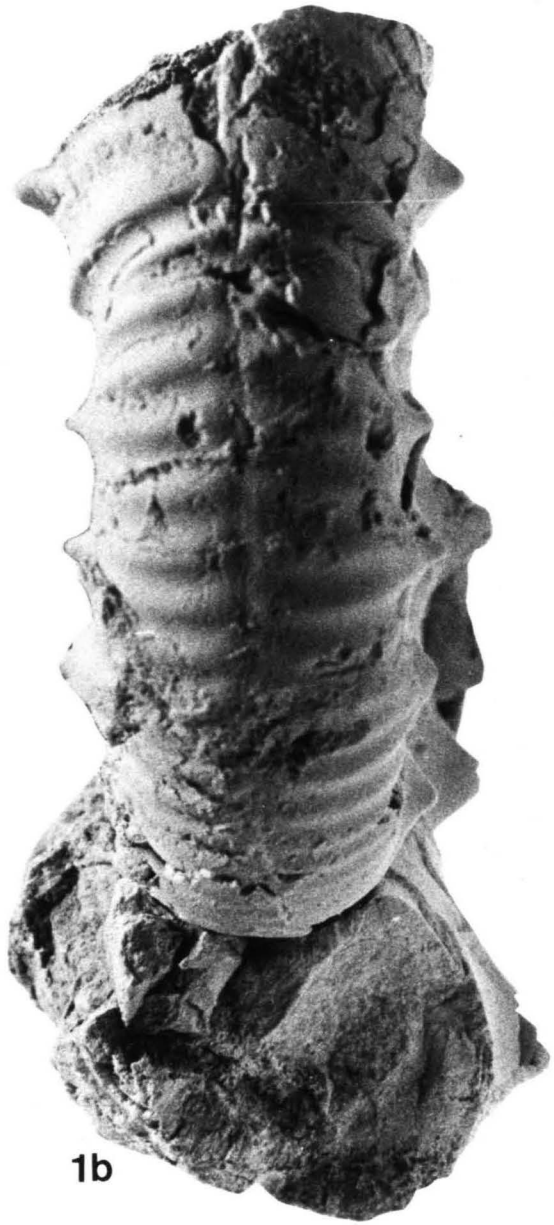

1b

PLATE 11

Figure 1a-b: Choffatia cf. subbackeriae (d'Orbigny), C1-6, 1X.
Figure 2: Choffatia cf. subbackeriae, C1-6, 1X.
Figure 3a-b: Reineckeia franconica (Quenstedt), C1-18, 1X.
Figure 4a-b: ?Choffatia sp. ♂, 1X.


1a
1b
2
3a
3b
4a
4b

PLATE 12

Figure 1: Choffatia aberrans (Burckhardt), C1-6, 1X.
Figure 2a-b: Choffatia suborion (Burckhardt), C1-3, 1X.
Figure 3a-b: Neuqueniceras (Frickites) bodenbenderi (Tornquist), C1-14, 1X.
Figure 4a-b: ?Choffatia (Homeoplanulites) sp. ♂, 1X.

1

3a

3b

2a

2b

4a

4b

PLATE 13

Figure 1a-b: Choffatia aff. jupiter (Steinmann), C3-2, 1X.
Figure 2: Choffatia suborion (Burckhardt), C1-3, 1X.
Figure 3: Choffatia aff. jupiter, C4-2, 1X.
Figure 4a-b: Oxycerites cf. prahecquense Petitclerc, C1-3, 1X.
Figure 5a-b: Prohecticoceras dominjoni Elmi, C3-2, 1X.

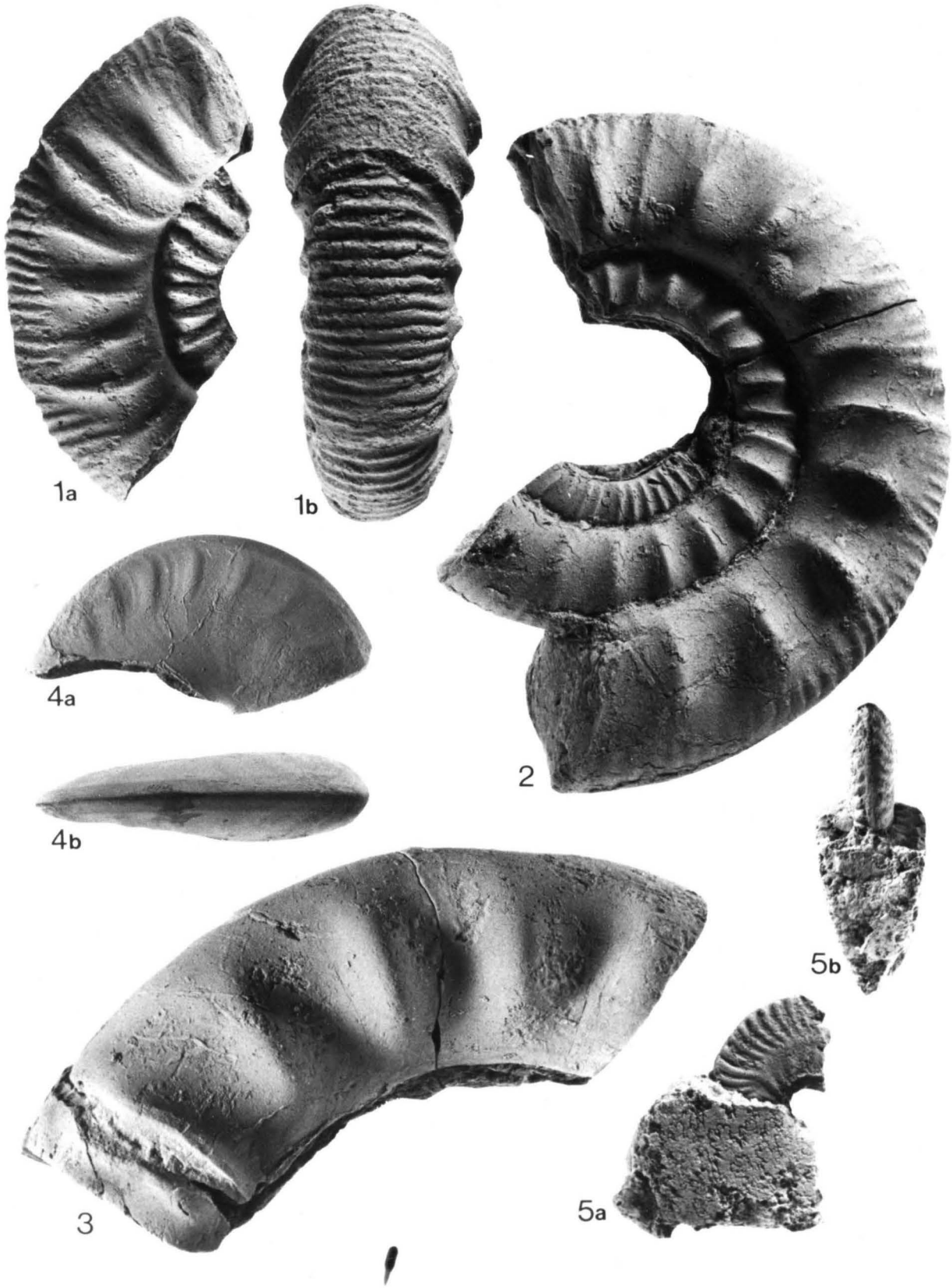
1a
1b
2
4a
4b
5b
3
5a

PLATE 14

Figure 1a-b: Reineckeia (Rehmannia) gr. "rehmanni-pictava" (Oppel)/(Burckhardt), C1-17, 1X.

Figure 2: Reineckeia (Rehmannia) gr. "rehmanni-pictava" C1-17, 1X.

Figure 3a-b: Reineckeia (Rehmannia) gr. "rehmanni-pictava" C1-17, 1X.

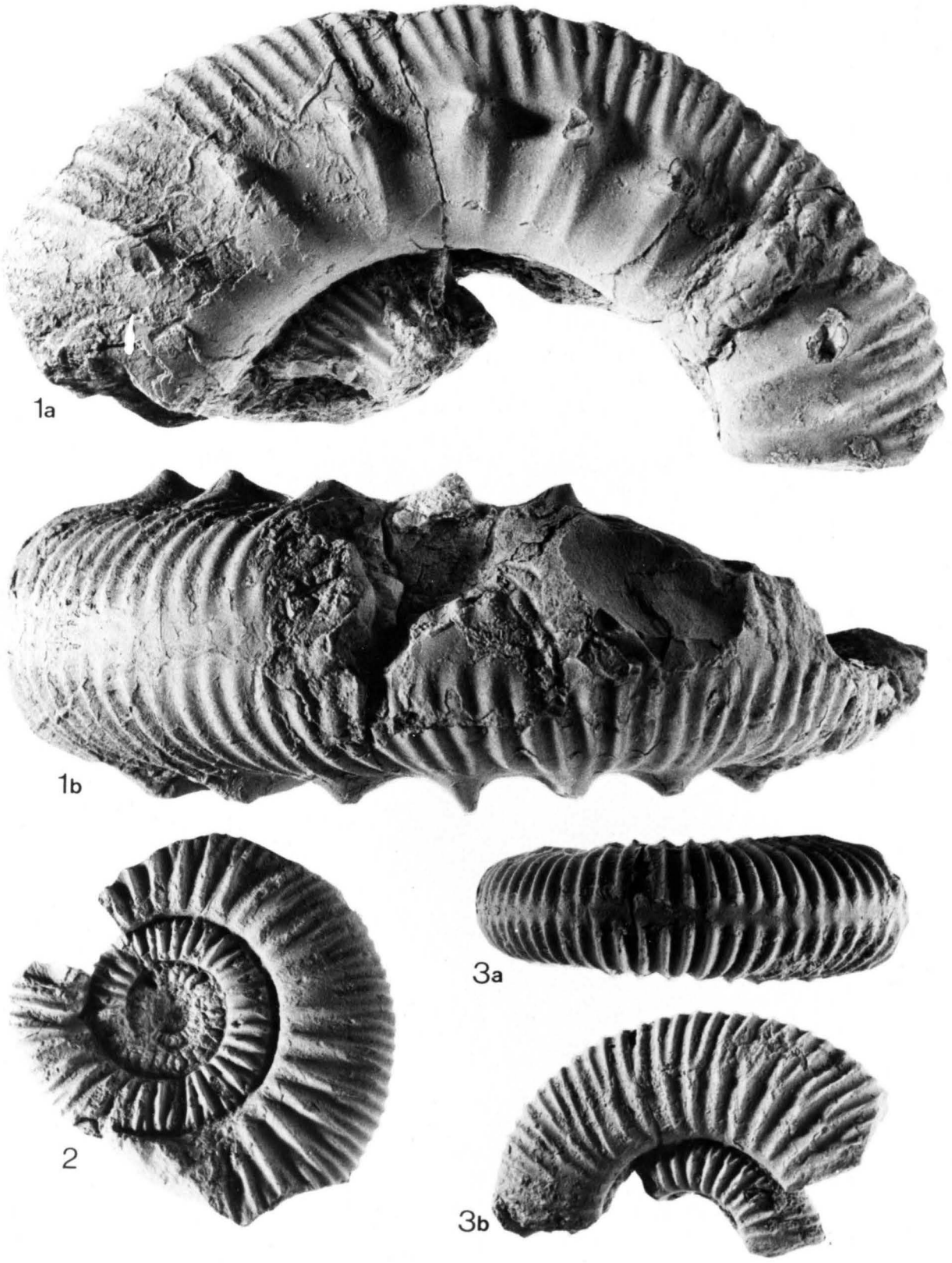
1a
1b
2
3a
3b

PLATE 15

Figure 1a-b: Mytilus (Falcimytilus) cf. stricapillatus Hayami, C3-2, 3. 1X.
Figure 2a-b: Unicardium cf. varicosum Sowerby, C4-1, 2. 1X.
Figure 3: Liostrea sp., C3-2, 3. 1X.
Figure 4a-b: Liostrea sp., C3-2, 3. 1X.
Figure 5a-b: Liostrea sp., C4-2. 1X.
Figure 6: Corbula oaxaquena Alencaster, C3-2, 3. 1X.
Figure 7a-b: Isocardia mixteca Alencaster, C3-2, 3. 1X.
Figure 8a-b: Isocardia mixteca Alencaster, C3-2, 3. 1X.

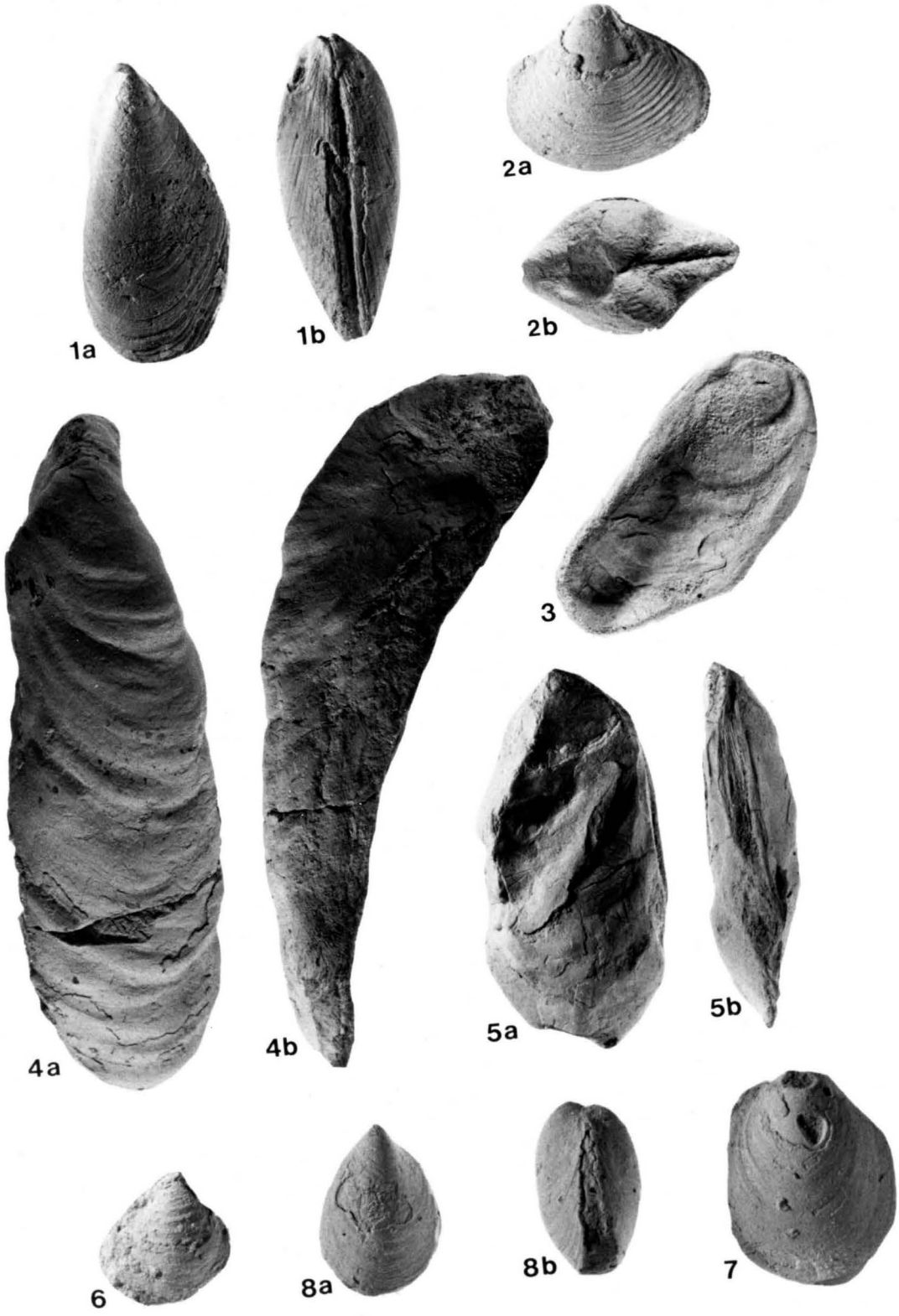
1a
1b
2a
2b
3
4a
4b
5a
5b
6
8a
8b
7

PLATE 16

Figure 1a-b: Vaugonia (Vaugonia) v-costata mexicana Alencaster, C4-1, 2; C3-2, 3. 1X.

Figure 2a-b: Anisocardia coxi Alencaster, C3; C1-6, 7. 1X.

Figure 3: Bositra sp., C1-15. 1X.

Figure 4a-b: Lucina magna Alencaster, C3-6, 1X.

Figure 5: Inoceramus cf. fuscus Quenstedt, C2-16, 1X.

Figure 6: Inoceramus cf. fuscus Quenstedt, C2-14, 1X.

Figure 7a-b: Capillirhynchia sp. C3-2, 3, 1X.

Figure 8: Cryptalaux sp., C4-8, 1X and 2X.

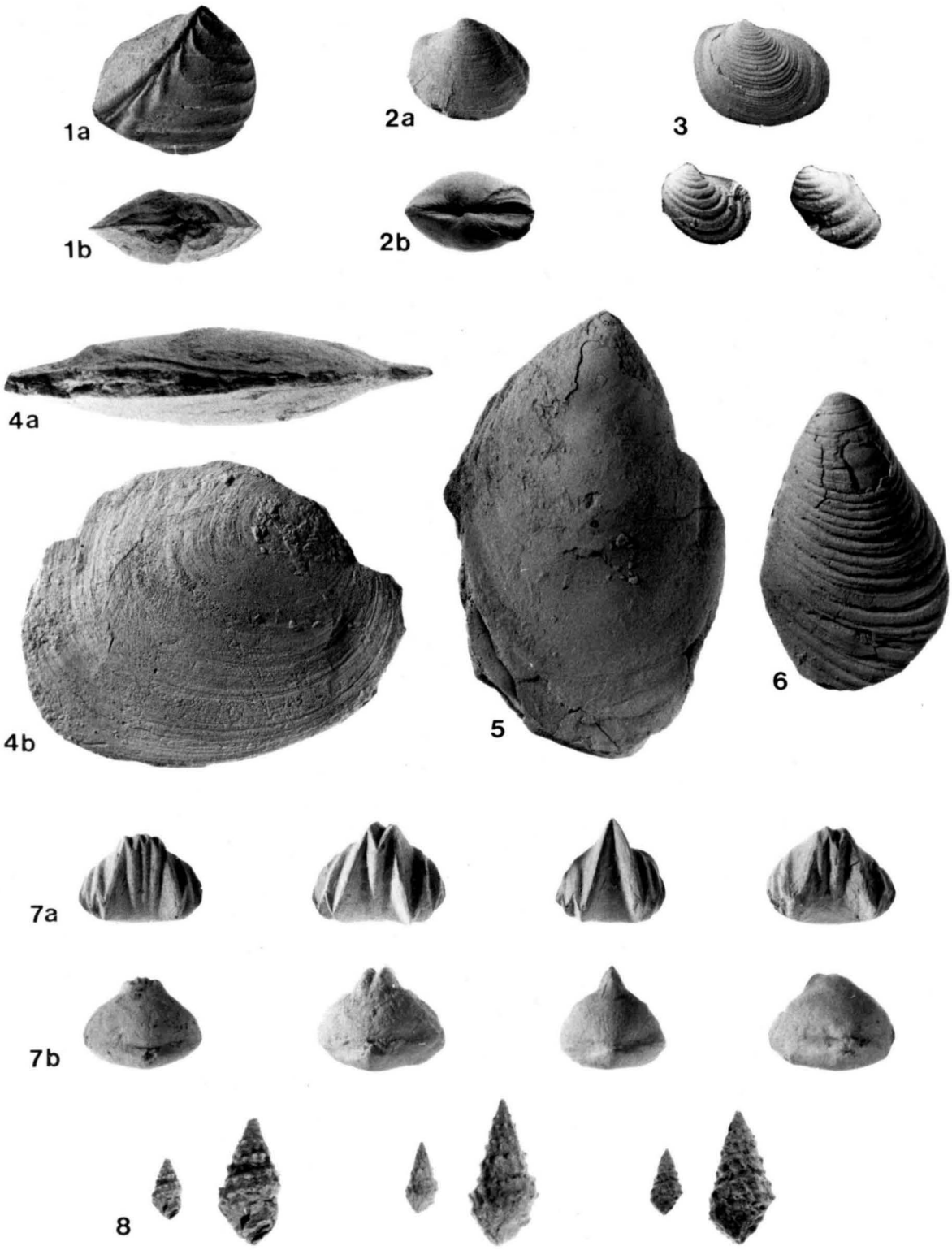
1a
1b
2a
2b
3
4a
4b
5
6
7a
7b
8

CHAPTER 5: PALEOECOLOGY

5.1 INTRODUCTION

Several faunal assemblages may be distinguished within the stratigraphic sequence of the Tecocoyunca Group near Coauilote, Mexico. These faunal assemblages are associated with specific sedimentary environments. The combination of faunal assemblages and their sediments permits the establishment of five communities specific to the Tecocoyunca Group. A community refers to a group of organisms living together in the same habitat (McKerrow, 1978). The following invertebrate communities have been distinguished: Sandy Mud, Shifting Sands, Restricted Mud, Open Marine Basinal and Black Mud. Block diagrams are presented in an attempt to diagrammatically visualize the habitat and characteristic organisms of each community. The upper planar surface (S_1) represents the living community, the lower planar surface (S_2) its fossil record.

5.2 SANDY MUD COMMUNITY

The diverse association of epifaunal and infaunal suspension feeding bivalves of the sandy mud community is seen in Facies A:interbedded sandstones, siltstones and shales. Other faunal components include suspension-feeding epifaunal brachiopods, large grazing gastropods, and nektonic ammonites (Fig. 5.1). Such a diverse population reflects several features of the environment. Firstly, the

Figure 5.1 SANDY MUD COMMUNITY

a. Epistrenoceras hystricoides (Rollier) (Mollusca: Cephalopoda: Ammonoidea)
b. Bullatimorphites (Kheraiceras) cf. bullatus (d'Orbigny)
c. 'Peltoceras' constrictum Burckhardt
d. Mytilus (Falcimytilus) cf. stricapillatus Hayami (Bivalvia: Mytilidae)
e. Liostrea sp. (Mollusca: Bivalvia: Pteroida-oyster)
f. Vaugonia (Vaugonia) v-costata mexicana Alencaster (Bivalvia: Trigoniidae)
g. ?Capillirhynchia sp. (Rhynchonellidae -brachiopod)
h. Unicardium varicosum Sowerby (Bivalvia: Mactromyidae)
i. Lucina magna Alencaster (Bivalvia: Lucinidae)
j. Corbula oaxaquena Alencaster (Bivalvia: Corbulidae)
k. Planolites sp. (ichnofossil)
l. Chondrites sp. (ichnofossil)

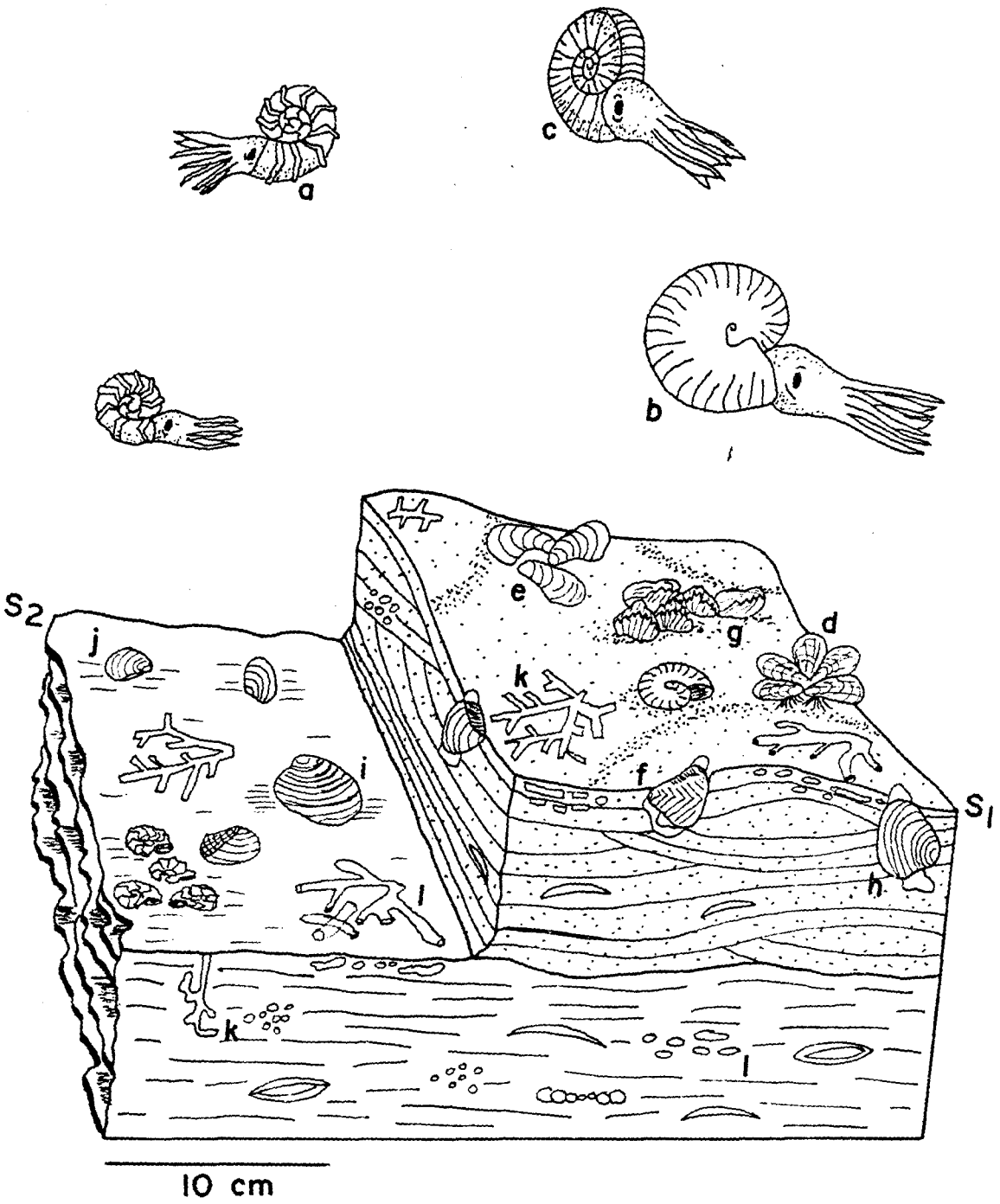
a
c
b
S2
S1
j
i
l
k
e
g
d
k
f
h
k
l
10 cm

proportion of sand and silt provided a more stable substrate than the muds. Some bivalves require sandier substrates while others prefer muddier substrates. The availability of these substrates within Facies A is conducive to bivalve diversity. The second feature indigenous to a suspension-feeding community is a relatively shallow water environment with sufficient turbulence to carry suspended organic matter (Sellwood, 1978). High rates of sedimentation excluded all deep burrowing bivalves.

The muds contained a flourishing population of shallow infaunal suspension-feeding bivalve species such as Anisocardia coxi Alencaster, Unicardium varicosum Sowerby, Isocardia mixteca Alencaster, Lucina magna Alencaster and Vaugonia (Vaugonia) v-costata mexicana Alencaster. Abundant feeding traces of Chondrites, and Planolites indicate that marine worms preferred the silty muds for burrowing.

The sands contained a sparser fauna of the previously mentioned bivalves due to episodic emplacement and high rate of deposition. Epifaunal and infaunal bivalves, as well as Chondrites and Planolites are found in the upper few centimetres of the sand beds suggesting colonization subsequent to deposition. The epifaunal bivalves Mytilus (Falcimytilus) cf. stricapillatus Hayami, Liostrea sp. and rhynchonellid brachiopods are associated with the sands. Occurrence of the rhynchonellids indicates that the water was clear and the seafloor stable enough for pedicle

attachment (Sellwood, 1978). Mytilus was also able to byssally attach to the stable substrate. The rhynchonellids and Mytilus occur in monospecific clusters. Shallow burrowing and mobile suspension-feeding bivalves such as Vaugonia also colonized the sands.

Salinity appears to have been normal marine, but some regions may have experienced slightly brackish salinities. Ammonites are stenohaline suggesting fully marine conditions. Liostrea is considered to be euryhaline (Sellwood, 1978). Small localized occurrences of Mytilus and Corbula suggest minor periodic influxes of freshwater causing slightly brackish salinities on a small scale. However, the seawater above the bottom possessed a sufficiently normal marine character to support ammonites.

Relatively shallow (10-20 metres) water depths, not too distant from shore, is indicated. Hummocky cross stratification (HCS), present within the sandstones, is formed below fairweather wave base (10-15 metres) by storm waves (Walker, 1984). Oysters and Mytilus are also generally associated with relatively shallow nearshore areas in modern environments (Kauffman, 1969).

5.3 SHIFTING SANDS COMMUNITY

The shifting sands community is found within the clean, fine- to medium-grained sandstones of Facies F, N, and P. Physical sedimentary structures are dominant over the

biogenic structures. Solitary vertical domichnia of the Skolithos ichnofacies predominate the faunal component of this community (Fig. 5.2). Body fossils are absent except for some 5-10 cm thick coquina layers consisting of fragmented oysters (Liostrea sp.).

The paleoenvironment was high energy intertidal and subtidal nearshore areas. The sands were constantly in motion due to fairweather wave activity. Common sedimentary structures are planar parallel bedding (swash cross stratification), planar tabular cross stratification and small- to medium- scale trough cross-bedding. Abrupt changes in rates of erosion, deposition, and reworking of the sediments were commmon. Storm activities greatly influenced the shifting sands community. Planar truncation surfaces demarcate periods of intense storm activity which eroded and lowered the angle of the nearshore profile (McCubbin, 1982).

High energy turbulent conditions of the shifting sands community were conducive to suspension-feeding organisms. Suspension-feeding polychaete worms and sea anenomes constructed vertical dwelling tubes assigned to Skolithos, Monocraterion and Diplocraterion. Deep vertical burrows permitted these organisms to feed on the suspended organic matter within the overlying water column, yet provided protection from moving sediments and scouring. Large storm-generated waves had catastrophic effects on the fauna

Figure 5.2 SHIFTING SANDS COMMUNITY

a. Liostrea sp. (Bivalvia: Pteroidea -oyster)
b. Skolithos sp. (ichnofossil)
c. Skolithos sp. burrow with annelid worm
d. Monocraterion sp. (ichnofossil)
e. Monocraterion sp. burrow with annelid worm
f. Diplocraterion sp. (ichnofossil)

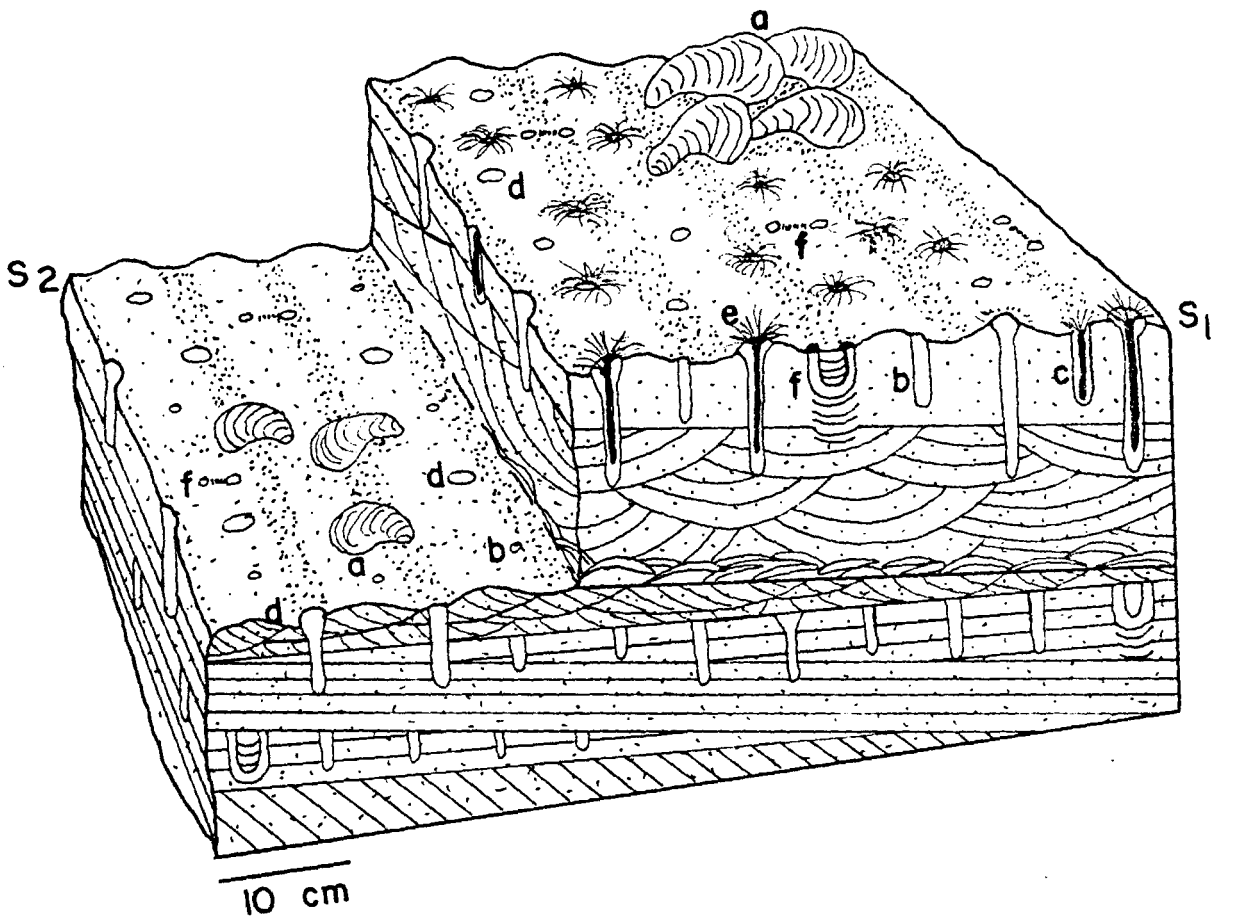
a
d
f
e
f
b
c
S2
S1
f
d
a
b
d
10 cm

of the shifting sands community. Extensive portions of the community were eroded as evidenced by the planar truncation surfaces. Burrows are truncated and even obliterated along the planar erosional surfaces depending on depth of erosion. Protrusive and retrusive spreiten in various sediment horizons of the community are indicative of episodic deposition and erosion of the sands. The paucity of macrofossils may be attributed to the inability of the unstable shifting sands to support populations of siphonate infaunal suspension-feeding bivalves. Some attached epifaunal suspension-feeding bivalves (oysters) were able to survive in "nests" or "reefs" of one species. Storm waves apparently destroyed these oyster colonies periodically and deposited the fragmented shells as coquina beds. Lack of macrofossils and bioturbation other than the Skolithos ichnofacies suggests that gastropods and bivalves other than oysters were absent or existed only in small numbers. The sands of the community are very porous, and many shells especially those composed of aragonite may have been dissolved. This may explain the preponderance of oyster shells, which consist of low-magnesium calcite.

In summary, the paleoenvironment of the shifting sands invertebrate community was intertidal to subtidal. Fairweather processes were very active and they retained organic matter in suspension within the water column. Suspension-feeding marine worms and sea anenomes lived in

vertical dwelling burrows, while macrofossils were rare.

5.4 RESTRICTED MUD COMMUNITY

Lithology of the resticted mud community is described under Facies R as slightly bioturbated, thinly bedded, dark grey shales with thin, sharp based interbeds of siltstone, sandstone, and silty laminations. Exposures are located at Arroyo Tecocoyunca within units 7_1 , 7_2 , 8_4-8_{14}. The shales are extremely rich in plant debris. Thin coal seams are also apparent, although not in great abundance. Sandstone and siltstone interbeds contain abundant shell fragments and are often moderately bioturbated.

The fauna of the restricted mud community is a low diversity-high abundance population consisting of the bivalve Anisocardia coxi Alencaster and the tiny cerithiacean gastropod Cryptalaux (Fig.5.3). The low diversity-high abundance nature of the fauna is indicative of high environmental stress. Cryptalaux can tolerate lowering of salinity. Low diversity combined with great abundance and dominance of cerithiaceans in a gastropod assemblage usually indicates brackish water conditions, and fluctuating salinities (J. Szabo, pers. comm.).

Bioturbation is significant within the restricted mud community. The shallow infaunal suspension-feeding bivalve Anisocardia was a sluggish burrower but would have accounted for some shallow bioturbation (McKerrow, 1978). Cryptalaux, a detritus feeder, probably grazed and burrowed

Figure 5.3 RESTRICTED MUD COMMUNITY

a. Anisocardia coxi Alencaster
(Mollusca: Bivalvia: Arcticidae)
b. Cryptalaux sp.
(Mollusca: Caenogastropoda: Cerithiacean)

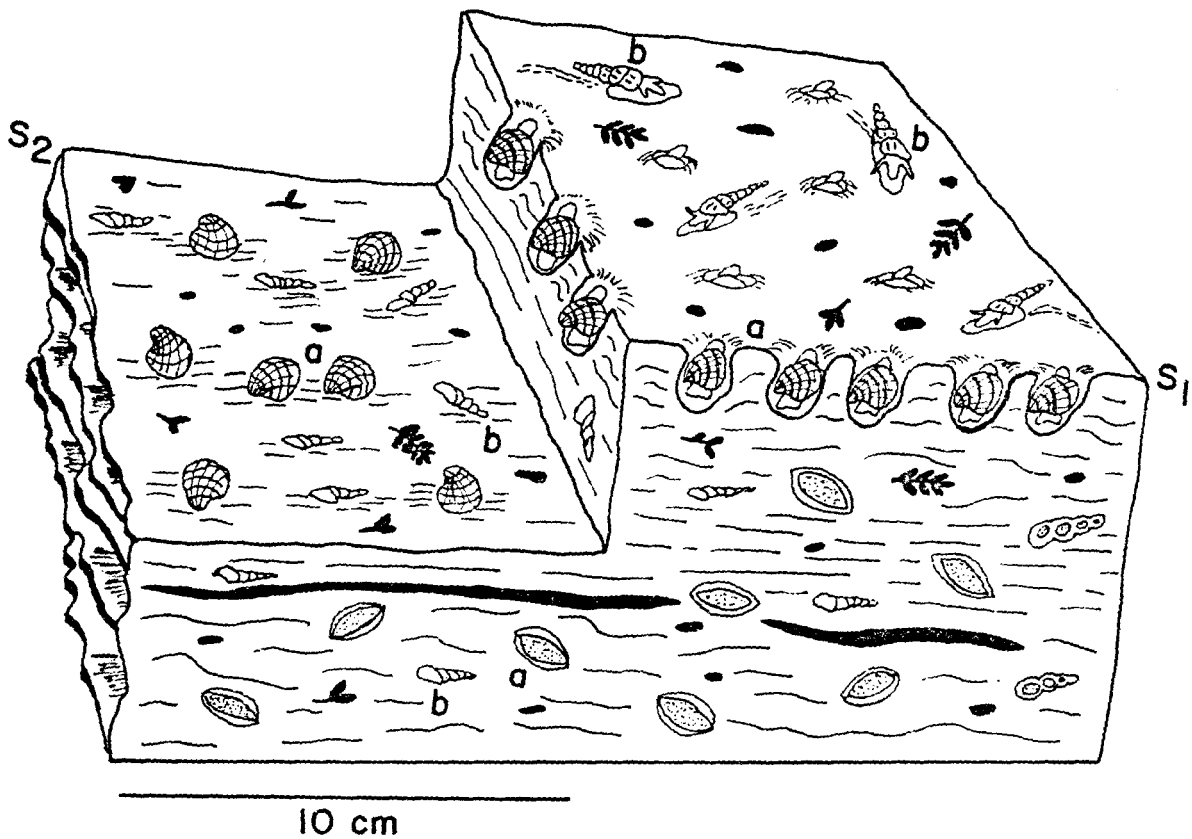
S2
S1
a
b
10 cm

at or near the sediment surface. Sedimentation rates of the mud must have been low to allow the organisms' bioturbation to keep pace. Horizons of poorly bioturbated fissile shale within Facies R indicate periods during which sedimentation rates exceeded those of bioturbation.

Muddy substrates and fluctuating brackish salinities excluded all organisms except those which could tolerate such conditions. Competition from other organisms was minimal and hence the members of the restricted mud community flourished. An abundant food supply may be inferred by: (1) high population density of Anisocardia and Cryptalaux, and (2) the quiet sheltered environment with freshwater influxes acting as an additional source of nutrients. Large volumes of plant debris provided a significant refractory carbon supply. Anisocardia and Cryptalaux were unable to utilize the refractory plant material directly. It was most likely exploited after partial decomposition by bacteria. The bacteria themselves would also have been an important food source, especially for Anisocardia. Cerithiacean gastropods such as Cryptalaux are thought to have grazed on algae and bacteria (J. Szabo, pers. comm.).

The restricted mud community seems to have been located in a muddy nearshore environment which was sheltered from open marine salinities. Sheltering may have been due to a physical barrier which also excluded wave energies, thus

allowing mud and plant debris to accumulate. Coarser grained sediments were carried episodically into the restricted water body during periods of elevated wave energy. Fluctuating brackish salinities of the restricted mud community existed as the result of freshwater influxes from proximal land areas.

5.5 BLACK MUD COMMUNITY

This community is observed within Facies T, consisting of thinly bedded, fissile bituminous black shale in levels C1-15 and C2-15 of Arroyo El Rincon and El Campamento. The fossil assemblage is composed of planktonic and nektonic macrofossils; ammonites (See Fig. 5.4 for typical genera) of stenohaline affinity and marine vertebrates (the crocodile Steneosaurus sp.). The assemblage also contains abundant "Posidonae" bivalves, especially Bositra sp. and carbonized plant fragments.

An anomaly in what otherwise appears to be a planktonic and nektonic fossil assemblage is Bositra sp.. The study of Jefferies and Minton (1965) suggests that Bositra was not a benthonic bivalve, but planktonic. Primary evidence is the facies association with black shales, which are bituminous and lacking in benthos. This is suggestive of anoxic or oxygen-poor bottom conditions. A second line of evidence is the extensive global distribution of Bositra sp. in sediments that usually lack any other benthos. Lateral

Figure 5.4 BLACK MUD COMMUNITY

a. Ptychophylloceras plasticum (Burckhardt) (Mollusca: Cephalopoda: Ammonoidea)
b. Clydoniceras inflatum Westermann ibid
c. Neuqueniceras (Frickites) bodenbenderi (Tornquist) ibid
d. Parapatoceras distans (d'Orbigny) ibid
e. Bositra sp. (Mollusca: Bivalvia: Pteroida)
f. Steneosaurus sp. (Reptilia: Teleosauridae: crocodile)

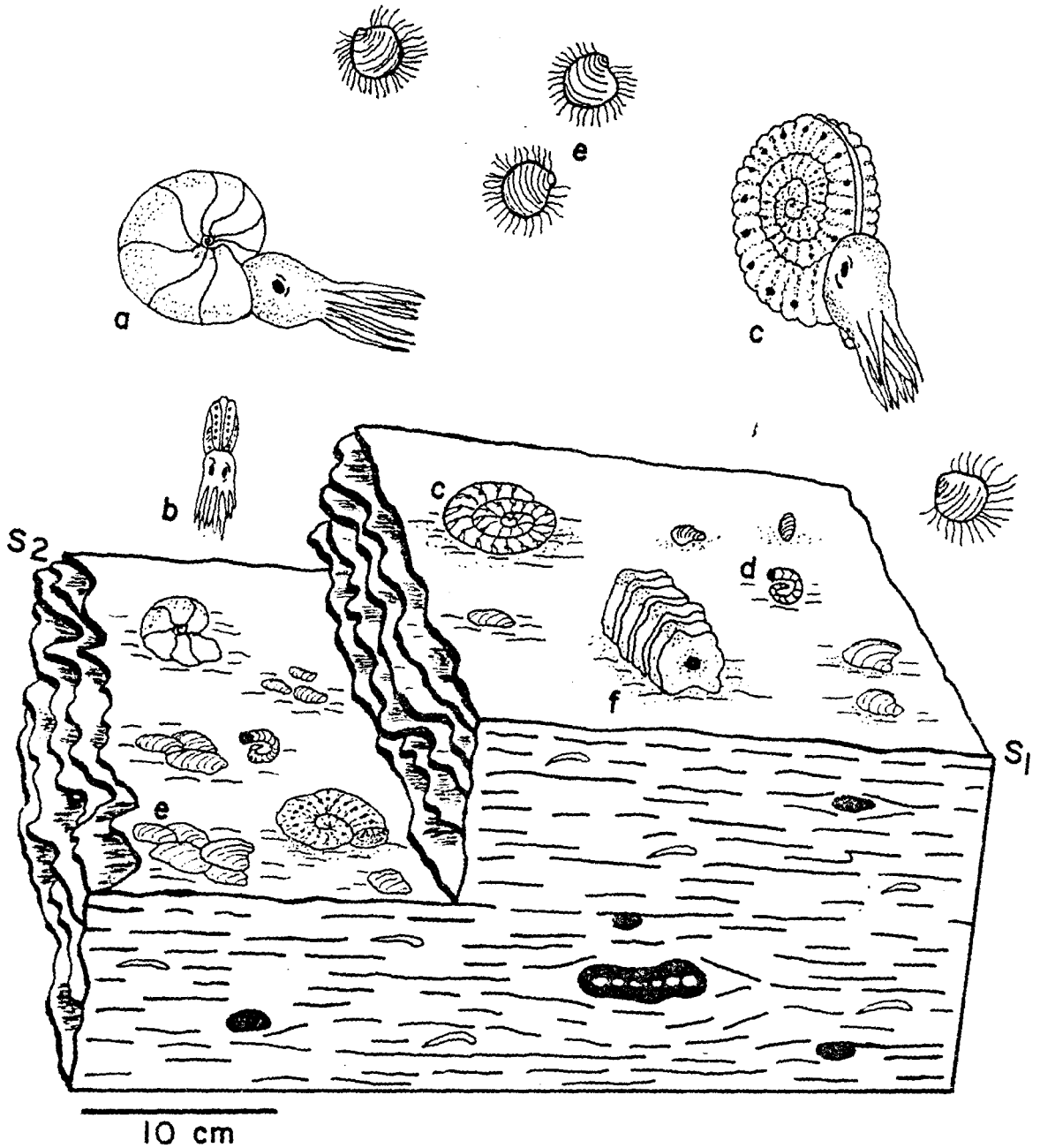
a
b
c
d
e
f
S2
S1
10 cm

distribution may be up to a hundred miles, even within one sedimentary basin (Jefferies and Minton, 1965). Finally, the shell morphology of Bositra is compatible with a planktonic mode of life. Ability to swim is suggested by anterior and posterior gapes, thin shell, and a hinge line which facilitates a wide marginal gape (Jefferies and Minton, 1965). There is no sign of attachment at any life stage and it has been proposed that Bositra had tentacles which would increase the drag and reduce the settling velocity (Jefferies and Minton,1965). Hydrodynamic experimentation confirmed that such a mode of life was feasible. Kauffman (1981) refuted this interpretation based on studies of Bositra in the German Posidonienschiefer. His lines of evidence, other than the morphology of Bositra apply only to the Posidonienschiefer. The characteristics of the Black Mud Community observed near Coauilote remain supportive of the interpretations of Jefferies and Minton (1965). A pseudoplanktonic mode of life is possible in which Bositra was attached to flotsam. This seems unlikely however, due to the lack of other pseudoplanktonic organisms and flotsam in the typical Bositra facies (Jefferies and Minton, 1965).

In summary, the fine mud,rich in organic matter from partially decomposed plant and animal remains,accumulated on an oxygen deficient sea floor. The organic remains had a high preservation potential due to the lack of oxygen and

benthos. The community formed in the deepest portions of the sedimentary basin, perhaps 200-300 metres water depth. Evidence for depth not exceeding 600-700 metres is the numerous non-imploded Ptychophylloceras plasticum Burckhardt. Nekton and plankton were present in the main body of sea water but limited water circulation allowed stagnant anoxic conditions to develop on the sea floor at or near the sediment-water interface.

5.6 OPEN MARINE BASINAL COMMUNITY

The open marine basinal community is associated with Facies S: medium grey shales containing thin interbeds of siltstone, sandstone and limestone. The coarser grained interbeds are interpreted as the result of storm-generated flows and contain some allochthonous shell fragments which are not considered to be part of this community. The fauna of the shales is dominated by pelagic organisms, especially ammonites which were nektobenthic (Fig. 5.5). The small planktonic bivalve Bositra sp. also occurs in minor abundance. Benthic faunal components include sparse Anisocardia coxi Alencaster, a slow and shallow burrowing suspension-feeding bivalve. Early in the appearance of the open marine basinal community, populations of the tiny cerithiacean gastropod Cryptalaux sp. were also present. Abundant disseminated plant debris is found in these same horizons even producing thin coal horizons (Unit C1-1). The

Figure 5.5 OPEN MARINE BASINAL COMMUNITY

a. Ptychophylloceras plasticum (Burckhardt) (Mollusca: Cephalopoda: Ammonoidea)
b. Neuqueniceras (Frickites) bodenbenderi (Tornquist) ibid
c. Reineckeia (Rehmannia) gr. rehmanni-pictava ibid
d. Reineckeia franconica (Quenstedt) ibid
e. Parapatoceras distans (d'Orbigny) ibid
f. Bositra sp. (Mollusca: Bivalvia: Pteroida)
g. Anisocardia coxi Alencaster (Bivalvia: Arcticidae)
h. Cryptalaux sp. (Caenogastropoda: Cerithiacea)

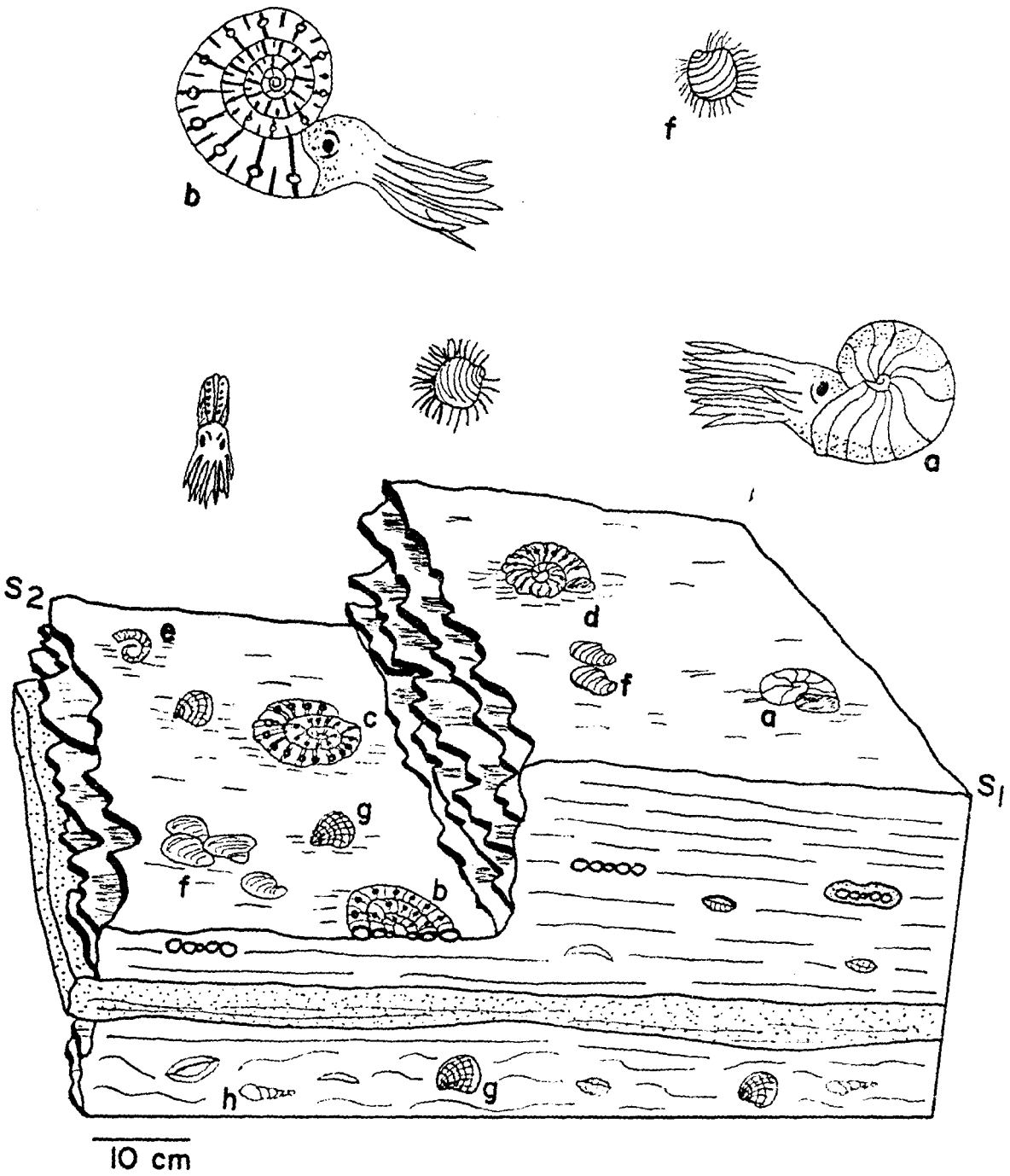
b
f
a
S2
S1
e
c
d
f
a
g
f
b
h
g
10 cm

amount of plant debris decreases upward within the community. Cryptalaux also disappears completely by Unit 7 of section C1-Arroyo El Rincon. Salinity of this community must have been normal marine to support large populations of stenohaline ammonites within the water column. However, the earliest stages of the community (Units C4-8_3-8_1; C1-1-3) contain very few ammonites. These same horizons contain considerable populations of Cryptalaux. Thus, it seems that early in the developmental stages of the open marine basinal community, the environment was somewhat restricted with some periodic influxes of freshwater, creating localized brackish conditions. The underlying restricted mud community also supports this interpretation.

In summary, the paleoenvironment appears to have been shallow to intermediate water depths (20-150 m). The shales are the result of mud accumulation in a quiet marine environment below fairweather wave base. Mud accumulation was interrupted episodically by density currents containing coarser sediments. Initial stages of the community indicate particularly shallow water depths and a more proximal environment affected by freshwater influxes. Reasons for this are: (1) abundance of cerithiacean gastropods (Cryptalaux), (2) very sparse ammonites, (3) considerable plant debris even to the extent of creating thin coal beds, and (4) some infaunal bivalves. During further development

of the community, water depth increased and salinities became normal marine. Eventually, benthic organisms disappeared completely while stenohaline ammonites flourished in the open marine environment.

CHAPTER 6: FACIES SEQUENCES AND DEPOSITIONAL ENVIRONMENTS

6.1 INTRODUCTION

The Middle Jurassic Tecocoyunca Group, seen as a whole, has an overall transgressive trend. Several minor fluctuations of base level are superimposed on the large-scale transgressive sequence. The following discussion of facies and depositional environments begins with the oldest (U. Bathonian) sediments of the Alto de Teeolutla section (C3), and proceeds upward through the continuous sections; C4-Arroyo Tecocoyunca, C1-Arroyo El Rincon and finally C2-Arroyo El Campamento. The facies within these sections are discussed in order of occurrence from the base to the top.

6.2 Section C3- Alto de Teeolutla

The lower 150 metres of this section contain Facies A interbedded sandstones and shales (Fig. 6.1). Limestone and massive limey siltstone beds (Facies B and C respectively) are intercalated. Sandstone beds of Facies A contain hummocky cross stratification indicative of reworking of sediments below fairweather wave base (10-20 m) by storm waves (Dott and Bourgeois, 1982; Walker, 1984). Characteristics of these sandstones are identical to those described by Aigner (1985) for proximal storm deposits found in the transition zone of offshore areas. The sandstone

Figure 6.1: Facies sequences within Section C3-Alto de Teeolutla.

C3 - Alto de Teeolutla

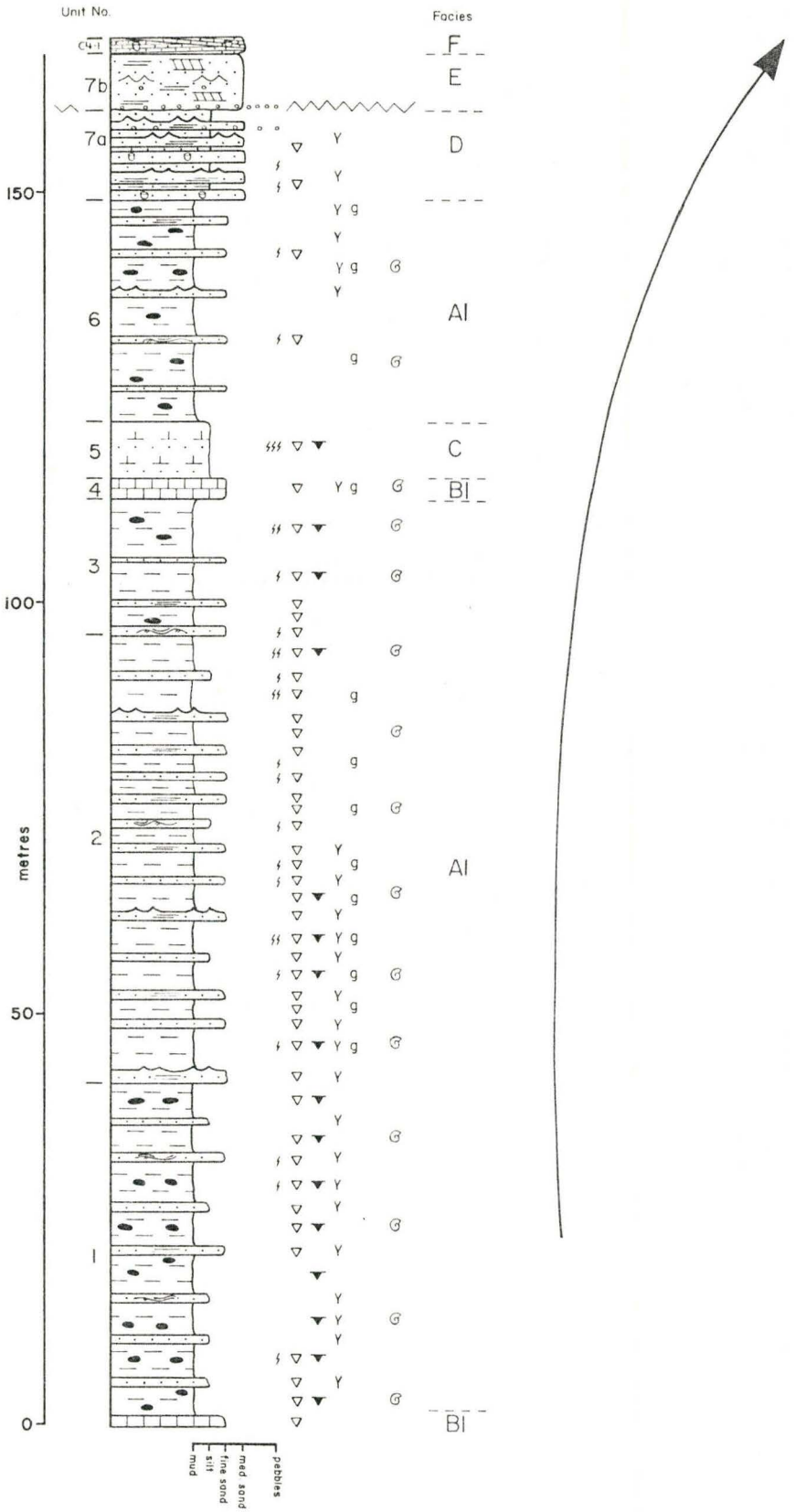

interbeds become slightly thicker and more abundant in the uppermost 50 metres of Facies A suggesting a proximality trend (Aigner, 1985). In summary, sedimentary and faunal characteristics of Facies A, B, and C are indicative of a shallow offshore marine environment below fairweather wave base (See Sandy Mud Community: Section 5.2).

Facies D lies above facies A, B, and C, and consists of 11 m of interbedded siltstones and sandstones interpreted as lower shoreface deposits. The sandstone beds have the definitive characteristics of shoreface storm deposits as described by Kumar and Sanders (1976) and Aigner (1985). The ratio of sandstone to siltstone beds increases upward, defining a coarsening-upward trend, whereas bioturbation decreases in intensity. This is characteristic of the transition from lower to upper shoreface (Howard, 1972). The fauna, especially the Skolithos ichnofacies, is typical of shifting substrates in a moderate to high energy littoral/infralittoral environment (Frey and Pemberton, 1984).

Facies E, blocky sandstones, is erosively based and contains sedimentary structures typical of upper shoreface sandstones (Howard, 1972; McCubbin, 1982; Reinson, 1984; Clifton et al., 1971; Davidson-Arnott and Greenwood, 1976).

Facies F (Section C4, Unit 1) contains 1.9 m of sandstone containing swash cross stratification, indicative of the wave swash zone of the foreshore, where fluctuating

water depths result from storm waves and tides (Harms et al., 1975; Clifton et al., 1971). The uppermost 15 cm contains high-density ($125/m^2$) Monocraterion burrows, typical of several metres water depth rather than the swash zone (Dr. M. J. Risk, pers. comm.). Small channel-form structures, interpreted as rip-current channels, have incised into the upper portion of Facies F (Units 1,8). Rip-current channels have been reported in water depths up to 5 m (Ingle, 1966) but generally occur 3-4 metres below mean sea level (Hunter et al., 1979).

The progression of Facies A to F is interpreted as a progradational (regressive) coarsening-upward sequence, in a wave-dominated climate. This sequence displays a proximality trend of storm deposits, ie. proximal storm deposits overlain by shoreface and intertidal storm deposits (Aigner, 1985). A deficiency of tidal sedimentary structures, and predominance of wave- and storm-related deposits is suggestive of a storm dominated shoreline (Clifton et al., 1971; Davis and Hayes, 1984). Preservation potential of moderate to high energy nearshore deposits is often relatively low except in subsiding basins where sedimentation is rapid (Clifton et al., 1971). A rapid rate of subsidence and sedimentation has been suggested for the Yucunuti Formation (see Section 1.6). The rate of sedimentation must have exceeded the rate of subsidence and/or sea-level variation to allow progradation of the

shoreline.

Total thickness of the progradational shoreface/foreshore deposits in Section C3 is approximately 20 m (Fig. 6.1). This is slightly thicker than most sequences which range from 6 to 12 m (e.g. Elliot, 1975; Howard and Reineck, 1972, 1981; Campbell, 1971). However, sequences up to 26 m have been documented by Hobday and Horne (1977) and Horne and Ferm (1976).

The shoreface sequence of Section C3 is a truncated coarsening-upward sequence (Fig. 6.1). Truncation occurs at the erosional base of Facies E. Erosion of the lower shoreface (Facies D) can be attributed to downcutting of the overlying upper shoreface sediments of Facies E. Evidence supporting such erosion is: 1) the erosional base of Facies E which contains a pebble lag, and 2) the significant deviation from a well developed coarsening-upward trend which is characteristic of the standard high-energy beach sequence (Howard and Reineck, 1981; McCubbin, 1982). This erosional truncation of lower shoreface deposits is most likely the result of an increase in base level (ie. sea level drop or tectonic uplift).

6.3 Section C4 - Arroyo Tecocoyunca

Eleven metres of Facies G sandstone gradationally overlie the coarsening-upward sequence of Section C3-Alto de Teeolutla (Fig. 6.2). This facies is characterised by low-angle inclined stratification consisting primarily of

Figure 6.2: Facies sequences within Section C4-Arroyo Tecocoyunca.

C4- Arroyo Tecocoyunca

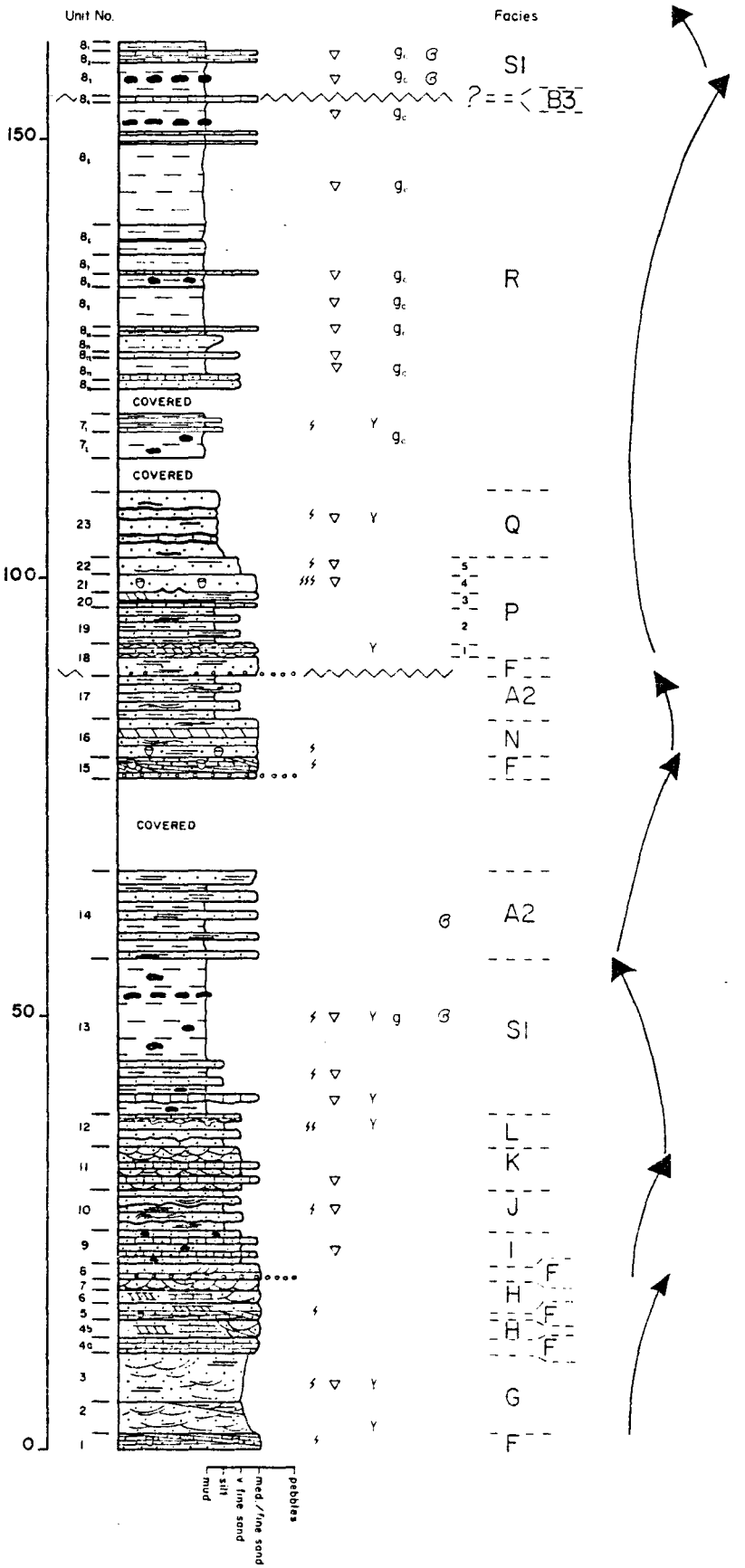

intersecting swaley deposits. It closely resembles swaley cross stratification (SCS), a storm-dominated structure formed in shallow water above fairweather wave base (Leckie and Walker, 1982). Facies G is bounded above and below by Facies F foreshore sediments suggesting that Facies G was deposited in the upper shoreface.

A 10 m thick alternation Facies F and H overlies Facies G. Paleocurrent orientations of tabular and trough cross stratification in Facies H indicate deposition by both longshore and shore-perpendicular currents. Facies H is interpreted as upper shoreface. This sequence represents a series of minor base level fluctuations.

Bioturbated fine-grained sandstone and silty limestone beds of Facies I lie immediately superjacent to the interbedded sequence of Facies F and H. Facies I is interpreted as lower shoreface deposits and they mark the beginning of an overall fining-upward (transgressive) sequence encompassing Facies J, K, L and S1 (Fig. 6.2).

Facies J consists of 4.6 m of amalgamated hummocky cross-stratified sandstones formed by waves of frequent storm events below fairweather wave base (Dott and Bourgeois, 1982; Walker et al., 1983).

Facies K sandstones are coarser-grained than in Facies J and represent a deviation from the overall fining-upward sequence. These sandstones are 5 m thick and contain small-scale trough cross stratification. Similar

stratification has been interpreted to have formed by migrating lunate megaripples in the Lunate Megaripple (outer rough) facies within the wave build-up zone of the lower to middle shoreface (Clifton et al., 1971; Davidson-Arnott and Greenwood, 1976). Facies K is bounded above and below by finer-grained facies (I, J) deposited slightly below fairweather wave base. This may be explained by an observation described by Clifton et al. (1971), in which lateral migration of zones of sedimentary structures may be up to 80 metres with as little as a 2 m tidal rise. Wave parameters and gradient of the shoreface are also important factors in this migration (Clifton et al., 1971).

Facies L consists of interbedded sandstones and siltstones, interpreted as lower shoreface deposits. Facies S and Subfacies A2, offshore marine shales, immediately overlie Facies L. A covered interval separates Subfacies A2 from the overlying Facies F foreshore sandstones (Unit 15).

Facies F, foreshore sandstones, appears again in Unit 15 (Fig. 6.2). The upper bounding surface contains abundant Monocraterion burrows indicative of increasing water depth. The sediments of Facies F are abruptly (unconformably ?) overlain by Facies N (parallel laminated, tabular cross-bedded and hummocky cross-stratified sandstones). These sedimentary structures support the interpretation of a shallow nearshore environment.

Facies F swash zone sediments appear once again as a 2

m thick package within Unit 18 (Fig. 6.2). The base is sharp and characterised by a pebble lag. These foreshore deposits abruptly overlie offshore deposits, with upper and lower shoreface deposits absent. This may be attributed to the downcutting of Facies F foreshore deposits. Based on average foreshore/shoreface deposits, 10 to 20 m of shoreface deposits may have been eroded (Elliot, 1975; Howard and Reineck, 1972, 1981; Campbell, 1971). This erosion surface marks the base of a regressive (progradational) sequence of overlying lagoonal sediments.

Facies P, with a 11.4 m thick sequence of thinly interbedded sandstones, siltstones, silty shales and coal, overlies Facies F (Fig. 6.2). The association of several interbedded lithologies is typical of lagoonal sequences with several overlapping subenvironments (McCubbin, 1982; Phleger, 1969). The erosionally based sandstones are interpreted as storm washover deposits, based on their sedimentary structures and stratigraphic position above beach sands and below lagoonal muds (McCubbin, 1982; Reinson, 1984; Schwartz, 1975; Leatherman, 1981). The abundance of plant debris and coal horizons suggests proximal marsh environments.

Marsh environments also supplied abundant plant debris to the overlying bioturbated siltstones of Facies Q. The shallow infaunal bivalve Anisocardia is profuse within the siltstones. This facies is interpreted as a mixed tidal

flat based on its sedimentological and faunal characteristics and sequential relationship with other facies.

Facies R consists of 38 m of thinly bedded, slightly bioturbated dark grey shales (Fig 6.2). These shales are interpreted as restricted marine (i.e. lagoon) in origin, based primarily on the fauna which is high in abundance and low in diversity (see Restricted Mud Community, Section 5.4). Facies R shales contain immense populations of the cerithiacean gastropod Cryptalaux sp. indicative of brackish salinities (J. Szabo, pers. comm.). Thin interbeds of sandstone, siltstone and limestone also occur within the shales. These beds are typified by erosive and undulatory bases which may be the result of erosion and/or loading, as the sediments were episodically emplaced by storms onto thixotropic muds of the lagoon. Facies R is also very rich in disseminated carbonaceous plant material and coal horizons suggestive of proximal marsh environments.

Taking into account the sequence of facies F to R, Facies F (Unit 18) may represent part of a sandy barrier which created a restricted lagoon environment landward of it (Fig. 6.2). The sequence contains brackish sediments which were deposited in an area restricted from open marine wave energies and salinities except during storms. This is the most important criterion in interpreting Facies F as a barrier.

Conditions conducive to the formation of a barrier island are: (1) a steady supply of sand to the shoreline, either by river input or longshore drift, and (2) a hydrodynamic setting characterised by low or moderate tidal ranges. The first condition seems probable in view of the thick sandy nearshore sequences observed within the Tecocoyunca Group outcrop. A low to moderate tidal range was suggested above, based on the absence of tidal sedimentary structures. Wave processes appear to have dominated.

The only enigma in the barrier interpretation is an apparent absence of tidal inlet deposits. However, this is accountable in several ways. Washover deposits are prominent in the lagoonal sediments of Facies P and R. These features are characteristic of a microtidal (<2 m) coast (Davis and Hayes, 1984). Tidal inlets are widely spaced and comprise a very small proportion of barrier complexes on coasts where tidal range is small and the supply of sediment is great (Davis and Hayes, 1984).

The brackish salinities suggested in the lagoonal sediments also indicates a microtidal regime. This is due to limited connection of the lagoon with an open marine water body because of the paucity of tidal inlets in a microtidal barrier (Elliot, 1978). These barrier islands are also frequently inundated or breached during storms because of insufficient passageways to accommodate

landward-directed storm surges (Hayes and Kana, 1976). As a result, washover fans are common (Facies P) and they often coalesce to produce an irregular apron of sand which projects out into the lagoon (Elliot, 1978). Such an apron may be represented by the massive sandstones in the upper portion of Facies P (Subfacies P4, P5) and, possibly, the massive siltstones of Facies Q. Facies Q siltstones are interpreted as mixed intertidal flats located on the lagoon side of the barrier. Similar situations of silts and sands along the backs of barriers are observed in modern barrier island environments (e.g. Laguna Madre; Rusnack, 1960).

The barrier/lagoonal package is a fining-upward progradational (regressive) sequence. The sequence of sediments from bottom to top is: nearshore, beach, washovers, marsh/tidal flat, and lagoon (Fig. 6.2). Other similar ancient progradational barrier island sequences have been discussed (Reineck, 1973; Davis and Hayes, 1984; Carter, 1978; Dickinson et al., 1972).

The top of the progradational sequence (i.e. Facies R lagoonal shales) is abruptly overlain by open marine offshore shales of Facies S (Subfacies S1) (Fig. 6.2). These are interpreted as having been deposited below fairweather wave base. This progression of lagoonal to offshore shales represents a significant and rapid transgressive event in the Late Bathonian-Early Callovian. The origin of this transgression appears to be a major

eustatic sea-level rise but subsidence is also implicated (see Section 7.5).

One of two possible mechanisms must have ensued. The first is landward barrier migration (shoreface retreat). As the sea level rises, sediment is eroded from the upper shoreface and emplaced either in the lower shoreface-offshore area or in the lagoon as a series of washover fans (Sanders and Kumar, 1975). When eustatic sea-level rise and/or subsidence rates are low relative to the rate of shoreface erosion, a relatively thin and incomplete transgressive sequence will result. A relatively rapid sea-level rise would result in the deposition of a thin sand sheet on the lagoonal muds as the barrier migrated landward. Sandstone beds within the base of Facies S or the top of Facies R may be representive of such a transgressive sand sheet (Fig. 6.2).

The alternative mechanism is termed "in-place drowning" (Rampino and Sanders, 1980), which involves a rapid rate of transgression. As sea-level rises, the barrier remains in place until the wave breaker zone reaches the crest of the barrier. At this point, the breaker zones leaps landward to the inner margin of the lagoon, and in the process, drowns the barrier. The vertical sequence for a drowned barrier from bottom to top is; barrier, lagoon, nearshore, and offshore sediments (Rampino and Sanders, 1980). Such a vertical sequence is observed in the Arroyo Tecocoyunca

section (C4). Either mechanism is difficult to prove conclusively from the outcrop data.

6.4 Sections C1-Arroyo El Rincon and C2- Arroyo El Campamento

The offshore shales of Facies S are approximately 400 m in total thickness (Fig. 6.3). They contain thin (5-60 cm) sharp-based interbeds of sandstone and siltstone, interpreted as distal storm deposits intercalated with shelf muds (Aigner, 1985). The fauna of Facies S is open marine (See Open Marine Basinal Community, Section 5.6).

Thirty-six metres of bituminous black shales of Facies T interrupt the sequence of Facies S shales in Unit 15 of the Arroyo El Rincon (C1) and Arroyo El Campamento (C2) sections. Facies T shales probably represent mud deposition in the deepest part of the basin (?200-300 m) with anoxic bottom conditions (See Black Mud Community, Section 5.5).

Facies T is overlain by shelf shales of Facies S, which in turn are overlain by sediments of Facies U, V, X, and Y all of which appear to represent a shallower and more proximal shelf environment (Fig. 6.4).

6.5 SUMMARY

The basal 150 m of the Tecocoyunca Group outcropping near Coauilote represent a coarsening-upward sequence of shallow offshore shales and sandstones deposited below fairweather wave base (10-20 m). This is overlain by 100 m containing four smaller coarsening-upward sequences of

Figure 6.3: Facies sequences within Section C1-Arroyo El Rincon.

C1 - Arroyo El Rincon

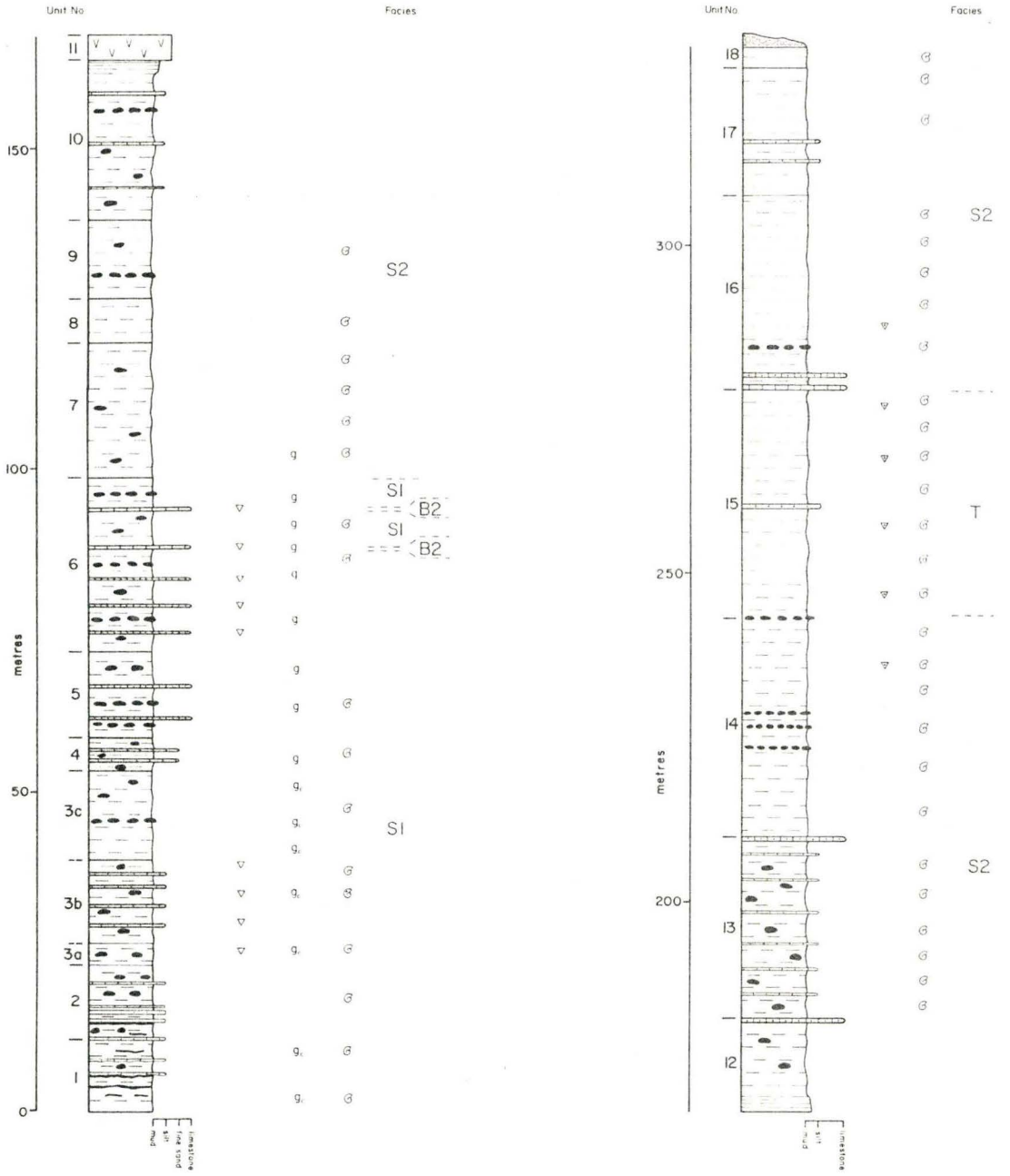

Figure 6.4: Facies sequences within Section C2-Arroyo El Campamento.

C2- Arroyo El Campamento

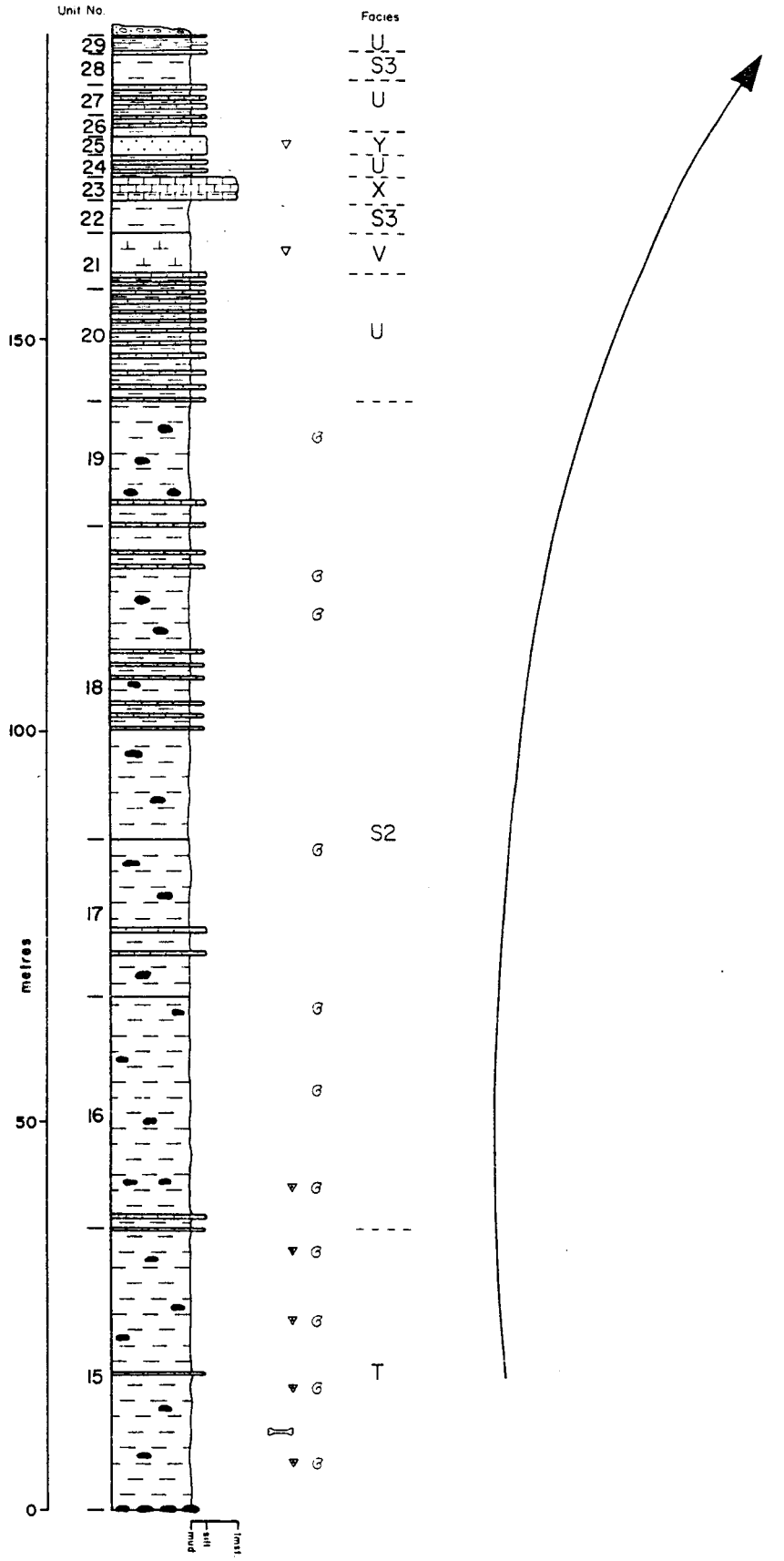

nearshore and beach sandstones. Each one of these represents fluctuations in base level due to: 1) tectonics, 2) eustatic sea-level variations, and 3) sediment supply. The fourth of these sequences is capped by beach and nearshore sediments interpreted as a barrier island. A fifth coarsening-upward trend, interpreted as washover and back-barrier sands, overlies the barrier sediments. Brackish lagoon shales lie superjacent to these sediments and terminate the barrier sequence.

These coastal sediments are abruptly overlain by 400 m of open marine shales which represent a major transgression initiated during the latest Bathonian. As the transgression continued into the Early Callovian, deep portions of the basin developed anoxic bottom conditions represented by 36 m of bituminous black shales. These are overlain by 100 m of open- marine shales. The entire outcrop sequence terminates with approximately 50 m of interbedded shales and siltstones deposited in shallower offshore areas. Figure 6.5 shows a schematic depositional environment and some of the associated facies for the Tecocoyunca Group.

The basin into which the Tecocoyunca Group sediments were deposited, appears to have undergone subsidence at a considerable rate (see Section 7.3). The rate of sedimentation in this basin was immense (e.g. ca. 1.1 m/Ka for the Yucunuti Fm; see Section 1.6). Approximately 900 m of sediments were deposited within ca. 4 ammonite standard

Figure 6.5: Block diagram illustrating the depositional environments of the various facies.

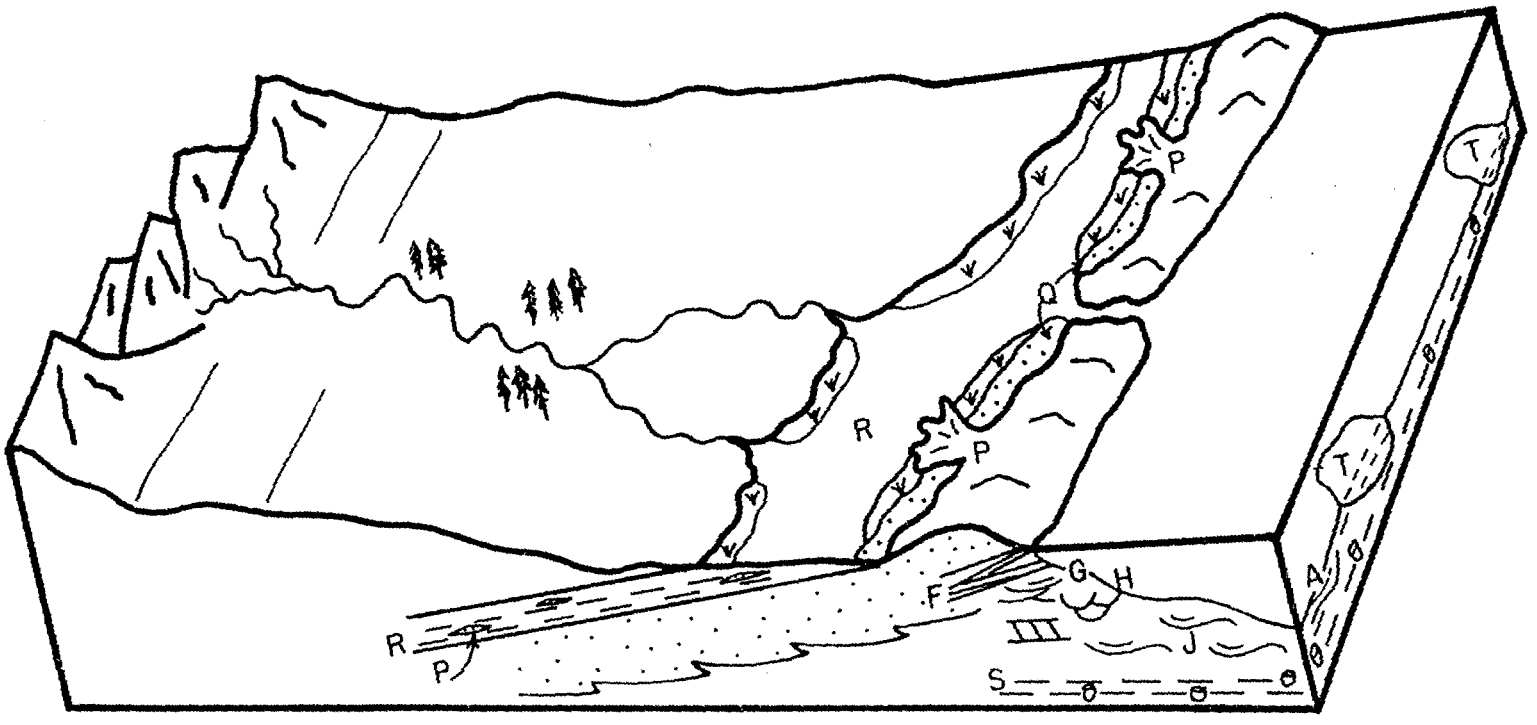
P
T
R
P
T
A
G
H
F
III
J
R
P
S

chronozones.

The Tecocoyunca group is characterised by abundant plant debris, especially in the nearshore sediments. This may be used to infer that the paleoclimate of the depositional area was humid or sub-humid (Dickinson et al., 1972; Elliot, 1978).

CHAPTER 7: SEA LEVEL VARIATIONS

7.1 INTRODUCTION

In recent years, considerable stratigraphic work has been done on Jurassic unconformities and eustatic sea-level cycles. Several global eustatic sea-level curves have been proposed for the Jurassic (e.g. Hallam, 1978, 1981; Vail et al., 1977, 1984; Vail and Todd, 1981). The chronological scale of these curves is based on the Jurassic time scale proposed by Van Hinte (1976a). There is an agreement between curves on most large-scale variations but discrepancies are apparent on smaller-scale variations. This is due to regional tectonics and precision of biostratigraphic correlation.

After detailed investigations, Vail and Todd (1984) concluded that sixteen eustatic sea-level cycles made up the Jurassic supercycle. These cycles correspond to depositional sequences which are recognizable from seismic, well, and outcrop data (Vail et al., 1984). Several of these cycles can be recognized on a global scale. Regional unconformities and marine transgressions-regressions are controlled by the interaction of three variables: subsidence, eustatics, and sediment supply (Vail et al., 1984).

Several chronostratigraphic scales have been proposed for the Jurassic and each one is based on different methods

and data (Fig. 7.1). Van Hinte (1976a) based his chronostratigraphic scale on glauconite radiometric ages. Westermann's (1984a) scale is based on ammonite standard subzones which were averaged between the Tethyan and Boreal faunal provinces. Note that there are significant age differences between period and stage boundaries of the various scales. Van Hinte's scale is adopted herein because chronostratigraphy of global eustatic sea-level curves continues to be based on his Jurassic time scale.

7.2 LATE BATHONIAN - EARLY CALLOVIAN

Arkell (1956) noted the presence of a major, world-wide Bathonian regression. Two world-wide lowstands have been recognized in Bathonian sedimentary sequences on the continents; Middle Bathonian and upper Upper Bathonian (post-Retrocostatum Zone). These two lowstands straddle a minor eustatic sea-level rise and highstand within the Retrocostatum Zone (Upper Bathonian). The Discus Zone (latest Bathonian) is usually completely absent in many sedimentary sequences world-wide.

Global eustatic sea-level curves for the Jurassic indicate a major sea-level fall near the end of the Bathonian followed by a significant rise in the Early Callovian (Hallam, 1978, 1981; Vail et al., 1977, 1984; Vail and Todd, 1981) (See Fig. 7.2). Until recently, the top of the regression (base of the transgression) was placed exactly at the Bathonian-Callovian boundary, dated as

Figure 7.1: Various chronostratigraphic scales proposed for the Jurassic. Van Hinte's (1976) scale is adopted in this study (After Westermann,1984).

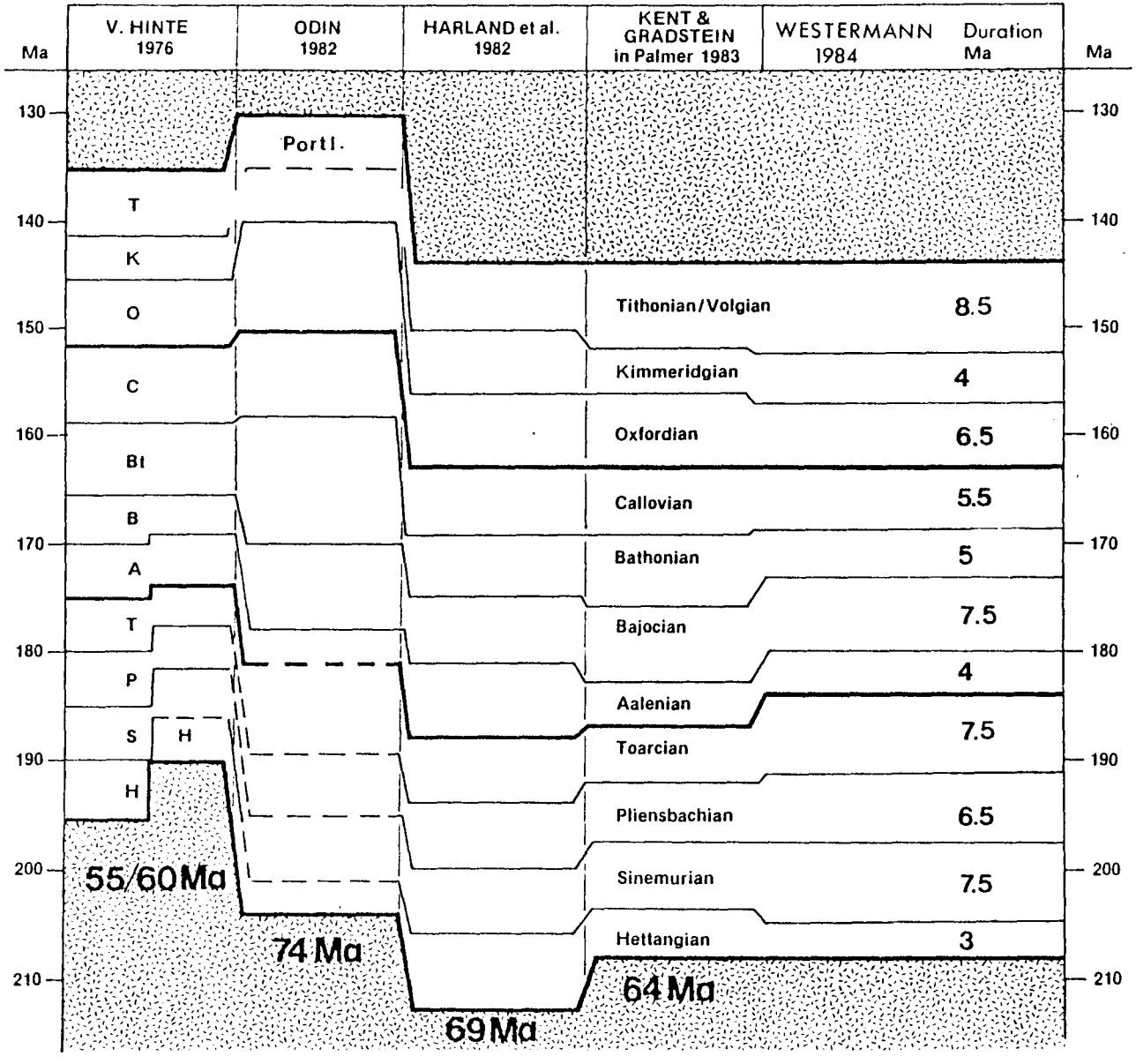
Ma
V. HINTE 1976
ODIN 1982
HARLAND et al. 1982
KENT & GRADSTEIN in Palmer 1983
WESTERMANN 1984
Duration Ma
Ma
130
140
150
160
170
180
190
200
210
Portl.
T
K
O
C
Bt
B
A
T
P
S
H
H
Tithonian/Volgian
8.5
Kimmeridgian
4
Oxfordian
6.5
Callovian
5.5
Bathonian
5
Bajocian
7.5
4
Aalenian
Toarcian
7.5
Pliensbachian
6.5
Sinemurian
7.5
Hettangian
3
55/60Ma
74 Ma
69Ma
64Ma

Figure 7.2: Global eustatic sea-level curves for the Jurassic.
A. Hallam (1981) B. Vail et al. (1977).

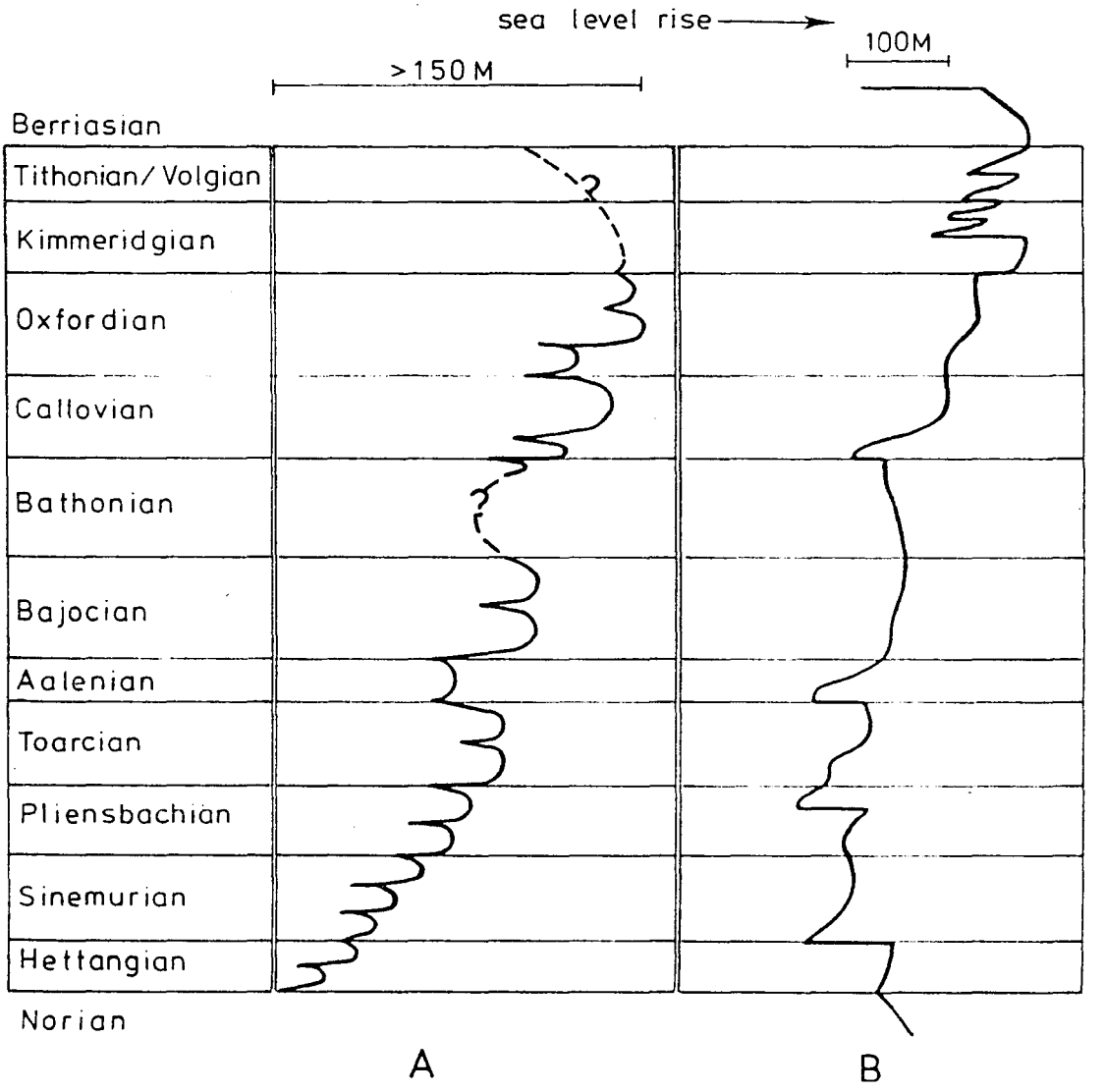
sea level rise
100M
>150 M
Berriasian
Tithonian/ Volgian
Kimmeridgian
Oxfordian
Callovian
Bathonian
Bajocian
Aalenian
Toarcian
Pliensbachian
Sinemurian
Hettangian
Norian
A
B

156 Ma (Van Hinte, 1976a). Hallam's (1981) curve has the Early Bathonian as a time of sea-level fall which reached its acme in the Middle Bathonian lowstand. This was followed by a gradual eustatic sea-level rise until the Upper Bathonian (Retrocostatum Zone) during which a rapid rise occurred. According to Hallam (1978), the highest eustatic sea-levels of the Bathonian occurred during the Discus zone. This is masked in the Tecocoyunca Group outcrop by high rates of sedimentation in the nearshore deposits. This is succeeded by a rapid eustatic sea-level fall at the end of the Retrocostatum Zone (Upper Bathonian). Vail et al. (1984) show the Bathonian as a period of stillstand with a slight sea-level fall in the Upper Bathonian, but a major fall at the Bathonian-Callovian boundary.

More careful dating by Vail et al. (1984) placed the global unconformity between the Late Bathonian regressive and transgressive cycles approximately 2 Ma ealier (158 Ma), in the basal Late Bathonian (See Fig. 7.3). This unconformity is considered to be Type 2 and of major magnitude by Vail et al. (1984). They state that a Type 2 unconformity is formed when the rate of eustatic sea-level fall is less than the rate of subsidence at the shelf edge, but exceeds the subsidence rate of the inner portion of the shelf. The depositional sequences above and below the unconformity are designated as J2.3 and J2.2 respectively

Figure 7.3 Revised global eustatic sea-level curve for the Jurassic. Note the Type 2 unconformity at 158 Ma (lowstand) followed by a sea-level rise in the Late Bathonian-Early Callovian. (After Vail et al., 1984).

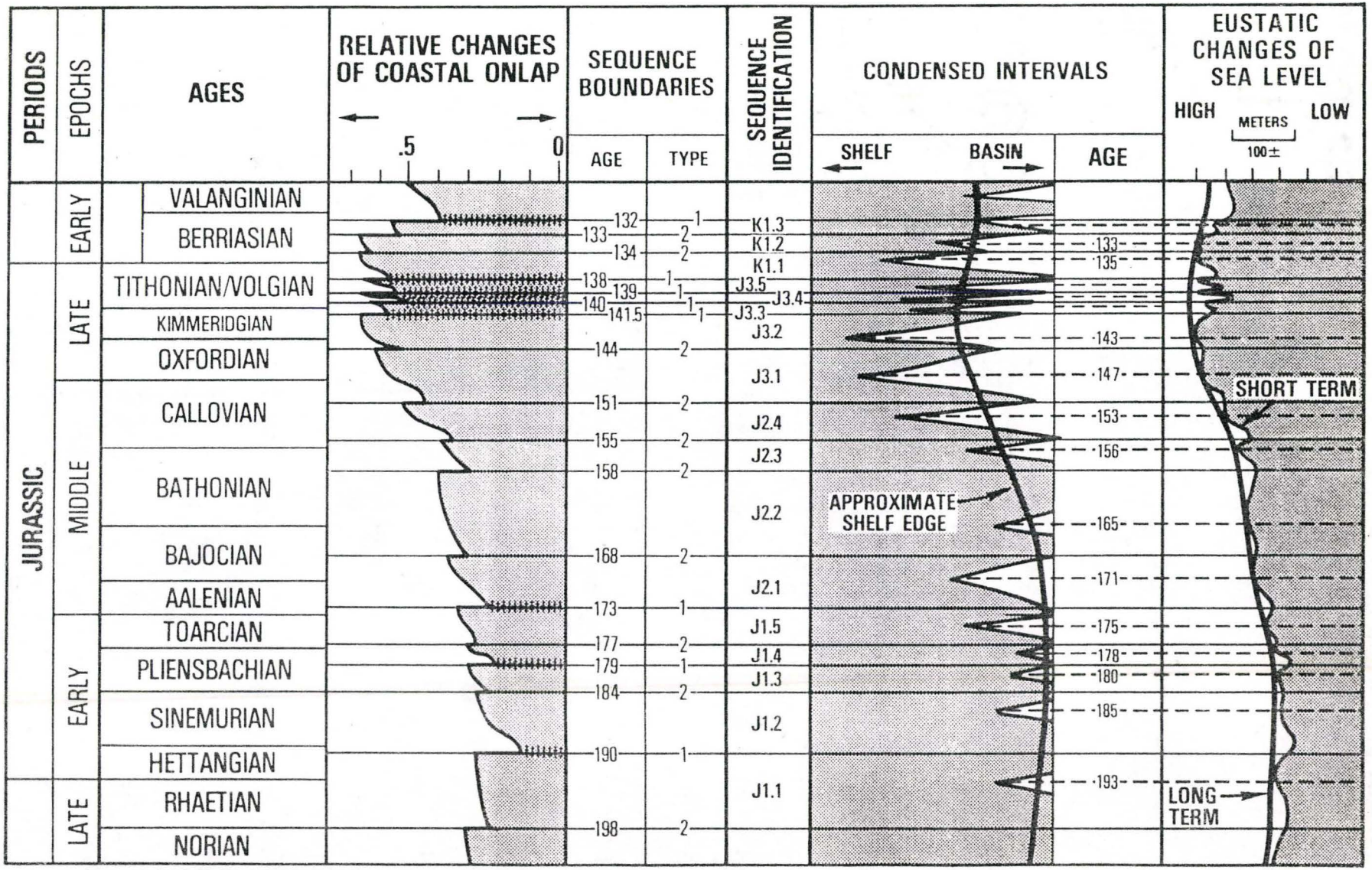

AGE FROM VAN HINTE 1976a

TIMES AT WHICH NO COASTAL ONLAP OCCURS

(Vail et al., 1984).

7.3 MIDDLE JURASSIC TECOCOYUNCA GROUP

The Middle Jurassic Tecocoyunca Group outcrop near Coauilote spans the Bathonian-Callovian boundary (See Fig. 7.4). Based on ammonite biostratigraphy, the age of the outcrop extends from the upper Retrocostatum Zone (160-159 Ma) to the Calloviense Zone (157-156 Ma) (Van Hinte, 1976). The depositional sequence of lithofacies within the Tecocoyunca Group outcrop is as follows (from bottom to top): (1) shallow offshore sandstones and shales, (2) shoreline sandstones, (3) lagoonal shales, and (4) shallow offshore shales of Bathonian age. This is overlain by: (1) offshore shales, and (2) deep water bituminous black shales of Callovian age. This sequence is interpreted to be the result of minor eustatic fluctuations, or stillstand in the Bathonian succeeded by a major Late Bathonian-Early Callovian eustatic sea-level rise.

Hallam (1984) noted that the degree of confidence in eustatic sea-level interpretation depends on: (1) reliable bathymetric estimates, (2) precise biostratigraphic correlation, and (3) extensive chronostratigraphic correlation, preferably between continents. Depositional depths of the Tecocoyunca Group marine facies may be approximated using sedimentological and paleoecological evidence, but absolute determinations are unattainable. A

Figure 7.4: European ammonite zones.
(Westermann, pers. comm.)

BOREAL-
SUBMEDITERRANEAN
STANDARD ZONES

CALLOVIAN	U	LAMBERTI
		ATHLETA
	M	CORONATUM
		JASON
	L	CALLOVIENSE
		MACROCEPHALUS
BATHONIAN	U	DISCUS
		ORBIS/RETROCOSTATUM
	M	MORRISI/?COSTATUS
		SUBCONTRACTUS
	L	ZIGZAG

prolific ammonite fauna within the Tecocoyunca Group provides precise biostratigraphic indices for correlation with the European ammonite zonation. This permits the establishment of chronological constraints and inter-continental correlations.

Local relative sea-level curves are drawn for the Tecocoyunca Group outcrop (Figs. 7.5-7.8) for purposes of comparison with eustatic sea-level curves of Hallam (1981) and Vail et al. (1984). The local curve approximates shallow water depths throughout most of the Late Bathonian. Depth increases rapidly and abruptly in the latest Bathonian, as shown by the offshore shales (Facies S) which overlie lagoonal shales (Facies R). Relative deepening continues in the Callovian, at least to the bituminous black shales of Facies T. A very slight shallowing occurs in the uppermost portion of the sequence, indicated by the sedimentology of Facies U, V, X and Y.

A change from shallow to deeper water facies could be the result of either; (1) a rise in sea-level or (2) an increase in the rate of subsidence beyond compensation by an increased sedimentation rate. Basin subsidence probably contributed to the observed relative sea-level rise in the Tecocoyunca Group. Chronostratigraphic controls placed on the outcrops by ammonites demonstrate that the change to deeper water facies commenced during the early Late Bathonian. This correlates well with the latest

Figure 7.5: Local relative sea-level curve for the facies of Section C3-Alto de Teeolutla.

C3 - Alto de Teeolutla

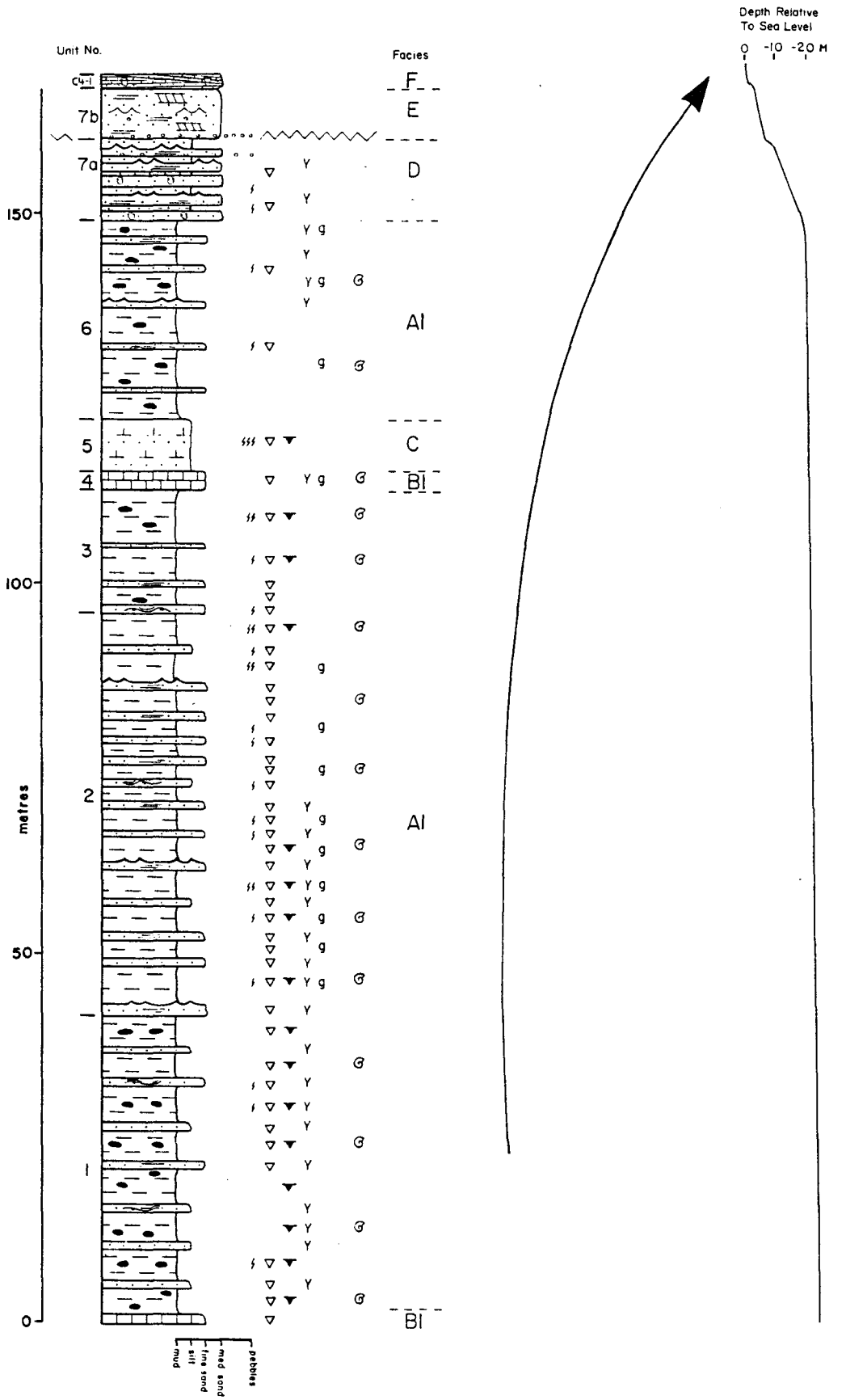

Figure 7.6: Local relative sea-level curve for the facies of Section C4-Arroyo Tecocoyunca.

C4- Arroyo Tecocoyunca

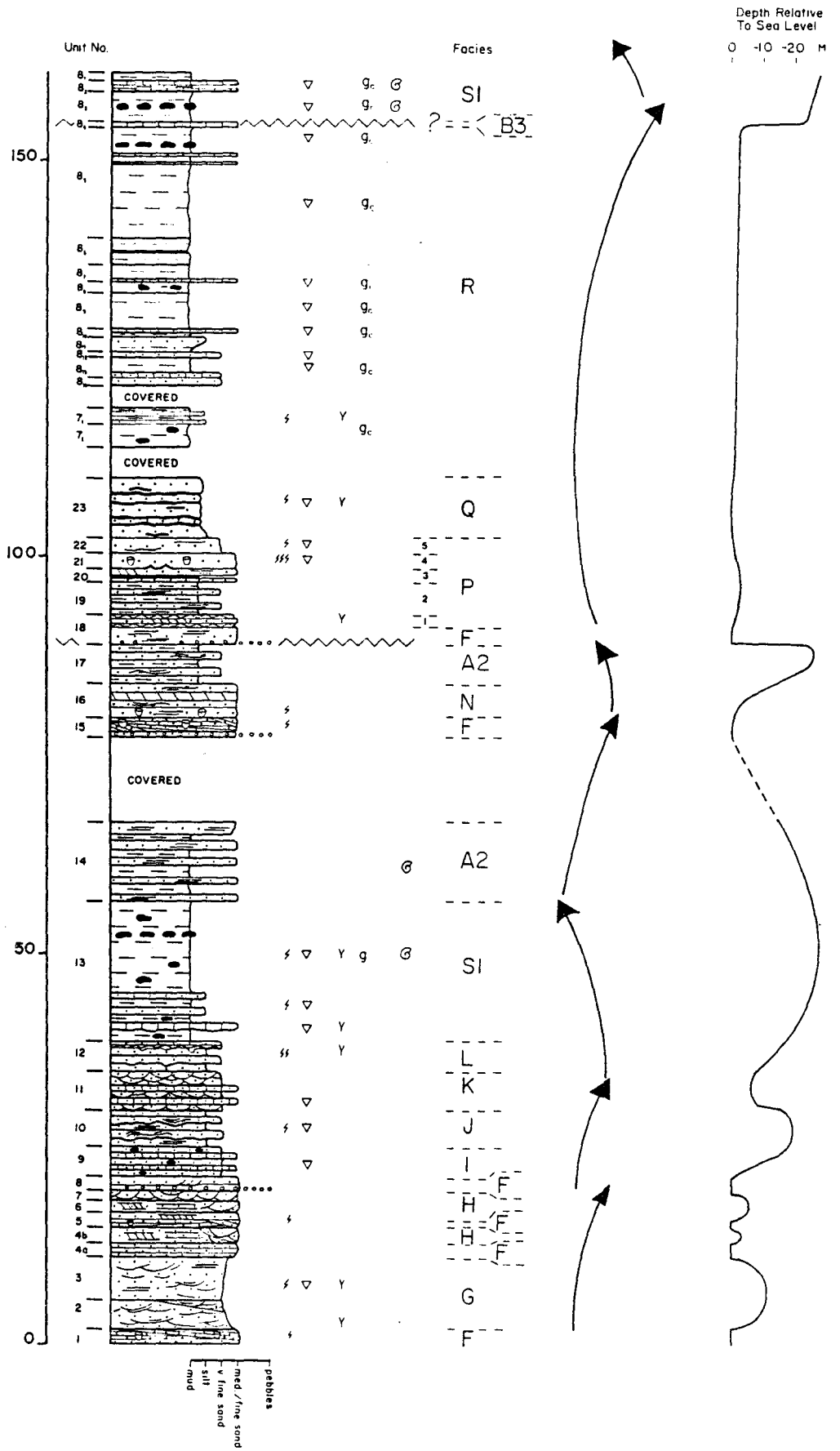

Figure 7.7: Local relative sea-level curve for the facies of Section C1-Arroyo El Rincon.

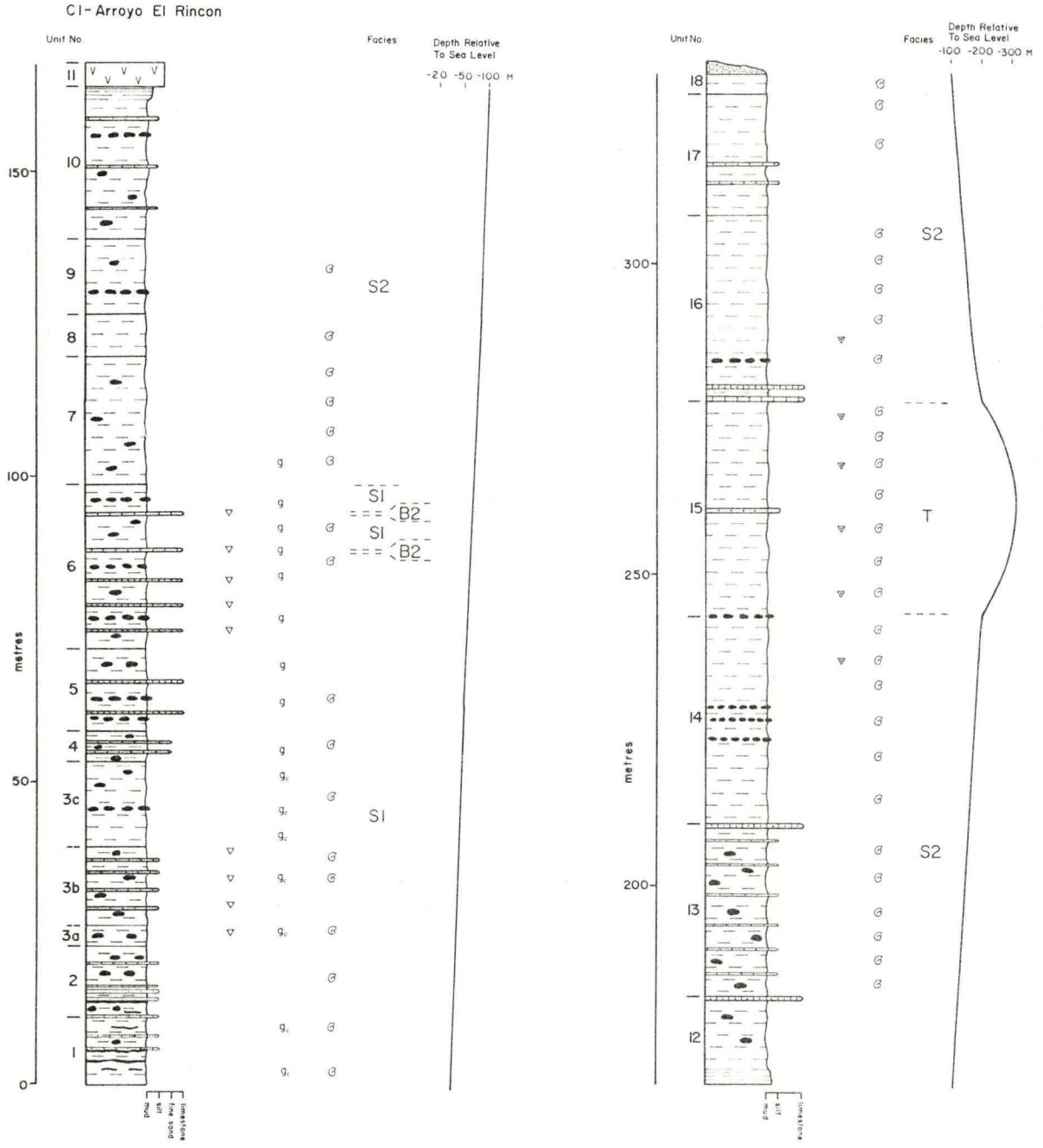
C1 - Arroyo El Rincon
Unit No.
Facies
Depth Relative To Sea Level
-20 -50 -100 M
metres
150
100
50
0
11
10
9
8
7
6
5
4
3c
3b
3a
2
1
S2
S1
B2
S1
B2
S1
mud
silt
fine sand
limestone
Unit No.
Facies
Depth Relative To Sea Level
-100 -200 -300 M
300
250
200
18
17
16
15
14
13
12
S2
T
S2
metres
mud
silt
limestone

Figure 7.8: Local relative sea-level curve for the facies of Section C2-Arroyo El Campamento.

C2- Arroyo El Campamento

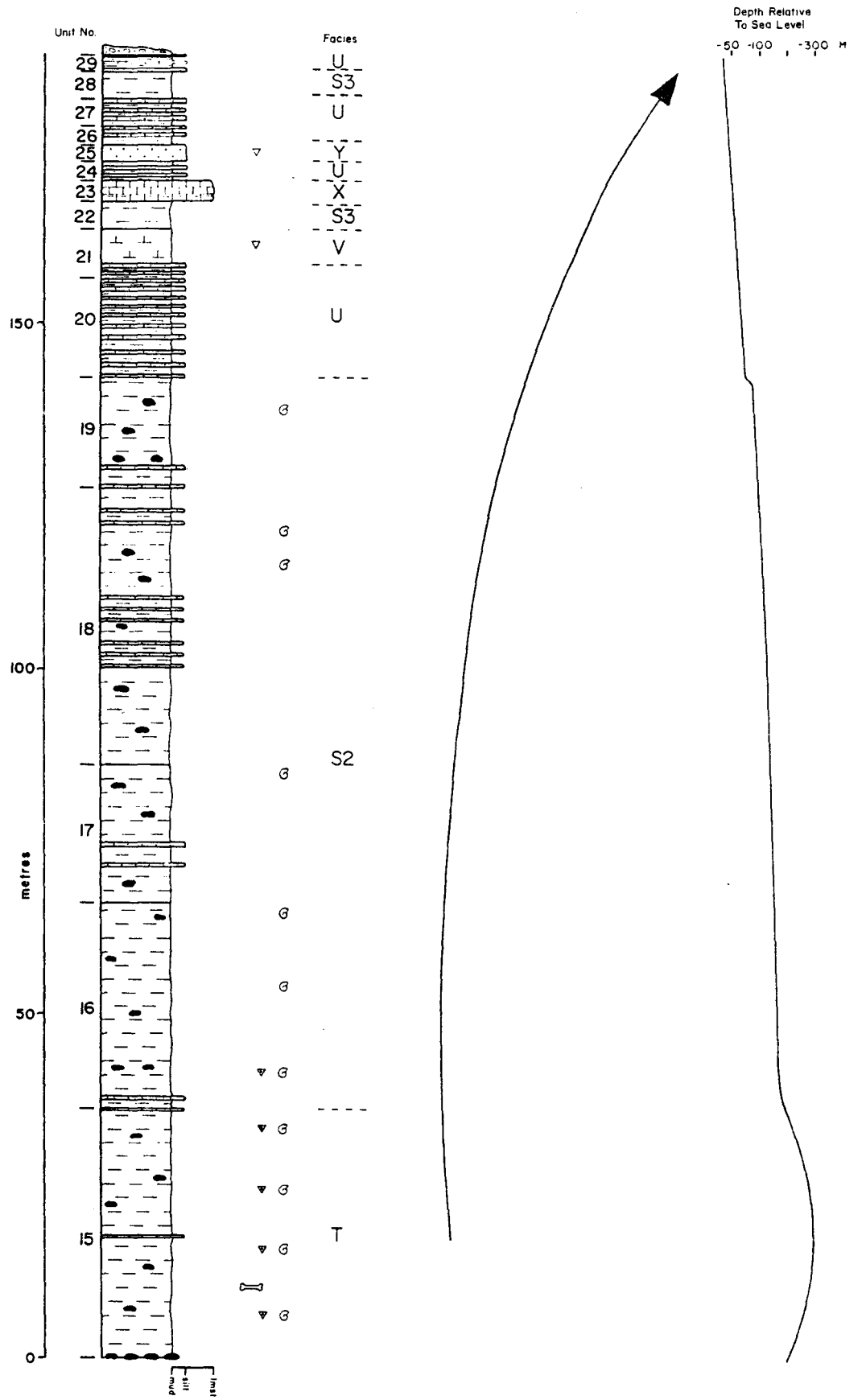

Bathonian-Early Callovian transgression depicted on the global eustatic curves of Hallam (1981) and Vail et al. (1984).

Bituminous shales (Facies T) are a second line of evidence supporting transgression due to eustatic sea-level rise. These shales are interpreted as having been deposited in deep portions of the basin where poor circulation allowed anoxic bottom conditions to develop. Hallam and Bradshaw (1979) noted that global occurrences of Phanerozoic bituminous shales characteristically occur close to the base of transgressive sequences. They proposed a model for the depositional environment of Jurassic bituminous shales involving topographic lows on the sea floor (See Fig. 7.9). Such irregularities would have locally inhibited bottom circulation thus allowing isolated pockets of stagnant water to persist. As some depressions filled in, circulation and bottom aeration improved, resulting in aerobic shales deposited on the bituminous shales. This model proposed by Hallam and Bradshaw (1979) accounts for the occurrence of Facies T bituminous shales bounded above and below by aerobic shales of Facies S in the Tecocoyunca Group.

Ammonite biostratigraphy of the Tecocoyunca Group facilitates inter-continental correlation with major portions of Europe. This fulfills the final criterion outlined by Hallam (1984) regarding confidence in eustatic sea-level interpretation. All lines of evidence suggest

Figure 7.9a: The irregular bottom topography model proposed for the depositional environment of Jurassic bituminous shales (After Hallam and Bradshaw,1979).

Figure 7.9b: Interpretations of conditions controlling the formation of bituminous or normal shales with respect to irregular bottom topography and sea level. A; early, B; late, stages of deposition in a shallow marine area of irregular topography. Stippling indicates sediments, black represents basement and cross-hatch symbolizes stagnant water. S.L.= sea level (After Hallam, 1978).

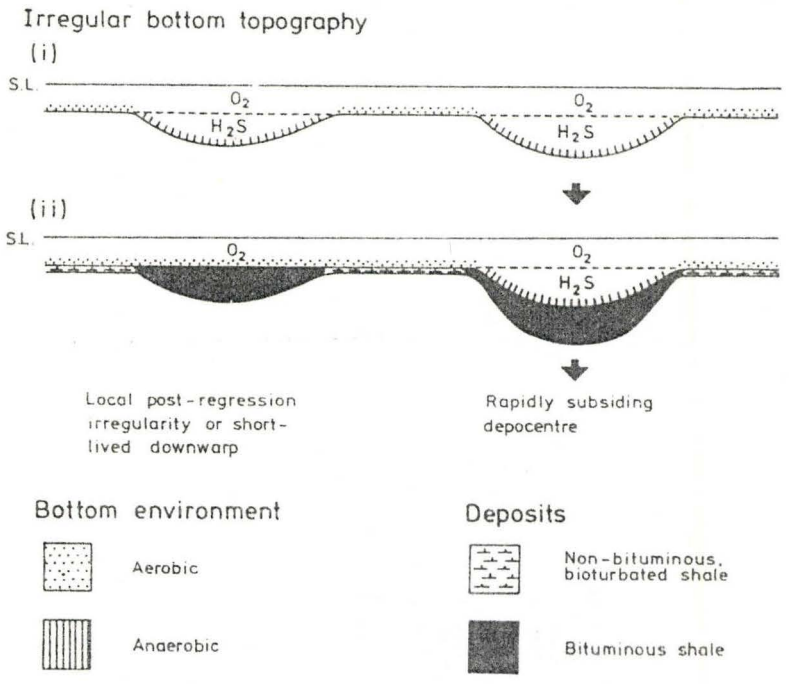
Irregular bottom topography
(i)
S.L.
O_2
H_2S
O_2
H_2S
(ii)
S.L.
O_2
O_2
H_2S
Local post-regression irregularity or short-lived downwarp
Rapidly subsiding depocentre
Bottom environment
Aerobic
Anaerobic
Deposits
Non-bituminous, bioturbated shale
Bituminous shale

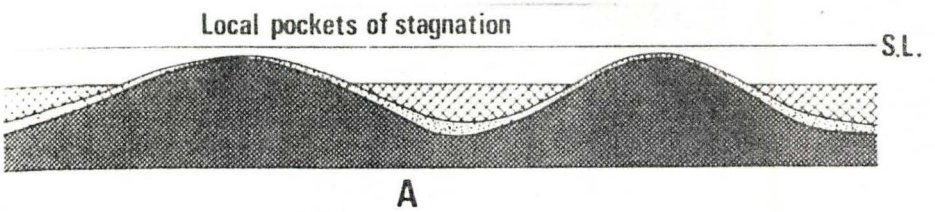
Local pockets of stagnation
S.L.

A

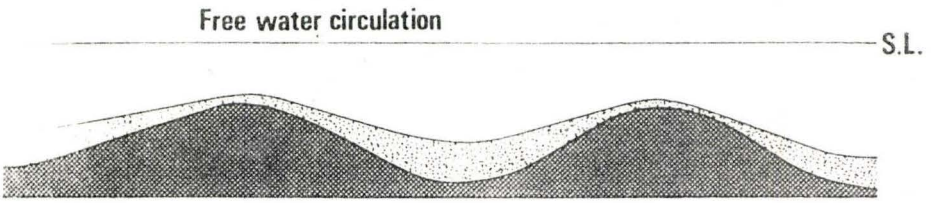
Free water circulation
S.L.

B

that the Late Bathonian-Early Callovian global eustatic sea-level rise is evident within the Tecocoyunca Group near Coauilote.

The rate of this transgression is more difficult to establish. The Yucunuti Formation includes all of the transgressive shales. A rate of sedimentation has been approximated as 1.1 m/Ka, based on ca. 550 m of shale deposited during 3 ammonite standard chronozones (approximately 1 Ma each). A conservative mud to shale compaction ratio of 6:1 was employed in this calculation. The actual rate of transgression and/or subsidence must have been greater to allow deepening of the water. My value of 1.1 m/Ka is extremely high compared to common values of a few centimeters per 1000 years for eustatic change (Hallam, 1978; Ramsbottom, 1979). Estimates of the net amount of sea level rise through the entire Jurassic only approximate 150 metres (Hallam, 1981)! Therefore, high rates of subsidence and sedimentation were important factors in addition to the eustatic rise in sea-level. Whatever the causes, the initial transgression was very rapid as indicated by the sequence of; lagoonal shales of Facies R being overlain abruptly by Facies S offshore shales without interspersed nearshore sands.

Bathonian nearshore deposits of the Tecocoyunca Group represent six small cycles of changing water depths. The water depths are interpreted as ranging from 0 m to 40 m.

Implications are that sea-level, subsidence, and sedimentation nearly balanced one another. Slight fluctuations of these three factors created the small-scale coarsening- and fining-upward cycles. The global eustatic sea-level curve of Vail et al. (1984) illustrates that the Bathonian was a time of sea-level stillstand or slight fall. Hallam's (1978) curve suggests a notable eustatic fall in the Middle Bathonian, but with a caveat. Therefore, variations in rates of sedimentation and subsidence were probably the most important factors in the Bathonian nearshore deposits of the Tecocoyunca Group.

7.4 RELATIONSHIP WITH AMMONITE FAUNAS

7.4.1 INTRODUCTION

Ammonites appear to have been stenotopic organisms highly susceptible to slight changes in salinity and temperature. As a result, the probability of extinction was great and the high rate of faunal turnover renders ammonites excellent for stratigraphy (Hallam, 1961).

Global analysis of the distribution of ammonite genera indicates an inverse correlation between sea-level stand and endemicity. High endemicity correlates with periods of regression and cosmopolitanism with periods of transgression, i.e. growth of epicontinental seas (Hallam, 1985). This general relationship is easily explained by the

comparative freedom of ammonites to migrate during periods of high sea-level (Hallam, 1985). Marine regressions, due to regional or global sea-level falls, correlate with episodes of increased extinction rate among ammonites. Major transgressions correlate with episodes of ammonite radiation. Changes within ammonite successions are recognizable independent of facies.

Bayer and Seilacher (1985) conclude that major sea-level changes may initiate faunal evolution in three ways: (1) changes of evolutionary rates due to variable extensions of environments, (2) diversity of faunas controlled by migration and evolutionary rates, and (3) the opening and closing of migration pathways. These changes are evident within the Tecocoyunca Group.

7.4.2 AMMONITE FAUNAS OF THE TECOCOYUNCA GROUP

Several characteristics of the Tecocoyunca Group ammonite faunas support the hypothesis of a significant early Late Bathonian regression followed by a major transgression extending into the Early Callovian. Firstly, a correlation between periods of regression and extinction is illustrated in the outcrop near Coauilote. Offshore sediments of Facies A contain abundant Late Bathonian (Retrocostatum Zone) ammonite genera such as Epistrenoceras, Prohecticoceras, and Bullatimorphites (Kheraiceras) (Fig. 4.2.1). Ammonites are completely absent in the

overlying nearshore sandstones and siltstones and lagoonal shales. This is not unusual for nearshore deposits where wave activity and coarse sediment drastically reduce the preservation potential of ammonites. However, with the abrupt reappearance of offshore shales (Facies S), a completely new ammonite fauna also appears (Fig. 4.2.1). This fauna is characterised by numerous Eurycephalitinae and Perisphinctidae (including Neuqueniceratinae) which are typical of the latest Bathonian-earliest Callovian (Thierry, 1976; Cariou, 1980). Reineckeiinae appear in the overlying Callovian shales. Faunal record for most of the Discus Zone (latest Bathonian) is lacking in the nearshore sediments. This is consistent with the general global absence of the Discus Zone.

An identical, but more rapid faunal replacement of Epistrenoceras and Prohecticoceras by the East-Pacific subfamilies Eurycephalitinae and Neuqueniceratinae was observed in the Andes (Thierry, 1976; Cariou, 1980). Most, if not all, of the Discus Zone is absent in many sequences throughout Europe. Therefore, this rapid faunal replacement appears to be inter-continental, and related to the proposed Late Bathonian (post-Retrocostatum Zone) regression.

Crude correlations have been observed between shell morphology of Jurassic ammonites and sedimentary facies (Westermann, 1954; Ziegler, 1967; Bayer, 1970; Bayer and McGhee, 1985). Smooth involute forms are often found in

deep water shale facies while evolute and sculptured forms are often found in moderate to shallow water facies. Involute sphaerocone forms are abundant in very shallow nearshore facies. However, numerous exceptions to these generalizations have been noted (Kennedy and Cobban, 1976; Lehmann, 1981). One exception is that sphaerocones with strong septa are often associated with deep water facies. Abundance of certain forms relative to others seems to be of utmost importance because there is always lateral overlap of shell forms with respect to facies. Most of this may be attributed to post-mortal drift. Bullatimorphites (Kheraiceras), an involute sphaerocone, occurs in the shallow offshore sediments of Facies A (Section C3-Alto de Teeolutla). Involute sphaerocones (Eurycephalitinae), and evolute sculptured platycones (Perisphinctidae) also occur within the reappearance of Upper Bathonian ammonites. This reappearance is associated with the early stages (Facies S) of the major transgressive sequence. As the transgression proceeded (Facies S, T), many smooth, involute non-keeled forms (Phylloceratina) appeared, followed by forms with carinate, bisulcate venters (Oppeliidae). Similar morphological sequences of ammonites have been reported by Donovan (1985) in the British Lower Jurassic transgressive cycles.

The final characteristic of the Tecocoyunca Group ammonite fauna involves the degree of

endemism/cosmopolitanism in relation to sea-level changes. Ammonites were relatively free to migrate along epicontinentalpathways during sea-level highstands, even though Pangea remained a coherent supercontinent throughout most of the Jurassic (Bayer and Seilacher, 1985). Evidence from the Jurassic Tecocoyunca Group ammonite fauna of Mexico and similar faunas of the Andes, suggests that the Hispanic Corridor between Africa and North America was important for migration. This area of the proto-Atlantic acted as an intermittent shallow epicontinental seaway which permitted ammonite migration between the Tethyan and East Pacific faunal provinces from the Pliensbachian to the Callovian (Westermann, 1984; Westermann et al., 1984; Westermann and Riccardi, 1985; Hallam, 1985).

Ammonite cosmopolitanism (Tethyan affinity) within the Tecocoyunca Group is highest (ie. low endemism) during the Bajocian and Middle Callovian (Westermann, 1984; Westermann et al., 1984; Westermann and Riccardi, 1985). Figure 4.3.1 illustrates the extent of endemism and Tethyan affinities of the ammonite fauna near Coauilote. Global eustatic sea level curves for the Jurassic indicate major sea-level rises in the Bajocian and Callovian. The sea-level highstands permitted ammonite migration between the Tethys Sea and east Pacific Ocean via the Hispanic Corridor. Many Early Callovian ammonites of the Tecocoyunca Group appear to be deep-water forms (eg. phylloceratids) which is suggestive

of considerable sea-level rise. However, the Middle Callovian is the first real opening of the seaway. In contrast, periods of eustatic sea-level lowstand allowed only shallow-water ammonites to migrate through the Hispanic Corridor. Shallow-water Bathonian ammonites (e.g. Bullatimorphites (Kheraiceras), Epistrenoceras) are characteristic of Facies A sediments (Fig. 4.2.1).

In summary, the ammonite faunas of the Tecocoyunca Group show: (1) rapid faunal replacement, (2) shell morphology trends, and (3) varying degrees of endemism/cosmopolitanism, all in relation to sea-level variations. Timing and character of these faunal changes correlate well with a significant global eustatic fall in the early Late Bathonian, followed by a global eustatic sea-level rise which extended into the Callovian.

7.5 SUMMARY

Sequences of lithofacies, biofacies and ammonite faunas of the Tecocoyunca Group suggest a major marine transgression in the Late Bathonian-Early Callovian. The cause of this transgression appears to be twofold; (1) a major global eustatic sea-level rise commencing in the early Late Bathonian and continuing into the Early Callovian (Hallam, 1978, 1981; Vail et al., 1977, 1984; Vail and Todd, 1981), and (2) considerable basinal subsidence during Late Bathonian-Early Callovian deposition of the Tecocoyunca

Group sediments.

There is no evidence of Jurassic polar ice caps or glaciation (Hallam, 1978). Therefore, the most widely favoured mechanism controlling eustasy in the Jurassic is changes in oceanic ridge volume. Sea-level oscillations were caused by variations in ridge spreading rates (Miall, 1984). Sea-level lowstands occurred during periods of slow spreading rates. Transgressions were produced during periods of accelerated sea-floor spreading or lengthening of the ridge system (Hallam, 1978). Based on several lines of evidence, including ammonite biogeography of this study and others, we know that the Atlantic Ocean was opening during the Middle Jurassic by sea-floor spreading.

CHAPTER 8: CONCLUSIONS

1. The age of the Middle Jurassic Tecocoyunca Group outcrop near Coauilote is Upper Bathonian (Retrocostatum Zone) to Lower Callovian (Calloviense Zone) based on ammonite chronostratigraphy.

2. The Tecocoyunca Group, seen as a whole, has an overall transgressive trend with a few minor fluctuations of base level. The lowermost 150 m (U. Bathonian) of sediments contain a vertical, coarsening-upward transition of shallow offshore facies to shoreface and foreshore facies on a wave- and storm-dominated coast. This is overlain by 100 m of sediments containing four smaller coarsening-upward sequences of shoreface and foreshore sandstones. The fourth sequence is a truncated coarsening-upward sequence, interpreted as barrier island sands capped by back-barrier sands, washover sands, and brackish lagoonal shales.

These nearshore sediments are abruptly overlain by 400 m of open marine shales which are thought to represent a major transgression beginning in the latest Bathonian. As the transgression continued into the Early Callovian, deep portions of the basin developed anoxic bottom conditions resulting in the deposition of bituminous black shales. The uppermost 150 m of the outcrop represent a minor shallowing trend of offshore shales and siltstone interbeds.

3. Petrographic investigations indicate that the provenance of the sandstones and siltstones is low rank metamorphic. The sediments are immature, which suggests relative proximity to the source. The offshore sandstone and siltstone interbeds are poorly sorted and rounded, which may indicate rapid deposition. The nearshore sands are "cleaner", well rounded, and well sorted.

The limestone interbeds contain random, poorly sorted fossil fragments and detrital mineral grains. These interbeds are interpreted as storm-related shell-rich sediments which were deposited episodically and subsequently cemented.

Limey-ferruginous concretions containing shell and plant debris formed during early diagenesis.

4. Biostratigraphic and lithostratigraphic investigations have elucidated minor base level fluctuations in the Upper Bathonian succeeded by a major transgression during the Late Bathonian due to a major eustatic sea-level rise. The latter is represented by brackish lagoonal shales overlain abruptly by offshore marine shales without interspersed nearshore sands. Preservation of both the regressive and transgressive sequences was facilitated by significant basinal subsidence. The rate of transgression and/or subsidence was greater than the rate of

sedimentation; 1.1 m/Ka for the Yucunuti Formation.

5. Five paleoecological communities of invertebrate organisms are recognized in the Tecocoyunca Group near Coauilote; Sandy Mud, Shifting Sands, Restricted Mud, Open Marine Basinal, and Black Mud. Each one contains diagnostic lithologies, sedimentary structures and organisms indicative of distinct paleoenvironments. Water depths inferred for these communities indicate an overall deepening-upward trend within the outcrop.

6. Several ammonite faunal associations are recognized in the Tecocoyunca Group:

(a) Epistrenoceras hystricoides Association - U. Bathonian, Retrocostatum Zone.

(b) Lilloettia/Neuqueniceras Association - latest Bathonian.

(c) Frickites bodenbenderi Association - L. Callovian, Macrocephalus Zone.

(d) Clydoniceras inflatum Association - Macrocephalus-Calloviense Zone.

(e) Rehmannia Association - Calloviense Zone.

7. Biogeographic affinity of the Coauilote ammonite fauna is mostly Andean with significant West-Tethyan/Mediterranean elements and a few endemic species.

8. The first known North American occurrences of the typically Tethyan/Mediterranean ammonite species; Phlycticeras cf. pustulatum (Reineck), Jeanneticeras cf. malbosi Elmi, and Paracuariceras cf. incisum Schindewolf are reported in this study.

9. The ammonite faunas show: (1) rapid faunal replacement, (2) shell morphology trends, and (3) varying degrees of endemism/cosmopolitanism, all in relation to sea-level variations.

(1) An abrupt faunal replacement of Upper Bathonian (Retrocostatum Zone) genera Epistrenoceras, Prohecticoceras, and Bullatimorphites (Kheraiceras) by genera of the Pacific subfamilies Eurycephalitinae and Neuqueniceratinae is observed. Record of the Discus Zone is missing at Coauilote. Similar faunal replacements have been observed in South America and Europe and they appear to be related to the proposed Late Bathonian (post-Retrocostatum Zone) eustatic sea-level fall (Vail et al., 1984).

(2) A sequence of shell morphology changes is observed in conjunction with the overall transgressive trend: sphaeroconic forms in shallow nearshore facies, evolute sculptured platycones in moderate

to shallow water facies, smooth involute forms in moderately deep water shale facies, and finally, forms with carinate bisulcate venters in the deepest facies.

(3) Increased cosmopolitanism of the Callovian ammonites is observed and may be attributed to greater capacity for migration through the Hispanic Corridor. This was facilitated by increased water depths associated with an Early Callovian global eustatic sea-level rise.

10. Vertebrae of the Tethyan crocodile genus Steneosaurus are reported for the first time in North America.

11. Sequences of lithofacies, biofacies and ammonite faunas of the Tecocoyunca Group suggest a major marine transgression in the Late Bathonian-Early Callovian. The cause of this transgression appears to be twofold: (1) a major global eustatic sea-level rise commencing in the early Late Bathonian and continuing into the Early Callovian (Vail et al., 1984), and (2) considerable basinal subsidence during Late Bathonian-Early Callovian deposition of the Tecocoyunca Group sediments.

12. Biogeography and lithostratigraphy of the Tecocoyunca Group suggest that:

a) this allochthonous Mixteca tectonostratigraphic terrane had a paleoposition, during the Middle Jurassic, near the Pacific opening of the Hispanic Corridor (proto-Atlantic) and the Andes of South America.

b) the Hispanic Corridor provided marine connections between the eastern Pacific Ocean and the western Tethys Sea.

c) preponderance of nearshore sediments in the Tecocoyunca Group suggests close proximity to a large continent i.e. South America.

REFERENCES

Aigner, T., 1985, Storm depositional systems, in G.M. Friedman, H.J. Neugebauer, and A. Seilacher (eds.), Lecture Notes In Earth Sciences 3, Springer-Verlag, Berlin, 174p.

Alencaster de Cserna, G., 1963, Pelecipodos del Jurasico Medio del Noroeste de Oaxaca y Noreste Guerrero: Paleontologia Mexicana, No. 15, 52 p.

Alencaster de Cserna, G., 1984, Late Jurassic-Cretaceous Molluscan paleogeography of the southern half of Mexico. in Westermann, G.E.G., (ed.). Jurassic-Cretaceous Biochronology & Biogeography of North America. Geological Association of Canada Special Paper 27. p. 77-88.

Arkell, W.J., 1951-1955. Monograph of the English Bathonian Ammonites. Pal. Society.

Arkell, W.J., 1956, Jurassic Geology of the World, Oliver and Boyd, Edinburgh, 806 p.

Bartok, P.E, Renz, O., Westermann, G.E.G., 1985, The Siquisique ophiolites, Northern Lara State, Venezuela: A discussion on their Middle Jurassic ammonites and tectonic

implications. Geological Society of America Bulletin. v. 96, p. 1050-1055.

Basu, A., Young, S.W., Suttner, W.C., James, W.C., Mack, G.H., 1975, Re-evaluation of the Use of Undulatory Extinction and Polycrystallinity in Detrital Quartz for Provenance Interpretation, Journal of Sedimentary Petrology, v. 45, p. 873-882.

Bathurst, R.G.C., 1975, Carbonate Sediments and their Diagenesis. Developments in Sedimentology v. 12, Elsevier Publ. Co., Amsterdam, 658 p.

Bayer, U., 1970, Anomalien bei Ammoniten des Aaleniums und Bajociums und ihre Beziehung zur Lebensweise. N. Jb. Geol. Palaont. Abh., v.135 (1), p. 19-41.

Bayer, U., McGhee, G.R., 1985, Evolution in marginal epicontinental basins: the role of phylogenetic and ecological factors (ammonite replacements in the German Lower and Middle Jurassic). in Bayer, U., Seilacher, A., Sedimentary and Evolutionary Cycles, Lecture Notes in Earth Sciences 1, Springer-Verlag, Berlin. 465p.

Bayer, U., Seilacher, A., (eds.), 1985, Sedimentary and Evolutionary Cycles, Lecture Notes in Earth Sciences 1,

Springer-Verlag, Berlin. 465p.

Beck, Jr., M.E., 1976, Discordant paleomagnetic pole positions as evidence of regional shear in the western Cordillera of North America. American Journal of Science. v. 276, p. 694-712.

Benavides, M.M.E., 1978, Estudio Geologico del Municipio de Cualac, Escuela Superior de Ingenieria Arquitectura, Inedita.

Berner, R.A., 1971, Principles of Chemical Sedimentology McGraw-Hill, New York, 239 p.

Berner, R.A., 1968, Calcium carbonate concretions formed by the decomposition of organic matter, Science, v. 159, p. 195-197.

Burckhardt, C., 1927, Cephalopodos del Jurasico medio de Oaxaca y Guerrero: Instituto de Geologia de Mexico, Boletin 47, 108 p.

Callomon, J.H., 1984, A review of the biostratigraphy of the post-Lower Bajocian Jurassic ammonites of western and northern North America. in Westermann, G.E.G., Jurassic-Cretaceous Biochronology & Biogeography of North

America. Geological Association of Canada Special Paper 27. p. 143-174.

Campbell, C.V., 1971, Depositional model -Upper Cretaceous Gallup beach shoreline, Ship Rock area, northwestern New Mexico, Journal of Sedimentary Petrology, v. 41, p. 395-409.

Campa, M.F., and Coney, P.J., 1983, Tectono-Stratigraphic Terranes and Mineral Resource Distributions in Mexico: Canadian Journal of Earth Sciences, Vol. 20, p.1040-1051.

Cant, D.J., 1984, Development of Shoreline-Shelf Sand Bodies in a Cretaceous Epeiric Sea Deposit, Journal of Sedimentary Petrology, vol.54, No. 2, p.541-556.

Cariou, E., 1980, L'Etage Callovien dans le Centre-Oueste de la France: These a l'Universite de Poitiers, Fascilles 1-3, 790 p.

Cariou, E., 1984, Structure, origine et paleobiogeographie de la famille des Reineckeiidae, Ammonitina, du Jurassic moyen. C.R. Acad. Sc. Paris, t. 298, Serie II, No. 6. p. 245-248.

Carter, C.H., 1978, A regressive barrier and

barrier-protected deposit: depositional environment and geographic setting of the Late Tertiary Cohansey Sand. Journal of Sedimentary Petrology, v. 48, p. 933-950.

Clifton, H.E., 1976, Wave -formed sedimentary structures- a conceptual model, in R.A. Davis Jr. and R.L. Ethington, (eds.), Beach and nearshore sedimentation, p. 126-148, Spec. Publ. Soc. econ. Paleont. Miner. 24, Tulsa.

Clifton, H.E., Hunter, R.E., Phillips, R.L., 1971, Depositional structures and processes in the non-barred high energy nearshore, Journal of Sedimentary Petrology, v. 41, p. 651-670.

Coney, P.J., 1972, Cordilleran tectonics and North America plate motion. American Journal of Science. v. 272, p. 603-628.

Coney, P.J., Jones, D.L., and Monger, H.W.H., 1980, Cordilleran suspect terranes. Nature, v. 288, p. 329-333.

Corona-Esquivel, R.J.J., 1981. Estratigrafia de la region de Olinala-Tecocoyunca, noreste del estado de Guerrero. Univ. Nat. Auton. Mexico. Inst. Geologia, Revista, v. 5 No. 1, p. 17-24.

Davidson-Arnott, R.G.D., and Greenwood, B., 1976, Facies relationships on a barred coast, Kouchibouguac Bay, New Brunswick, Canada. in R.A. Davis Jr. and R.L. Ethington (eds.), Beach and nearshore sedimentation, p. 149-168. Spec Publ. Soc. econ. Paleont. Miner., 24, Tulsa.

Davis, R.A.Jr., and Hayes, M.O., 1984, What is a wave-dominated coast? in B. Greenwood, and R.A.Jr. Davis, (eds.), Hydrodynamics and Sedimentation in Wave-Dominated Coastal Environments. Elsevier, New York, 1984.

Dickenson, K.A., Berryhill, H.L. Jr., and Holmes, C.W., 1972, Criteria for recognizing ancient barrier coastlines. in J.K. Rigby, and W.K. Hamblin (eds.), Recognition of ancient sedimentary environments, Society of Economic Paleontologists and Mineralogists, Spec. Publ. No. 16, p. 192-214.

Dickson, J.A.D., 1966, Carbonate identification and genesis as revealed by staining, Journal of Sedimentary Petrology, v. 36, p. 491-505.

Dietl, G., 1978, Die heteromorphen Ammoniten des Dogger: Stuttgarter Beitrage zur Naturkunde, Serie B (Geologie and Palaontologie), Nr. 87, 21 p.

Donovan, D.T., 1985, Ammonite Shell Form and Transgressions in the British Lower Jurassic. in Bayer, U., Seilacher, A., Sedimentary and Evolutionary Cycles. Lecture Notes in Earth Sciences. Springer-Verlag. Berlin. 465p.

Dott, R.H. Jr., and Bourgeois, J., 1982. Hummocky stratification:significance of its variable bedding sequences. Bulletin of the Geological Society of America, v. 93, p. 663-680.

Elliot, T. 1975, The sedimentary history of a delta lobe from a Yoredale (Carboniferous) cyclothem, Proc. Yorks. geol. Soc., v. 40, p. 505-536.

Elliott, T., 1978, Clastic Shorelines, in H.G. Reading (ed.), Sedimentary Environments and Facies, Elsevier, New York. 557 p.

Elmi, S., 1967, Le Lias et le Jurassique Moyen de l'Ardeche. Labratoirs de Geologie de la Faculte de Sciences de Lyon, Documents 19, 845 p.

Enay, R., 1959. Note sur Quelques Tulitides (Ammonitina) du Bathonien: Societe Geologique de France, 7e Series, Bulletin 1, p. 252-259.

Erben, H.K., 1956, El Jurasico Medio y el Calloviano de Mexico: XX Congreso Geologico International (Mexico 1956), 140 p.

Erben, H.K., 1957b, New biostratigraphic correlations in the Jurassic of Eastern and South-Central Mexico. Congress Geologie International XX Sesion, Section II, p. 44-52.

Folk, R.L., 1962, Spectral subdivision of limestone types. in W.E. Ham (ed.), Classification of Carbonate Rocks. American Association of Petroleum Geologists, Tulsa, okla., p. 62-84.

Frey, R.W., Pemberton, S.G., 1984, Trace Fossils Facies Models, in R.G. Walker (ed.), 1984, Facies Models, 2nd Ed, 317 p.

Ginsburg, R.N., 1975, Tidal deposits: A case-book of recent examples and fossil counterparts. Springer-Verlag, New York. 428p.

Gottsche, C., 1878, Uber jurassische Vertsteinerungen aus der Argentinischen Cordillere: Palaontographica Supplement 3, Lieferung 2, Abteilung, 3, 50p.

Guzman, E.J., 1950, Geologia al Noreste de Guerrero:

Asociation Mexicana de Geologia y Petrologia, Boletin 2, p. 95-156.

Hallam, A., 1961, Cyclothems, transgressions and faunal change in the Lias of northwest Europe. Trans. Edinburgh Geological Society, v. 18, p. 132-174.

Hallam, A., 1978, Eustatic cycles in the Jurassic, Paleogeography, Paleoclimatology, Paleoecology, v. 23, p. 1-32.

Hallam, A., 1981, A revised sea-level curve for the early Jurassic. Journal of the Geological Society of London. v. 138, p. 735-734.

Hallam, A., 1984, Pre-Quaternary sea-level changes, Ann. Rev. Earth Planet. Sci.. v. 12, p. 205-43.

Hallam, A., 1985, Jurassic molluscan migration and evolution in relation to sea level changes. in Bayer,U., Seilacher, A., Sedimentary and Evolutionary Cycles, Lecture Notes in Earth Sciences 1, Springer-Verlag, Berlin. 465p.

Hallam, A., Bradshaw, M.J., 1979, Bituminous shales and oolitic ironstones as indicators of transgressions and regressions. J. Geol. Soc. London. v. 136, p.157-164.

Harms, J.C., Southard, J.B., Spearing, D.R., and Walker,R.G., 1975, Depositional environments as interpreted from primary sedimentary structures and stratification sequences. Society of Economic Paleontologists and Mineralogists, Short Course 2, 161.

Hayes, M.O., and Kana, T.W., 1976, Terrigenous Clastic Depositional Environments- Some Modern Examples, p. 1-131, II-184, Tech. Rept.. 11-CRD, Coastal Res. Div., Univ. South Carolina.

Hillebrandt, A.von, 1970, Zur Biostratigraphie und AmmonitenFauna des sudamerikanischen Jura (insbes. Chile): Neues Jahrbuch fur Geologie and Palaontologie, Abhandlungen, vol. 136, p. 166-211.

Hobbs, B.E., Means, W.D., Williams, P.F., 1976, An Outline of Structural Geology, John Wiley & Sons. Inc., New York. 571p.

Hobday, D.K., and Horne, J.C., 1977, Tidally influenced barrier island and estuarine sedimentation in the Upper Carboniferous of southern West Virginia, Sedim. Geol.., v. 18, p. 97-122.

Horne, J.C., and Ferm, J.C., 1976, Carboniferous depositional environments in the Pocahontas Basin, Eastern Kentucky and Southern West Virginia: A Field Guide, p. 129, Dept. of Geology, University of South Carolina.

Howard, J.D., 1972, Trace fossils as a criteria for recognizing shorelines in the stratigraphic record, in J.K. Rigby and W.K. Hamblin (eds.), Recognition of Ancient Sedimentary Environments, pp. 215-225, Spec. Publ. Soc. econ. Paleont. Miner, 16, Tulsa.

Howard, J.D., Reineck, H.E., 1972, Physical and biogenic sedimentary structures of the nearshore shelf. Senckenberg. Mar., v. 4, p. 81-123.

Howard, J.D., and Reineck, H.E., 1981, Depositional facies of high-energy beach-to-offshore sequence: comparison with low energy sequence. American Association of Petroleum Geologists, Bulletin, v. 65, p. 807-830.

Hunter, R.E., Clifton, H.E., Phillips, R.L., 1979, Depositional processes, sedimentary structures, and predicted vertical sequences in barred nearshore systems, northern Oregon coast, Journal of Sedimentary Petrology, v. 49, p. 711-726.

Imlay, R.W., 1980, Jurassic Paleobiogeography of the Conterminous United States and its Continental Setting: Geological Survey Professional Paper 1062, 134 p.

Ingle, J.C., 1966, The movement of beach sand. Developments in Sedimentolgy, v.5, p. 221. Elsevier, Amsterdam.

Irving, E., 1979. Pole positions and continental drift since the Devonian, in M.W. McElhinay, ed., The earth: its origin, structure, and evolution. Academic Press,London. p. 567-593.

Jefferies, R.P.S., and Minton, D., 1965, The mode of life of two Jurassic species of Posidonia. Paleontology, v. 8, p. 156-185.

Jenny, H., 1933, Geological Reconnaissance Survey of the Northeastern Part of the State of Guerrero: Archivo Petroleos Mexicanos, Reporte Geologico no. 418.

Kauffman, E.G., 1969, Form, function and evolution. in Treatise on Invertebrate Paleontology, Part N. R.C. Moore (ed.)., Mollusca 6, Bivalvia. p. 129-205.

Kauffman, E.G., 1981. Ecological reappraisal of the German Posidonienschiefer (Toarcian) and the stagnant basin model. in Gray, L., Bonco, A.J., and Berry, W.B. (eds.),

Communities of the Past. Hutchinson Ross Publishing Co. 623p.

Kennedy, W.J., Cobban, W.A., 1976, Aspects of ammonite biology, biogeography, and biostratigraphy. Spec. Pap. Paleontol. 17.

Kumar, N., and Sanders, J.E., 1976, Characteristics of shoreface storm deposits, modern and ancient examples, Journal of Sedimentary Petrology, v. 46, p. 145-162.

Leatherman, S.P. (ed.), 1981, Overwash Processes, Benchmark Papers in Geology No. 58, Hutchinson Ross Publishing Company, Stroudsberg, Pennsylvania. 376 p.

Leckie, D.A., and Walker, R.G., 1982, Storm and tide-dominated shorelines in Cretaceous Moosebar-Lower Gates interval-outcrop equivalents of deep basin gas trap in Western Canada, American Association of Petroleum Geologists, Bulletin, v. 66, p. 138-157.

Lehmann, U., 1981, The ammonites. Their Life and their world. Cambridge University Press.

Lindholm, R.C., and Finkelman, R.B., 1971, Calcite staining semi-quantitative determination of ferrous iron, Journal of

Sedimentary Petrology., v. 42, p. 239-242.

Mattes, B.W., and Mountjoy, E.W., 1980, Burial dolomitization of the Upper Devonian Miette Buildup, Jasper National Park, Alta., Society of Economic Paleontologists and Mineralogists., Spec. Publ., No. 28, p. 259-297.

McBride, E.F., 1963, A classification of common sandstones. Journal of Sedimentary Petrology, v. 33, p. 664-669.

McCubbin, D.G., 1982, Barrier-island and strand plain facies in P.A. Scholle and D.R. Spearing (eds.), Sandstone Depositional Environments, American Association of Petroleum Geologists, Memoir 31, p. 247-280.

McKerrow, W.S. (ed.), 1978, The Ecology of Fossils: an illustrated guide, Gerald Duckworth and Co. Ltd., London. 383 p.

Miall, A.D., 1984, Principles of Sedimentary Basin Analysis, Springer-Verlag, New York. 490p.

Ochoterena, H., 1966, Amonitas del Jurasico Medio de Mexico. II. Infrapatoceras gen. nov.: Paleontologia Mexicana 23, 18 p.

Orbigny, A., d', 1842-51, Paleontologie Francaise; Terrains Jurassiques, I. Cephalopodes: Masson, Paris, 642 p., 234 pl.

Ortega, G.F., 1978, Estratigraphia del Complejo Acatlan en la Mixteca Baja, Estados de Puebla y Oaxaca: Univ.Nal. Auton.de Mexico, Instituo de Geologia, Revista 2.

Parona, C.F. and Bonarelli, G., 1897, Fossili Albiani d'Escragnolles del Nizardo e della Liguria occidentale: Paleontogr. Italica, tomo 2 (1896), 112p.

Pettijohn, F.J., Potter, P.E., Siever, R., 1972, Sand and Sandstone, Springer-Verlag. New York. 618p.

Powers, M.C., 1953, A new roundness scale for sedimentary particles: Journal of Sedimentary Petrology, v. 23, p. 117-119.

Quenstedt, F.A., 1845-49, Petrefactenkunde Deutschlands; Die Cephalopoden. 580p.

Rampino, M.R. and Sanders, J.E., 1980, Holocene transgression in south-central Long Island, New York, Journal of Sedimentary Petrology, v. 50, p. 1063-1080.

Ramsbottom, W.H.C, 1979, Rates of transgression and

regression in the Carboniferous of NW Europe. J. Geol. Soc. London. v. 136, p. 147-153.

Reading, H.G., (ed.), 1978, Sedimentary Environments and Facies, Elsevier, New York. 557 p.

Reineck, H.E., 1973, Bibliographic geolgischer Arbeiten uber rezente und fossil kalk- und Silikatwatten. (Bibliography of recent and ancient tidalites. Cour. Foursch. Inst. Senckenberg 6, Frankfurt a.M, 57p.

Reineck, H.E., Gutmann, W.F., Hertweck, G., 1967, Das schlickgebiet sudlich Helgoland als Beispiel rezenter schelfablagerungen. Senckenberg. leth., v. 48, p. 219-275.

Reineck, H.E., and I.B. Singh, 1973, Depositional Sedimentary Environments, Springer-Verlag, New York. 439 p.

Reineck, H.E., and Singh, I.B., 1980, Depositional sedimentary environments with reference to terrigenous clastics, Berlin, Springer-Verlag, 549 p.

Reinson, G.E., 1984, Barrier island and associated strand plain systems, in R.G. Walker (ed.), Facies Models, Geoscience Reprint Series 1. 2nd Edition, 317 p. GAC, Toronto.

Riccardi, A.C., 1984. Los Eurycephalitinae en America Del Sur, Actas del 3rd Congreso Argentino de Paleontologia y Bioestratigrafia. p. 151-164.

Riccardi, A.C., 1985, Los Eurycephalitinae Andinos (Ammonitina, Jurasico Medio): Modelos Evolutivos y Resolucion Paleontologica. Bol. Gent. Inst. Fitolec. Castelar, p.1-27.

Richter, D.K., and Fuchtbauer,H., 1978, Ferroan calcite replacement indicates former magnesian calcite skeletons, Sedimentology, v. 25, p. 843-860.

Rusnack, G.A., 1960, Sediments of Laguna Madre, Texas. in F.P. Shepard, F.B. Phleger, and T.H. van Andel (eds.), Recent sediments, Northwest Gulf Of Mexico, p. 153-196, American Association of Petrol. Geologists., Tulsa.

Salas, G.P., 1949, Bosquejo Geologico de la Cuenca Sedimentaria de Oaxaca: Asociacion Mexicana de Geologia y Petrologia, Boletin 1, p. 79-156.

Sanders, J.E., and Kumar, N., 1975, Evidence of shoreface retreat and in-place "drowning" during Holocene submergence of barriers, shelf off Fire Island, New York,

Bull. geol. Soc. Amer.., 86, p. 65-76.

Scholle, P.A. and Spearing, D., eds. 1982, Sandstone Depositional Environments, American Association of Petroleum Geologists, Memoir 31, 410 p.

Schwartz, M.L., (ed.), 1973, Barrier Islands, Dowden, Hutchinson and Ross Inc., Stroudsberg, Pennsylvania. 451 p.

Schwartz, R.K., 1975, Nature and genesis of some storm washover deposits, U.S. Army Corps. Engin. Coastal Eng. Res. Centre Tech. Mem., 61, pp. 69.

Sellwood, B.W., 1978, Jurassic. in McKerrow, W.S., The Ecology of Fossils: An illustated guide. Duckworth Press, London. 383p.

Silver, L.T. and Anderson, T.H., 1974. Possible left lateral Early to Middle Mesozoic disruption of the southwestern north American Craton margin. Geological Society of America, Abstracts with Programs, v. 6, p.955.

Spath, L.F., 1927-33, Revision of the Jurassic cephalopod faunas of Kacch (Cutch). India Geol. Survey Mem., Palaeont. Indica.

Stehn, E., 1923, Beitrage zur Geologie und Paleotologie von Sudamerika. XXV, Beitrage zur Kenntnis des Bathonien und Callovien in Sudamerika: Neues Jahrbuch fur Mineralogie, Geologie und Palaontologie, Beilage-Band XLIX, p. 52-158.

Steinmann, G., 1881, Zur Kenntnis der Jura- und Kreideformation von Caracoles (Bolivia). Neues Jahrbuch fur Geologie, Mineralogie und Palaontologie, Beilage-Band 1, p. 239-301.

Stipanicic, P.N., 1966, El Jurasico en Vega de la Veranada (Neuquen), el Oxfordense y el Diastrofismo Divesiano (Agassiz-Yaila) en Argentina. Asociacion Geologica Argentina, Revista XX, p. 403-478.

Tasch, P., 1980, Paleobiology of the Invertebrates, Data Retrieval from the Fossil Record, 2nd Edition, John Wiley and Sons, New York, 975 p.

Taylor, D.G., Callomon, J.H., Hall, R., Smith, P.L., Tipper, H.W., Westermann, G.E.G., 1985, Jurassic Ammonite Biogeography of Western North America: The Tectonic Implications. in Westermann, G.E.G., Jurassic-Cretaceous Biochronology & Biogeography of North America, Geological Association of Canada, Special Paper 27. 315p.

Thierry, J., 1976, Le Genre Macrocephalites ou Callovien Inferieur (Ammonites, Jurassic Moyen): Memoire Geologique de Universite de Dijon 4, 490 p.

Tornquist, A., 1898, Der Dogger am Espinazito-Pass. Palaeontologische Abhandlungen, Neue Folge, Band VII, 2, p.3(135)-69(201).

Vail, P.R., Mitchum, R.M., Todd, R.G., Widmier, J.M., et al., 1977, Seismic stratigraphy and global changes of sea level. in Stratigraphic Interpretation of Seismic Data, ed. C.E. Payton, p.49-212. Am. Assoc. Pet. Geol. Mem. No. 26.

Vail, P.R., Todd, R.G., 1981, Northern North Sea Jurassic unconformities, chronostratigraphy and sea-level changes from seismic stratigraphy. in Petroleum Geology of the Continental Shelf of North-west Europe. p. 216-235. London:Heyden.

Vail, P.R., Hardenbol, J., Todd, R.G., 1984, Jurassic unconformities, chronostratigraphy, and sea-level changes from seismic stratigraphy and biostratigraphy. in Schlee,J.S. (ed.), Interregional Unconformities and Hydrocarbon Accumulation. Am. Assoc. Petroleum Geol. Memoir 36.

Van Hinte, J.E., 1976, A Jurassic time scale. Am. Assoc. Petrol. Geol. Bulletin. v. 60. p.489-497.

Waagen. W., 1873-1875, Jurassic fauna of Kutch; Cephalopoda. India Geol. Survey Mem., Palaeont. Indica.

Walker, R.G., 1982. Hummocky and swaley cross stratification. in Walker, R.G., ed., Clastic units of the Front Ranges, Foothills and Plains in the area between Field B. C. and Drumheller, Alberta. International Association of Sedimentologists, 11th International Congress on Sedimentology (Hamilton, Canada), Guidebook to Excursion 21A, p. 22-30.

Walker, R.G.,(ed.), 1984, Facies Models, 2nd Edition, Geoscience Canada, G.A.C., 317 p.

Walker, R.G., 1984, Geological evidence for storm transportation and deposition on ancient shelves. in Tillman, R.W. et al., (eds.), Shelf sands and sandstone reservoirs, Society of Economic Paleontologists and Short Course, San Antonio, TX., p.1-58.

Walker, R.G., Duke W.L., Leckie, D.A., 1983, Hummocky stratification: significance of its variable bedding

sequences: discussion, Bulletin of the Geological Society of America, v.94, p. 1245-1249.

Ward, P.D., 1976, Stratigraphy, Paleoecology and Functional Morphology of Heteromorph Ammonites of the Upper Cretaceous Nanaimo Group, British Columbia and Washington. unpublished Ph.D. thesis, McMaster University, Hamilton, Canada.

Weeks, L,G., 1957, Origin of carbonate concretions in shales of the Magdelena Valley, Colombia, Geological Society of America Bulletin, v. 68, p. 95-102.

Weimer, R.J., Howard, J.D., and Lindsay, D.R., 1982, Tidal flats and associated tidal channels. in Scholle, P.A., and Spearing, D. (eds.), Sandstone Depositional Environments. Amer. Assoc. Petrol. Geol. Memoir 31, p. 191-245.

Westermann, G.E.G., 1954, Monographie der Otoitidae (Ammonoidea). Beih. Geol. Jb. 15, 364p.

Westermann, G.E.G., 1958, Ammoniten-Fauna und Stratigraphie des Bathonien NW-Deutschlands: Beihefte zum Geologischen Jahrbuch 32, 152 p.

Westermann, G.E.G., 1984a, Gauging the duration of stages: A

new approach for the Jurassic, Episodes, v. 7, No. 2.

Westermann, G.E.G., 1984b, The Late Bajocian Duashnoceras Association (Jurassic Ammonitina of Mixteca in Oaxaca, Mexico: Congreso Latinamericano de Paleontologia Memoria 3, p. 192-199.

Westermann, G.E.G.,(ed.), 1984c, Jurassic-Cretaceous Biochronology & Biogeography of North America. Geological Association of Canada, Special Paper 27. 315p.

Westermann, G.E.G., Corona, R., Carrasco, R., 1984, The Andean Mid-Jurassic Neuqueniceras Ammonite Assemblage of Cualac, Mexico. in Westermann G.E.G., (ed.), Jurassic-Cretaceous Biochronology & Biogeography of North America. Geological Association of Canada, Special Paper 27. 315p.

Westermann , G.E.G., Riccardi, A. C., 1985. Middle Jurassic ammonite evolution in the Andean Province and emigration to the Tethys. in Bayer, U., Seilacher, A., Sedimentary and Evolutionary Cycles, Lecture Notes in Earth Sciences 1, Springer-Verlag, Berlin. 465p.

Winkler, H.G.F., 1979. Petrogenesis of Metamorphic Rocks, 5th Edition, Springer-Verlag, New York. 348p.

Ziegler, B., 1967, Ammoniten-Ökologie am Beispiel des Oberjura. Geol. Rundschau. v. 56,p.439-646.

APPENDIX 1

Staining techniques

The method of staining developed by Lindholm and Finkelman (1971) was used in the identification of ferroan/non-ferroan calcite and dolomite. Both the calcite and dolomite readily stained. Non-ferroan calcite stains red, ferroan calcite mauve to purple, and dolomite blue.

Method:

1/ The solution consists of 1 gram of Alizarin Red-S and 5 grams of K-ferricyanide, dissolved in 1 litre of 0.2 HCL.

2/ The 0.2 solution of HCL was prepared by adding 2 ml of concentrated (12 normal) HCL to 998 ml of distilled water (always add acid to water).

3/ 0.5 g of Alzarin Red-S and 2.5 g of K-ferricyanide were dissolved in 500 ml of the 0.2 HCL solution.

4/ One half of the thin section was immersed in the 0.2 HCL etching solution for 30 seconds.

5/ The etched half was then immersed in the staining solution at room temperature for 2-4 minutes.

6/ After staining the sections were rinsed in distilled water and allowed to air dry.

The solution must be prepared fresh, since it gradually oxidizes, to ensure proper stain colouration.